



University of
Salford
MANCHESTER

**Organic and Inorganic Contaminants along the Qatari Coast: A Case Study
of The Pearl Oyster (*Pinctada radiata*)**

© **Noora Mahmood Aljathelah Al-Shamary**

This thesis is presented to the School of Environment & Life Sciences, University of Salford, in fulfilment of the requirements for the degree of Ph.D.

Supervised by Dr. Simon Hutchinson and Dr. Debapriya Mondal

June 2021

Table of Contents

Table of Contents	i
List of Figures.....	v
List of Tables	vii
Acknowledgment.....	viii
Glossary	ix
Abstract.....	x
Chapter 1: Introduction	1
1.1 General Introduction.....	2
1.2 Aims and Objectives of the Study.....	5
1.3 Thesis Outline and Structure	5
Chapter 2: Literature Review	8
2.1 The Geography and Geology of the Region.....	10
2.1.1 Geography of the Gulf Region	10
2.1.2 Geography and Geology of the Arabian Peninsula.....	11
2.1.3 Geography and Geology of the Arabian Gulf.....	12
2.1.4 Geology of Qatar	14
2.2 Total Petroleum and Polycyclic Aromatic Hydrocarbons (TPHs and PAHs).....	17
2.2.1 Total Petroleum Hydrocarbons (TPHs).....	17
2.2.2 Polycyclic Aromatic Hydrocarbons (PAHs).....	20
2.2.3 Distribution of TPHs and PAHs	28
2.3 Trace metals	33
2.3.1 Sources of trace metals	33
2.3.2 Routes of exposure	34
2.3.3 Transport and fate in the environment.....	34
2.3.4 Human Health Effects	35
2.3.5 Metabolism	36
2.3.6 Removal from the Environment	36
2.3.7 Distribution of Trace Metals.....	40
2.4 Total Mercury	47
2.4.1 Sources of mercury	47
2.4.2 Exposure routes of mercury	48

2.4.3 Health effects of mercury	48
2.4.4 Metabolism of mercury	48
2.4.5 Distribution of Total Mercury in marine environment	49
2.4.6 Distribution of Total Mercury in Qatar’s Marine Environment.....	51
2.5 Summary.....	52
Chapter 3: Study Area and Methodology	54
3.1 Sampling Locations.....	55
3.1.1 Simaisma site:.....	56
3.1.2 Umm Bab site:	57
3.1.3 Al Khor site:	58
3.1.4 Al Wakra site:	59
3.2 Sampling Collection Techniques.....	60
3.2.1 Collection of Seawater	61
3.2.2 Collection of Surface Coastal Sediment	61
3.2.3 Collection of Pearl Oysters.....	62
3.2.4 Collection of Sediment Cores	62
3.3 Sample Preparation	64
3.3.1 Coastal Sediment Samples.....	64
3.3.2 Sediment Core Samples	65
3.3.3 Oyster Tissue Samples.....	65
3.4 Extraction of Samples for Organic Contaminants.....	66
3.4.1 Seawater Extraction for GC Analysis	66
3.4.2 Coastal Sediment and Oyster Tissues Extraction for GC Analysis.....	66
3.5 Digestion of Samples for Inorganic Contaminants	67
3.5.1 Digestion of Samples for Trace Metals.....	67
3.5.2 Sample Preparation for Total Mercury	68
3.6 Analysis Methodology	70
3.6.1 In-situ parameters analysis of seawater	70
3.6.2 Abiotic parameter of seawater and sediment	70
3.6.3 Organic Contaminants (TPHs and PAHs).....	71
3.6.4 Inorganic Contaminants (Trace metals and Total Mercury).....	72
3.6.5 Quality Assurance and Quality Control (QA/QC).....	73
3.6.6 Statistical Analysis	75

Chapter 4: Physicochemical Parameters of Seawater and Sediment	76
4.1 In-situ parameters of seawater	77
4.2 Abiotic parameters of seawater and sediment.....	79
4.2.1 Total Organic Carbon	79
4.2.2 Grain size	83
4.3 Summary.....	85
Chapter 5: Distribution of organic contaminants (TPHs, PAHs) in seawater, surface sediment, core sediment, and oyster tissues around the coastline of Qatar	86
5.1 Introduction.....	87
5.2 Methodology	90
5.2.1 Sampling and study area	90
5.2.2 Laboratory techniques protocols.....	90
5.2.3 Quality Assurance and Quality Control (QA/QC).....	91
5.2.4 Statistical Analysis	91
5.3 Results and Discussion.....	91
5.3.1 TPHs and PAHs in Surface Seawater	92
5.3.2 TPHs and PAHs in Surface Coastal Sediment	94
5.3.3 TPHs and PAHs in sediment cores	101
5.3.4 TPHs and PAHs in oyster tissues.....	106
5.3.5 Seasonal Variation of TPHs and PAHs.....	114
Chapter 6: Occurrence of trace metals and total mercury in seawater, surface sediment, and oyster tissues around the coastline of Qatar	119
6.1 Introduction.....	120
6.2 Methodology	122
6.2.1 Sampling and Study Area.....	122
6.2.2 Laboratory technique protocols	122
6.2.2.2 Glassware and General Instruments.....	122
6.2.2.3 Sample Preparation and Analysis	123
6.2.3 Quality Assurance and Quality Control (QA/AC).....	124
6.2.4 Statistical Analysis	124
6.3 Results and Discussion.....	124
6.3.1 Trace Metals and Total Mercury in Seawater	124
6.3.2 Trace Metals and Total Mercury in Surface Coastal Sediment	131
6.3.3 Trace Metals and Total Mercury in Sediment Cores	140

6.3.4 Trace Metals and Total Mercury in Oyster Tissues	143
6.4 Conclusion	154
Chapter 7: Integration and Discussion	155
7.1 General Finding and Integration	156
7.2 Theoretical Patterns of Organic and Inorganic Contaminants	162
7.3 Assessment of Current Status of Organic and Inorganic Contaminants in Qatar's Coastal Environment	165
7.4 Recommendations and Future Directions	167
References	169
Appendixes	186
Appendix A: Physical parameters for the four locations from the four sampling rounds in summer and winter.	186
Appendix B: Seasonal concentrations of TOC in seawater, marine sediment, and core sediment from four different sites	191
Appendix C: Grain size	194
Appendix D: TPHs results for the two-years sampling	196
Appendix E: PAHs results for the two-years sampling	202
Appendix F: Trace metals results for two years sampling.....	206
Appendix G: Total mercury results for two years sampling.....	214

List of Figures

Figure 1. 1: Thesis structure and the organization of chapters	6
Figure 2. 1: Geographical map of Arabian Gulf Region.....	10
Figure 2. 2: Major contaminant sources areas in the Arabian Gulf region	11
Figure 2. 3: Geological map of Arabian Gulf Peninsula.....	12
Figure 2. 4 :Spatial distribution of highest daily maximum wet-bulb temperature, in the modern record	13
Figure 2. 5 : Predominant surface water circulation patterns in the Arabian Gulf.	13
Figure 2. 6 : Major sedimentary domains of The Gulf.	14
Figure 2. 7 : Geological map of Qatar	15
Figure 2. 8 : Location of major coral reef, mangrove, and seagrass ecosystems in coastal and marine systems of Qatar...	16
Figure 2. 9 : Coastal sediment in Qatar	16
Figure 2. 10: The structures of common PAHs	21
Figure 2. 11: Sources of PAHs from natural and anthropogenic sources	22
Figure 2. 12: PAHs distribution in the environments	23
Figure 2. 13: Major pathways involved in the metabolism of PAHs by bacteria, fungi and algae.....	26
Figure 2. 14: Multiple mechanisms by which PAHs cause lung cancer.....	26
Figure 2. 15: Pathways of metals to humans	34
Figure 2. 16: The Median lethal dose "LD ₅₀ " for metals. (A) All metals for which the data are available. (D) The toxicity rating based on the corresponding table from Hazardous Chemicals Handbook.	36
Figure 3. 1: Location of the sampling points around the coastline of Qatar.....	55
Figure 3. 2: Simaisma site.....	56
Figure 3. 3: Umm Bab site.....	57
Figure 3. 4: Al Khor site.....	58
Figure 3. 5: Al Wakra site.....	59
Figure 3. 6: Sampling scheme.....	60
Figure 3. 7: Sampling of seawater samples.....	61
Figure 3. 8: Sampling of surface marine sediment samples.....	61
Figure 3. 9: Scuba diving during collection of pearl oysters (<i>P. radiata</i>) from the Simaisma site.....	62
Figure 3. 10: Sampling locations of sediment core samples.....	63
Figure 3. 11: Sampling of core samples in the field.....	64
Figure 3. 12: Preparation of core samples in the lab prior of extraction.....	65
Figure 3. 13: Preparation of homogenized oyster samples for each batch.....	66
Figure 3. 14: Extraction procedure for sediment and oyster tissues samples.....	67
Figure 3. 15: The EXO3 Multiparameter Sonde- YSI.....	70
Figure 4. 1: Summary of the physicochemical parameters over the two years for the four sampling sites, A: temperature, B: salinity, C: pH.....	78
Figure 4. 2: The TOC in seawater samples. (A- In summer seasons. B- In winter seasons).	80
Figure 4. 3: The TOC in surface sediment samples. (A- In summer seasons. B- In winter seasons).	81
Figure 4. 4: Correlation between TOC in seawater and sediment	81
Figure 4. 5: The mean concentration of TOC in sediment core.....	82
Figure 4. 6: The mean grain size fractions in coastal surface sediment of the four sites in all seasons	84
Figure 4. 7: The mean grain size of sediment core samples from the four different locations	84

Figure 5. 1: Concentration of TPHs in seawater samples in summer seasons and winter seasons.....	92
Figure 5. 2: Ranges of TPHs in seawater from different area.....	93
Figure 5. 3: Concentration of TPHs in surface sediment samples in Summer seasons and Winter seasons.....	95
Figure 5. 4: Concentration of PAHs in surface sediment samples in summer seasons and winter seasons.....	96
Figure 5. 5: Concentration of most detected PAHs in the surface coastal sediment samples ($\mu\text{g}/\text{kg}$ dry weight).....	96
Figure 5. 6: Ranges of TPHs and PAHs in surface sediment from different area.....	97
Figure 5. 7: Correlation between TPHs/ PAHs and TOC in surface sediment samples.....	100
Figure 5. 8: The mean concentration of TPHs in sediment Core ($\mu\text{g}/\text{kg}$).....	101
Figure 5. 9: The mean TPHs concentration in sediment cores across sites and depth.....	102
Figure 5. 10: The mean concentration of PAHs in sediment core ($\mu\text{g}/\text{kg}$ dry weight).....	102
Figure 5. 11: The mean TPHs concentration in sediment cores across sites and depth.....	103
Figure 5. 12: Concentration of detected PAHs in the sediment core samples ($\mu\text{g}/\text{kg}$ dry weight).....	104
Figure 5. 13: Mean concentration of TPHs and PAHs by depth in sediment core samples.....	105
Figure 5. 14: Correlation between TOC content and PAHs level in sediment core samples.....	106
Figure 5. 15: Concentration of TPHs in oyster tissues samples in summer seasons and winter seasons.....	107
Figure 5. 16: Concentration of PAHs in oyster tissues samples in summer seasons and winter seasons.....	108
Figure 5. 17: Concentration of highest detected PAHs in the oyster tissues samples ($\mu\text{g}/\text{kg}$ dry weight).....	109
Figure 5. 18: Ranges of TPHs and PAHs in oyster tissues from different area.....	110
Figure 5. 19: Relationship of TPHs between coastal sediment and oyster tissues.....	112
Figure 5. 20: Relationship of PAHs between coastal sediment and oyster tissues.....	113
Figure 5. 21: Seasonal variations of TPHs concentration in seawater, surface sediment and oyster tissues.....	114
Figure 5. 22: Seasonal variations of PAH concentration in the surface coastal sediment and oyster tissues.....	115
Figure 5. 23: Mean TPHs and PAHs concentration in biotic and abiotic matrixes from Qatar Coastal Environment...	116
Figure 6. 1: Seasonal variations of trace metals concentration in Seawater samples from the four sites	125
Figure 6. 2: Concentration of Total Mercury in seawater samples in summer and winter seasons	129
Figure 6. 3: Concentration of total Hg in seawater samples ($\mu\text{g}/\text{L}$).....	130
Figure 6. 4: Seasonal variations of trace metals concentration in coastal sediment samples.....	134
Figure 6. 5: Concentration of Total Mercury in surface sediment samples in summer and winter seasons	137
Figure 6. 6: Concentration of total Hg in surface sediment samples ($\mu\text{g}/\text{g}$)	138
Figure 6. 7: The mean concentration of trace metals in sediment cores from the four sites	141
Figure 6. 8: The mean concentration of total mercury in sediment Cores ($\mu\text{g}/\text{g}$)	142
Figure 6. 9: The mean concentration of Total Mercury in sediment cores across sites and depth.....	143
Figure 6. 10: Seasonal variations of trace metals concentration in oyster tissues samples.....	146
Figure 6. 11: Concentration of Total Mercury in pearl oyster tissues samples in summer and winter seasons	149
Figure 6. 12: Concentration of total Hg in oyster tissues samples ($\mu\text{g}/\text{g}$) from different areas.....	149
Figure 6. 13: Seasonal variations of total mercury concentration in seawater, coastal sediment, and oyster tissues samples	152
Figure 7. 1: The overall mean concentration of organic and inorganic contaminants from the four sample sites	157
Figure 7. 2: PCA Biplot of organic and inorganic contaminants.	159
Figure 7. 3: Vertical profiles of mean concentration of organic and inorganic contaminants in sediment cores	161
Figure 7. 4: The theoretical accumulation pattern of organic and inorganic contaminants in this study	162
Figure 7. 5: Distribution patterns of organic and inorganic contaminants in the depth profiles of different four cores. ...	164

List of Tables

Table 2. 1: Cancer classification of individual polycyclic aromatic hydrocarbons (VDH, 2012)	24
Table 2. 2: Toxicity of some PAHs based on lab experiments	24
Table 2. 3: Concentrations of TPHs and PAHs in abiotic and biotic matrices from different locations in the world .	29
Table 2. 4: Concentration profile of some PAHs.....	30
Table 2. 5: Concentrations of TPHs and PAHs in abiotic and biotic matrices from Arabian Gulf countries	31
Table 2. 6: Concentrations of TPHs and PAHs in marine sediment from Qatar environment	32
Table 3. 1: Timetable for each category in each site	60
Table 3. 2: Hot Block program for sediment acid digestion	68
Table 3. 3: Hot Block program for acid digestion.	68
Table 3. 4: Operating Conditions for Mercury Analyzer AULA-254 ASD.....	69
Table 3. 5: Operating Conditions for Mercury Analyzer AULA-254 ASD.....	69
Table 3. 6: GC/FID conditions used for analysis of TPHs	72
Table 3. 7: GC/MS conditions used for analysis of PAHs.....	72
Table 3. 8: Limit of Detection (LOD) for organic and inorganic contaminates	73
Table 3. 9: CRM recoveries for TPHs and some PAHs compounds	74
Table 3. 10: CRMs recoveries for trace metals and total mercury.....	75
Table 4. 1: The Mean Concentration of TOC in Surface Seawater (mg/L \pm SD).....	79
Table 4. 2: The Mean Concentration of TOC in surface Sediment (mg/kg \pm SD)	80
Table 4. 3: The mean grain size measurement of surface coastal sediment.....	83
Table 5. 1: The range of diagnostic ratios for PAHs sources.....	98
Table 6. 1: The Mean Concentration of Trace Metals in Surface Seawater (μ g/L)	126
Table 6. 2: The Mean Concentration of Total Mercury in Surface Seawater (μ g/L).....	128
Table 6. 3: The Mean Concentration of Trace Metals in surface coastal sediment (μ g/g)	133
Table 6. 4: The Mean Concentration of Total Mercury in surface coastal sediment (μ g/g)	136
Table 6. 5: The Mean Concentration of Trace Metals in Tissues of Pearl Oyster (<i>P. radiata</i>) (μ g/g)	144
Table 6. 6: The Mean Concentration of Total Mercury in Tissues of Pearl Oyster (<i>P. radiata</i>) (μ g/g)	148
Table 7. 1: National and international limits for organic and inorganic contaminants	166

Acknowledgment

This dissertation was carried out in a challenging interdisciplinary field and I wish to thank the many persons who contributed in different ways to the realization of the work. First, I would like to express my deepest gratefulness to my two supervisors Dr. Simon M. Hutchinson and Dr. Debapriya Mondal who were an encouraging, trustful and at the same time challenging supervisors. I am also thankful to my second father Mr. Ismail Al-Shaikh who was the first and main supporter to complete my postgraduate degree and achieve my goal. Many thanks also to Dr. Alexandra Leitão-Ben Hamadou, Dr. Stéphane Bayen and Dr. Hassan Hassan, the team of the NPRP project, for their support and help in the sampling field area and in the lab. Deep thanks also goes to the staff of Environmental Science Center "ESC" at Qatar University for their help in sample's analysis. I am especially thankful to my friends for the invaluable compensation to the daily routine. You supported me throughout these years by just being there.

An extra big “thank you” goes to my husband "Mohammed", who support me from the beginning until this time. Finally, I am deeply grateful to my parents and to my brother Awad and sisters for always encouraging me in any possible way.

Glossary

DRO	Diesel Range Organics
GC	Gas Chromatography
GC/FID	Gas Chromatography/ Flame Ionization Detector
GC/MS	Gas Chromatography/ Mass Spectrometry
ICP-OES	Inductively Coupled Plasma - Optical Emission Spectrometry
PAHs	Polycyclic Aromatic Hydrocarbons
POPs	Persistent Organic Pollutants
TC	Total Carbon
T-Hg	Total mercury
TIC	Total Inorganic Carbon
TOC	Total Organic Carbon
TPHs	Total Petroleum Hydrocarbons

Abstract

Qatar sits in the middle of the world's most important hydrocarbon producing areas where significant regional refining activity and shipping traffic take place. In addition, significant local coastline development, prominently along the eastern coast, has taken place over recent decades. Protecting Qatar's marine ecosystems from the adverse effects of environmental contaminants is a core component of the Environmental Development pillar within the National Vision 2030. However, a limited number of studies have investigated contaminant concentrations in the coastal environment of Qatar. The accumulation of contaminants in aquatic environments can affect coastal and marine ecosystems and cause adverse effect for marine organisms and human health.

This study aims to determine environmental contamination in Qatar's coastal environment by measuring organic and inorganic contaminants, along with physiochemical parameters, at four sites located on the contrasting east and west coasts of the country. The Pearl Oyster *Pinctada radiata*, which is considered an iconic organism in Qatar, was used to determine a baseline of contaminants in an aquatic organism. Surface seawater, surface sediment and oysters were collected four times over two years in different seasons from the four sites. In-situ parameters (temperature, pH, and salinity), and abiotic parameters (TOC and grain sizes) were measured for seawater and sediment. Organic (TPHs, PAHs) and inorganic contaminants (trace metals including Cd, Cu, Cr, Ni, Pb and Zn, T-Hg) were measured in all samples.

Overall, high PAHs were observed in oyster tissues and sediment cores while high Pb was noted in seawater and high Zn was observed in sediment and oyster. Benzo (a) pyrene was the highest PAHs compound detected in oyster tissues exceeding the permissible level of 5 µg/kg in fishery products (EUCR, 2014). The concentrations found were 1507.2, 1261.9, 374.8, 218.2 µg/kg dry weight in Al Wakra, Al Khor, Umm Bab and Simaisma tissues samples respectively. However, high TPHs were also noted in oyster tissues and sediment cores from Simaisma. At Al Khor, also on the east coast, high level of TPHs were recorded in seawater, while high PAHs and TOC were observed in surface sediment, which had a relatively higher clay and silt content than the other sites. High level of Pb was observed in seawater samples collected from Al Khor site (56.1 µg/L) exceeding the toxicity level of 50 µg/L (WHO, 2003). Umm Bab (with a desalination plant near the coast), the sole sample site on the west coast, showed the highest level of TOC in seawater and sediment and highest Ni in seawater. In addition, high total mercury in oyster tissues

collected from Umm Bab was observed (1.18 $\mu\text{g/g}$) that exceeded the permissible level of 1 $\mu\text{g/g}$ (EC, 2001; USEPA, 2002). Moreover, levels of Zn in oyster tissues (551.8 to 2807.2 $\mu\text{g/g}$) exceeded the maximum limit allowed for oysters (1000 $\mu\text{g/g}$) according to Australian acceptable limits as recommended by the National Health and Medical Research Council (Hungspreugs and Yaunghthong, 1984).

Our results, in general, report lower levels in seawater and sediment compared to other studies in the region and more widely; however, in oysters most of the contaminants are higher when compared to international guideline values. These higher levels indicate the potential for these filter feeding organisms to absorb contaminants into their tissues from the environment that surrounds them. Additionally, bioaccumulation can occur. This study provides background information for further investigation to understand the presence and distribution of organic and inorganic contaminants in Qatar's rapidly changing coastal environment. It indicates the usefulness of applying a holistic view to environmental monitoring including the use of biomonitoring.

Chapter 1:

Introduction

1.1 General Introduction

The State of Qatar is a small peninsular land mass, just over 11,000 km² with 900 km of coastline, off the Arabian Peninsula and connected to the south to Saudi Arabia. High salinity and great temperature fluctuations make the Gulf surrounding Qatar unique and extreme (Richer, 2008). Marked solar pumping (evaporation) and restricted water exchange with the open water of the Arabian Sea makes the Gulf's seawater saline, this lack of exchange means that pollutants in the Gulf can take longer to dissipate (Brook et al. 2006). Qatar has witnessed a rapid expansion in coastal development, linked to its industrial and population growth in recent decades (Burt et al., 2017). While economically and socially valuable, the growth comes with an associated environmental cost and Qatar's marine environment now faces many pressures including eutrophication, inputs of domestic sewage, discharge of industrial waste and the resuspension of sediment due to coastal construction (Leitão-Ben Hamadou et al., 2016). Major point sources of pollution include the numerous wastewater outfalls around Qatar and inputs associated with the oil and desalination industry. In combination, these various activities have resulted in an increased influx of different types of chemical contaminants into the Gulf (Al-Sarawi et al., 2015), including those which are known to have a range of adverse impacts on marine organisms.

Biomonitoring of marine environment involves the systematic measurement of compounds in living organisms (biomarkers/bioindicators) to identify and assess potential hazardous exposure and effects to chemicals (Costa and Teixeira, 2014). The aquatic organisms and the other members of the food chain accumulate the contaminants into their tissues and organs (Taylan and Ozkoc, 2007). The process of the increase in concentration of a substance in an organism's tissues or organs which it exposes to the surrounding environment is known as bioaccumulation. Bioaccumulation of substances taken in by the organism from water is termed bioconcentration (Türe et al., 2009).

The presence of chemical contaminants has also been shown in food products harvested from the sea, and certain species of fish and shellfish collected from the Gulf are known to fail international food safety limits (Stentiford et al., 2014). With Qatar relying heavily on clean seawater for the production of potable water and seafood as the only real source of protein production, these contaminant related pressures are seen as posing a real threat to national water and food security (Hussein and Lambert, 2020). As such, protecting Qatar's marine ecosystems, drinking water and food resources from the adverse effects of chemical contaminants is a core component of the Environmental Development pillar within the National

Vision 2030(Qatar National Vision 2030, 2008). It is now internationally agreed that the assessment of environmental ‘health’, and the design and implementation of measures to improve environmental quality, are best undertaken on the basis of an integrated approach using both chemical measurements and appropriate biological measurements in key sentinel or ‘guardian’ species (EPA, 2019). As such, bivalve molluscs, including mussels and oysters, have been used extensively in marine coastal monitoring programs, from the early U.S. “Mussel Watch” program in the 1970s to more recent European research programs (e.g., National Oceanic and Atmospheric Administration NOAA's Mussel Watch Program) in 2015 to 2019 (Johnson et al., 2019) and initiatives in the Arabian Gulf under the guise of ROPME “Regional Organization for the Protection of The Marine Environment” in 2011(ROPME, 2011). Bivalve molluscs are ideal sentinel organisms, with high ecological importance, a wide geographical distribution, sessile in nature, which bioaccumulate contaminants and exhibit a range of biological responses when stressed or exposed to environmental contaminants.

In Qatar, the pearl oyster, *Pinctada radiata*, represents an integral part of the nation’s cultural heritage and is one of the main economic foundations upon which the country developed. Historically, pearl oyster formed extensive beds along the western coastline of the Gulf extending from Kuwait in the north to Oman in the South. During the early part of the 20th century nearly half the male population of Qatar were involved in the pearl oyster industry, which, at present day prices, would be worth an estimated \$2.5 billion per annum to the nation’s economy (Smyth et al., 2016). However, as Qatar has prospered and developed coastal urban and industrial areas, *P. radiata* populations have significantly declined. Therefore, due to its biological characteristics, ecological status and sensitivity to anthropogenic stress, this symbolic species of Qatar’s maritime history is now ideally positioned to be selected as a sentinel species to monitor and assess the health of the country’s marine environment.

Previous research in Gulf countries has assessed the levels of organic and inorganic contaminants in the marine environment. However, relatively few studies have investigated organic and inorganic contaminants in Qatar’s coastal environment although this environment has been impacted by marked industrial expansion and anthropogenic pressures over the last several decades. In particular, little is known about the levels of organic contaminants such as Total Petroleum Hydrocarbons (TPHs) and Polycyclic Aromatic Hydrocarbons (PAHs), and inorganic contaminants, such as trace metals and total mercury, in seawater, sediment and biota.

Organic contaminants have only been assessed in one study of TPHs and PAHs in Qatari seawater and pearl oyster tissues (Leitão et al. (2017), three studies have reported levels of TPHs in Qatari marine sediment (Rushdi et al., 2017; Leitão et al., 2017; Tolosa et al., 2005), while seven studies have reported levels of PAHs in Qatari marine sediment (Soliman et al., 2019; Soliman et al., 2014; Rushdi et al., 2017; Hassan et al., 2018; Leitão et al., 2017; de Mora et al., 2010; Tolosa et al., 2005). For inorganic contaminants, only two studies have investigated trace metals concentrations (Aboul Dahab and Al-Madfa, 1997; Leitão et al. 2017) and three examined total mercury (Al-Madfa et al., 1994; Kreish & Al-Madfa, 1999; Leitão et al. 2017) in Qatari seawater; four studies reported trace metals (Basaham and Al-Lihaibi, 1993; Aboul Dahab and Al-Madfa, 1997, Al-Naimi et al., 2015; Leitão et al., 2017) and three examined total mercury concentrations (Al-Madfa et al., 1994; Kreish & Al-Madfa, 1999; Leitão et al. 2017) in Qatari marine sediment. Two studies have examined levels of trace metals (Al-Madfa et al., 1998; Leitão et al., 2017) and three reported level of total mercury (Kreish & Al-Madfa, 1999; Al-Maslamani et al., 2015; Leitão et al. 2017) in Qatari pearl oyster tissues.

Thus, this thesis aims to overcome the research gap, specifically the lack of wider geographical coverage and a holistic approach. This study will also provide more recent data of chemical contaminants in the coastal environment of Qatar, which is significant given the rapid rate of the country's coastal development.

Qatar sits in the middle of the world's most important hydrocarbon producing areas where significant regional refining activity and shipping traffic take place, in addition to local coastline development. However, there is a paucity of data to properly assess the pollution status of Qatar's coastal environment. Thus, within the frame of 'National Priority Research Program' NPRP 9 project, entitled "The Pearl Oyster from national icon to a guardian of Qatar's marine environment" (commenced 2017-2019), an assessment of contaminants in Qatar's coastal environment have been applied. In particular, baseline concentrations and distributions of organic and inorganic contaminants of Qatar's coastline have been determined using a pearl oyster '*Pinctada Radiata*' as an indicator organism. Two organic contaminants including Total Petroleum Hydrocarbons (TPHs) and 16 compounds of Polycyclic Aromatic Hydrocarbons (PAHs) (USEPA, 1982), and two inorganic contaminants including six trace metals and total mercury are investigated and reported.

1.2 Aims and Objectives of the Study

The aim of this study is to determine the environmental contamination of Qatar's coastal environment by measuring organic and inorganic contaminants using pearl oyster as the indicator study organism for contaminants level in an aquatic environment.

In particular, the specific objectives are:

1. To quantify the levels of organic and inorganic contaminants (TPHs, PAHs, heavy metals and total mercury) in abiotic matrices (seawater and sediments) and biotic tissues of *P. radiata* from different sites located on the contrasting east and west coasts of Qatar.
2. To determine the relationship between organic and inorganic contaminants within the matrices of sediments and oyster tissues.
3. To assess the current status of organic and inorganic contaminants levels in Qatar coastal environment by comparing it with the National and International standards.

1.3 Thesis Outline and Structure

This thesis has seven chapters:

- **Chapter 1** provides a general introduction to the study including the rationale, aims and objectives for the study.
- **Chapter 2** provides a literature review of organic contaminants (TPHs and PAHs) and inorganic contaminants (trace metals, and total mercury) in the environment.
- **Chapter 3** describes the sampling area and methodology used in this study, including: sampling locations, collection techniques, sample preparation and analytical methods.
- **Chapter 4** presents the physicochemical parameter of seawater and sediment, including: in-situ parameters (temperature, pH, and salinity) and abiotic parameters (TOC and grain sizes).
- **Chapter 5** illustrates the levels of organic contaminants (TPHs and PAHs) in seawater, surface marine sediment, core sediment, and pearl oyster tissues (*P. radiata*) samples collected from four sites around Qatar coastline in different seasons.
- **Chapter 6** shows the trace metals and total mercury concentration found in same collected samples (seawater, surface marine sediment, and pearl oyster tissues (*P. radiata*)) around the coastline of Qatar.
- **Chapter 7** provides an integration and general discussion of the study including the general finding and integration, theoretical patterns of organic and inorganic contaminants,

assessment of the current status of contaminants by comparing it with the National and International standards, recommendation and future direction.

Figure 1.1 summarizes the structure of this thesis:

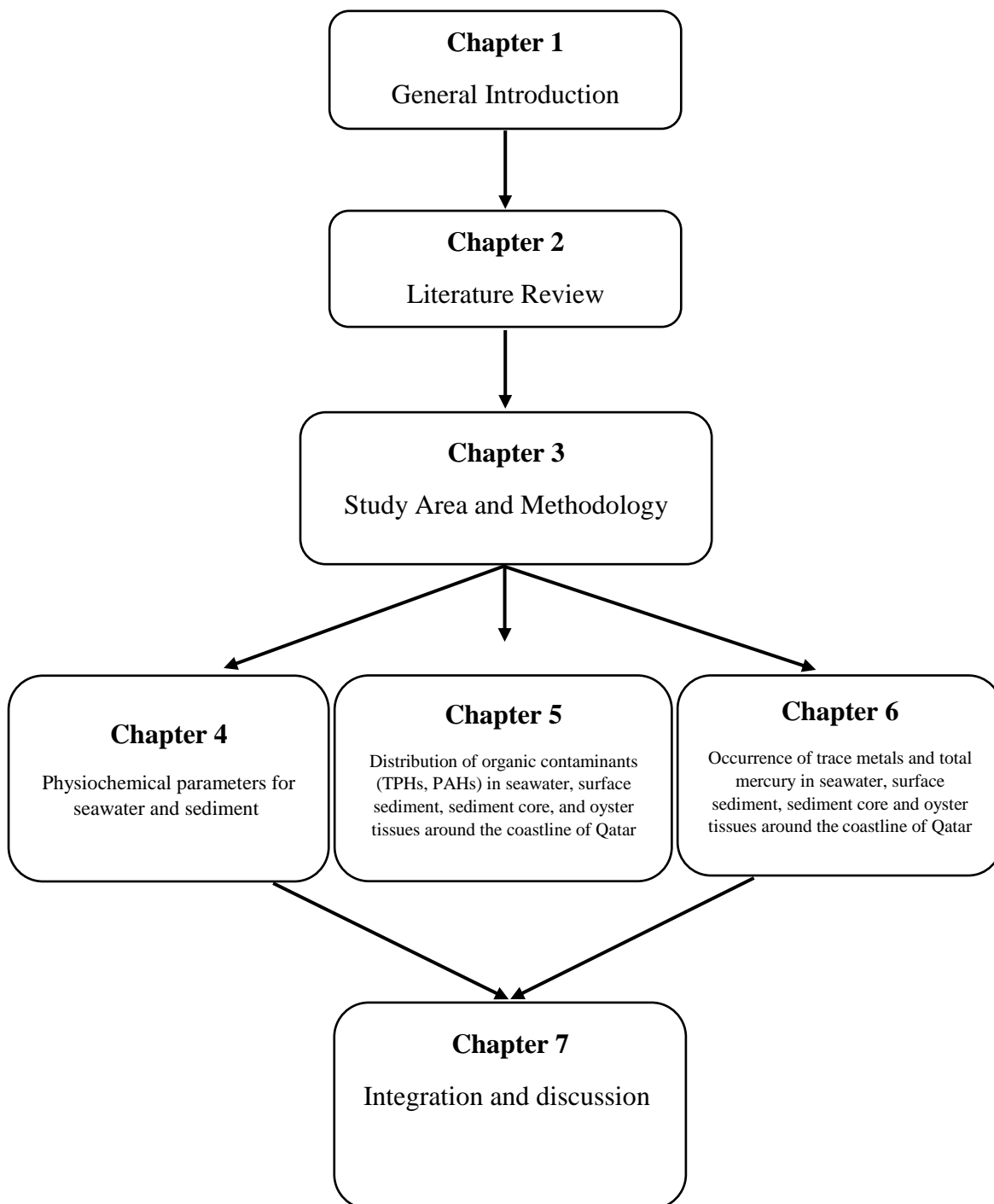


Figure 1. 1: Thesis structure and the organization of chapters

In addition to the main body of this thesis, there are seven appendices:

Appendix A offers an overview of the abiotic parameters (temperature, pH, and salinity) for the seawater in the four locations from the four sampling rounds in summer and winter seasons (March 2017, December 2017, May 2018, and November 2018).

Appendix B presents the seasonal concentrations of TOC in seawater, surface marine sediment, and core sediment samples from four different sites around the coastline of Qatar.

Appendix C illustrates the particle size measurement of surface marine sediment and core sediment.

Appendix D provides detailed data for levels of TPHs in seawater, sediment, and pearl oyster tissues samples collected from four sites around Qatar coastline in different seasons. Also provides the statistical analysis data for each matrix.

Appendix E offers detailed data for levels of PAHs in seawater, sediment, and pearl oyster tissues samples collected from four sites around Qatar coastline in different seasons. Also offers the statistical analysis data for each matrix.

Appendix F provides trace metals concentration detailed data found in seawater, sediment, and pearl oyster tissues samples collected from four sites around Qatar coastline in different seasons. Also provides the statistical analysis data for each matrix.

Appendix G offers detailed data for total mercury concentration found in seawater, sediment, and pearl oyster tissues samples collected from four sites around Qatar coastline in different seasons. Also offers the statistical analysis data for each matrix.

Chapter 2:

Literature Review

"Chemical contamination of the marine environment is a highly complex issue" (Alvarez-Muñoz et al., 2016). The issue includes organic and inorganic contaminants that may originate from a wide range of sources. The nature of the chemical contaminant differs depending on the type of anthropogenic activity and the chemicals used in various industrial processes (Thompson and Darwish, 2019). The most known organic contaminants include "Total Petroleum Hydrocarbons" (TPHs) and "Polycyclic Aromatic Hydrocarbons" (PAHs). Inorganic contaminants include trace metals and total mercury. For all these contaminants, accumulation in aquatic environments can cause environmental problems and potentially impact human health.

Many researchers around the world studied the distribution and accumulation of organic and inorganic contaminants in aquatic environments including seawater, marine sediment, and oyster tissues. Few studies in Arabian Gulf region have examined levels of these contaminants in the marine environment, while limited studies have reported concentration of these contaminants in Qatari marine environment.

This chapter provide a brief overview of regional and local geography and geology. Furthermore, it gives a short description of organic (TPHs and PAHs) and inorganic (selected trace metals and total mercury) contaminants including their sources, exposure routes, ways of transportation, human health effects, metabolism and methods of removal from environment.

2.1 The Geography and Geology of the Region

2.1.1 Geography of the Gulf Region

The Gulf is situated in Southwest Asia. It is an extension of the Indian Ocean located between Iran and the Arabian Peninsula. The Gulf is about 251,000 km² and connected to the Gulf of Oman to the east by the Strait of Hormuz. It is about 989 km length, where the northern coast is occupied mostly by Iran and the southern coast by Saudi Arabia. The gulf is about 56 km wide at its narrowest point which lies in the Strait of Hormuz (Yetiv, 1997). Overall, it is a very shallow water body with an average depth of 50m (Konyuhov and Maleki, 2006). The coastline of Arabian Gulf surrounded by the Iran, Oman , United Arab Emirates, Saudi Arabia, Qatar, Bahrain , Kuwait, and Iraq (Figure 2.1). Within this Gulf, several small islands lie, which are subject to territorial disputes by the states of the region.



Figure 2. 1: Geographical map of Arabian Gulf Region (Source: Pahl-Weber et al., 2013)

At present, more than 180 million people live in the Arabian Gulf region countries, more than 26 million of this population live in the coastal zone. The Arabian Gulf region countries are well known for their role as the world's biggest energy providers and possess 40% of the world's oil and 44% of gas reserves (Figure 2.2). As a result, the oil and gas industries are currently the main economic drivers of these countries (El-Katiri and Fattouh, 2017). Around 60% of the world's crude oil shipping occurs along Arabian Gulf maritime routes and the region is responsible for around 5.2% of the world's container trade (World Bank Group, 2019). More than 98% of the region's energy demands are met by oil and gas, with the remainder coming from renewable hydraulic energy provided by Iraq and Iran (World Bank Group, 2019). In addition to more exploitation of ordinary sources of fresh water, the Arabian

Gulf region relies heavily on desalination plants. Of the 15,900 operational desalination plants in the world, half of them are in the region (Frenken, 2009).

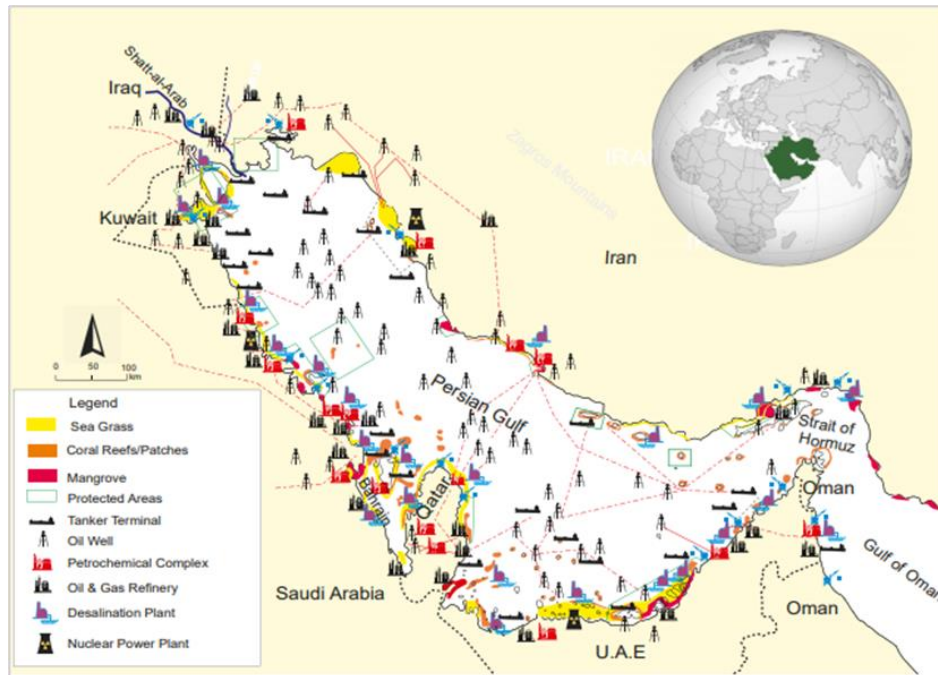


Figure 2 .2: Major contaminant sources areas in the Arabian Gulf region (Source: Beni et al., 2021)

2.1.2 Geography and Geology of the Arabian Peninsula

The bulk of Arabian Peninsula consists of two main geomorphological areas: the Arabian shield in the west; and sedimentary areas (Figure 2.3) dipping away from the shield to the northeast, east, and southeast into the great basin consisting of lower Iraq, the Persian Gulf, and the eastern part of the Rub ‘ al-Khali desert (Chapman, 1978). The eastern edge of the shield curves eastward from the head of the Gulf of Aqaba, a northern extension of the Red Sea, to a point midway across the peninsula and then trends southwestward and southward to the Yemeni highlands. Extinct volcanoes overlies the shield; their eruptions, which ceased seven centuries ago, produced the broad black lava beds that are characteristic of the western Arabian landscape (Rentz and Nijim, n.d.).

Different seasonal winds blow over the Arabian Gulf region. The Shamal wind is the most prolonged and intensive one to blow near the surface and transports around 90 million tons of dust per year into the Gulf region, mainly from the deserts of the Arabian Peninsula, Iraq and Syria (Prakash et al., 2015). The wind occurs in the region during winter and summer. The activity in summer reaches its maximum in June and July (Prospero et al., 2002) while in winter it is more active in November and March (Thoppil and Hogan, 2010).

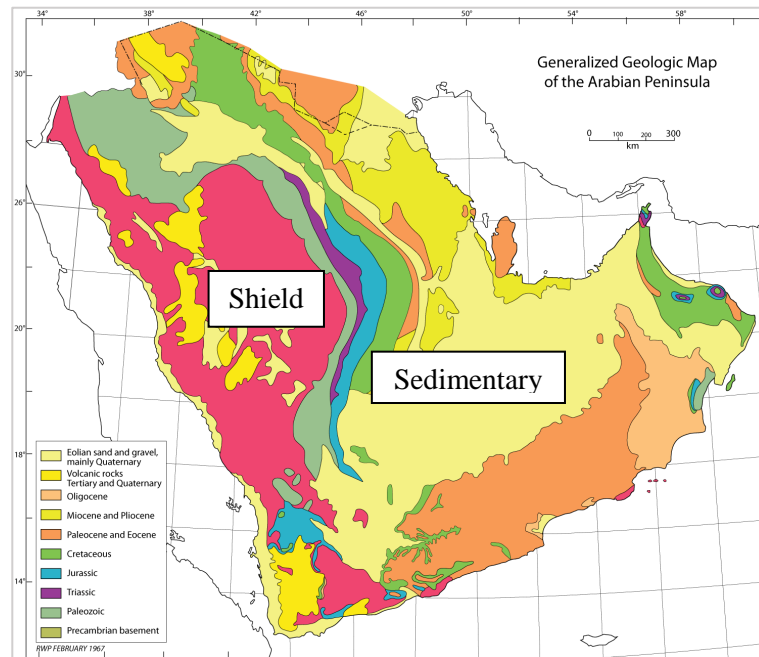


Figure 2. 3: Geological map of Arabian Gulf Peninsula (Source: Powers, 2010)

2.1.3 Geography and Geology of the Arabian Gulf

The Arabian Gulf region lies in a subtropical, hyper-arid zone that is generally characterized by high temperatures and low precipitation. The average annual temperature and rainfall in the region varies significantly and is largely dependent on geography and orography. The average annual rainfall on the southern coasts and over the Gulf is less than 100 mm while the northern watershed areas (Iran and Iraq) receive, on average, 355 mm of precipitation annually (World Bank Group, 2019). Air temperature in lowland areas of the Arabian Gulf region can exceed 50°C during summer (June to August), where the average monthly temperature in summer is > 32°C. The low-lying areas of the Arabian Gulf region experience mild temperatures during winters and the most precipitation is received from November to March in the whole area. Sea surface temperatures can exceed 35°C in summer (Figure 2.4), while in winter they can fall to <10°C (Vaughan et al., 2019). Water loss through evaporation (high temperatures and strong winds) exceeds the net freshwater input and increases the salinity of the water body to more than 39 g/L in most parts of the Gulf (Kampf and Sadrinasab, 2006) and even up to 70 to 80 g/L on the southern coast of the Gulf namely in coastal waters of Bahrain (Sheppard et al., 2010).

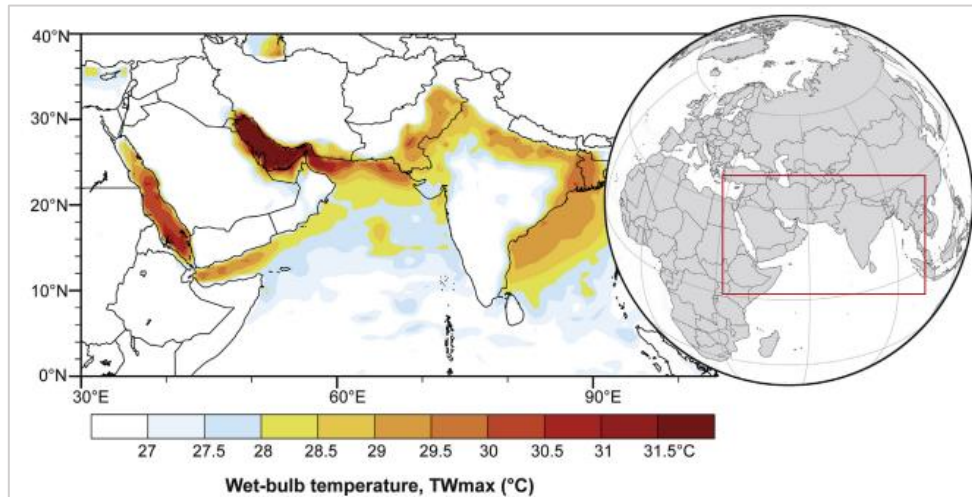


Figure 2. 4 : Spatial distribution of highest daily maximum wet-bulb temperature, in the modern record (1979–2015). (Source: Im et al., 2017)

The average depth of the Arabian Gulf basin is around 35 m; the bathymetry increases eastward with a depth of >110 m at the Strait of Hormuz (Reynolds, 1993). The bathymetry of the basin is complex. More than 60 islands exist in this Gulf. Their origin is mostly related to regional geological structures. Moreover, salt domes, the accumulation of sediments in shallow waters, and coral reefs construct other island types (Ross et al., 1986). The existence of these islands, along with the complicated bottom topography of the gulf, limits maritime routes to just a few narrow waterways, closer to the Iranian coast.

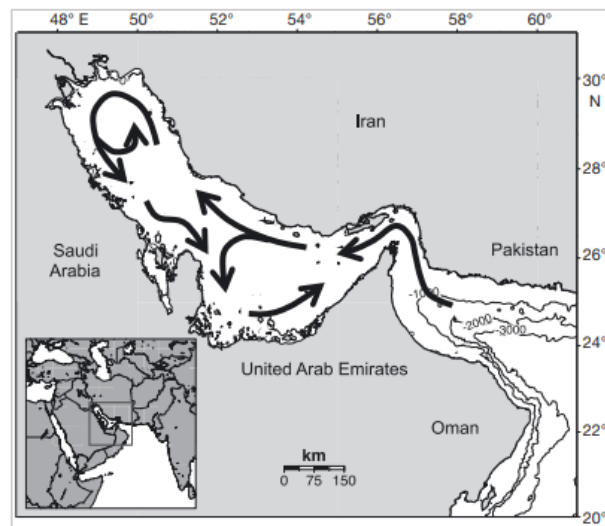


Figure 2 .5 : Predominant surface water circulation patterns in the Arabian Gulf. (Source: Kämpf & Sadrinasab, 2005)

The Arabian Gulf is a meso-tidal water body with maximum tidal range of more than 3.5 m in the northwest flank of the Gulf (Najafi and Noye, 1997). Predominant currents in the

Gulf generally move counterclockwise (Figure 2.5), and prevailing winds over long-term were from the north and northwest (Kampf and Sadrinasab, 2006). The water residence time in the Gulf is around 2–5 years (Reynolds, 1993).

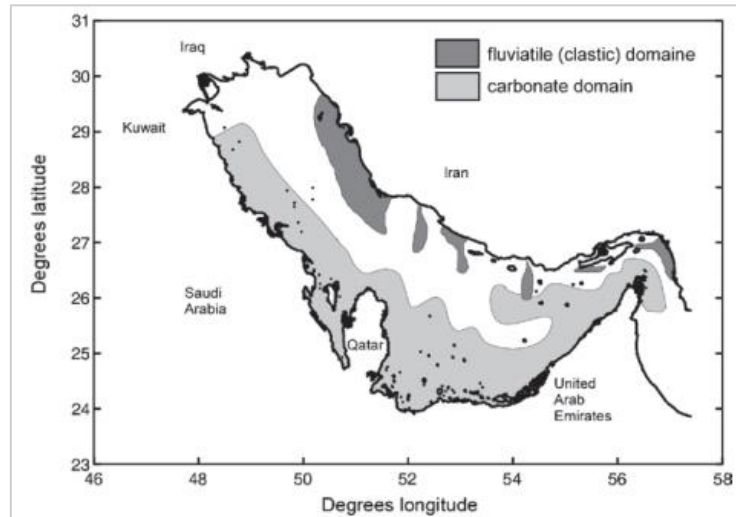


Figure 2 .6 : Major sedimentary domains of The Gulf. (Source: Combined from Diester-Haas 1973; Uchupi et al. 1999)

The Gulf is separated into two major sedimentary realms: a northern, Iranian, domain strongly influenced by fluviatile sedimentation, and a southern, Arabian, carbonate domain of mainly autochthonous, pure carbonates with aeolian-derived siliciclastic admixture (Figure 2.6; Diester-Haas 1973; Uchupi et al. 1999).

2.1.4 Geology of Qatar

Qatar is a peninsula with an approximate area of 11610 km² (Smyth et al., 2016). The topography of the country in general is a deflation surface shaped by the persistent Shamal wind except for some low hills in the North West. The geological map of Qatar is shown in Figure 2.7.

Generally, the surface topography has been described as low relief ranging from around 103m above sea level in the southwest to nearly 6m below sea level in Dukhan sabkha (Sadooni, 2014). Though, most of the country is less than 40m above sea level. A remarkably uniform limestone beds underlie the larger part of Qatar, as thus it contrast with the rest of the southern coast of the Gulf (Figure 2.4). In some places the limestone is overlain by younger strata, which form numerous mesa-type hills (Rivers et al., 2019). The oldest exposed rocks are the Lower Eocene Rus Formation that made up of dolomite, limestone and some scattered outcrops of Miocene that cover around 8% of the total area of the country.

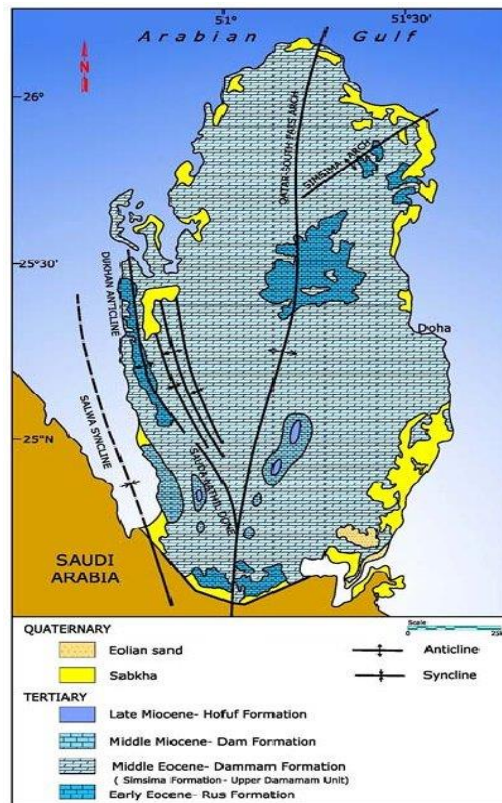


Figure 2.7 : Geological map of Qatar (Source: Cavalier, 1970)

Many studies were classified the physiographic features of Qatar; however (Ashour, 1987) performed the most comprehensive one. He classified Qatar's physiographic features into eight groups as following:

1. Sand accumulation (Nebkhas, Sand dunes and Sand sheets)
2. Duricrusts
3. Coastal sediments (Subtidal zone and Intertidal flats)
4. Dohool (Krust features)
5. Sabkhas (Dukhan Sabkha and Umm Saied Sabkha)
6. Fluvial sediments
7. Hamada Plain sediments
8. Depression soil (Rauda)

2.1.4.1 Qatar Coast

2.1.4.1.1 Coastal system

The coastlines and marine systems of Qatar contain a mosaic of biologically important and interconnected ecosystems. Coral reefs, mangrove forests and seagrasses are among Qatar's most well-known ecosystems (Figure 2.8, Burt et al., 2017) but sabkha (i.e., salt flats), mud-flats, and beaches serve important, though underappreciated, ecological roles as well (Burt, 2014).

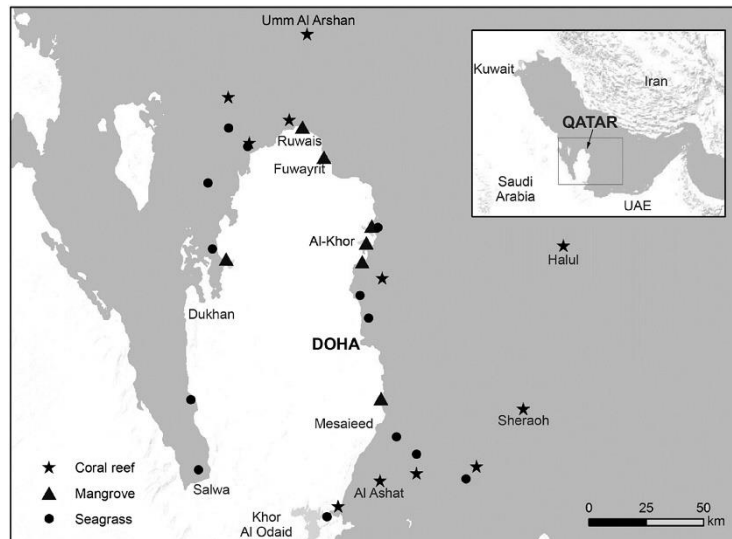


Figure 2 .8 : Location of major coral reef, mangrove, and seagrass ecosystems in coastal and marine systems of Qatar (Source: Burt et al., 2017)

2.1.4.1.2 Coastal sediment

Coastal sediments are associated with the shallow marine environment and resulted from the combined effect of accumulation and erosion (Figure 2.9) (Sadooni, 2014), and can be divided into two groups (Intertidal flats and Subtidal zone). The intertidal flats represent the area that covered by seawater during high tide and exposed during the low tide. They range in width from few meters to several kilometers depending on the tidal range and local topography. They are characterized by the presence of microbial mats and mangrove stands. The sediments are formed of carbonate sand, silt and mud of either chemical or biochemical origin (Rushdi et al., 2017). While the area of the marine environment that covered with water all the time represent the subtidal zone. This area formed mainly of silt and clay-sized carbonate sediments with skeletal grains such as shell fragments and coral debris with nonskeletal grains such as ooliths and pellets (Kureishy and Ahmad, 1994).



Figure 2 .9 : Coastal sediment in Qatar (Source: Sadooni, 2014)

2.2 Total Petroleum and Polycyclic Aromatic Hydrocarbons (TPHs and PAHs)

2.2.1 Total Petroleum Hydrocarbons (TPHs)

The most common group of persistent organic contaminants is the TPHs (Huang et al., 2005). They can be divided into two categories, short chain alkanes (C₆-C₁₀) which represent gasoline range organics (GRO), and long-chain alkanes (C₁₀-C₄₀) which represent diesel range organics (DRO) (Vazquez-Duhalt & Quintero-Ramirez, 2004, p. 447). Relatively high hydrophobicity of petroleum hydrocarbons results in a considerable increase of their ability to accumulate in soil and sediment in comparison to water (Karthikeyan et al., 2001).

2.2.1.1 Sources of TPHs

Total Petroleum Hydrocarbons can come into the environment from many sources. The sources include refineries, oil spill sites, waste disposal pits, petrochemical sites and storage areas (Vazquez-Duhalt & Quintero-Ramirez, 2004, p. 447).

2.2.1.2 Routes of human exposure

Human can be exposed to TPHs from many sources. At the pump via gasoline fumes, on the pavement, by split oil, at home or work they can be exposed to chemicals (Kuppusamy et al., 2020). People working in petroleum production industries could have high exposure levels of TPHs by polluted air inhalation or body contact.

Todd et al. (1999) stated that underground water could be poisoned by TPHs when leakage of underground oil storage tank occurs. Also, he found that air can be accidentally contaminated by TPHs when these compounds get evaporated from the oil spill or leakage. Contaminated soil and sediments are considered to be as a source of exposure.

2.2.1.3 Transport and Fate in marine environment

When petroleum hydrocarbons released into the water environment, they have the affinity to float on the water surface and form a thin surface layer, while the heavier fractions have a tendency to accumulate in the bottom sediment. Petroleum hydrocarbons interact with numerous biotic and abiotic factors such as physical factors and microorganisms. The concentration of petroleum hydrocarbons at contaminated sites can be reduced by biotic processes which includes biodegradation and naturally occurring processes such as spreading, evaporation, dispersion, sinking, dissolution, emulsification and photo-oxidation (Al-Majed et al., 2012; Souza et al., 2014). The biodegradation rate of petroleum hydrocarbons is influenced by temperature, oxygen level, and number of rings in aromatic hydrocarbons (Wang et al., 1998). Evaporation is considered to be the fastest process in removing volatiles during

massive spill which is influenced by physical parameters such as temperature, wind velocity, water turbulence or surface characteristics (Fingas 1998; Payne et al. 1991). In the water column of aquatic ecosystem, the distribution of petroleum hydrocarbons depends on their viscosity and density (Wang et al., 2005).

There are two general pathways for migration of petroleum products through the soil. It can migrate in soil by the gravity and action of the capillary as bulk oil, whereas in water and air, petroleum products migrate as individual compounds. Eastcott et al. (1989) stated that the flow of bulk oil lead to low separation process of product mixture to individual compounds, and usually the dissolution speed is slower than the infiltration rate. Many compounds are hydrophobic so that it can migrate along with the bulk oil flow. Soil moisture content, vegetation, terrain, climate, soil particle size, and oil viscosity were considered to be the main factors that affect the bulk oil infiltration speed (Zhang et al., 2020).

When bulk oil migrates through the soil column, little product mass quantity is retained by soil particles, these small products called “residual saturation.” These products can potentially reside in the land for years depending on the bulk oil persistence (Dragun, 1988). Todd et al. (1999) illustrate that if the quantity of soil is greater than the number of contaminants, these contaminants are transformed to ‘residual saturation’ compounds and downward migration of the contaminant stops before reaching groundwater site. However, negative impacts to groundwater may occur when rainwater enhances the movement of these contaminants downwards to the underground water table.

2.2.1.4 Human Health Effects

Inhalation exposure of short aliphatic hydrocarbons fraction (C₆-C₁₅) have been studied on humans and rats (Zahlsen et al., 1992). These studies found that these fractions are easily absorbed in the lungs and is distributed, which then accumulates in fatty tissues where the rate of elimination from these tissues is slow. Also, they examined that the speed of metabolism of short aliphatic hydrocarbons is slower than the aromatic hydrocarbons. Other researchers found that the rate of absorption of inhaled aliphatic hydrocarbons in rats declined as the carbon number increases (Richard et al., 2015).

Dietary exposure of long aliphatic hydrocarbons fraction (C₁₆-C₄₀) were studied in animals. These fractions were found to have a low rate of absorption and were found to be distributed into the liver and fatty tissues producing fatty acids or triglycerides that metabolised at a slow rate and were eliminated into the faeces gradually by bile or were excreted as urinary

metabolites. These aliphatic hydrocarbons fraction have a low rate of metabolism according to the presence of lipogranulomata in human liver and spleen tissue which composed of lipids that cover them by lymphocytes and macrophages after dietary exposure (Todd et al., 1999). In general, hepatotoxicity is the main toxic endpoint for TPHs (Turczynowicz, 2003). Some TPH compounds can affect the central nervous system causing headaches and dizziness at high levels in the air; others can cause a nerve disorder called "peripheral neuropathy" consisting of numbness in the feet and legs (ATSDR, 2014).

2.2.1.5 Metabolism

Short aliphatic hydrocarbons fractions are metabolised by an oxidation process to alcohols and fatty acids catalysed by cytochrome P-450 isozymes (Moorthy et al., 2019; Miller et al., 1996). Many evidence sources from metabolism studies of this fraction in humans or animals have established that the rate of metabolism is slow (Nzila, 2019; Pedersen et al., 1984). Zahlsten et al. (1992) studied the metabolism of short-chain hydrocarbons in rats after inhalation exposure, and observed that the rate of metabolism of this fraction was slower than aromatic hydrocarbons. In animals or humans, the long aliphatic hydrocarbons fractions were found to be slowly metabolised.

In monkeys, two days after intramuscular injection of a mineral oil emulsion with a radiolabeled C₁₆ hydrocarbon, substantial portions (30-90s) of radioactivity in various tissues were noted as unmetabolised n-hexadecane. Free fatty acids, sterol esters, phospholipids and triglycerides constitute radioactivity residue. In water-soluble fractions, the absence of radioactivity occurs (Todd et al., 1999). Regarding the slow metabolism of aliphatic hydrocarbons in this fraction, lipogranulomata in human autopsies and the widespread dietary exposure to mineral oils and waxes are existing (Wanless & Geddie, 1985).

2.2.1.6 Removal from Environment

Organic compounds found in many natural sources can be degraded by indigenous microbes (Das & Chandran, 2011). Microbes in the biodegradation process get their energy by using the organic contaminants. Regardless of other processes which diffuse environmental pollutants, biodegradation process helps in removing these contaminants without moving them to other media. Production of CO₂, H₂O, and microbial biomass are the final products of microbial degradation (Todd et al., 1999).

The chemical composition of the released product and site-specific environmental parameters are the main factors affecting the rate of hydrocarbon degradation. In general, the highly branched aliphatic compounds have lower degradation than the straight chain hydrocarbons and aromatics hydrocarbons (Das & Chandran, 2011). The C₁-C₄ hydrocarbons ranges are slightly biodegradable by a variety of specialised hydrocarbon degraders, and the C₅-C₉ hydrocarbons range are biodegradable at low concentrations by some microorganisms. The most degradable hydrocarbons are in the C₁₀-C₂₂ range (Todd et al., 1999).

The rate of biodegradation can be affected by environmental factors, including pH, oxygen, moisture, nutrient levels and microbiota. Oxygen is considered to be the main factor for oil biodegradation. The degradation of petroleum hydrocarbons by anaerobic decomposition is low (Frankenberger, 1992). Effective biodegradation occurs in a pH ranged from 6 to 8. Dragun (1988) found that optimal pH is slightly alkaline for most of the species.

The level of moisture in polluted soil or sediment has an effect on the oil biodegradation because of the remaining compounds dissolution and microbial metabolism activity. It also has effects on the locomotion of microbes, dispersion of solute and metabolic by-products elimination. High-level of moisture can inhibit the exchange of oxygen gas which plays an important role in petroleum hydrocarbons decomposition (Todd et al., 1999).

Temperature can affect most of the biological transformations. In general, there is a positive correlation between temperature and biological activity, which reach equilibrium when denaturation of enzymes occurred. Soil temperature, especially at the surface increases depending on the amount of oil. The heat capacity by adsorption of radiation increases as the colour of the oil becomes darker. Frankenberger (1992) mentioned that the best ranges where the effective biodegradation process occur is between 18 °C to 30 °C.

2.2.2 Polycyclic Aromatic Hydrocarbons (PAHs)

Polycyclic aromatic hydrocarbons (PAHs) are defined as a group of aromatic hydrocarbons with two or more single or fused aromatic rings with a pair of carbon atoms shared between rings in their molecules. Regardless of the presence of many PAHs compounds in the environment, the most important and most analyzed PAHs compounds range from 14 to 20 compounds. Small PAHs compounds contain a maximum of six rings, while large PAHs compounds contain more than 6 rings. The small PAHs were mostly detected in most studies

since they are present in many samples (Abdel-Shafy & Mansour, 2016). When no chemical interaction interfered with the PAHs, the adsorption onto particles will mainly depend on physical characteristics, the size of the carrier particle and scavenging processes, including wet and dry deposition (National Research Council, 1983). Figure 2.10 shows the most commonly analyzed PAHs.

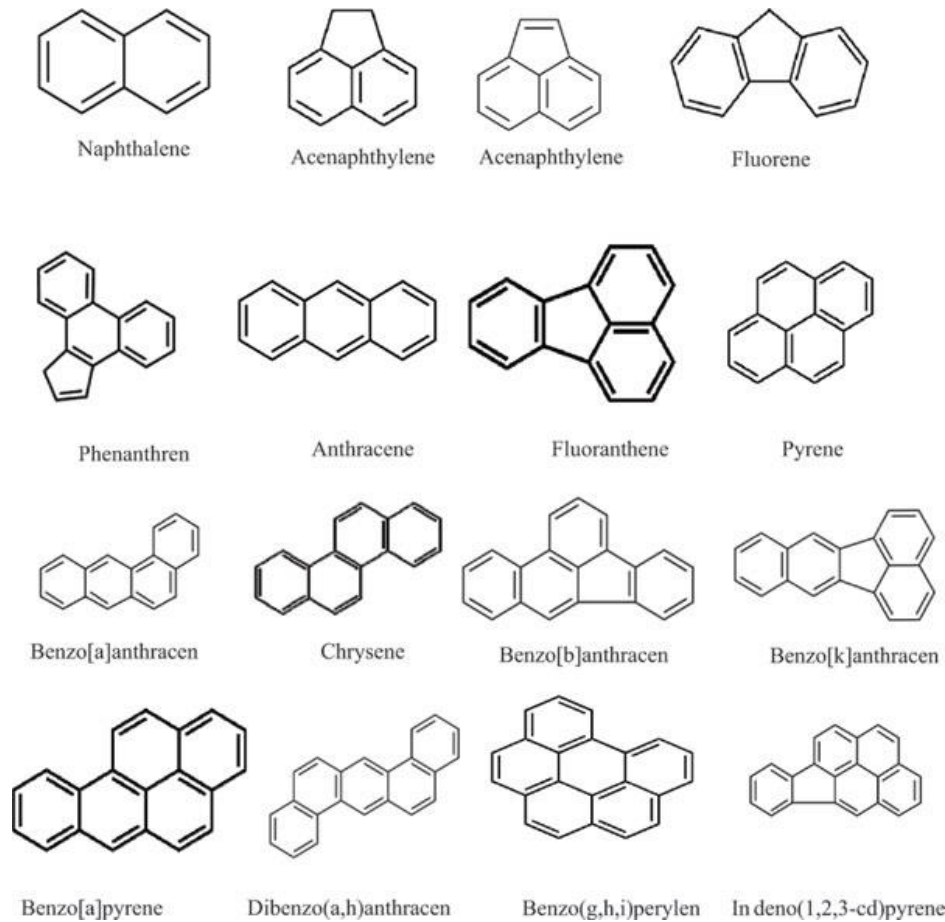


Figure 2. 10: The structures of common PAHs (Source: US EPA)

2.2.2.1 Source of PAHs

The major PAHs sources in the environment are pyrogenic and petrogenic. Pyrogenic PAHs formed from pyrolysis process (temperature range 350°C to more than 1200°C), where organic compounds are exposed to high temperature and low oxygen level. Petrogenic sources of PAHs include manufacturing of crude oil and other related processes. These sources are widely available in the environment because of the many uses of crude oil and their products as well as great transportation of contaminants (Tolosa et al., 1996; WHO, 2003). In general, PAHs can come from natural or anthropogenic sources (Figure 2.11).

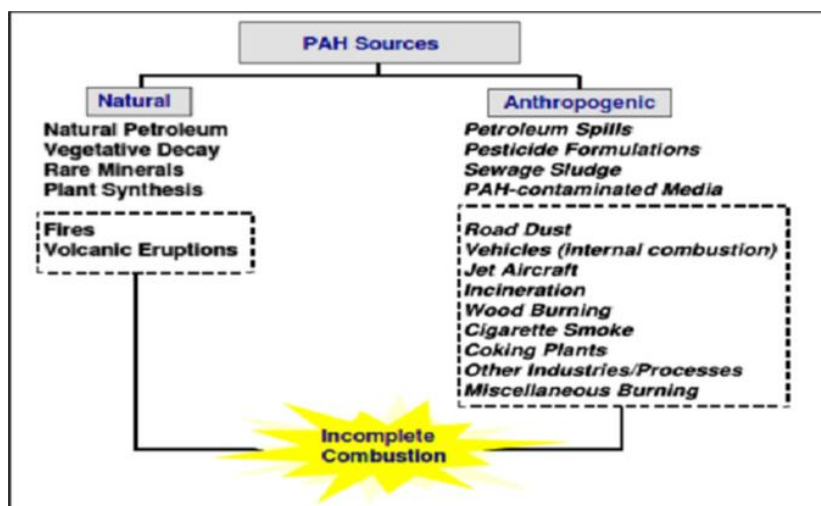


Figure 2. 11: Sources of PAHs from natural and anthropogenic sources (Source: Abdel-Shafy & Mansour, 2016)

2.2.2.2 Routes of Exposure

Inhaling polluted air, ingesting polluted food and cigarettes smoking are considered to be the main route of PAHs exposure (ACGIH, 2005). Creation or absorption of PAHs contaminants from the environment can occur in various crops including wheat, lentils and rye. Oil spills in the marine environment, industrial effluents and soil leaching processes are the main routes that can contaminate water resources (Pichtel, 2016). Ciecierska et al., (2013) mentioned that airborne fallout is the primary route of PAHs contamination in soil.

2.2.2.3 Transport and Fate

Figure 2.12 represents the transportation of PAHs compounds from air to land and marine environment (Hussain et al., 2018). PAHs compounds can transport in the environment by addition, dispersion and degradation processes. Humans are exposed to PAHs through inhaling, ingesting, and direct contact of these contaminants (Abdel-Shafy & Mansour, 2016).

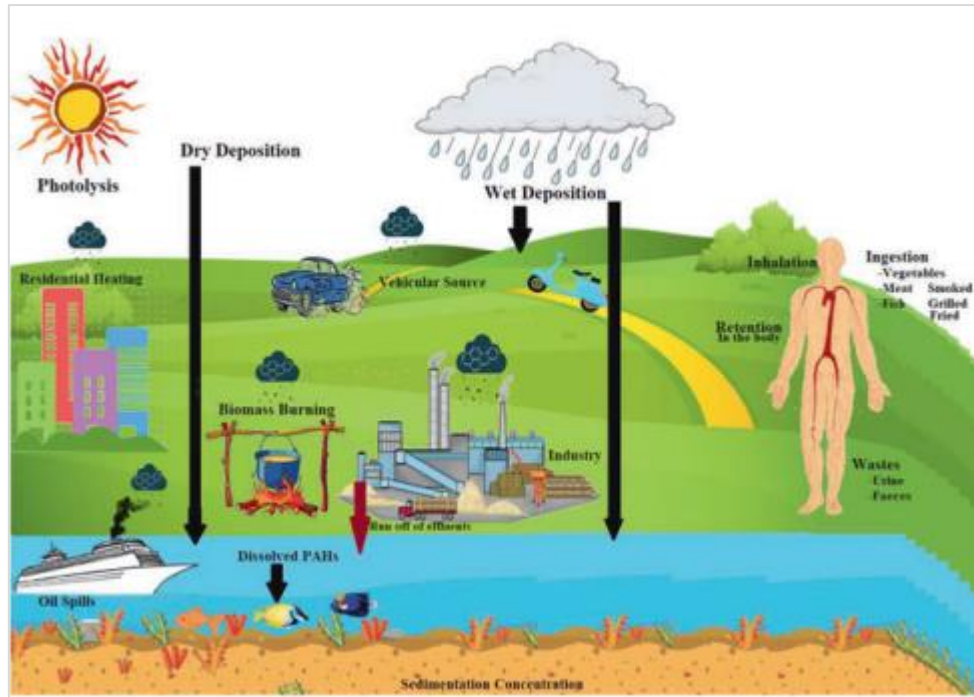


Figure 2. 12: PAHs distribution in the environments (Source: Hussain et al., 2018).

2.2.2.4 Human Health Effects

Humans are commonly exposed to 16 PAH compounds which can cause various negative health effects. The diffusion and the toxicological impact of PAHs are the main concerns for the monitoring of these compounds in the environment. The International Agency for Research on Cancer grouped the PAHs compounds according to the carcinogenic effects (IARC, 2010). The benzo[a]pyrene grouped in the first cluster as the most carcinogenic PAH compound (G1). Five PAHs compounds are clustered as group 2B including naphthalene, chrysene, benzo[a] anthracene, benzo[k]fluoranthene and benzo[b]fluoranthene (IARC, 2010). The most significant endpoint of PAH toxicity is cancer. Cancers in the lungs are the main disease that is caused by the direct inhalation of PAHs from the polluted air (Kim et al., 2013).

Table 2. 1: Cancer classification of individual polycyclic aromatic hydrocarbons (VDH, 2012)

Polycyclic aromatic hydrocarbon	Cancer Classification		
	DHHS*	EPA*	IARC*
Flouranthene		D	3
Benzo (a) pyrene	2	B2	1
Indeno(1,2,3-cd) pyrene	2	B2	2B
Dibenz(a,h) anthracene	2	B2	2A
Benzo (ghi) perylene		D	3

*DHHS: Department of Health and Human Services, EPA: Environmental Protection Agency, IARC: International Agency for Research on Cancer. (2=Reasonably anticipated to be a carcinogen. D=Not classified as to human carcinogenicity. B2=Probable human carcinogen (inadequate human, sufficient animal studies). 3=Not Classifiable. 2B=Possibly carcinogenic to humans (limited human evidence; less than sufficient evidence in animals). 2A=Probably carcinogenic to humans (limited human evidence; sufficient evidence in animals).

There are sufficient evidences that the benzo (a) pyrene, indeno(1,2,3-cd) pyrene and dibenz(a,h) anthracene are carcinogenic to experimental animals (IARC, 2010). Table 2.1 shows the cancer classification of PAHs compounds by different institutions. The Department of Health and Human Services (DHHS) classified the three earlier compounds as reasonably anticipated to be a carcinogen. Moreover, the Environmental Protection Agency (EPA) classified them as probable human carcinogen compounds. The toxicity of common PAHs based on lab experiments presented in Table 2.2.

Table 2. 2: Toxicity of some PAHs based on lab experiments

PAHs	Dose	Organism	Toxicity	Reference
Flouranthene	1500 mg /kg BW/day at the 90day time point.	rats	affects specific hematological parameters and kidneys	(Knuckles et al., 2004)
	1.27 μ mol at 26 weeks	new-born male and female mice	incidence of lung tumours	(Busby et al., 1989)
Benzo (a) pyrene	3, 10, 30, and 90 mg/kg BW/day	rats	immunotoxicity	(DeJong et al. (1999)
	200 μ g for 25 weeks	mice	Cancer-skin tumours	(Shimizu et al., 2000)
Indeno(1,2,3-cd) pyrene	0.1-5 mg/kg	Carassius auratus fish	Induce EROD and GST activity	(Lu et al., 2009)
	4.0 μ mol [1105 μ g] for 20 weeks	Female mice	papillomas	(Rice et al. 1990)
Dibenz(a,h) anthracene	0.06mg (8-32 weeks)	new born mice	Induce Multiple tumors of the lung, subcutaneous fibrosarcomas, leukemias, sebaceous-gland adenomas, and hepatomas	(Kelly & O'Gara, 1961)
	83.5 μ g/100 μ l acetone (24 weeks)	Female NMRI mice	Skin tumours	(Platt et al., 1990)
Benzo (ghi) perylene	0.1-10mg/kg	Carassius auratus fish	Induce EROD activity	(Lu et al., 2009)
	1-10mg/kg		Induce GST activity	

2.2.2.4.1 Short-term health effects (acute)

The route and length of exposure, the level of PAHs, and the toxicity of PAHs congeners are the main factors influencing the human health effect (ACGIH, 2005). Also, other factors like human age and health history can induce health impacts. Unwin et al. (2006) examined the effects of high-level PAHs indoor exposures; the resulting effects include eye irritation, nausea, vomiting, diarrhea and confusion. However, they could not have examined exactly which PAH individually caused these symptoms. Other symptoms caused by PAHs include skin irritation and inflammation. The IPCS (2010) reported that two PAHs individuals (anthracene and benzo(a)pyrene) might influence the skin allergic reaction in animals and humans.

2.2.2.4.2 Long-term health effects (chronic)

A decline in the immune system, inhalation difficulties, kidney, lung and liver failure are the main negative impacts from long-term PAHs exposure. Continuous direct contact of skin with PAHs compounds can cause redness and inflammation symptoms. High-level of naphthalene compound inhalation can induce the red blood cells to break down. In general, the route of exposure to PAHs contaminants is the main factor that can control the occurrence of health effects (Bach et al., 2003, Diggs et al., 2011 & Olsson et al., 2010).

2.2.2.5 Metabolism

In general, PAHs are metabolized by cytochrome P450 (CYPs) and other metabolic enzymes into phenols, catechols, and quinones, resulting in the formation of diol-epoxides, radical cations, or reactive and redox-active o-quinones, which may all react with DNA to produce DNA adducts (Moorthy et al., 2015). Figure 2.13 illustrated the major pathways involved in the metabolism of PAHs by bacteria, fungi and algae (Mueller et al., 1996). The mechanisms of PAHs to cause lung cancer is well described in Figure 2.14.

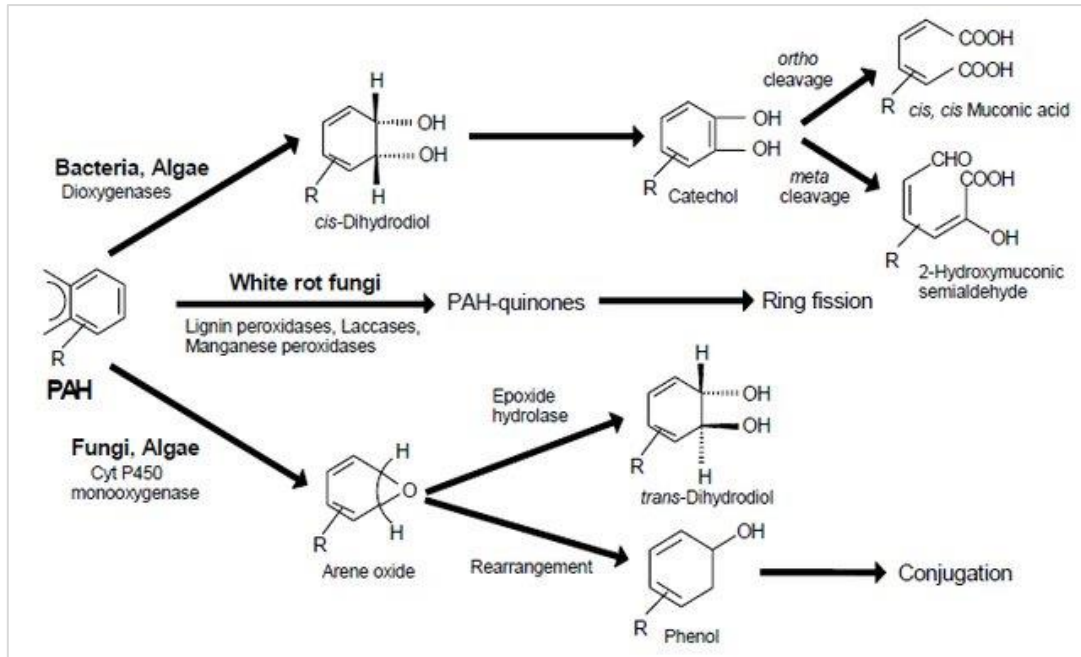


Figure 2. 13: Major pathways involved in the metabolism of PAHs by bacteria, fungi and algae (Mueller et al., 1996).

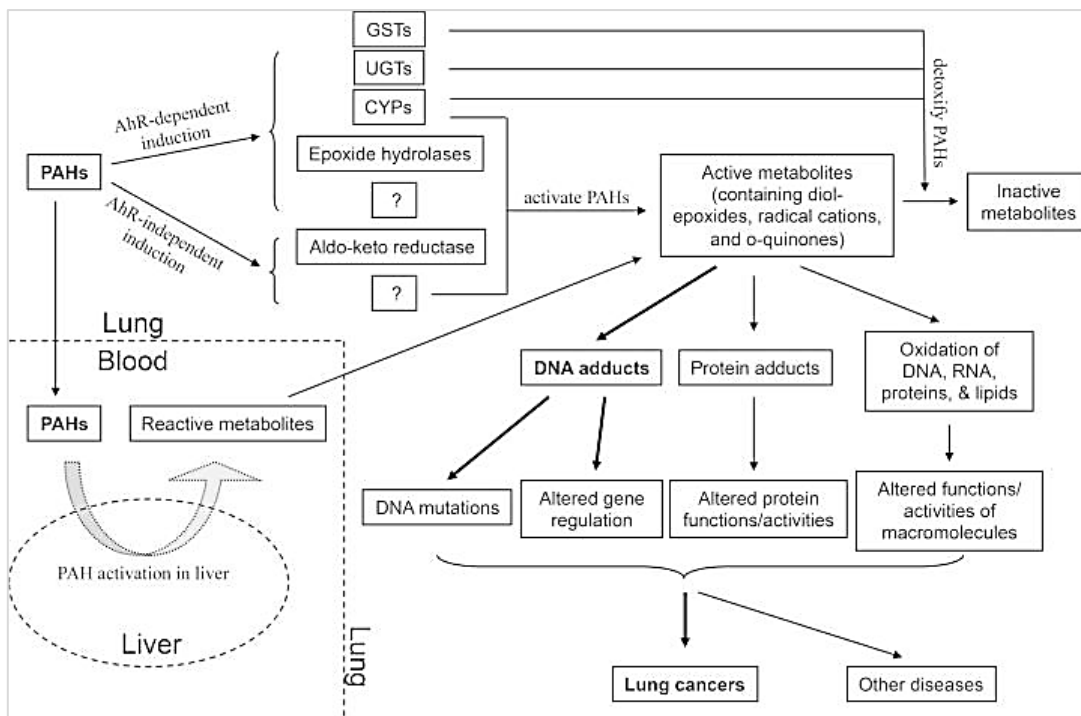


Figure 2. 14: Multiple mechanisms by which PAHs cause lung cancer (Moorthy et al., 2015).

2.2.2.6 Removal from the Environment

The PAHs are eliminated from the environment through several ways including biodegradation, photolysis degradation and chemical degradation (Abdel-Shafy et al., 2014 & Perera et al., 2011). Most of the studies discussed the biodegradation process, and a few talked about the other types of degradation (photolysis or chemical degradations) (Nadarajah et al., 2002).

Most of the earlier studies on the biodegradation of PAHs concentrated on aerobic degradation, although some demonstrate other conditions (Haritash & Mater, 2009 & Peng et al., 2008). PAHs tend to be bioavailable in two phases (vapour and aqueous). The solubility factor of the PAHs influences their bioavailability, and this factor depends on the molecular mass of these compounds (Thorsen et al., 2004 & Chen and Aiken, 1999). Competitive inhibition can affect the degradation process of PAHs, i.e. the active sites of the enzymes are nonspecific.

The other type of PAHs removal is photolysis degradation, which involves the absorption of light (Manahan, 1994). Electrons within the molecules excited by light and convert the molecular structure to unstable arrangement causing various processes within the compound (physical and chemical processes). Like biodegradation, the photolysis process works effectively when the PAHs are in vapour or aqueous phases (Finlayson-Pitts Jr., Pitts, 1997). As the particle surface area of the compound increases, the effectiveness of photolysis reaction increases. Moreover, low molecular weight PAHs compounds (e.g. Naphthalene) have high photolysis degradation, since they have high bioavailability (Korfmacher et al., 1980).

The last, and less available PAHs removal is by chemical degradation. This process is affected by many properties including structure and molecular weight, temperature and the oxidising agent efficiency (Abdel-Shafy and Mansour, 2016). Chemical treatment has been found to be effective degradation process for removing PAHs from surface water (Abdel-Shafy et al., 2014). In polluted soil, removal of PAHs by UV irradiation and TiO₂ or ZnO catalysis found to be an ideal degradation process (Zhang et al., 2016).

2.2.3 Distribution of TPHs and PAHs

2.2.3.1 Distribution of TPHs and PAHs worldwide

Most of the global studies and projects concentrate more on measuring the level of PAHs rather than the level of TPHs in abiotic and biotic matrices as summarized in Table 2.3, which shows the TPHs and Σ PAHs reported in seawater, sediment and oyster samples from various locations in the world. [Keshavarzifard et al. \(2017\)](#) studied the PAHs in sediments from the northern Persian Gulf and reported a concentration of (12.8- 81.25 $\mu\text{g}/\text{kg}$). Many other authors reported a high-level of PAHs in marine sediment from different countries, Italy (112000 $\mu\text{g}/\text{kg}$, [Fabbri, 2003](#)), UK (4171- 79648 $\mu\text{g}/\text{kg}$, [Brettell, 2013](#), 626- 3766 $\mu\text{g}/\text{kg}$, [Vane et al., 2007](#)), and USA (487-718360 $\mu\text{g}/\text{kg}$, [Shiaris & Sweet, 1986](#)). Based on the publications selected, the overall ranges for PAHs in surface sediment and marine sediment is 11.54-1825.35 $\mu\text{g}/\text{kg}$, and 12.8- 718360 $\mu\text{g}/\text{kg}$ respectively, excluding one study from New York surface sediment that showed high level (152088 $\mu\text{g}/\text{kg}$). In general, seawater has lower levels of contaminants than sediment and biota. The overall range of PAHs in seawater from the selected publications is (0.0007- 758 $\mu\text{g}/\text{L}$). Levels of PAHs in oysters reported worldwide ranged from (26- 1700 $\mu\text{g}/\text{kg}$); high level was reported in 2005 from San Francisco estuary (184–6899 $\mu\text{g}/\text{kg}$).

The level of TPHs in surface sediment and marine sediment based on the selected publications is higher than PAHs. The overall range of TPHs in surface sediment is 5290- 616000 $\mu\text{g}/\text{kg}$, while in marine sediment is 5000-971500 $\mu\text{g}/\text{kg}$. The range of TPHs in seawater reported worldwide is 1.5- 7310 $\mu\text{g}/\text{L}$. Few studies reported the concentration of TPHs in oyster. Two studies from Nigeria and Malaysia reported high level of TPHs of 6370-8440 $\mu\text{g}/\text{kg}$ and 56661-262515 $\mu\text{g}/\text{kg}$ respectively.

Flouranthene, benzo (a) pyrene, indeno(1,2,3-cd) pyrene, dibenz(a,h) anthracene, and benzo (ghi) perylene are present as a component of the total content of polycyclic aromatic hydrocarbons in the environment. Smoking, inhalation of polluted air and by ingestion of food and water contaminated by combustion effluents are the main human exposure sources of PAHs ([IARC, 2010](#)). Table 2.4 displays levels of these compounds examined in different matrixes all over the world.

Table 2. 3: Concentrations of TPHs and PAHs in abiotic and biotic matrices from different locations in the world

Location	Matrices	Concentrations Reported	Reference
China	Seawater	Σ PAHs (0.03- 0.75 μ g/L)	(Hong et al., 2016)
	Oyster	Σ PAHs (33.1-125 μ g/kg w wt.)	
	Surface sediment	Σ PAHs (37.2-206.6 μ g/kg dry wt.)	(Qian et al., 2016)
	Seawater	Σ PAHs (mean 0.35 μ g/L)	(Xiang et al., 2018)
	Surface sediment	Σ PAHs (13.59-166.5 μ g/kg dry wt.)	(Zhang et al., 2016)
	Seawater	TPHs (20-508 μ g/L)	(Li et al., 2010)
	Surface sediment	TPHs (6300–535000 μ g/kg dry wt.)	(Zhou et al., 2014)
Korea	Seawater	TPHs (1.5 to 7310 μ g/L)	(Kim et al., 2013)
Northern Persian Gulf	Marine Sediments	Σ PAHs (12.8- 81.25 μ g/kg dry wt.)	(Keshavarzifard et al., 2017)
England	Surface sediment	Σ PAHs (464-1014 μ g/kg dry wt.)	(Woodhead et al., 1999)
Sochi, Black Sea, Russia	Marine Sediments	Σ PAHs (61.2– 368 μ g/kg dry wt.)	(Readman et al., 2002)
Pialassa, Baiona, Ravenna, Italy	Marine Sediments	Σ PAHs (112000 μ g/kg dry wt.)	(Fabbri, 2003)
The Humber Estuary, UK	Marine Sediments	Σ PAHs (4171- 79648 μ g/kg dry wt.)	(Brettell, 2013)
Boston Harbour, USA	Marine Sediments	Σ PAHs (487– 718360 μ g/kg dry wt.)	(Shiaris and Sweet,1986)
Delaware River Estuary, USA	Surface sediment	TPHs (38000–616000 μ g/kg)	(Kim et al., 2018)
	Surface sediment	Σ PAHs (3749- 22324 μ g/kg)	
Mersey Estuary, United Kingdom	Marine Sediments	Σ PAHs (626- 3766 μ g/kg dry wt.)	(Vane et al., 2007)
Cotonou, Benin, Africa	Marine Sediments	Σ PAHs (80–1411 μ g/kg dry wt.)	(Soclo et al., 2000)
Bosphorus, Black Sea, Turkey	Marine Sediments	Σ PAHs (13.8–531 μ g/kg dry wt.)	(Readman et al., 2002)
Danube Coastline, Black Sea, Ukraine	Marine Sediments	Σ PAHs (30.5–608 μ g/kg dry wt.)	(Readman et al., 2002)
Todos os Santos Bay, Brazil	Surface sediment	Σ PAHs (11.45-1825.35 μ g/kg dry wt)	(Nascimento et al., 2017)
New York	Surface sediment	Σ PAHs (15-152088 μ g/kg dry wt.)	(EPRI, 2008)
Malaysia	Surface sediment	TPHs (5390 μ g/kg)	(Ali et al., 2015)
	Oyster	TPHs (56661- 262515 μ g/kg)	(Vaezzadeh et al., 2017)
Nigeria	Marine sediment	TPHs (5000-232000 μ g/kg)	(Benson, 2009)
	Oyster	TPHs (6370 -8440 μ g/kg)	(Inam et al., 2012)
Saronikos Gulf, Greece	Seawater	Σ PAHs (113-459 μ g/L)	(Valavanidis et al., 2008)
Egypt	Seawater	Σ PAHs (mean 0.047 μ g/L)	(El Nemr and Abd-Allah, 2003)
Atlantic Ocean	Seawater	Σ PAHs (0.0007- 0.001 μ g/L)	(Nizzetto et al., 2008)
Tunisia	Oyster	Σ PAHs (107.4- 430.7 μ g/kg)	(Barhoumi et al., 2016)
San Francisco estuary	Oyster	Σ PAHs (184–6899 μ g/kg)	(Oros and Ross, 2005)
French Atlantic Coast	Oyster	Σ PAHs (81- 236 μ g/kg)	(Acosta et al., 2015)
France	Oyster	Σ PAHs (66 to 961 μ g/kg)	(Ramdine et al., 2012)
Japan	Oyster	Σ PAHs (26- 1700 μ g/kg)	(Nakata et al., 2014)
Iran, Musa Bay	Marine sediment	TPHs (16480- 97150 μ g/kg)	(Tehrani et al., 2016)
Romanian Black Sea	Seawater	TPHs (6- 758 μ g/L)	(Țigănuș et al., 2016)

Table 2. 4: Concentration profile of some PAHs

PAHs	Matrix	location	Concentration	Reference	
Flouranthene	Seawater	North China	Mean 0.00759 µg/L	(Hong et al., 2016)	
		Hainan Island, China	Mean 0.01299 µg/L	(Xiang et al., 2018)	
	Sediment	North China	Mean 100 µg/kg	(Hong et al., 2016)	
		Northeast China	Mean 16 µg/kg	(Qian et al., 2016)	
		Coast of Weihai, China	Mean 43.92 µg/kg	(Zhang et al., 2016)	
	Qatar		Mean 1.1±1.7µg/kg	(Soliman et al.,2014)	
		Kuwait	Mean 48 µg/kg	(Beg et al., 2003)	
	Hainan Island, China		Mean 5.01 µg/kg	(Xiang et al., 2018)	
		Oyster	North China	Mean 1.72 µg/kg	(Hong et al., 2016)
	Benzo (a) pyrene	Seawater	North China	Mean 0.00818 µg/L	(Hong et al., 2016)
Hainan Island, China			Mean 0.000002µg/L	(Xiang et al., 2018)	
North China			Mean 0.00252± 0.00129 µg/L	(Hong et al., 2016)	
Sediment		North China	Mean 71.5 µg/kg	(Hong et al., 2016)	
		Northeast China	Mean 14.1 µg/kg	(Qian et al., 2016)	
		Coast of Weihai, China	Mean 17.21 µg/kg	(Zhang et al., 2016)	
Qatar			Mean 0.6±0.8 µg/kg	(Soliman et al.,2014)	
		Kuwait	Mean 31.20 µg/kg	(Beg et al., 2003)	
Hainan Island, China			Mean 9.84 µg/kg	(Xiang et al., 2018)	
		Oyster	North China	Mean 1.42 µg/kg	(Hong et al., 2016)
Indeno(1,2,3-cd) pyrene		Seawater	Hainan Island, China	Mean 0.000005µg/L	(Xiang et al., 2018)
			Spain	Mean0.0681± 0.0947µg/L	(Carrera et al., 2007)
		Sediment	North China	Mean 57.0 µg/kg	(Hong et al., 2016)
			Northeast China	Mean 2.9 µg/kg	(Qian et al., 2016)
	Coast of Weihai, China		Mean 0.66 µg/kg	(Zhang et al., 2016)	
	Qatar		Mean 0.6±0.7µg/kg	(Soliman et al.,2014)	
		Oyster	Mexico	0.65- 6.91 µg/kg	(Barroso et al., 1999)
	Dibenz(a,h) anthracene	Seawater	Hainan Island, China	Mean 0.000006µg/L	(Xiang et al., 2018)
Sediment		North China	Mean 50.0 µg/kg	(Hong et al., 2016)	
		Northeast China	Mean 4.0 µg/kg	(Qian et al., 2016)	
		Coast of Weihai, China	Mean 0.50 µg/kg	(Zhang et al., 2016)	
Qatar			0.2±0.3 µg/kg	(Soliman et al.,2014)	
		Oyster	Mexico	0.34- 6.18 µg/kg	(Barroso et al., 1999)
Benzo (ghi) perylene	Seawater	Spain	0.000157-0.000295 µg/L	(Carrera et al., 2007)	
	Sediment	North China	Mean 68.1 µg/kg	(Hong et al., 2016)	
		Northeast China	Mean 4.1 µg/kg	(Qian et al., 2016)	
		Coast of Weihai, China	Mean 1.24 µg/kg	(Zhang et al., 2016)	
		Qatar	0.8±1.0 µg/kg	(Soliman et al.,2014)	
	Oyster		Mean 4.1 µg/kg	(Qian et al., 2016)	
			3.79- 39.1 µg/kg	(Barroso et al., 1999)	

2.2.3.2 Distribution of TPHs and PAHs in Gulf Countries

In 1992, in the light of the Kuwait oil slick follow warfare in the region, oil pollution in the Arabian Gulf was investigated by measuring TPHs and total organic carbon (TOC) in 77 core samples from the bottom sediments of the Arabian Gulf (Massoud et al., 1996); the TPHs

reported were in the range of (50000–1122000 $\mu\text{g}/\text{kg}$). The total levels of TPHs and PAHs were examined in biota and coastal sediments from Bahrain, UAE, and Oman (Tolosa et al., 2005) (Table 2.5). The ΣPAHs in marine sediment from Bahrain and UAE were (mean, 6600 $\mu\text{g}/\text{kg}$) and (6500-940 $\mu\text{g}/\text{kg}$) respectively. de Mora et al. (2010) examine the levels of TPHs in marine sediment from Bahrain and oyster tissues from Oman (1850000 $\mu\text{g}/\text{kg}$ and 572000 $\mu\text{g}/\text{kg}$ respectively). Five studies reported the levels of PAHs in Kuwait's marine sediment; the concentration range were 12.9-190 $\mu\text{g}/\text{kg}$ (Lyons et al., 2015), 5.65-1333.6 $\mu\text{g}/\text{kg}$ (Beg et al., 2003), 5.65–1333.6 $\mu\text{g}/\text{kg}$ (Bach et al., 2003), 7200 - 80000 $\mu\text{g}/\text{kg}$ (Readman et al., 1996), 10- 910 $\mu\text{g}/\text{kg}$ (Saeed et al., 1996). Levels of TPHs in marine sediments were reported from Saudi Arabia and Kuwait 62000-1400000 $\mu\text{g}/\text{kg}$ (Fowler et al., 1993) and 4200-41000 $\mu\text{g}/\text{kg}$, (Lyons et al., 2015) respectively.

Table 2. 5: Concentrations of TPHs and PAHs in abiotic and biotic matrices from Arabian Gulf countries

Country	Matrices	Concentrations Reported	Reference
Arabian Gulf	Marine Sediments	TPHs (50000–1122000 $\mu\text{g}/\text{kg}$ dry wt.)	(Massoud et al., 1996)
Saudi Arabia	Marine Sediments	TPHs (62000–1400000 $\mu\text{g}/\text{kg}$ dry wt.) TPHs (11000- 6900000 $\mu\text{g}/\text{kg}$ dry wt.) ΣPAHs (1400- 1400000 $\mu\text{g}/\text{kg}$ dry wt.)	(Fowler et al., 1993) (Readman et al., 1996)
Bahrain	Marine Sediments	TPHs (16600- 779000 $\mu\text{g}/\text{kg}$ dry wt.) ΣPAHs (13- 6600 $\mu\text{g}/\text{kg}$ dry wt.) TPHs (mean, 185000 $\mu\text{g}/\text{kg}$ dry wt.)	(Tolosa et al., 2005)
	Pearl oyster	TPHs (38500- 98000 $\mu\text{g}/\text{kg}$ dry wt.), ΣPAHs (58.3- 105 $\mu\text{g}/\text{kg}$ dry wt.) TPHs (22900- 69700 $\mu\text{g}/\text{kg}$ dry wt.) ΣPAHs (8- 24 $\mu\text{g}/\text{kg}$ dry wt.)	(de Mora et al., 2010)
UAE	Marine Sediments	TPHs (19200- 26400 $\mu\text{g}/\text{kg}$ dry wt.) TPHs equiv. (100–16400 $\mu\text{g}/\text{kg}$ dry wt.), ΣPAHs (0.39–9.4 $\mu\text{g}/\text{kg}$ dry wt.)	(Banat et al., 1998) (Tolosa et al., 2005)
	Rock oyster	TPHs equiv. (219000 $\mu\text{g}/\text{kg}$ dry wt.), ΣPAHs (846 $\mu\text{g}/\text{kg}$ dry wt.)	
	Pearl oyster	TPHs (25600- 237000 $\mu\text{g}/\text{kg}$ dry wt.), ΣPAHs (36.6- 251 $\mu\text{g}/\text{kg}$ dry wt.) TPHs (20300- 33900 $\mu\text{g}/\text{kg}$ dry wt.), ΣPAHs (2- 31 $\mu\text{g}/\text{kg}$ dry wt.)	(de Mora et al., 2010)
Oman	Rock oyster	TPHs (37600-632000 $\mu\text{g}/\text{kg}$ dry wt.) ΣPAHs (4- 419 $\mu\text{g}/\text{kg}$ dry wt.)	
	Rock oyster	TPHs (23200- 130000 $\mu\text{g}/\text{kg}$ dry wt.), ΣPAHs (17- 173 $\mu\text{g}/\text{kg}$ dry wt.)	(Tolosa et al., 2005)
Kuwait	Marine Sediments	TPHs (4200–41000 $\mu\text{g}/\text{kg}$ dry wt.) ΣPAHs (12.9–190.1 $\mu\text{g}/\text{kg}$ dry wt.) ΣPAHs (5.65–1333.6 $\mu\text{g}/\text{kg}$ dry wt.) TPHs (6700- 2070000 $\mu\text{g}/\text{kg}$ dry wt.) ΣPAHs (6- 1334 $\mu\text{g}/\text{kg}$ dry wt.) TPHs (40,000-240000 $\mu\text{g}/\text{kg}$ dry wt.) ΣPAHs (7200 - 80000 $\mu\text{g}/\text{kg}$ dry wt.) ΣPAHs (10- 910 $\mu\text{g}/\text{kg}$ dry wt.)	(Lyons et al., 2015) (Bach et al., 2003) (Beg et al., 2003) (Readman et al., 1996) (Saeed et al., 1996)
	Seawater	ΣPAHs (154.89 $\mu\text{g}/\text{L}$)	(Saeed et al., 2011)

2.2.3.3 Distribution of TPHs and PAHs in Qatar

Limited studies are available on the presence of TPHs and PAHs in Qatar's environment. Thus, the first aim of this study is to quantify the levels of TPHs and PAHs surface seawater, surface coastal sediments and pearl oysters tissues from different locations in Qatar.

2.2.3.3.1 TPHs and PAHs in Qatari Sediment

Only two newly published studies in 2017 and older study in 2005 with three ESC-QU Internal Projects in 2009 and 2011 reported the concentration of TPHs in Qatar's marine sediment. While five published studies in (2005, 2010, 2014, 2017 and 2018) reported the concentration of PAHs in Qatari sediment with two ESC-QU Internal Projects (Table 2.6). The range of TPHs measurements found in all studies was between 17.3 to 84000 $\mu\text{g}/\text{kg}$, whereas the range of PAHs measurements found was 0.29 to 1560 $\mu\text{g}/\text{kg}$.

Table 2. 6: Concentrations of TPHs and PAHs in marine sediment from Qatar environment

Organic Pollutant	Concentration ($\mu\text{g}/\text{kg}$ dry wt.)	Reference
TPHs	17.3- 79.3	(Rushdi et al., 2017)
	160- 1700	(Leitão et al., 2017)
	Mean 2530	(ESC internal project, March 2011)
	100- 19400	(ESC internal project, Dec. 2009)
	170- 1230	(ESC internal project, May 2009)
	2200- 84000	(Tolosa et al., 2005)
Σ PAHs	0.6 -1560	(Soliman et al., 2019)
	2.6-1025.1	(Soliman et al., 2014)
	0.3- 7.8	(Rushdi et al., 2017)
	3.15- 14.35	(Hassan et al., 2018)
	0.29- 18.15	(Leitão et al., 2017)
	6.0- 138.6	(de Mora et al., 2010)
	0.55- 92	(Tolosa et al., 2005)
	Mean 2.53	(ESC internal project, March 2011)
	0.75- 18.33	(ESC internal project, May 2009)

2.2.3.3.2 TPHs and PAHs in Qatari Seawater

Only one author examined the level of TPHs and PAHs in Qatar's seawater (Leitão et al., 2017). The TPHs level ranged from 10 to 60 $\mu\text{g}/\text{L}$, and the Σ PAHs ranged from 0.15 to 2.65 $\mu\text{g}/\text{L}$. Regardless of the published studies, there was an internal project in the ESC at Qatar University which measured the levels of TPHs and PAHs in Qatari seawater in 2011. Researchers in this project collected seawater samples from Ras Laffan in the North of Qatar, they found a low level of mean TPHs and PAHs of 10 $\mu\text{g}/\text{L}$ and 0.13 $\mu\text{g}/\text{L}$ respectively.

2.2.3.3.3 TPHs and PAHs in Qatari Oyster (*Pinctada radiata*)

Recently, only one author studied the level of TPHs and PAHs in Qatar's oyster (Leitão et al., 2017). The TPHs level ranged from 2120 to 7410 $\mu\text{g}/\text{kg}$, and the ΣPAHs ranged from 8.08 to 23.13 $\mu\text{g}/\text{kg}$.

2.3 Trace metals

Trace metals are elements that normally occur at very low levels in the environment (Tchounwou et al., 2014). Some of them are considered to be essential in humans, animals and plants to maintain various biochemical and physiological functions. The nutritional requirements of these trace metals which called microelements, including: cobalt (Co), copper (Cu), chromium (Cr), zinc (Zn), nickel (Ni) iron (Fe), manganese (Mn), molybdenum (Mo) and selenium (Se) are generally low (Hejna et al., 2018). These trace elements are present in various matrices in trace concentrations (ppb or ppm) with a different bioavailability (Hambidge, 2003). They are usually added as nutritional additives in animal feed to promote health and to optimize production, though, excessive exposure with higher concentration could represent a source of pollution and has been linked with cellular or systemic disorders (Rossi et al., 2014).

Other metals, such as: arsenic (As), cadmium (Cd) and lead (Pb) have no established biological functions and are considered as contaminants and undesirable substances in animal feed (Hambidge, 2003). Furthermore, these nonessential metals which considered prior hazard to public health, present a high toxicity because they can induce organ damage, even at lower exposure levels (Hejna et al., 2018).

2.3.1 Sources of trace metals

Trace metals can enter the environment via many sources including natural and anthropogenic sources (Kroon et al., 2020). The natural sources include: rocks (soil), volcanic emission, undersea smokers, extra-terrestrial material (Goldberg, 1995). The anthropogenic sources include metal mining, mineral processing, smelting, coal mining, power generation, oil, natural gas production, petroleum utilization, industrial wastes and byproducts, municipal waste incinerators, landfills, sewage sludge disposal, agricultural, households, and fuels (Islam & Tanaka, 2004).

2.3.2 Routes of exposure

The main routes of exposure of trace metals are via inhalation, ingestion or dermal contact (Figure 2.15). Metals emitted into air as dust or fume can be transported to the receptor where they are inhaled and subsequently absorbed, and some can be vaporized and inhaled (Life Sciences Research Reports, 1983). Metals may also be transfer through two or more environmental media and can be ingested involuntarily through food or drink (Al Osman et al., 2019). Uptake of metals can also be absorbed through skin, where mass transfer occurs by diffusion (Islam et al., 2018).

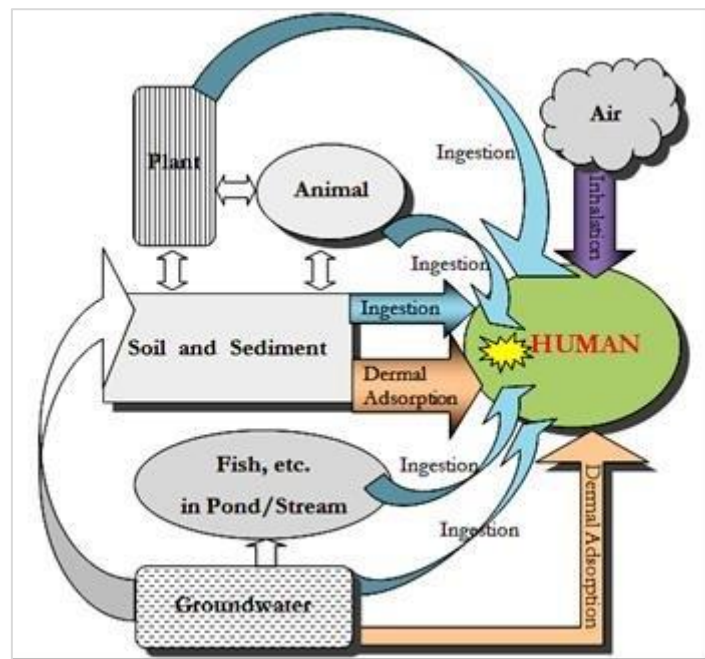


Figure 2. 15: Pathways of metals to humans (Source: Islam et al., 2018)

2.3.3 Transport and fate in the environment

When the metals enter the environment, they may be transported or transformed into other chemicals. Transport can occur within or between compartments (Pachana et al., 2010). Transformation of metals in the environment occurs via several processes such as photodegradation, chemical degradation or biodegradation, which involve ultraviolet, hydrolysis, or bacterial decomposition respectively (Gautam et al., 2016). Another type of transformation that may occur is the Biotransformation where the transformation of heavy metals takes place within organisms (Boonsaner, 2006).

2.3.4 Human Health Effects

Heavy metals are nonbiodegradable, thus they tend to bioaccumulate at various trophic levels through food chain and can cause human health problems (Alvarenga et al., 2009). The cationic forms can cause serious problems to living organisms since they have the capacity to bind with short carbon chains. These forms bioaccumulate in protein-rich tissues of marine organisms and may eventually end up in humans (Hassan et al., 2018). Wang & Shi (2001) found that exposure to certain trace metals can affect cellular components such as cell membrane, mitochondria, etc., and they can interfere with cellular metabolic functions causing harmful side effects (Davis, 1979). Excess exposure to metals, particularly the nutritionally nonessential metals, can produce toxicity or pathological effects on most organ systems (Goyer et al., 2004). Table 2.7 illustrated the toxicity of the six trace metals. The dose required to achieve 50% mortality from toxicity represented in Figure 2.16 based on rat oral values provided in material safety data sheets (MSDSs) for all available metals (Egorova & Ananikov, 2017).

Table 2.7: Toxicity of the selected trace metals

Metal	Toxicity	Reference
Cd	▪ Acute pneumonitis with pulmonary oedema.	(Leonard et al., 2009)
	▪ Acute gastroenteritis	(Gautam et al., 2016)
	▪ Severe chronic effects, predominantly in the lungs and kidneys	(Zhu et al., 2009)
	▪ The most severe from Cd (II) toxicity in humans is "itai- itai", a disease characterized by excruciating pain in the bone	(Loganathan et al., 2008)
Cr	▪ Lung cancer, liver necrosis, brain damage, premature death and kidney problems	(Covington, 1997)
	▪ Mutagenic in bacteria, mutagenic and carcinogenic in humans	(Losi et al., 1994)
	▪ Ingestion of chromium in large doses may cause death in animals and humans	(Loganathan et al., 2008)
Cu	▪ Cellular damage leading to Wilson disease in humans	(ATSDR,2002; Tchounwou et al., 2008)
Ni	▪ lungs, nose and bone cancer	(Tchounwou et al., 2014)
	▪ Dermatitis (Ni itch)	(Gautam et al., 2016)
Pb	▪ Impaired development, lower IQ, shortened attention span, hyperactivity and mental deterioration in children	(Halim et al., 2003)
	▪ Loss of memory, anorexia, weakness of the joints, failures of reproduction, inhibition of hem synthesis, and producing tumor	(Drexler & Brattin, 2007)
	▪ Encephalopathy	(Gautam et al., 2016)
Zn	▪ Skin irritations, vomiting, nausea and stomach cramps	(McBride et al., 2009)
	▪ Liver damage, respiratory disorders and disturb protein metabolism	(Beesley & Marmiroli, 2011)

A										B		
Sc 21 44.96	Ti 22 47.88	V 23 50.94	Cr 24 52.00	Mn 25 54.94	Fe 26 55.85	Co 27 58.93	Ni 28 58.69	Cu 29 63.55	Zn 30 65.38	Rating	Common description	LD ₅₀ (single oral dose for rats, mg kg ⁻¹)
Y 39 88.91	Zr 40 91.22	Nb 41 92.91	Mo 42 95.94	Tc 43 98.91	Ru 44 101.07	Rh 45 101.07	Pd 46 106.37	Ag 47 107.87	Cd 48 112.41	1	Extremely toxic	≤1
Hf 72 178.49	Ta 73 180.95	W 74 183.85	Re 75 186.21	Os 76 190.23	Ir 77 192.22	Pt 78 195.08	Au 79 196.97	Hg 80 200.59		2	Highly toxic	1-50
Rf 104 261.10	Db 105 262.11	Sg 106 263.10	Bh 107 264.10	Hs 108 265.10	Mt 109 266.10	Ds 110 267.10	Rg 111 268.10			3	Moderately toxic	50-500
										4	Slightly toxic	500-5000
										5	Practically non-toxic	5000-15000
										6	Relatively harmless	>15000

Figure 2. 16: The Median lethal dose "LD₅₀" for metals. (A) All metals for which the data are available. (D) The toxicity rating based on the corresponding table from Hazardous Chemicals Handbook (Carson, 2002, source: (Egorova & Ananikov, 2017)).

2.3.5 Metabolism

Metabolism of metals is usually limited to oxidation-reduction reactions or alkylation/dealkylation reactions (Goyer et al., 2004). In these reactions, new inorganic species or metal organic complexes may be formed but the metal ion persists. Metals and their complexes are often ionized, with tissue uptake (membrane transport) having greater potential to be diffusion-limited or use specialized transport processes. Metals typically do not require bioactivation, at least not in the sense that an organic molecule undergoes enzymatic modification that produces a reactive chemical species (Waalkes, 1995). However, metals use other detoxification mechanisms, such as long-term storage (e.g., cadmium) and biliary and/or urinary excretion (Goyer et al., 2004).

2.3.6 Removal from the Environment

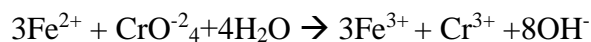
Over the last few decades, several methods have been devised for the treatment and removal of heavy metals. Pollution by metal ions has become a major issue throughout many countries (Mukhopadhyay and Konar, 1982) because the contents of metal ions in potable waters and wastewaters often exceed the permissible sanitary standards. Therefore, there is a requirement for newer and effective methods which are also cost-effective and there is a continuing interest in the development of more economic and environmentally-benign processes of selective removal of heavy metals from dilute wastewater streams (Gautam et al., 2016). The methods include precipitation, evaporative and electrolytic recovery, solvent extraction, cementation, reverse osmosis, electrodialysis, ion exchange and floatation.

2.3.6.1 Chemical Precipitation

It is one of the oldest and most widely used methods for the removal of metals from wastewater (Gautam et al., 2016). Chemical precipitation involves the addition of chemicals to modify the physical state of dissolved and suspended solids and facilitate their removal by sedimentation (Barman and Bhattacharya, 2001). Precipitation of metals is achieved by the addition of coagulants such as alum, lime, iron salts and other organic polymers (Wuana et al., 2010). Chemical precipitation is employed for most of the metals. Common precipitants include hydroxide (OH)⁻, carbonate (CO₃)²⁻ and sulfide (S)²⁻.

2.3.6.2 Chemical Reduction

Reduction of hexavalent chromium can also be accomplished with electro-chemical units (Kousi et al., 2007). The electrochemical chromium reduction process uses consumable iron electrodes and an electric current to generate ferrous ions that react with hexavalent chromium to give trivalent chromium as follows:



Another application of reduction process is the use of sodium borohydride, which has been considered effective for the removal of mercury, cadmium, lead, silver and gold (Gautam et al., 2016).

2.3.6.3 Xanthate Process

Insoluble starch xanthate (ISX) is made from commercial cross-linked starch by reacting it with sodium hydroxide and carbon disulphide (Gautam et al., 2016). To give the product stability and to improve the sludge settling rate, magnesium sulphate is also added. ISX works like an ion exchanger, removing the heavy metals from the wastewater and replacing them with sodium and magnesium (Alvarez and Crespo, 2007). ISX is most commonly used by adding to it the wastewater as slurry for continuous flow operations or in the solid form for batch treatments. The effectiveness of soluble starch xanthate (SSX) for removal of Cd (II), Cr (VI) and Cu (II) and insoluble starch xanthate (ISX) for Cr (VI) and Cu (II) have been evaluated under different aqueous phase conditions. Insoluble starch xanthate had better binding capacity for metals (Ku and Lung, 2001).

2.3.6.4 Solvent Extraction

Liquid-liquid extraction of metals from solutions on a large scale has experienced a phenomenal growth in recent years due to the introduction of selective complexing agents (Chang et al., 2002). In addition to hydrometallurgical applications, solvent extraction has gained widespread usage for waste reprocessing and effluent treatment. Solvent extraction

involves an organic and an aqueous phase. The aqueous solution containing the metal or metals of interest is mixed with the appropriate organic solvent and the metal passes into the organic phase (Duan et al., 2010). In order to recover the extracted metal, the organic solvent is contacted with an aqueous solution whose composition is such that the metal is stripped from the organic phase and is reextracted into the stripping solution. Once the metal of interest has been removed, the organic solvent is recycled either directly or after a fraction of it has been treated to remove the impurities (Gautam et al., 2016).

2.3.6.5 Membrane Process

Important examples of membrane process applicable to inorganic wastewater treatment include reverse osmosis and eletrodialysis (Basta and Gradwohl, 2000). These processes involve ionic concentration by the use of selective membrane with a specific driving force. For reverse osmosis, pressure difference is employed to initiate the transport of solvent across a semipermeable membrane and electro dialysis relies on ion migration through selective permeable membranes in response to a current applied to electrodes (Khanmirzaei et al., 2013). The application of the membrane process described is limited due to pretreatment requirements, primarily, for the removal of suspended solids. The methods are expensive and sophisticated, requiring a higher level of technical expertise to operate (Sampera et al., 2009). Liquid membrane is a thin film that selectively permits the passage of a specific constituent from a mixture. Unlike solid membranes, however liquid membranes separate by chemistry rather than size, and thus in many ways liquid membrane technology is similar to solvent extraction. Since liquid membrane technology is a fairly recent development, a number of problems remain to be solved. A major issue with the use of supported membranes is the long-term stability of the membranes, whereas the efficient breakup of microspheres for product recovery is one of the difficulties encountered frequently with emulsion membranes (Nemeh and Van Peteghem, 1992).

2.3.6.6 Cementation

Cementation is the displacement of a metal from solution by a metal higher in the electromotive series (Ruppert et al., 1988). It offers an attractive possibility for treating any wastewater containing reducible metallic ions. In practice, a considerable spread in the electromotive force between metals is necessary to ensure adequate cementation capability (Gallego-Lizon and Pérez de Ortiz, 2000). Due to its low cost and ready availability, scrap iron is the metal used often. Cementation is especially suitable for small wastewater flow because a long contact time is required. Some common examples of cementation in wastewater

treatment include the precipitation of copper from printed etching solutions and the reduction of Cr (VI) in chromium plating and chromate inhibited cooling water discharges (El-Ashtoukhy and Abdel-Aziz, 2013). Removal and recovery of lead ion by cementation on iron sphere packed bed has been reported (Karavasteva, 2005).

2.3.6.7 Ion Exchange

Ion exchange resins are available selectively for certain metal ions. The cations are exchanged for H^+ or Na^+ . The cation exchange resins are mostly synthetic polymers containing an active ion group such as SO_3H . The natural materials such as zeolites can be used as ion exchange media (Gautam et al., 2016). The modified zeolites like zeocarb and chalcarb have greater affinity for metals like Ni and Pb (Pakzadeh and Batista, 2011).

2.3.6.8 Electrodeposition/Electrochemical Recovery

Electrolytic metal recovery is one of a number of technologies capable of removing metals from process wastewaters. The technology has been used for many years in the mining industry for electrorefining of ores, and has been used to recover copper from pickle liquors (Dudzinska and Clifford, 1991). During the last 25-30 years, electrolytic metal recovery has been investigated for recovery of metals plating tanks. In electrolytic recovery, a direct current is passed through an aqueous solution containing metal ions between cathode plates and insoluble anodes. The positively charged metallic ions adhere to the negatively charged cathodes leaving a metal deposit that can be stripped off and recovered (Juang and Shiau, 1998).

2.3.6.9 Floatation

Floatation is employed to separate solids or dispersed liquids from a liquid phase using bubble attachment (Gautam et al., 2016). The attached particles are separated from the suspension of heavy metal by the bubble rise. Floatation can be classified as: dispersed-air flotation, dissolved-air flotation, vacuum air flotation, electro-floatation, and biological floatation (Carcía and Montero-Ocampo, 2010). Adsorptive bubble separation employs foaming to separate the metal impurities from water (Juttner et al., 2000). The target floated substances are separated from bulk water in a foaming phase. Although it is only a kind of physical separation process, heavy metal removal by floatation has the potential for industrial application (Gautam et al., 2016).

2.3.7 Distribution of Trace Metals

2.3.7.1 Distribution of Trace Metals worldwide

Many studies worldwide measured the level of trace metals in abiotic and biotic matrices as summarized in Table 2.8, which shows the reported concentration of six trace metals (cadmium, chromium, copper, nickel, zinc and lead) in seawater, sediment and oysters from various locations in the world.

[Yuan et al., \(2020\)](#) reported concentrations of five trace metals in seawater from South China Sea (Cd, Cr, Cu, Zn and Pb). The highest trace metal detected in seawater was zinc (mean 12.25 µg/L), followed by copper (mean 1.48 µg/L), lead (mean 0.77 µg/L), chromium (mean 0.72 µg/L), then cadmium (mean 0.08 µg/L). Seawater samples collected from the Eastern Black Sea Region of Turkey contained 0.00917 µg/L Cu, 0.00620 µg/L Pb, and 0.00439 µg/L Zn ([Baltas et al., 2017](#)). [El-Sorogy and Attiah \(2015\)](#) reported low levels of trace metals in seawater of the Mediterranean Sea coast of Egypt, with mean concentration of 1.3×10^{-6} µg/L Zn, 6×10^{-6} µg/L Ni, 6×10^{-6} µg/L Pb, and 4×10^{-6} µg/L Cr.

[Fang and Lien \(2020\)](#), reported levels of trace metals in surface sediment from East China Sea with concentration range of 32.2-142.5 µg/g Cr, 18.2-143.3 µg/g Zn, 13.3-108 µg/g Ni, 6.2-46 µg/g Pb, 1.9-47.1 µg/g Cu, and 0.02-0.36 µg/g Cd. While study conducted in sediments from coastal environment of USA reported lower levels of trace metals with mean concentration of 45.3 µg/g Zn, 32 µg/g Cr, 10.5 µg/g Pb, and 9 µg/g Cu ([Paul et al., 2021](#)). Other study investigated the contents of Cu, Zn and Pb in sediment samples collected from Turkey with mean concentration of 576.31 µg/g, 357.02 µg/g, 97.33 µg/g respectively ([Baltas et al., 2017](#)). [El-Sorogy and Attiah \(2015\)](#) measured levels Ni, Pb, Zn and Cr in seawater from sea coast of Egypt with mean of 803.2, 405.71, 340.23, and 0.26 µg/g respectively.

The most trace metals found in bivalves from South China Sea was zinc (mean 10.78 µg/g) but with more high concentration than seawater; other trace metals in bivalves were 3.07 µg/g Cu, 0.9 µg/g Cr, 0.47 µg/g Pb, 0.44 µg/g Cd [Yuan et al., \(2020\)](#). [Lu et al. \(2020\)](#) reported levels of trace metals in oysters from the Pearl River Estuary with high level observed with zinc (mean 4100 µg/g), followed by copper (mean 1520 µg/g), cadmium (mean 12.4 µg/g), nickel (mean 4.17 µg/g), chromium (mean 1.66 µg/g), then lead (mean 1.46 µg/g). Previous study reported that the mean concentrations of Zn, Cu, Cr, Cd, Ni, and Pb in the oyster tissues from the entire Chinese coastal waters were 3346, 1182, 2.57, 8.59, 9.00, and 5.13 µg/g, respectively ([Lu et al., 2019](#)). Another study in bivalves from southeast coast of India found that Zn and Cu were the highest concentration with 19 and 11.15 µg/g, respectively

(Satheeswaran et al., 2019). El-Sorogy and Attiah (2015) reported levels of Ni, Zn, Pb, and Cr in bivalves collected from Egypt with mean of 1.92, 1.69, 0.426, and 0.133 µg/g, respectively.

Table 2. 8: Concentrations of trace metals in abiotic and biotic matrices from different locations worldwide

Metal	Location	Matrices	Concentration (µg/g dry wt., µg/L)	Reference	
Cadmium (Cd)	China	Bivalve	0.44 ± 0.41	(Yuan et al., 2020)	
		Oyster	7.66	(Lu et al., 2019)	
			12.4	(Lu et al., 2020)	
		Seawater	0.08 ± 0.08	(Yuan et al., 2020)	
		Marine sediment	0.02–0.36	(Fang and Lien, 2020)	
		India	Bivalve	0.86	(Satheeswaran et al., 2019)
Chromium (Cr)	China	Bivalve	0.90 ± 0.51	(Yuan et al., 2020)	
		Oyster	10.65	(Lu et al., 2019)	
			1.66	(Lu et al., 2020)	
		Seawater	0.72 ± 0.66	(Yuan et al., 2020)	
		Marine sediment	32.2–142.5	(Fang and Lien, 2020)	
		India	Bivalve	0.34	(Satheeswaran et al., 2019)
	USA	Coastal sediment	32	(Paul et al., 2021)	
	Egypt	Seawater	0.004	(El-Sorogy and Attiah, 2015)	
		Coastal sediment	0.26	(El-Sorogy and Attiah, 2015)	
		Bivalve	0.133	(El-Sorogy and Attiah, 2015)	
	Copper (Cu)	China	Bivalve	3.07± 4.40	(Yuan et al., 2020)
			Oyster	522	(Lu et al., 2019)
			1520	(Lu et al., 2020)	
Seawater			1.48 ± 0.87	(Yuan et al., 2020)	
			Marine sediment	1.9–47.1	(Fang and Lien, 2020)
			India	Bivalve	11.15
USA		Coastal sediment	9	(Paul et al., 2021)	
Turkey		Seawater	9.17	(Baltas et al., 2017)	
		Sediment	576.31	(Baltas et al., 2017)	
Nickel (Ni)		China	Oyster	7.14	(Lu et al., 2019)
				4.17	(Lu et al., 2020)
			Marine sediment	13.3–108	(Fang and Lien, 2020)
	India	Bivalve	0.46	(Satheeswaran et al., 2019)	
	Egypt	Seawater	0.006	(El-Sorogy and Attiah, 2015)	
		Coastal sediment	803.2	(El-Sorogy and Attiah, 2015)	
	Bivalve	1.92	(El-Sorogy and Attiah, 2015)		
Lead (Pb)	China	Bivalve	0.47 ± 0.20	(Yuan et al., 2020)	
		Oyster	0.91	(Lu et al., 2019)	
			1.46	(Lu et al., 2020)	
		Seawater	0.77 ± 0.35	(Yuan et al., 2020)	
			Marine sediment	6.2–46	(Fang and Lien, 2020)
			India	Bivalve	0.94
	USA	Coastal sediment	10.5	(Paul et al., 2021)	
	Egypt	Seawater	0.006	(El-Sorogy and Attiah, 2015)	
		Coastal sediment	405.71	(El-Sorogy and Attiah, 2015)	
		Bivalve	0.426	(El-Sorogy and Attiah, 2015)	
	Turkey	Seawater	6.20	(Baltas et al., 2017)	
		Sediment	97.33	(Baltas et al., 2017)	
	Zinc (Zn)	China	Bivalve	10.78 ± 0.76	(Yuan et al., 2020)
			Oyster	2068	(Lu et al., 2019)
				4100	(Lu et al., 2020)
Seawater			12.25 ± 5.60	(Yuan et al., 2020)	
			Marine sediment	18.2–143.3	(Fang and Lien, 2020)
			India	Bivalve	19
USA		Coastal sediment	45.3	(Paul et al., 2021)	
Egypt		Seawater	0.013	(El-Sorogy and Attiah, 2015)	
		Coastal sediment	340.23	(El-Sorogy and Attiah, 2015)	
		Bivalve	1.694	(El-Sorogy and Attiah, 2015)	
Turkey		Seawater	4.39	(Baltas et al., 2017)	
		Sediment	357.02	(Baltas et al., 2017)	

2.3.7.2 Distribution of Trace Metals in Gulf Countries

The effect of the Gulf War in 1991 and the ensuing oil spills on the concentration levels of several heavy metals in the marine environment and in aquatic organisms was the highlight of several studies (Al-Sayed et al., 1996; Madany et al., 1996). Levels of selected trace metals from Gulf countries in seawater, sediment, and oysters illustrated in Table 2.9.

Marine pollution in the territorial water of the kingdom of Bahrain was assessed by analyzing trace metals in seawaters from 23 different sites known as fishing areas in the year 2007, the concentrations of Cd, Cu, Ni, Pb and Zn were in the range of 0.06-5.20, 4.53-119.00, 0.71-20.1, 1.13-2.01 and 4.06-118.0 µg/L, respectively (Juma and Al-Madany, 2008). The metals (Cd, Cu, Ni, Pb, and Zn) were measured in seawater collected from two stations around Bahrain between March 1991 and March 1992 with mean concentration of 0.13, 0.2, 0.24, 0.14, and 2.99 µg/L (Al-Sayed et al., 1994). Which mean that the levels of trace metals in seawater of Bahrain increased after 1992.

Measuring levels of heavy metals in marine sediments has been used in monitoring and assessment of environmental disasters and industrial pollution in the Arabian Gulf (Naser, 2013). An assessment of contamination in marine sediment due to heavy metals in the Arabian Gulf was conducted during 2000– 2001 (de Mora et al., 2004). This study noted two hotspots of heavy metals in Bahrain and on the east coast of the UAE. Elevated levels of heavy metals Cu, Pb, and Zn with mean concentrations of 48.3, 99.0, and 52.2 µg/g respectively were recorded off the oil refinery in Bahrain. Higher concentrations of heavy metals Cr and Ni were reported at Akkah beach on the east coast of the UAE with maximum concentrations of 303, and 1010 µg/g respectively and attributed to the metal-rich mineralogy of the region. Elevated Cd levels (19.14 µg/g) were also reported near a desalination plant off the eastern coastline of Bahrain and attributed to petroleum industries as well as effluents from a variety of factories and industrial facilities (Naser, 2013). A baseline survey of sediment contamination due to heavy metals was undertaken at twenty-nine locations around Kuwait (Lyons et al., 2015). The reported range of trace metals were Cr (108.2–429.0 µg/g), Ni (86.2–169.3 µg/g), Cu (21.7–53.4 µg/g), Zn (55.3–140.7 µg/g), Cd (<0.178–0.5 µg/g), and Pb (9.7–32.2 µg/g). Previous study in marine sediment from Kuwait in 1985 reported lower levels of trace metals (Cd, Cu, Ni, Pb and Zn) with mean concentrations of 0.26, 2.59, 10.07, 3.55, and 13.7 µg/g respectively (Al-Hashimi and Salman, 1985). Alharbi and El-Sorogy (2017) measured levels of Cd, Cr, Cu, Ni, Pb and Zn in sediment from Saudi Arabia marine environment with mean concentration of 0.23, 51.03, 182.97, 75.10, 5.36, and 52.68 µg/g respectively.

Historically, pearl oysters represented a major marine resource in the Arabian Gulf countries. Several studies have been conducted to detect heavy metal contamination in the pearl oyster, *Pinctada radiata* in the Arabian Gulf. [Bu-Olayan et al. \(1997\)](#) investigated the contribution of the 1991 oil spill to heavy metal contamination in the pearl oyster, *Pinctada radiata* for their heavy metal contents before and after the spill. Concentrations of copper (Cu), nickel (Ni), lead (Pb) and zinc (Zn) were determined in oyster samples from three coastal stations of Kuwait during 1990 and 1994. In the 1990 samples, the metal mean concentrations in oysters were 0.86 µg/g for Cu, 0.88 µg/g for Ni, 0.56 µg/g for Pb and 0.494 µg/g for Zn, while in the 1994 samples, the metal mean concentrations for Cu, Ni, Pb and Zn were 55.00, 16.96, 0.57 and 486.61 µg/g respectively. Due to a contribution from the 1991 Gulf War oil spill, the 1994 samples have significantly higher mean concentrations of metals than the 1990 samples. Between March 1991 and March 1992, levels of Cd and Pb were measured in pearl oyster *Pinctada radiata* collected from two stations around Bahrain ranged from (0.25-3.8 µg/g) and (1.25-14.0 µg/g) respectively ([Al-Sayed et al., 1994](#)). Levels of Cu, Ni, Pb and Zn in bivalves from Bahrain, UAE, Saudi Arabia and Oman were measured in 1991 by [Fowler et al. \(1993\)](#). The highest concentrations of trace metals in oysters was Zn collected from UAE, Saudi Arabia and Oman with mean concentration of 1261, 1618, and 477 µg/g respectively. Moreover, oysters collected from Saudi Arabia showed high level of Ni (260 µg/g), while oysters collected from Oman showed high level of Cu (129.83 µg/g) compared to other countries. During 2000–2001, very high concentrations of Zn (4290 µg/g), and Pb (3.92 µg/g) were found in pearl oysters near the BAPCO site in Bahrain and relatively high concentrations of Cr (2.36 µg/g), Ni (7.02 µg/g) and Cu (17.3 µg/g) were found in pearl oysters from Abu Dhabi ([de Mora et al., 2004](#)).

Table 2. 9: Concentrations of selected trace metals in abiotic and biotic matrices from Arabian Gulf countries

Metal	Country	Matrices	Concentration ($\mu\text{g/g}$ dry wt., $\mu\text{g/l}$)	Reference		
Cadmium (Cd)	Kuwait	Marine sediment	<0.178–0.5	(Lyons et al., 2015)		
		coastal sediments	0.26	(Al-Hashimi and Salman, 1985)		
	Saudi Arabia	coastal sediments	0.23	(Alharbi and El-Sorogy, 2017)		
	Bahrain	Pearl oyster	0.25–3.8	(Al-Sayed et al., 1994)		
		Seawater	0.13	(Al-Sayed et al., 1994)		
			0.06-5.20	(Juma and Al-Madany, 2008)		
			Sediments	109–195	(de Mora et al., 2004)	
Chromium (Cr)	Kuwait	Marine sediment	19.14	(Naser, 2010)		
	Kuwait	Marine sediment	108.2–429.0	(Lyons et al., 2015)		
	Saudi Arabia	coastal sediments	51.03	(Alharbi and El-Sorogy, 2017)		
	UAE	Sediments	303	(de Mora et al., 2004)		
Copper (Cu)	Kuwait	Marine sediment	21.7– 53.4	(Lyons et al., 2015)		
		coastal sediments	2.59	(Al-Hashimi and Salman, 1985)		
			Pearl oyster	55.00	(Bu-Olayan et al., 1997)	
	Bahrain	Sediments	48.3	(de Mora et al., 2004)		
		Seawater	4.5–119	(Juma and Al-Madany, 2008)		
			Seawater	0.2	(Al-Sayed et al., 1994)	
			Pearl oyster	1.41	(Al-Sayed et al., 1994)	
			Pearl oyster	4.60	(Fowler et al., 1993)	
	UAE	Pearl oyster	3.00	(Fowler et al., 1993)		
	Saudi Arabia	Oyster	16.00	(Fowler et al., 1993)		
		Coastal sediments	182.97	(Alharbi and El-Sorogy, 2017)		
	Oman	Oyster	129.83	(Fowler et al., 1993)		
	Nickel (Ni)	Kuwait	Marine sediment	86.2–169.3	(Lyons et al., 2015)	
			coastal sediments	10.07	(Al-Hashimi and Salman, 1985)	
				Pearl oyster	16.96	(Bu-Olayan et al., 1997)
		Bahrain	Pearl oyster	0.44	(Fowler et al., 1993)	
			Seawater	0.24	(Al-Sayed et al., 1994)	
			0.71-20.1	(Juma and Al-Madany, 2008)		
UAE		Sediments	1010	(de Mora et al., 2004)		
		Pearl oyster	1.64	(Fowler et al., 1993)		
Saudi Arabia		Oyster	260	(Fowler et al., 1993)		
		coastal sediments	75.10	(Alharbi and El-Sorogy, 2017)		
Oman		Oyster	1.59	(Fowler et al., 1993)		
Lead (Pb)		Kuwait	Marine sediment	9.7–32.2	(Lyons et al., 2015)	
			coastal sediments	3.55	(Al-Hashimi and Salman, 1985)	
			Pearl oyster	0.57	(Bu-Olayan et al., 1997)	
	Bahrain	Pearl oyster	1.25–14.0	(Al-Sayed et al., 1994)		
				3.92	(de Mora et al., 2004)	
			3.90	(Fowler et al., 1993)		
			Seawater	0.14	(Al-Sayed et al., 1994)	
			1.13-2.01	(Juma and Al-Madany, 2008)		
			Sediments	99	(de Mora et al., 2004)	
	UAE	Pearl oyster	0.14	(Fowler et al., 1993)		
	Saudi Arabia	Oyster	0.43	(Fowler et al., 1993)		
		coastal sediments	5.36	(Alharbi and El-Sorogy, 2017)		
	Oman	Oyster	0.97	(Fowler et al., 1993)		
Zinc (Zn)	Kuwait	Marine sediment	55.3–140.7	(Lyons et al., 2015)		
		coastal sediments	13.7	(Al-Hashimi and Salman, 1985)		
			Pearl oyster	486.61	(Bu-Olayan et al., 1997)	
	Bahrain	Pearl oyster	4290	(de Mora et al., 2004)		
				8.98	(Fowler et al., 1993)	
			Sediments	52.2	(de Mora et al., 2004)	
			Seawater	2.99	(Al-Sayed et al., 1994)	
			4.06-118.0	(Juma and Al-Madany, 2008)		
	UAE	Pearl oyster	1261	(Fowler et al., 1993)		
	Saudi Arabia	Oyster	1618.00	(Fowler et al., 1993)		
		coastal sediments	52.68	(Alharbi and El-Sorogy, 2017)		
	Oman	Oyster	477.00	(Fowler et al., 1993)		

2.3.7.3 Distribution of Trace Metals in Qatar

Few studies examined levels of trace metals in Qatari marine environment. [Kureishy \(1993\)](#) investigated the contribution of the 1991 oil spill to heavy metal contamination in marine organisms around Qatar. He found Cd concentrations ranging from 0.21 to 1.32 mg/kg in 13 fish species around Doha, Qatar, and ranging from 0.31 to 1.21 mg/kg in 16 fish species from Halul Island (an oil storage and transfer facility), offshore of Qatar. [Abdel-Moati and Nasir \(1997\)](#) study the bioaccumulation of some metals including Cr, Ni, and Pb in some fish and prawn from Qatari waters. The range of levels in fish were 0.06- 0.64 µg/g, 0.03-0.93 µg/g, and 0.31 -2.23 µg/g for Cr, Pb, and Ni respectively; while in prawn corresponding values were 0.3- 0.99 µg/g for Cr, 0.88- 2.9 µg/g for Pb, and 1.14- 3.63 µg/g for Ni indicating higher concentration of metals in prawn compared to fish. The edible portions including skin of 20 popular fish species in Qatar were examined for Cu, Zn, Pb and Hg and proven to be safe for human consumption ([Al-Jedah and Robinson, 2001](#)). Limited studies investigated trace metals concentrations in seawater, sediment, and oyster tissues in marine environment of Qatar.

2.3.7.3.1 Trace Metals in Qatari Seawater

[Aboul Dahab and Al-Madfa \(1997\)](#) studied Chromium distribution in seawater of the eastern side of the Qatari peninsula. Average Cr concentrations in the investigated waters during the period of study were 0.08, 0.66 and 0.54 µg/L respectively for Cr (III), Cr (VI), and particulate phases. After 10 years of the previous study, only one author examined the level of trace metals in Qatar's seawater ([Leitão et al., 2017](#)). They showed that most of the heavy metal concentrations were below the limits set by the Ministry of Environment of Qatar, Environmental Law No. 30/2002, amended in 2009 by decree Law No. 45. Of the metals detected, most were in the range of 0.01 µg/L–4.52 µg/L, with the exception of Zn, which had a range of 13.8µg/L–21.12µg/L during the summer sampling and 27.3 µg/L to 148.57 µg/L during the winter sampling.

2.3.7.3.2 Trace Metals in Qatari Sediment

Trace metals (Cr, Co, Cu, Zn, and Ni) concentrations were investigated in marine sediment from North Western of Qatar with mean concentration of 4, 1, 3, 13, and 6 µg/g respectively ([Basaham and Al-Lihaibi, 1993](#)). [Aboul Dahab and Al-Madfa \(1997\)](#) examined Cr concentration in sediments of the eastern side of the Qatari peninsula with concentration ranged from 11.6 to 46.5 µg/g dry wt. and an average of 25.4 ± 8.7 µg/g dry wt. Concentrations of trace metals in surface sediments along the Qatari Doha Bay from 10 transects each with five stations were studied by ([Al-Naimi et.al., 2015](#)). The overall results of metal analyses were

within the international standards criteria, and the results were comparable to the previous studies conducted around Qatar. [Leitão et al. \(2017\)](#) measured levels of trace metals in sediment from three sites around Qatar coastline (AlKhor, Doha Harbor and AlWakra Harbor) during summer and winter seasons. In summer, levels of Cd, Cr, Cu, Ni, and Zn were (0.05, 15.97, 2.92, 1.10 and 4.72 $\mu\text{g/g}$) in AlKhor, and levels of Cd, Cr, Cu, and Zn were (0.06, 1.13, 2.74, and 1.31 $\mu\text{g/g}$) and (0.06, 3.81, 0.74, 0.58, 2.20 $\mu\text{g/g}$) in Doha Harbor and AlWakra Harbor respectively. While in winter, levels of Cd, Cr, Cu, Ni, and Zn were (0.07, 4.90, 2.11, 2.81, and 4.71 $\mu\text{g/g}$) in AlKhor, and levels of Cd, Cr, Cu, and Zn were (0.04, 1.29, 1.08, and 1.37 $\mu\text{g/g}$) and (0.18, 29.80, 9.73, 5.34, and 14.34 $\mu\text{g/g}$) in Doha Harbor and AlWakra Harbor respectively.

2.3.7.3.3 Trace Metals in Qatari Oyster (*Pinctada radiata*)

A wealth of knowledge exists for heavy metals in oysters in many areas of the world while very limited appears for the Qatari coastline species. [Al-Madfa et al. \(1998\)](#) collected pearl oysters *P. radiata* from eight sites around Eastern coastline of Qatar to assess trace metals concentration. The mean concentration of Cd, Cu, Pb, and Ni in *P. radiata* collected from all the sites were 0.49, 2.79, 3.88 and 7.08 $\mu\text{g/g}$ dry weight respectively. This study reported high mean concentrations for Pb and Ni in *P. radiata* collected from areas that were subject to dredging and shipping activities along the Qatari coastline.

The latest study done by [\(Leitão et al, 2017\)](#) measured levels of trace metals in *P. radiata* from three sites around Qatar coastline (AlKhor, Doha Harbor and AlWakra Harbor) during summer and winter seasons. In AlKhor and Doha Harbor, the levels for most trace metals were high in winter compared to summer, while in AlWakra same trend was maintained during the summer and winter. In summer, levels of Cd, Cr, Cu, Ni, Pb and Zn were (9.02, 1.32, 3.84, 0.58, 0.04, and 840.63 $\mu\text{g/g}$), (0.06, 1.13, 2.74, ND, ND, 1.31 $\mu\text{g/g}$), and (3.22, 2.64, 12.92, 1.42, 0.33, and 2529.49 $\mu\text{g/g}$) in AlKhor, Doha Harbor and AlWakra Harbor respectively. While in winter, levels of Cd, Cr, Cu, Ni, Pb and Zn were (7.13, 1.29, 5.75, 0.50, 0.21, and 1792.39 $\mu\text{g/g}$), (6.35, 1.33, 4.81, ND, 0.10, and 4205.70 $\mu\text{g/g}$), and (2.45, 2.37, 6.65, 1.28, 0.06, and 2066.83 $\mu\text{g/g}$) in AlKhor, Doha Harbor and AlWakra Harbor respectively. Overall, Zn presented high values in the *P. radiata* samples in all three sites.

2.4 Total Mercury

Mercury (Hg) is among the most highly toxic trace metals and a well-recognized global persistent pollutant that is known to bioaccumulate in aquatic organisms and in some cases display biomagnification in the food web (Arcagni et al., 2013; Eagles-Smith et al., 2018). According to the World Health Organization (WHO, 2017), Hg is “one of the top ten chemicals or groups of chemicals of major public health concern”. Moreover, the Government Agency for Toxic Substances and Disease Registry of the United States, ranked Hg third on their substances priority list in 2017 (ATSDR, 2017). There are three forms of Mercury: elemental, organic and inorganic mercury compounds (CDC, 2007). These forms have different properties, usage and degree of toxicity.

2.4.1 Sources of mercury

Mercury enters the environment through volcanism, fossil fuel and waste burning and from other human as well as natural processes. The distribution of mercury into the environment occurs through the natural degassing of the earth’s crust (Berlin et al., 2015). Mercury is circulated naturally in the biosphere, with 30,000-50,000 tons being released into the atmosphere by degassing from the Earth’s crust and the oceans. In addition, 20,000 tons of mercury is released into the environment each year through human activities such as combustion of fossil fuels and other industrial releases (Streets et al., 2017). The sources of Hg in an aquatic environment originate from a number of natural processes, e.g. weathering of rocks, degassing of the earth's crust and volcanism. In addition, anthropogenic activities as a consequence of rapid urbanization and industrialization, such as coal combustion, the mining industry and by-products, agriculture fertilizer, and waste incineration are also important sources of Hg (Nicklisch et al., 2017; Ordiano et al., 2011; Radomyski et al., 2018).

When Hg is released into the environment, it becomes a part of the biogeochemical cycle including transformation and transposition between the atmosphere, soil and aquatic ecosystems (Sheehan et al., 2014; Rice et al., 2014). Elemental Hg (Hg^0) is the most common form found in the atmosphere and it can travel long distances before being deposited far from its original source (Fitzgerald et al., 1998). Deposited inorganic Hg (Hg^{2+} and Hg^{3+}) can be transformed in the aquatic environment to organic Hg by anaerobic bacteria, mainly forming methyl mercury (MeHg) or dimethyl mercury (Me_2Hg) compounds. MeHg is able to readily bioaccumulate in aquatic biota and even biomagnify in higher trophic levels of the aquatic food web (Arcagni et al., 2013).

2.4.2 Exposure routes of mercury

In the general population, mercury exposure were reported as inhalation of mercury vapor in a family while burning charms (Lee et al., 2010), ingestion of herbal medication for vertigo treatment (Chung et al., 1980), inhalation of mercury vapor for pain relief of arthralgia (Lee et al., 1991), inhalation of mercury vapor for hemorrhoid treatment (Lim et al., 1998), intravenous injection of metallic mercury for suicide (Choi et al., 1999), dermal applications of inorganic mercury compounds (Eum et al., 2006), and children's exposure from house paints and lacquer (Ji et al., 1983).

2.4.3 Health effects of mercury

Elemental and methylmercury are toxic to the central and peripheral nervous systems (Myers et al., 2009). Further, the World Health Organization (WHO, 2017) reported that, inhalation of mercury vapor can produce harmful effects on the nervous, digestive and immune systems, lungs and kidneys, and may be fatal. Mercury exposure has also been noted to cause eye and skin corrosion, leading to neurocognitive disorders such as impaired memory (Tang et al., 2015; Aaseth et al., 2018; Kaur et al., 2018), insomnia (Zhou et al., 2014; Do et al., 2017) and tremors (WHO, 2017; Calabrese et al., 2018).

2.4.4 Metabolism of mercury

Metabolism of mercury by microorganisms in aquatic sediments creates methyl mercury, an organic form of mercury, which can bioaccumulate in aquatic and terrestrial food chains (CDC, 2017). The ingestion of methyl mercury, predominantly from fish and other seafood, constitutes the main source of dietary mercury exposure in the general population. Apart from methyl mercury, synthetic organomercury compounds were once used in pharmaceutical applications of organomercury, and mercury compounds are still used as preservatives (e.g., thimerosal, phenylmercuric acetate) or topical antiseptics (e.g., merbromin) (CDC, 2017).

The kinetics of the different forms of mercury vary considerably. Poorly absorbed from the gastrointestinal tract, elemental mercury is absorbed mainly by inhaling volatilized vapor, undergoes distribution to most tissues, with the highest concentrations in the kidneys (Barregard et al., 1999; Hursh et al., 1980; IARC, 1993). After elemental mercury is absorbed, it is oxidized in the tissues to inorganic forms. Blood concentrations decline initially with a rapid half-life of approximately 1-3 days followed by a slower half-life of approximately 1-3 weeks (Barregard et al., 1992; Sandborgh-Englund et al., 1998). The slow-phase half-life may

be several weeks longer in persons with chronic occupational exposure (Sallsten et al., 1993). After exposure to elemental mercury, excretion of mercury occurs predominantly through the kidney (Sandborgh-Englund et al., 1998), and peak urine levels can lag behind peak blood levels by days to a few weeks (Barregard et al., 1992); thereafter, for both acute and chronic exposures, urinary mercury levels decline with a half-life of approximately 1-3 months (Jonsson et al., 1999; Roels et al., 1991).

Less than 15% of inorganic mercury is absorbed from the human gastrointestinal tract (Rahola et al., 1973). Lesser penetration of inorganic mercury occurs through the blood-brain barrier than occurs with either elemental or methyl mercury (Hattula and Rahola, 1975; Vahter et al., 1994). The half-life of inorganic mercury in blood is similar to the slow-phase half-life of mercury after inhalation of elemental mercury; excretion occurs by renal and fecal routes (CDC, 2017).

The fraction of methyl mercury absorbed from the gastrointestinal tract is about 95% (Miettinen et al., 1971). Methyl mercury enters the brain and other tissues (Vahter et al., 1994) and then undergoes slow dealkylation to inorganic mercury. Human pharmacokinetic studies indicate that methyl mercury declines in blood and the whole body with a half-life of approximately 50 days, with most elimination occurring through in the feces (Sherlock et al., 1984; Smith et al., 1994; Smith and Farris, 1996). Methyl mercury is incorporated into growing hair, a measure of accumulated dose (Cernichiari et al., 1995; Suzuki et al., 1993), and which has served as a useful marker of exposure in epidemiologic studies (Grandjean et al., 1999 ; McDowell et al., 2004).

2.4.5 Distribution of Total Mercury in marine environment

Most of the studies around the world concentrate more on measuring the level of total mercury in sediment and water, and few in oyster tissues, as summarized in Table 2.10. In South China Sea, the level of total mercury in seawater was ranged between 0.0008 to 0.0023 µg/L (Fu et al., 2010). Mao et al., (2020) measured the level of total mercury in surface seawater of the Jiaozhou Bay of China and reported a concentration of (0.00846 - 0.02732 µg/L). Many other studies in seawater reported low levels of total mercury from English Channel, South Florida Estuaries, USA, and Xiamen Western Sea Area with concentration ranged from (0.0002- 0.0041 µg/L, 0.003- 0.0074 µg/L, 0.00151- 0.09288 µg/L) respectively (Cossa and Fileman, 1991; Kannan et al., 1998; Liang et al., 2010). Other authors reported higher level of total mercury in seawater from Bahrain (0.13-0.38 µg/L, Juma and Al-Madany, 2008), and

Sadia Arabia (Tarut Island, 0.19- 0.44 µg/L, [Youssef et al., 2016](#) and Al-Khobar, 0.25- 1.01 µg/L, [Alharbi et al., 2017](#)).

Table 2. 10: Concentrations of total mercury in seawater, sediment and oyster species of different areas of the world

Matrices	Location	Concentration (µg/g dry wt., µg/L)	Reference
Seawater	South Florida Estuaries, USA	0.003- 0.0074	(Kannan et al., 1998)
	Bahrain	0.13-0.38	(Juma and Al-Madany, 2008)
	Jiaozhou Bay, China	0.00846- 0.02732	(Mao et al., 2020)
	South China Sea, China	0.0008- 0.0023	(Fu et al., 2010)
	English Channel	0.0002- 0.0041	(Cossa and Fileman, 1991)
	Xiamen Western Sea Area	0.00151- 0.09288	(Liang et al., 2010)
	Jordanian Gulf of Aqaba	0.018–0.123	(Al-Taani et al., 2014)
	Tarut Island, Saudi Arabia	0.19- 0.44	(Youssef et al., 2016)
	Al-Khobar, Saudi Arabia	0.25- 1.01	(Alharbi et al., 2017)
Sediment	South Florida Estuaries, USA	0.012- 0.219	(Kannan et al., 1998)
	Southern Baltic Sea, Poland	0.0058- 0.225	(Bełdowski et al., 2014)
	Northern Gulf of Mexico, USA	0.01-0.2	(Apeti et al. ,2012)
	Japan	1.4–4.3	(Tomiyasu et al., 2006)
	Minamata Bay, Japan	1.17- 4.75	(Matsuyama et al., 2011)
	China	0.0037- 0.19	(Fang and Lien, 2020)
	Jiaozhou Bay, China	0.0246- 0.14516	(Mao et al., 2020)
	Pearl River Estuary, China	0.109- 0.453	(Yu et al., 2012)
	Kaštela bay, Yugoslavia	0.50- 6.13	(Mikac et al., 1985)
	Northeastern Chukchi Sea	0.005- 0.055	(Fox et al., 2014)
	Iran	0.01-0.056	(Agah et al., 2009)
	Arabian Gulf	0.032-0.27	(Kureishy and Ahmad, 1994)
	Kuwait	<0.097– <0.236	(Lyons et al., 2015)
	Tarut Island, Saudi Arabia	0.3- 1.7	(Youssef et al., 2016)
	Al-Khobar, Saudi Arabia	0.05- 1.61	(Alharbi et al., 2017)
	UAE	0.0006–0.0022	(de Mora et al., 2004)
	Bahrain	0.0025–0.220	
Oman	<0.0001–0.011		
Oysters	Northern Gulf of Mexico, USA	0.03–0.5	(Apeti et al. ,2012)
	Zhejiang, China	0.11 ± 0.04	(Fang et al. ,2004)
	Minamata Bay, Japan	Mean 10	(Eisler ,1987)
	Ebro Delta, Spain	0.12–0.27	(Ochoa et al. ,2013)
	Arabian Sea, Oman	0.07 ± 0.03	(Yesudhason et al., 2013)
	Kaštela bay, Yugoslavia	0.05- 13.28	(Mikac et al., 1985)

Distribution of total mercury in marine sediment was reported from many areas around the world. The sedimentary mercury in the Southern Baltic of Poland was investigated by [Bełdowski et al. \(2014\)](#), who reported concentration of total mercury ranged between 0.0058 to 0.225 µg/g. Many authors studied levels of total mercury in marine sediment of China ([Yu et al., 2012](#); [Mao et al., 2020](#); [Fang and Lien, 2020](#)) with concentration ranged between 0.109- 0.453 µg/g, 0.0246- 0.14516 µg/g, and 0.0037- 0.19 µg/g respectively. Concentration of total mercury in marine sediment of USA studied in different decade by [\(Kannan et al., 1998\)](#) and [\(Apeti et al. ,2012\)](#) who reported same levels with concentration ranged from 0.012- 0.219 and 0.01 - 0.2 µg/g respectively. [Tomiyasu et al. \(2006\)](#) investigated slightly high level of total

mercury in surface marine sediments collected from Minamata Bay and Fukuro Bay of Japan with concentration ranged from 1.4–4.3 µg/g and 0.3–4.8 µg/g respectively. Moreover, [Matsuyama et al. \(2011\)](#) measured the total mercury in the Minamata Bay and he found (1.17–4.75 µg/g) approximately same levels reported by the previous author.

Other authors investigated levels of total mercury in marine sediment from Arabian Gulf region. [Kureishy and Ahmad \(1994\)](#) reported (0.032–0.27 µg/g) of total mercury from Arabian Gulf sea. [de Mora et al. \(2004\)](#) reported levels of total mercury from UAE, Bahrain and Oman marine sediment with levels ranged between 0.0006–0.0022 µg/g, 0.0025–0.220 µg/g, and <0.0001–0.011 µg/g respectively. Concentration of total mercury in Kuwait marine sediment was ranged from <0.097– <0.236 µg/g ([Lyons et al., 2015](#)), while in Saudi Arabia were (0.3– 1.7 µg/g, Tarut Island) and (0.05– 1.61 µg/g, Al-Khobar) ([Youssef et al., 2016](#); [Alharbi et al., 2017](#)).

Oysters have been widely used to determine the levels of trace metals and mercury contamination in coastal ecosystems ([Ochoa et al., 2013](#)). Oysters have relatively long life spans and are sedentary and filter feeders, thus bioaccumulation of metals and mercury can be expected to occur ([Funes et al., 2006](#)). Nevertheless, few studies around the world reported the total mercury concentration in oysters as shown in Table 9.

In the '80s, high level of total mercury reported in oyster tissues collected from Minamata Bay of Japan with mean concentration of 10 µg/g ([Eisler, 1987](#)). Moreover, [Mikac et al. \(1985\)](#) studied the total mercury level on oysters from Kaštela bay of Yugoslavia and he reported a range of 0.05– 13.28 µg/g. In China, especially in Zhejiang, the mean concentration of total mercury in oyster tissues was 0.11 ± 0.04 ([Fang et al., 2004](#)). [Apeti et al. \(2012\)](#) investigated the levels of total mercury in oysters from Northern Gulf of Mexico with range of 0.03–0.5. Oysters collected from Ebro Delta of Spain contained total mercury ranged from 0.12–0.27 ([Ochoa et al., 2013](#)). [Yesudhason et al. \(2013\)](#) studied the levels of total mercury from Arabian Sea of Oman; he reported a concentration of 0.07 ± 0.03 .

2.4.6 Distribution of Total Mercury in Qatar's Marine Environment

Limited studies are available on the bioavailability of mercury in Qatar's marine environment (Table 2.11). [Al Madfa et al. \(1994\)](#) observed concentration of total mercury in Qatar's seawater ranged between 0.0033–0.03 µg/L. After five years, levels slightly became higher with ranged of 0.032 to 0.128 µg/L ([Kreish & Al Madfa, 1999](#)). The latest study done by ([Leitão et al, 2017](#)) reported 0.01– 0.16 µg/L of total mercury in Qatari seawater.

Table 2. 11: Concentrations of total mercury ($\mu\text{g/g}$ dry wt.) in abiotic and biotic matrices of Qatar marine environment

Matrices	Concentration ($\mu\text{g/g}$ dry wt., $\mu\text{g/L}$)	Reference
Seawater	0.0033-0.03	(Al Madfa et al.,1994)
	0.032-0.128	(Kreish & Al Madfa, 1999)
	0.01 - 0.16	(Leitão et al, 2017)
Sediment	0.19-1.75	(Al Madfa et al.,1994)
	0.0239 - 0.201	(Kreish & Al Madfa, 1999)
	0.01 - 0.04	(Leitão et al, 2017)
Oysters	0.038-0.065	(Kreish & Al Madfa, 1999)
	Mean 0.008, max. 0.014	(Al-Maslamani et al., 2015)
	0.01 - 0.15	(Leitão et al, 2017)

Total mercury concentration in marine sediment of Qatar seemed to decline by time. The concentration range were 0.19-1.75 $\mu\text{g/g}$ (Al Madfa et al., 1994), 0.0239 - 0.201 $\mu\text{g/g}$ (Kreish & Al Madfa, 1999), and 0.01- 0.04 $\mu\text{g/g}$ (Leitão et al, 2017).

Only three authors investigated total mercury concentration in oyster tissues around Qatar's coastline. Kreish & Al Madfa (1999) reported levels of total mercury ranged from 0.038 to 0.065 $\mu\text{g/g}$. The other author reported the maximum total mercury concentration of 0.014 $\mu\text{g/g}$ with an average of 0.008 $\mu\text{g/g}$ (Al-Maslamani et al., 2015). The latest was (Leitão et al, 2017) who examined slightly higher concentration of total mercury in oyster tissues ranged between 0.01 to 0.15 $\mu\text{g/g}$.

2.5 Summary

The Gulf region lies in a subtropical, hyper-arid zone that is generally characterized by high temperatures and low precipitation. Currently, more than 180 million people live in the Arabian Gulf region countries, more than 26 million of this population live in the coastal zone. Historically, pearl oysters represented a major marine resource in the Arabian Gulf countries. Qatar is a peninsula with an approximate area of 11610 km^2 . The coastlines and marine systems of Qatar contain a variety of biologically important and interconnected ecosystems; however, Qatar aquatic environments vulnerability to pollution coupled with the rapid development and urbanization of the coastal zone. Bioaccumulation of environmental contaminants may not only cause health impact to aquatic organisms but can also lead to human health issues.

Many researchers around the world studied the distribution and accumulation of organic and inorganic contaminants in aquatic environments including seawater, marine sediment, and oyster tissues. Few studies in the Gulf region have examined levels of these contaminants in the marine environment, while limited studies have reported concentration of these contaminants in Qatari marine environment. Accumulation of these contaminants in aquatic

environments can potentially impact human health, as described above in human health effects section for each contaminant.

Chapter 3:

Study Area and Methodology

An overview of the Qatar and a regional perspective have been provided in chapter 2 (Section 2.1). This chapter will give details about the sampling locations. It also details the methodology for sample collection in the field and sample preparation in the lab. General analytical techniques and instrumentation are also illustrated. However, the details for specific methodologies for organic and inorganic contaminants are provided in chapter 5 and 6 respectively.

3.1 Sampling Locations

Four coastal sampling sites were selected to represent different anthropologically impacted areas around the coastline of Qatar (Figure 3.1), three located on the east coast (Simaisma, Al Khor, and Al Wakra) and one on the west coast (Umm Bab). The dots in the figure below show the points where the surface seawater, surface sediment and pearl oysters samples were collected.

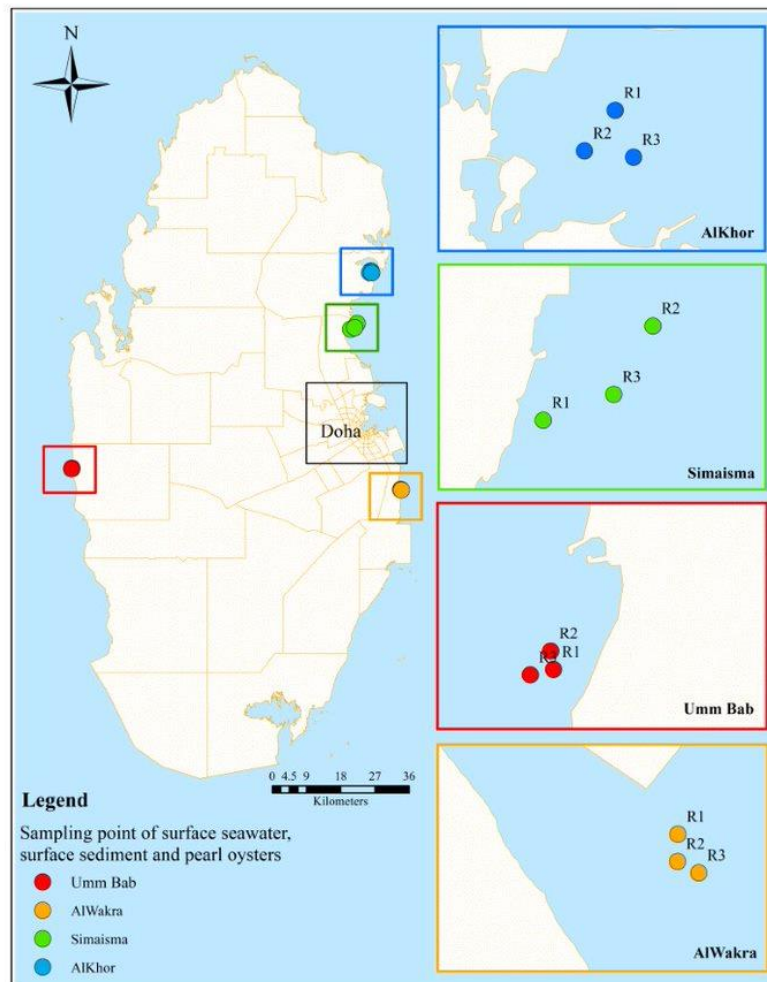


Figure 3. 1: Location of the sampling points around the coastline of Qatar

The temporal and spatial dimension are both constrained by the funding of the National Priority Research Program (NPRP 9 project), as well as practical considerations such as road access along the coast (permission / ownership). The four sampling sites are contrasting sites geographically as the maps of the land show this. The time intervals reflect the seasons. However, there are limitations especially in terms of the sites i.e., there could be more. Though, we assume they are representative given that this study considers at-a-site variability. The four sites are described individually below.

3.1.1 Simaisma site:

Simaisma is located on the east coast of Qatar with a water depth of 1–5 m. The area is situated at the bottom of a small bay about midway between Lusail and Al Khor and is rich in bivalves. The area is populated but not near the coast. Beach filling has been undertaken creating a ‘new’ Simaisma beach in 2011. The General Directorate of Coast Guard Qatar and its port located in its coast (Figure 3.2). The markers mark in the figure below and for other sites represent the location points for samplings of the three matrixes in each round.

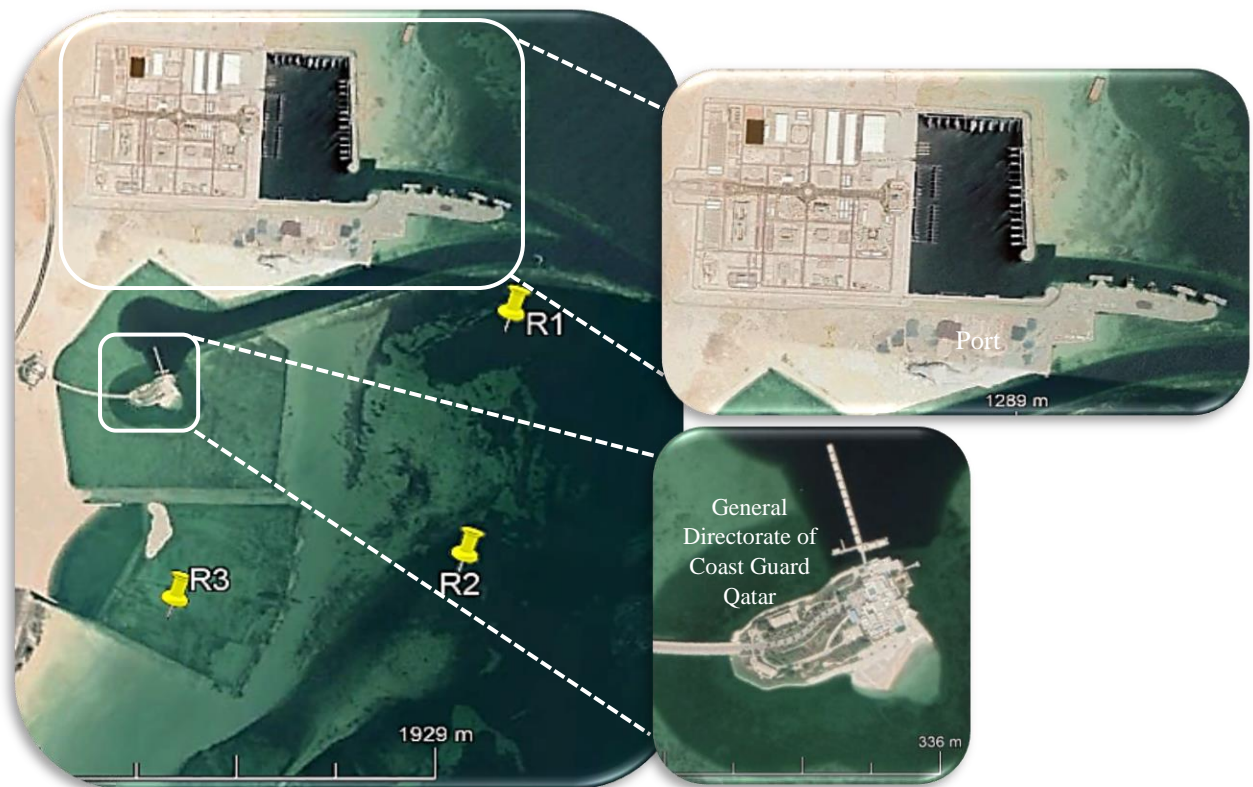


Figure 3. 2: Simaisma site

3.1.2 Umm Bab site:

Umm Bab located in western Qatar, a highly industrialized area and only 25 km away from the industrial city of Dukhan. It is enclosed area and less densely populated. It has two ports to supply all the industrial locations in the area. It also has seawater desalination plant near the coast and a cement manufacturing plant. The brine and outlets from the industries are the main source of pollution beside the regional source that might come from the north west of the Arabian Gulf.

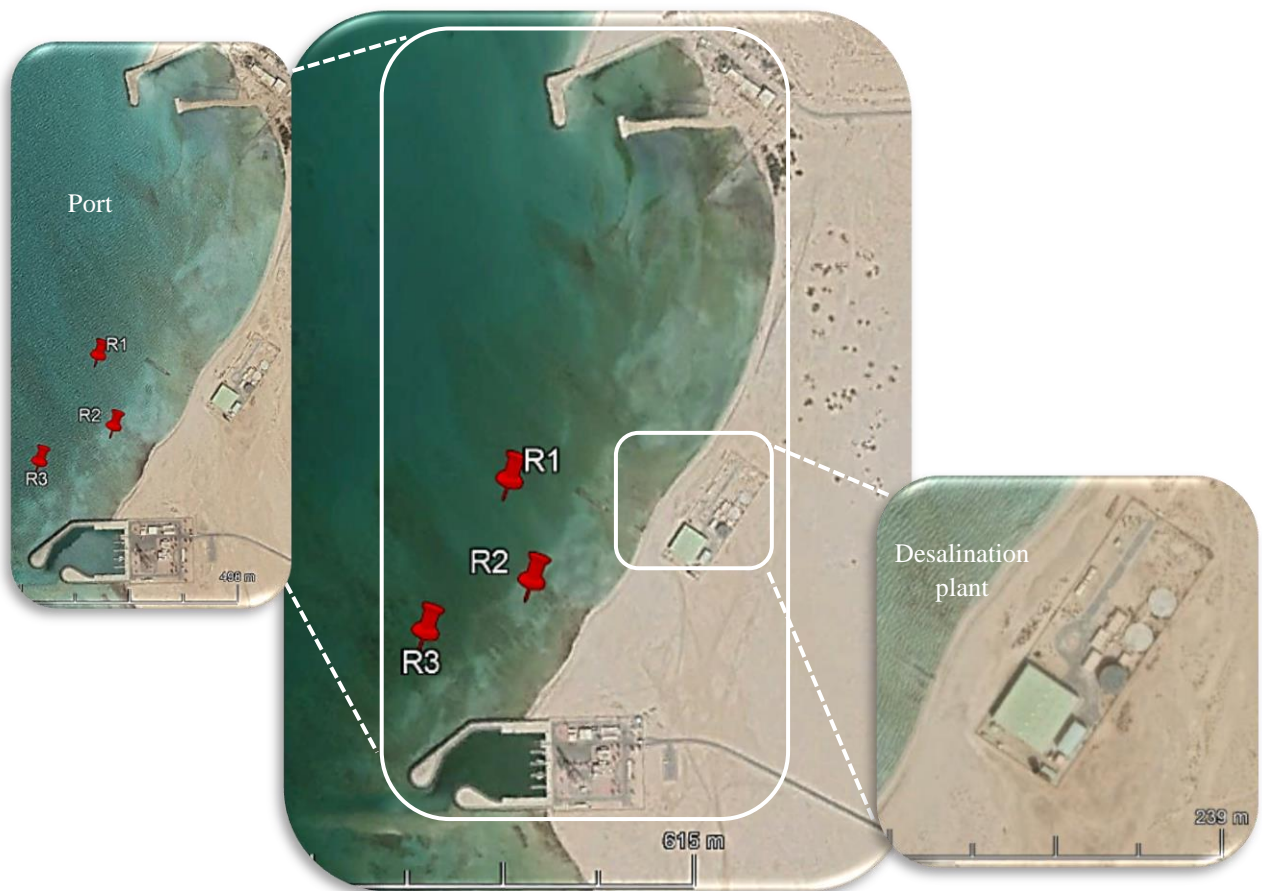


Figure 3. 3: Umm Bab site

3.1.3 Al Khor site:

Al Khor is a near shore site with clear waters with a depth of 0.5–1.0 m (Leitão et al., 2017). The bottom sediment is sandy and the area is relatively free from any industrial facilities. However, in the north side of this area there are a port, mangrove area and boat jetties.



Figure 3. 4: Al Khor site

3.1.4 Al Wakra site:

The fourth location situated in eastern Qatar, 15 km south of the capital Doha with a water depth of 0.5–1 m, the bottom sediment is mainly sandy in nature. The area is densely populated and has a harbor that makes it very busy with recreational boat traffic and fishing fleet movement. Recently, in August 2019 (after the sampling finished), they started to expand and construct a new section of the harbor (highlighted in the figure 3.5). There is a boat yard where minor repairs are carried out on seagoing vessels, fueling activities are also found within the area where fishing and recreational vessels are refuelled. In addition, there is a new recreational beach in the coast of this site.

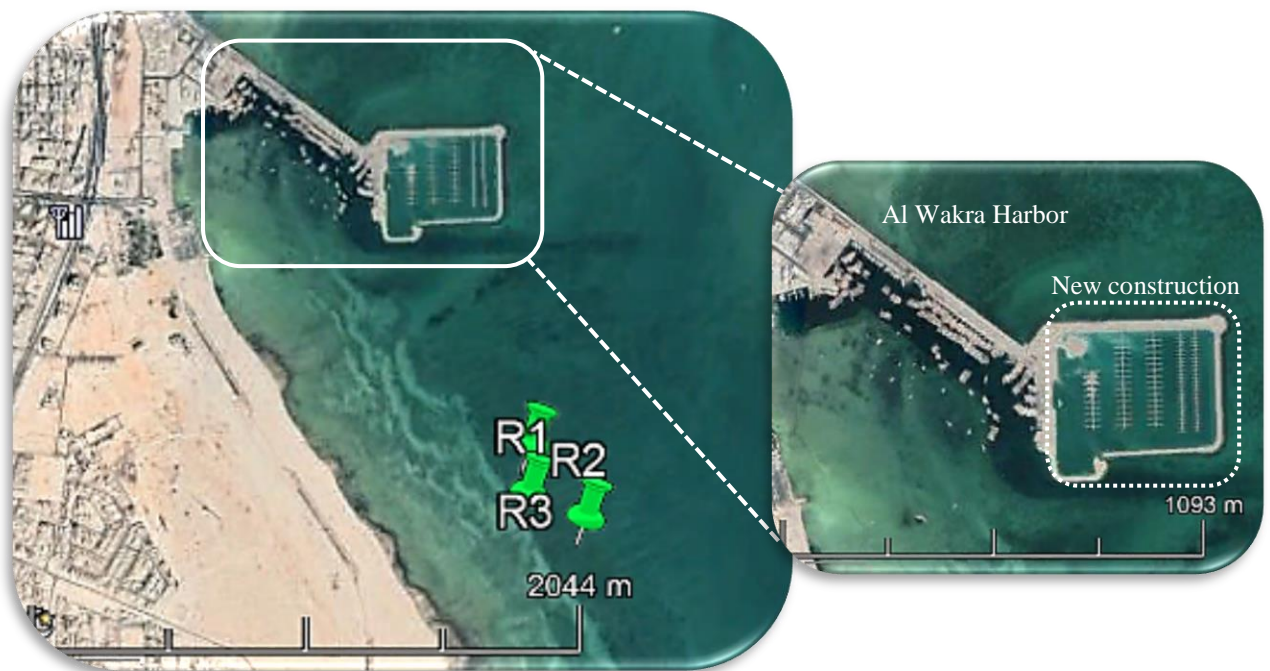


Figure 3. 5: Al Wakra site

3.2 Sampling Collection Techniques

Sampling was performed two times a year over two years at the four sampling sites to allow the assessment of the impact of any variability in abiotic parameters on the contamination profile and concentrations in oysters. At each sampling period and site, water temperature, water column depth, salinity, pH and dissolved oxygen were measured using a multi-parameter probe and water- depth probe. The sampling scheme is presented in figure 3.6.

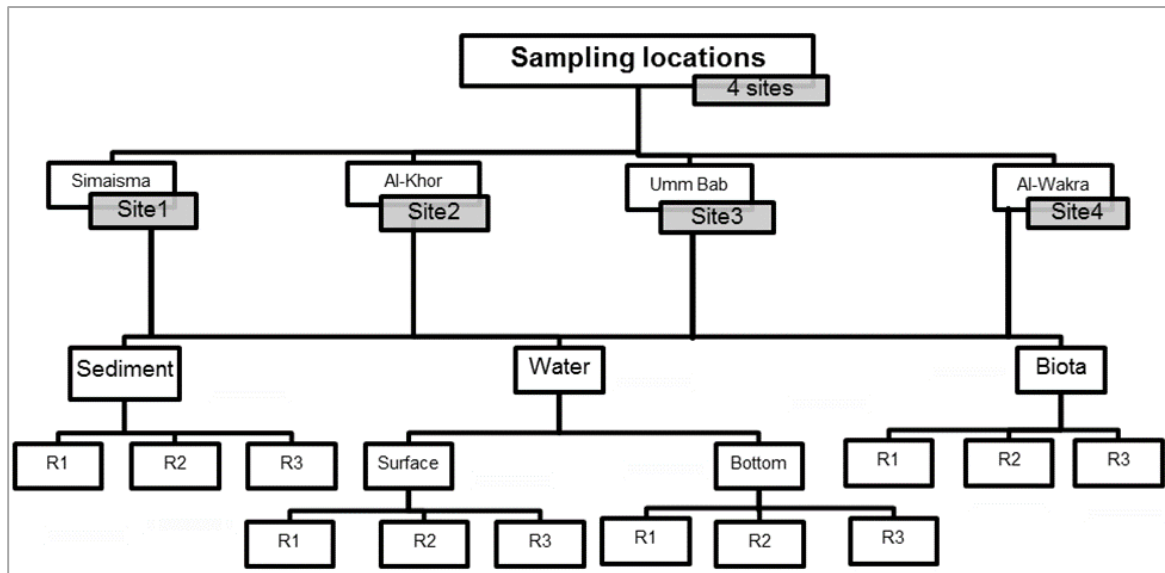


Figure 3. 6: Sampling scheme

Table 3.1 summarizes the timetable for seawater, sediment and biota in individual site. The core sediment samples were collected in May 2019 from the same four sites in total of 12 cores, 3 cores from each site.

Table 3. 1: Timetable for each category in each site

Category	Seawater	Marine Sediment	Oysters
Summer 2017 (March 2017)	3 samples	3 samples	3 groups of samples
Winter 2017 (December 2017)	3 samples	3 samples	3 groups of samples
Summer 2018 (May 2018)	3 samples	3 samples	3 groups of samples
Winter 2018 (November 2018)	3 samples	3 samples	3 groups of samples

3.2.1 Collection of Seawater

Seawater samples collection were carried out using acid cleaned 1 L amber glass bottles for organic contaminants analysis and 1 L plastic bottles for metals analysis at the subsurface, preservation of samples was immediately carried out by acidifying the samples to pH 2 using 2M hydrochloric acid (Leitão et al., 2017). The samples were then transported to the Qatar University-Environmental Science Center (ESC) laboratories in a cooled icebox and stored in the refrigerator at 2–8 °C, until analysis.



Figure 3. 7: Sampling of seawater samples

3.2.2 Collection of Surface Coastal Sediment

Composite sediment samples (n=3 composites per site) were collected using a Van-Veen grab (0.05m²). From each grab mixed sample, a sub-sample was removed using a plastic corer for trace metal determination, a further sub sample was collected using a stainless-steel spatula for organic analysis (Hassan et al., 2018) (Figure 3.8). The samples were placed in plastic and glass containers respectively, transported to the ESC laboratories and stored in the freezer until analysis.



Figure 3. 8: Sampling of surface marine sediment samples

3.2.3 Collection of Pearl Oysters

Collection of *P. radiata* specimens was conducted through scuba diving sessions (Figure 3.9) conducted in the targeted sites where depth does not allow direct collection of samples. Specimens were transported to the ESC in iceboxes containing freshly collected seawater until reaching the lab, and then they were kept in refrigerator until laboratory processing.



Figure 3. 9: Scuba diving during collection of pearl oysters (*P. radiata*) from the Simaisma site.

For each site, three batches of a minimum of twelve *P. radiata* specimens were collected for each sampling round, totaling 48 batches (Leitão et al., 2017). Hence, in total, 576 oysters were caught and analyzed as composites. The individual size and total biomass of all sampled oysters were recorded.

3.2.4 Collection of Sediment Cores

For core sampling, three core samples were collected inshore from each site when the tide went out (Figure 3.10). A tube on a T-handle that is pushed into the sediment was used (Containers, H., 1994) (Figure 3.11). To improve the success rate, piston using a ball (same diameter as tube) was used. Samples were carefully wrapped, labelled (site, top-bottom) immediately and store at <4 C and sectioned in 5cm intervals on the day of analysis.

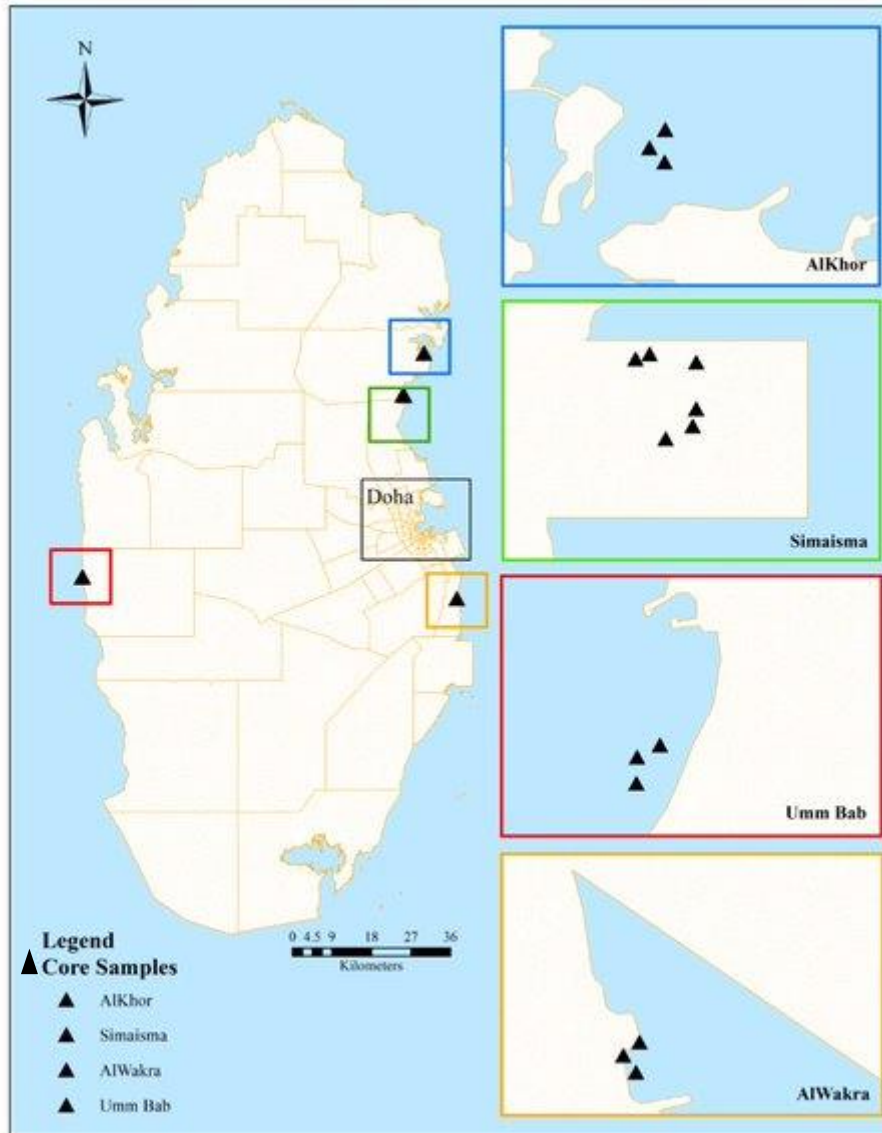


Figure 3. 10: Sampling locations of sediment core samples

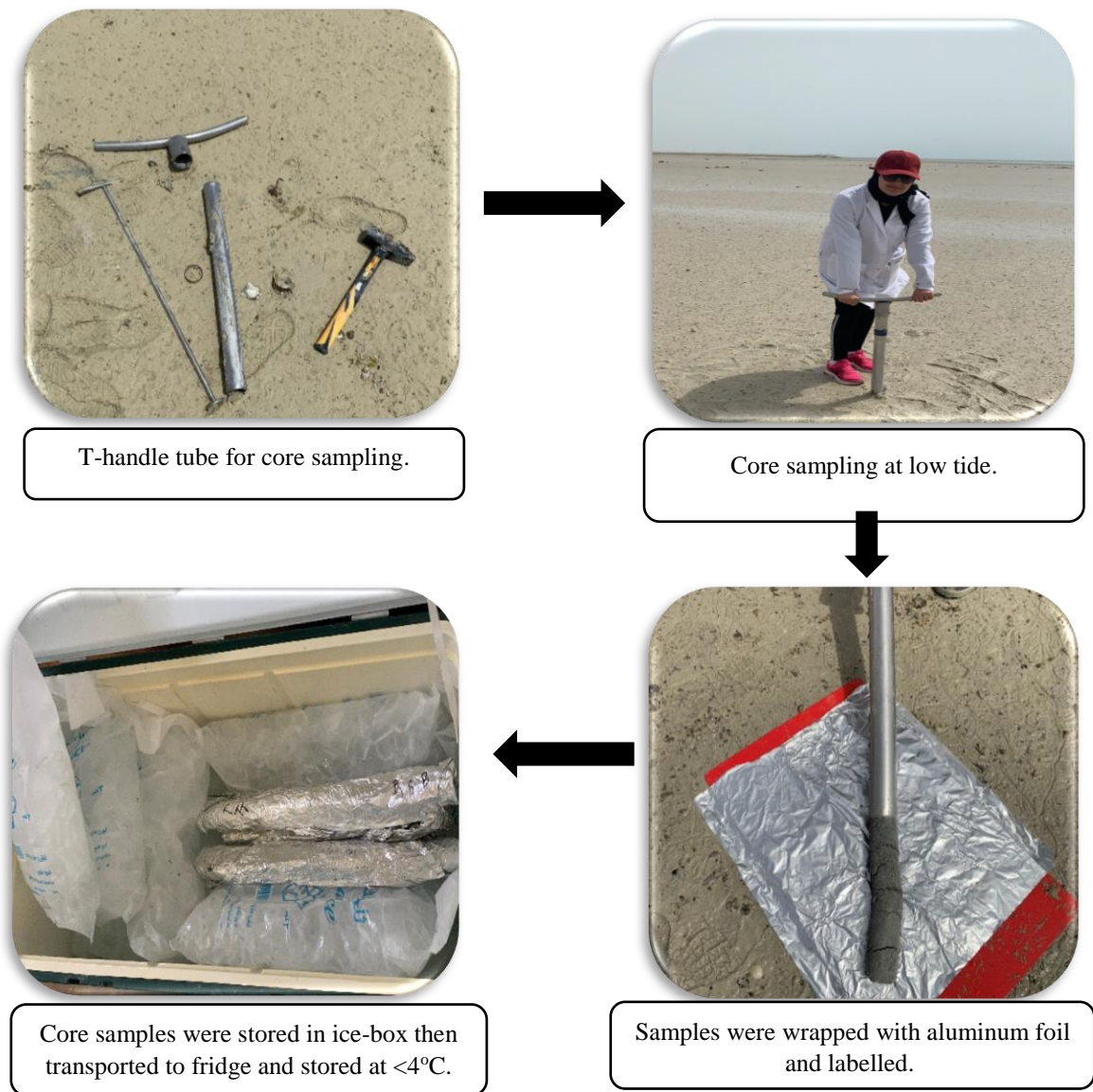


Figure 3. 11: Sampling of core samples in the field

3.3 Sample Preparation

3.3.1 Coastal Sediment Samples

In the laboratory, all sediment samples were freeze-dried by the AdVantage Pro Freeze Dryer. Then the sediment samples were grinded by Planetary Ball Mill, Type PM400 (Retsch, Germany) to obtain a well-mixed sample (Leitão et al., 2017). The ground sediment samples were placed in a glass jars prior of extraction and digestion.

3.3.2 Sediment Core Samples

In the lab, the core samples were taken from the freezer and defrosted. Then each core sample sectioned in 5cm intervals (Oyo-Ita et al., 2016) started from top to bottom and each section was transferred into a glass jar labeled with (5, 10, 15, 20, 25, and 30 cm) for each site. Each sub-sectioned sample was freeze-dried using an AdVantage Pro Freeze Dryer, and then ground by Planetary Ball Mill, Type PM400 to obtain a well-mixed sample (Figure 3.12). The samples then were placed in a glass jars prior of extraction.

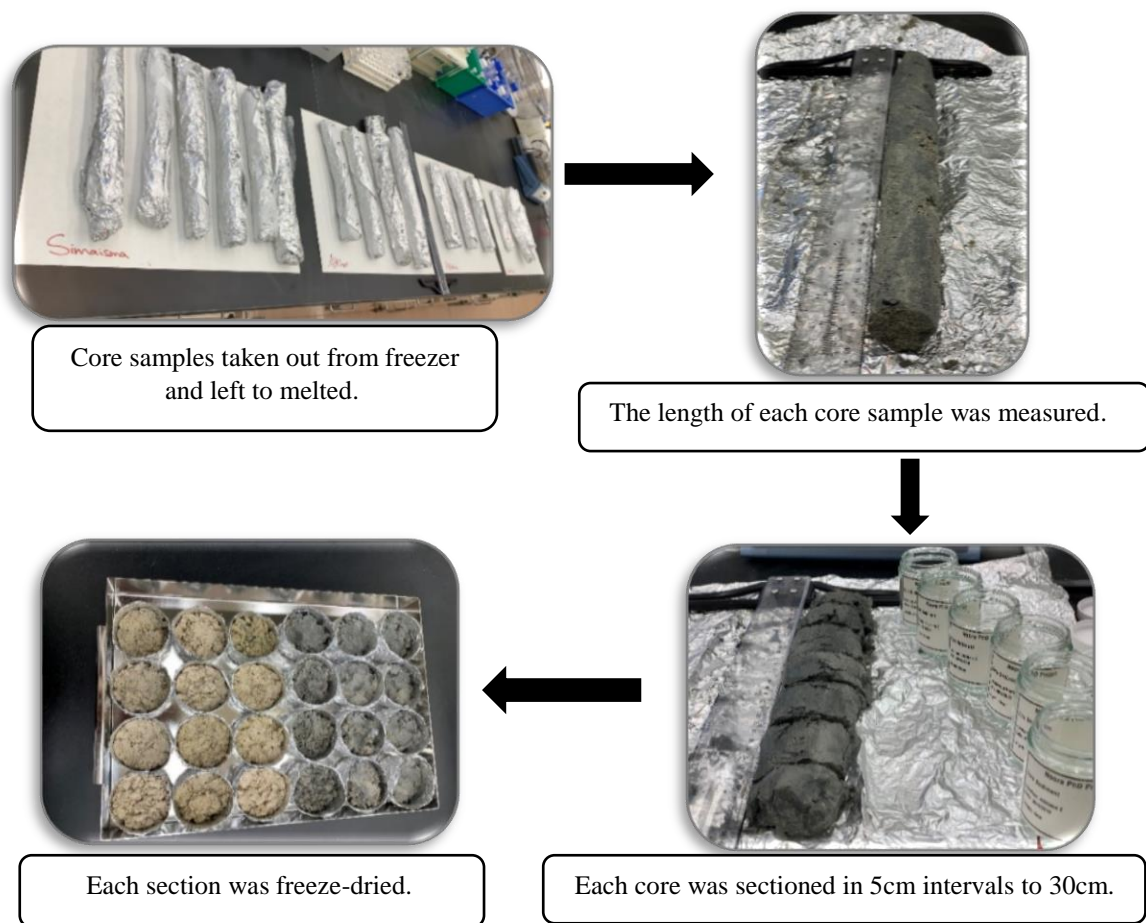


Figure 3. 12: Preparation of core samples in the lab prior of extraction

3.3.3 Oyster Tissue Samples

The pearl oysters were subsequently opened, rinsed with ultrapure water. The soft tissue including the GI tract contents were separated from the shells, mixed using blender to have a homogenized sample for each batch (3 batches for each site in each year) (Figure 3.13), then these samples were freeze-dried by the AdVantage Pro Freeze Dryer and placed in a glass jars prior of extraction (Leitão et al., 2017).



Figure 3. 13: Preparation of homogenized oyster samples for each batch

3.4 Extraction of Samples for Organic Contaminants

3.4.1 Seawater Extraction for GC Analysis

The EPA (3510C) extraction process for organic pollutants from water samples by the liquid-to-liquid extraction was followed. Briefly, 1L of water sample was separated in separating funnel by adding 30 mL of hexane and shaking for 2 minutes resulting in the formation of two layers. Then, the organic layer was taken off and cleaned by SP cartridge before concentrating it to 1 mL using nitrogen gas (Leitão et al., 2017). Then the sample was ready to inject into GC/FID and GC/MS for TPH and PAHs analysis.

3.4.2 Coastal Sediment and Oyster Tissues Extraction for GC Analysis

To extract the TPHs and PAHs from sediments and biota samples, a Dionex 350 Accelerated Solvent Extractor (ASE) (US-EPA method 8015B) was used (Accredited by A2LA- ISO 17025). Ten grams of sediment sample (or 1g of biota sample) was mixed with 5 g diatomaceous earth and placed in an extraction cell that contains 20g alumina (Figure 3.14), where the extraction was performed by using dichloromethane as a solvent mixture at a temperature of 105 °C and a pressure of 1500 psi (Rushdi et al., 2017).

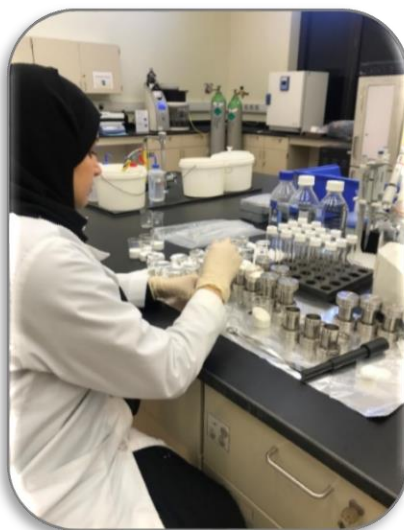


Figure 3. 14: Extraction procedure for sediment and oyster tissues samples

Next, the extracted solvent was concentrated to about 1mL by gentle nitrogen gas. The concentrated solvent was then cleaned by SP extraction cartridge and 20mL of dichloromethane. This cleaned extract underwent further evaporation process using nitrogen gas to about 1000 μ l. Then the sample was ready to inject into GC/FID and GC/MS for TPH and PAHs analysis.

3.5 Digestion of Samples for Inorganic Contaminants

3.5.1 Digestion of Samples for Trace Metals

3.5.1.1 Seawater Sample Preparation for Trace Metals

For the seawater sample analyses we followed the trace metals analysis method used by Environmental Science Center (ESC) at Qatar University (Accredited by A2LA- ISO 17025). Exactly 10ml of seawater sample transferred into a Teflon tube, then 0.5ml of concentrated nitric acid was added into the tube and sealed. The sealed tube was placed at 105°C hot block for 2 hours. Then diluted with 2% nitric acid using 50 ml volumetric flask with deionized distilled water up to the mark. Samples were analysed by Inductively Coupled Plasma-Optical Emission Spectrometry (ICP-OES) (Perkin-Elmer, Optima 7300 DV model).

3.5.1.2 Sediment Sample Preparation for Trace Metals

For the coastal sediment and sediment cores samples analyses we followed the procedure used by Environmental Science Center (ESC) at Qatar University for metals analysis in sediment (Accredited by A2LA- ISO 17025). Approximately 0.25 ± 0.05 g of oyster tissues sample weighted in TFM Vessel and follow the below given steps for acid digestion (Table 3.2). Then 3ml of nitric acid (HNO_3) followed by 20ml deionized water. Boil until clear, cool,

and quantitatively transfer into a 100 ml volumetric flask, make up to volume with deionized water. Then samples were analysed by Inductively Coupled Plasma-Optical Emission Spectrometry (ICP-OES) (Perkin-Elmer, Optima 7300 DV model).

Table 3. 2: Hot Block program for sediment acid digestion

Steps	Time	Temperature	To be digested
1	30 minutes	95°C	Sample + 9ml HNO ₃
2	30 minutes	95°C	Mixture + 3ml HF
3	60 minutes	135°C	Evaporate to reduce volume
4	--	155°C	Evaporate to almost dryness

3.5.1.3 Oyster Tissues Sample Preparation for Trace Metals

For the oyster tissues samples we followed the below method procedure used by Environmental Science Center (ESC) at Qatar University for analysis of metals in biota tissues. Approximately 0.5 ± 0.05 g of oyster tissues sample were weighted in TFM Vessel and follow the below given steps for acid digestion (Table 3.3). Then 2ml of nitric acid (HNO₃) followed by 20ml deionized water. Boil until clear, cool, and quantitatively transfer into a 50 ml volumetric flask, make up to volume with deionized water. Then samples were analysed by Inductively Coupled Plasma-Optical Emission Spectrometry (ICP-OES) (Perkin-Elmer, Optima 7300 DV model).

Table 3. 3: Hot Block program for acid digestion.

Steps	Time	Temperature	To be digested
1	60 minutes	95°C	Sample + 5ml HNO ₃
2	60 minutes	135°C	Evaporate to reduce volume
3	--	155°C	Evaporate to almost dryness

3.5.2 Sample Preparation for Total Mercury

3.5.2.1 Seawater Sample Preparation for Total Mercury

Approximately 10ml is directly introduced through a peristaltic pump to a mixer which mixes a sample with oxidizing reagents, then heated at 98°C. The heated mixture is introduced into a reaction cell, and argon gas carries the elemental mercury from the sample to the detector, which measures the mercury concentration. Table 3.4 shows the operating conditions for Mercury Analyzer AULA-254 ASD.

Table 3. 4: Operating Conditions for Mercury Analyzer AULA-254 ASD

Analytical wavelength	253.65 nm
UV source	Electrodeless low-pressure mercury discharge lamp (EDL)
Stripping gas	Argon, 4~6 l/h, stabilized with an electronic mass flow controller (MFC)
Software	AULA-WIN 254, Windows TM based
Electrical power supply	115 V / 230 V~; 50 - 60 Hz, consumption ca. 100 W
AULA-254-ASD	150 W

3.5.2.2 Sediment and Oyster Tissues Samples Preparation for Total Mercury

The sediment and biota samples followed the same procedure for Total Mercury analysis using Method Validation done in Environmental Science Center (ESC) at Qatar University (Abou Elezz et al., 2018). Approximately 0.1 g of freeze-dried and homogenized sample weighed into a 50 ml Teflon tube. Then 1ml HF, 5ml HNO₃, and 3ml H₂SO₄ (Suprapur, Merck) were added to the tube. The sample was digested using a hot block set at 125°C for 12 hours with the cap closed. After complete digestion, the tube was left to cool to room temperature. The resulting mixture was then transferred into a 50ml measuring flask together with 2ml potassium dichromate, and the volume made up to the mark with deionized water. Then the flask was shaken for 2 minutes to homogenize the matrix. About 10 ml of the sample was taken into an instrument vial. Samples are analyzed using the Automatic Mercury Analyzer AULA-254 ASD (Table 3.5). Samples introduced into a mixer with stannous chloride solution (tin (II)), then to a reaction cell, and argon gas carries the elemental mercury from the sample to the detector which measures the mercury concentration.

Table 3. 5: Operating Conditions for Mercury Analyzer AULA-254 ASD

Analytical wavelength	253.65 nm
UV source	Electrodeless low-pressure mercury discharge lamp (EDL)
Stripping gas	Argon, 4~6 l/h, stabilized with an electronic mass flow controller (MFC)
Software	AULA-WIN 254, Windows TM based
Electrical power supply	115 V / 230 V~; 50 - 60 Hz, consumption ca. 100 W
AULA-254-ASD	150 W

3.6 Analysis Methodology

3.6.1 In-situ parameters analysis of seawater

In each sampling station, the temperature, pH, and salinity were measured and recorded in-situ using a portable meter (EXO3 Multiparameter Sonde- YSI) (Figure 3.15).



Figure 3. 15: The EXO3 Multiparameter Sonde- YSI

3.6.2 Abiotic parameter of seawater and sediment

3.6.2.1 Total Organic Carbon (TOC) Analysis

3.6.2.1.1 TOC in seawater

Seawater samples are acidified with hydrochloric acid, then measured indirectly by Multi N/C 2100S (TOC /TN Analyzer). The samples sparked with oxygen injected into a heated reaction chamber packed with platinum catalyst. The CO₂ formed is transported and measured directly by an infrared detector. The amount of CO₂ is directly proportional to the concentration of carbonaceous material in the sample.

3.6.2.1.2 TOC in sediment

TOC content in marine sediment samples was measured indirectly by analysing total carbon (TC) and total inorganic carbon (TIC) using (PrimacsSNC100 – SKALAR instrument). Peak area results for TC and TIC obtained from the instrument were used in the standard calibration curve equation to calculate % TC and % TIC in sediment. The % TOC was determined by the following formula: % TOC = % TC - % TIC.

3.6.2.1.2.1 Total Carbon (TC)

Approximately 75 mg to 80 mg of ground dry weight sediment samples were added to the ceramic crucibles. The crucibles were placed in the PrimacsSNC100 instrument rack to determine the TC content in sediment through the combustion of the sample in pure oxygen at 1200 °C. Following combustion, the gas mixture containing CO₂ is led by a carrier gas through

a splitter where a part of the combustion gas is collected. The remaining gas is led to the IR detector where the CO₂ content is measured.

3.6.2.1.2.2 Total Inorganic Carbon (TIC)

Approximately 25 mg to 30 mg of ground dry weight sediment samples were added to the IC glass test tubes and about 1 ml of carbon-free water was added to each test tube and swirl to wet the sample. The TIC test tubes were placed in the PrimacsSNC100 instrument rack to determine the TIC content in sediment through acidification and sparging at 150 °C. Following the reaction of carbonates with o-phosphoric acid, the gas mixture containing CO₂ is led by the oxygen carrier gas through the IR detector. The IR detector measures the CO₂ concentration from which the TIC content of the sample is calculated.

3.6.2.2 Grain Size Analysis

About 2 to 5 g (depending on the sediment texture) of fresh wet marine sediment samples were sieved through 2 mm mesh size sieve and analysed for size distribution by Mastersizer 3000, Malvern analyser.

3.6.3 Organic Contaminants (TPHs and PAHs)

The TPHs ranged from C₄ to C₃₆ and 16 PAHs compounds, listed as priority contaminants by the US EPA were analysed in seawater, sediment and oyster tissues samples, including: Naphthalene, Acenaphthylene, Acenaphthene, Fluorene, Phenanthrene, Anthracene, Fluoranthene, Pyrene, Benzo(a) anthracene, Chrysene, Benzo(b) fluoranthene, Benzo(k) fluoranthene, Benzo(a) pyrene, Indeno(1,2,3-cd) pyrene, Dibenzo(a,h) anthracene, and Benzo(ghi) perylene.

The TPHs was analyzed using an Agilent 6890N Network Gas Chromatograph (GC) with Flame Ionization Detector (FID), and for the PAHs analysis Agilent 7890B gas chromatograph coupled to a 5975C triple-axis mass spectrometer (GCMS) was used. Table 3.6 and Table 3.7 show the conditions of the GC used for the analysis of TPHs and PAHs respectively.

Table 3. 6: GC/FID conditions used for analysis of TPHs

GC/FID conditions	
Inlets	Splitless mode, 250 °C, 7.90 psi, 6.3 mL/min
Injection volume	1 µl
Carrier gas	Helium; 0.6 ml/min
Column	Agilent HP-1 (30 m × 250 µm × 0.10 µm)
Oven temperature program	40 °C hold (2 min) to 320 °C hold (10 min) @ 10 °C/min. Total run time 40 min

Table 3. 7: GC/MS conditions used for analysis of PAHs

GC/MS conditions	
Inlets	Pulsed splitless mode, 300 °C, 11.747 psi
Injection volume	1 µl
Carrier gas	Helium; 1.4 ml/min
Column	Restek Rxi-5SILMS (30 m × 250 µm × 0.25 µm)
Oven temperature program	50 °C hold (0.5 min) to 250 °C @ 25°C /min to 290 °C hold (3.5 min) @ 5 °C/min. Total run time 20 min.

3.6.4 Inorganic Contaminants (Trace metals and Total Mercury)

The trace metals including Cd, Cr, Cu, Ni, Pb and Zn were analyzed in seawater, sediment and oyster tissues samples using ICP-OES (Inductively coupled plasma - optical emission spectrometry) (Perkin-Elmer, Optima 7300 DV model).

For total mercury, samples are analysed using the Automatic Mercury Analyzer AULA-254 ASD. Samples introduced into a mixer with stannous chloride solution (tin (II)), then to a reaction cell, and argon gas carries the elemental mercury from the sample to the detector which measures the mercury concentration.

3.6.5 Quality Assurance and Quality Control (QA/QC)

For quality assurance and quality control checks, field blanks and certified reference materials (CRM) were used. For water samples, field blanks were used to verify if sample contamination occurred as a result of reagent and/or environmental contamination, such as from contaminated air at the sampling location. Distilled water was used as a blank water filled in the same sampling containers for water samples. For each sampling site, one field blank was taken for each round. For sediment and oyster samples, the blank samples followed the same extraction and/or digestion methods. For each samples set, at least one blank was used. Duplicate samples account for 5% of the samples.

Table 3. 8: Limit of Detection (LOD) for organic and inorganic contaminates

Compounds	Instrument	LOD (mg/kg)
Organic contaminants		
TPHs	GC/FID	0.47
PAHs		
Naphthalene	GC/MS	0.09
Acenaphthylene	GC/MS	0.09
Acenaphthene	GC/MS	0.09
Fluorene	GC/MS	0.09
Phenanthrene	GC/MS	0.16
Anthracene	GC/MS	0.16
Fluorathene	GC/MS	0.16
Pyrene	GC/MS	0.16
Benzo(a) anthracene	GC/MS	0.19
Chrysene	GC/MS	0.19
Benzo(b) fluoranthene	GC/MS	0.19
Benzo(k) fluoranthene	GC/MS	0.16
Benzo(a) pyrene	GC/MS	0.16
Indeno(1,2,3-cd) pyrene	GC/MS	0.13
Dibenzo(a,h) anthracene	GC/MS	0.13
Benzo(ghi) perylene	GC/MS	0.13
Inorganic contaminants		
Cd	ICP-OES	0.00017
Cr	ICP-OES	0.0012
Cu	ICP-OES	0.00027
Ni	ICP-OES	0.0060
Pb	ICP-OES	0.0012
Zn	ICP-OES	0.0011
Hg	Automatic Mercury Analyzer AULA-254 ASD	0.007

The limit of detection is the smallest amount or concentration of analyte in the test sample that can be reliably distinguished from zero (Currie, 1995). The limit of detection (LODs) were calculated for all analytes using 10 samples of the lowest concentration of standard. Table 3.8 shows the calculated LOD for each analyzed compounds.

Certified reference materials (CRM) for TPHs, PAHs, trace metals and total mercury were used as quality assurance and quality control checks for sediment and oyster tissues samples. Table 3.9 illustrates the recoveries of TPHs and PAHs analytes. For sediment sample, CRM361 (Sigma Aldrich) and NIST 1941b (US NIST) were used for TPHs and PAHs analytes respectively. Whereas for oyster tissues samples, NIST 2974a was used for PAHs. All analyte's recoveries were in the acceptable range of (80%–120%).

Table 3. 9: CRM recoveries for TPHs and some PAHs compounds

Matrix	CRM	Analyte	1	2	Average	Certified value	Percentage Recovery
Sediment	CRM361 (mg/kg)	Total TPHs	374.5	401.4	388	455	85.3
	NIST 1941b (µg/kg)	Naphthalene	852.29	927.20	889.74	848	104.92
		Fluoranthene	743.06	669.83	706.45	651	108.52
		Pyrene	575.18	509.78	542.48	581	93.37
		Benzo(a)anthracene	346.47	285.72	316.10	335	94.36
		Benzo(k)fluoranthene	244.23	198.70	221.47	225	98.43
		Dibenzo(a,h)anthracene	66.77	56.55	61.66	53	116.34
Mussel tissues	NIST 2974a (µg/kg)	Benzo (a) pyrene	10.19	8.04	9.12	9.73	106.75
		Phenanthrene	70.01	63.54	66.78	74.4	111.42
		Benzo (b) fluranthene	38.56	32.36	35.46	41.5	117.03
		Indeno(1,2,3-cd) pyrene	14.02	12.59	13.31	14.9	111.99

The CRM recoveries for trace metals and total mercury for different matrixes (water, coastal sediment, and mussel tissues) are illustrated in Table 3.10. The obtained recoveries were within (85-110%) for selected analytes. The Standard Reference Materials (1641d, 1643F, and 2976) were provided from (NIST/ UK), and Marine Sediment Certified Reference Material (PACS-3) was provided from National Research Council Canada.

Table 3. 10: CRMs recoveries for trace metals and total mercury

Matrix	CRM	Metals	1	2	3	4	Average	Certified value	Percentage Recovery
Water	SRM 1643F (µg/L)	Cd	6.31	6.21	6.54	5.60	6.16	5.89	104.64
		Cr	19.48	18.22	18.70	19.07	18.87	18.50	102.00
		Cu	19.43	18.13	17.96	19.83	18.83	21.66	86.95
		Ni	59.69	59.97	61.59	63.64	61.22	59.80	102.38
		Pb	18.52	18.83	20.38	18.98	19.18	18.49	103.73
		Zn	75.62	78.53	81.73	71.58	76.86	74.40	103.31
	SRM 1641d (µg/L)	Hg	0.72	0.62	0.60	0.60	0.63	0.62	102.34
Sediment	PACS-3 (mg/kg)	Cd	2.30	2.39	2.35	2.40	2.36	2.23	105.81
		Cr	92.61	83.25	87.93	93.86	89.41	91.60	97.61
		Cu	310.27	310.08	310.17	335.98	316.62	327.00	96.83
		Ni	43.27	41.78	42.52	42.60	42.54	39.90	106.62
		Pb	201.76	196.58	199.17	174.39	192.98	188.00	102.65
		Zn	410.21	370.58	390.40	378.97	387.54	379.00	102.25
		Hg	2.73	2.46	3.15	2.84	2.80	2.97	94.11
Mussel tissues	SRM 2976 (mg/kg)	Cd	0.82	0.81	0.81	0.86	0.83	0.82	100.75
		Cr	0.43	0.41	0.42	0.52	0.44	0.50	88.99
		Cu	3.98	4.08	4.03	3.54	3.91	4.02	97.17
		Ni	0.90	0.88	0.89	0.84	0.88	0.93	94.44
		Pb	1.33	1.19	1.26	1.31	1.27	1.19	106.87
		Zn	133.40	127.97	130.69	137.24	132.33	137.00	96.59
		Hg	0.064	0.059	0.062	0.06	0.06	0.06	98.77

3.6.6 Statistical Analysis

The statistical analyses were performed using Excel and SPSS software. The Normality test was applied to all data to check the distribution of data. For normal distributed data, One-way ANOVA was performed followed by a Tukey HSD (Tukey's Honestly-Significant Difference) post-hoc test to determine which pairs of the factor levels are significantly different from each other. Whereas for non-normal distributed data, the nonparametric test (Kruskal-Wallis test) was performed. Post-hoc pairwise comparisons were only applied where a significant difference was noted. The LOD divided by the square root of 2 was used for samples below the limit of detection.

Chapter 4:
**Physicochemical Parameters of
Seawater and Sediment**

This chapter gives details for the general physicochemical parameters for seawater and sediment samples collected in this study, which may have an effect on the accumulation of organic and inorganic contaminants in the three types of matrices. Refer to chapter 3 (section 3.1) for the sampling locations, (section 3.2) for sampling collection techniques, and (section 3.3) for sample preparation. The analysis methodology used for in-situ parameters (temperature, pH, and salinity), TOC for seawater and sediment, and particle size for sediment are well described in chapter 3 (section 3.4).

In brief, the temperature, pH, and salinity for seawater were measured at the four sampling stations in-situ using a portable meter (EXO3 Multiparameter Sonde - YSI). The TOC for surface seawater, surface sediment and sediment core samples were measured in the lab using (Multi N/C 2100S - TOC /TN Analyzer) for seawater samples and (PrimacsSNC100 – SKALAR instrument) for sediment samples. Grain size of sediment samples were measured using Mastersizer 3000.

4.1 In-situ parameters of seawater

The seawater parameters (temperature, salinity, and pH) at the four sites over two years are illustrated in Figure 4.1. For the first-year's sampling (summer 2017 and winter 2017) there was a slight variation in water temperature from (23°C to 28°C) in March 2017 and from (18°C to 23°C) in December 2017 (Figure 18-A). The level of salinity varied between (43psu to 57psu) in summer and from (40psu to 52psu) in winter (Figure 18-B). Umm Bab showed a higher salinity value at both sample intervals which may reflect its proximity to a desalination plant (Richer, 2008). The seawater pH of the four locations in the summer sampling was almost the same (from 8.1 to 8.3), while in winter it ranged from 7.8 to 8.2. For the second-year's sampling (summer 2018 and winter 2018) the water temperature was almost the same at all four sites (28°C to 29°C) in May 2018, while there was a slight variation from (24°C to 27°C) in November 2018. The level of salinity varied between 43psu and 57psu in summer and from (39psu to 58psu) in winter. The pH ranged from 7.9 to 8.2 in the summer sampling, whereas in the winter it ranged from 8 to 8.3. Appendix A-1 shows the in-situ parameters for the four sites from the four rounds in summer and winter seasons in details.

Based on statistical analysis, the temperature at Al Khor was significantly higher ($p = 0.045$) than at the other three sites in summer while in winter no significant differences was observed ($P > 0.05$) (post-hoc Kruskal-Wallis test). Salinity at Umm Bab was significantly higher ($p = 0.01$) than at the other three sites in summer while in winter it was only significantly

higher than Al Wakra (post-hoc Kruskal-Wallis test). The pH at Al Khor was significantly higher ($p = 0.001$) than at the other three sites in summer while in winter no significant differences across sites was observed (post-hoc Kruskal-Wallis test). Appendix A-2 display the Normality and Kruskal-Wallis H test in detail for all parameters.

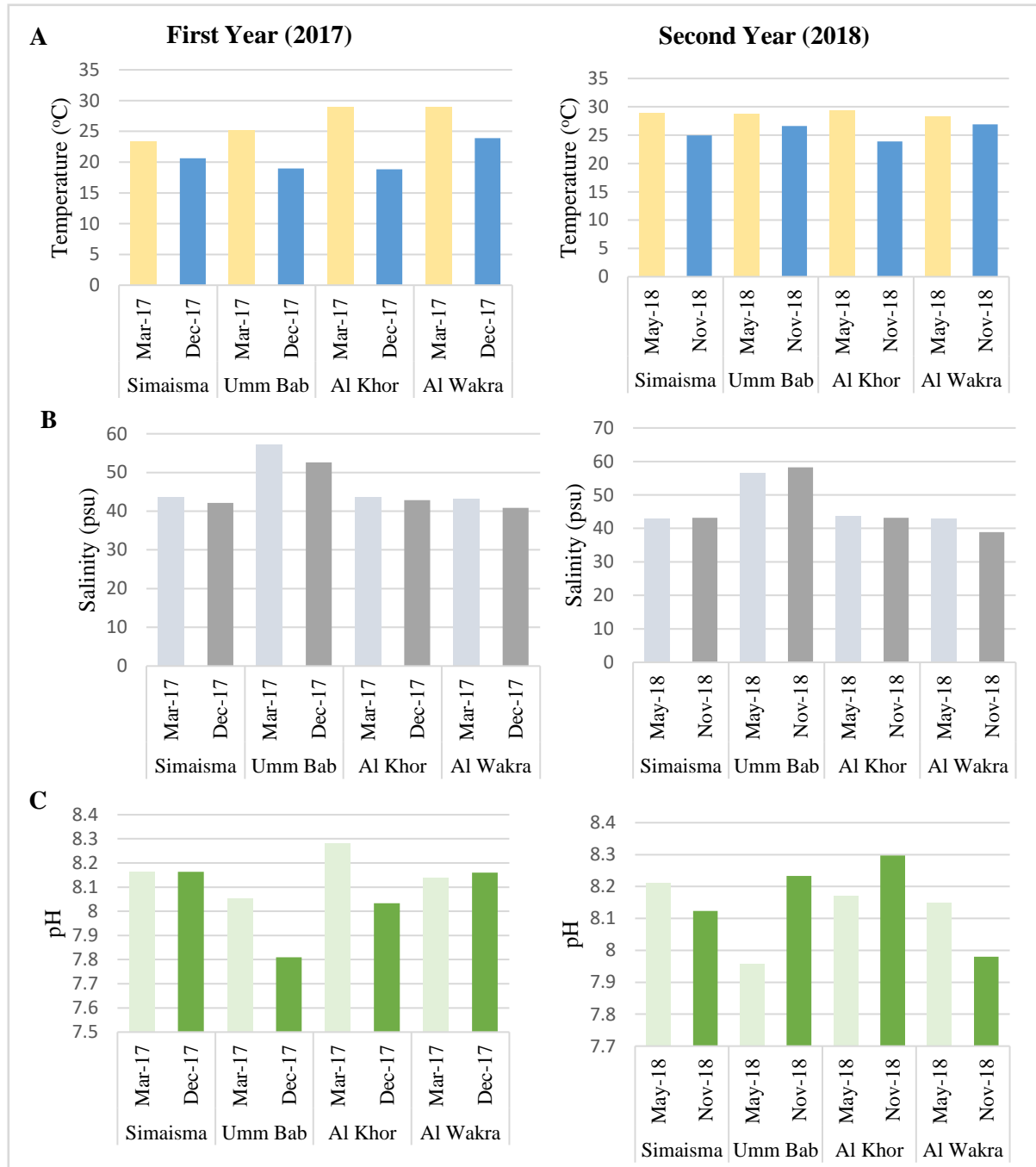


Figure 4. 1: Summary of the physicochemical parameters over the two years for the four sampling sites, A: temperature, B: salinity, C: pH

Comparing the two years, the temperature and salinity had a same trend in both years. There was a significant difference with season, as in summer the values for temperature and

salinity were higher in summer than winter. The temperature in second year (2018) was slightly higher than first year (2017) across all sites. Salinity was almost same for each site in both years with highest values recorded in Umm Bab. While pH values were fluctuated over sites and seasons. Umm Bab and Al Khor in both years shows a slight difference in pH value across seasons.

Overall, the surface seawater temperature range recorded in this study in summer (23.1-30.4 °C) and winter (17.9-26.9 °C) were in the range of historical data for the last seven years (from January to May, 17-31 °C) and (June to December, 18-36 °C) (Sea Temperature, 2021). Likewise, the pH measured in summer (7.95-8.29) and winter (7.8-8.3) was in the ranged recorded for Qatar coastal seawater (8-8.6) (Rivers et al., 2019). For salinity, the average salinity in open ocean is about 35psu “power supply unit” (National Ocean Service, 2021), while those of the Arabian Gulf are higher (around 45psu) (Richer, 2008) because the Arabian Gulf is surrounded by desalination plants with about 50% of worldwide capacity to desalinate seawater. In this study, a high salinity level was recorded. In Simaisma, Al Khor and Al Wakra the salinity ranged from (38.4-44.6psu), while in Umm Bab was from (52.2-58.2psu). This high salinity recorded in Umm Bab is probably due to the desalination plant that disposes a hyper-saline effluent (brine) via surface and near-shore outfall into the coastline (Richer, 2008).

4.2 Abiotic parameters of seawater and sediment

4.2.1 Total Organic Carbon

4.2.1.1 TOC in surface seawater

The TOC concentrations in surface seawater of Qatar during two-year sampling conducted from March 2017 to November 2018 ranged from 26.4 mg/L to 30.3 mg/L with an overall seasonally weighted mean of 28.5 mg/L (Table 4.1). Appendix B-1-1 shows the TOC concentration for each site with the three replicates.

Table 4. 1: The Mean Concentration of TOC in Surface Seawater (mg/L \pm SD)

	Mar-17	Dec-17	May-18	Nov-18	Weighted mean*
Simaisma	28.29 \pm 0.30	28.33 \pm 0.16	27.23 \pm 0.86	27.39 \pm 0.13	27.81
Umm Bab	30.26 \pm 0.59	29.53 \pm 0.75	29.23 \pm 0.26	28.97 \pm 0.26	29.49
Al Khor	27.84 \pm 1.14	29.44 \pm 0.46	26.44 \pm 0.90	27.73 \pm 0.37	27.86
Al Wakra	28.88 \pm 1.09	30.09 \pm 0.18	28.08 \pm 0.10	28.23 \pm 0.78	28.82
Overall mean	28.82	29.35	27.75	28.08	28.50**

*Average of the four rounds. ** Overall seasonally weighted mean

Statistical analysis showed that TOC at Umm Bab was significantly higher than Simaisma ($p = 0.042$) and Al Wakra ($p = 0.026$) in summer, while in winter no significant differences across sites was observed (post-hoc Kruskal-Wallis test).

Generally, seawater samples collected from Al Wakra site had wide range of TOC, while Al Khor samples had a small range in summer but wider range in winter (Figure 4.2). In contrast, the TOC of samples from Umm Bab had a bigger range in summer than winter.

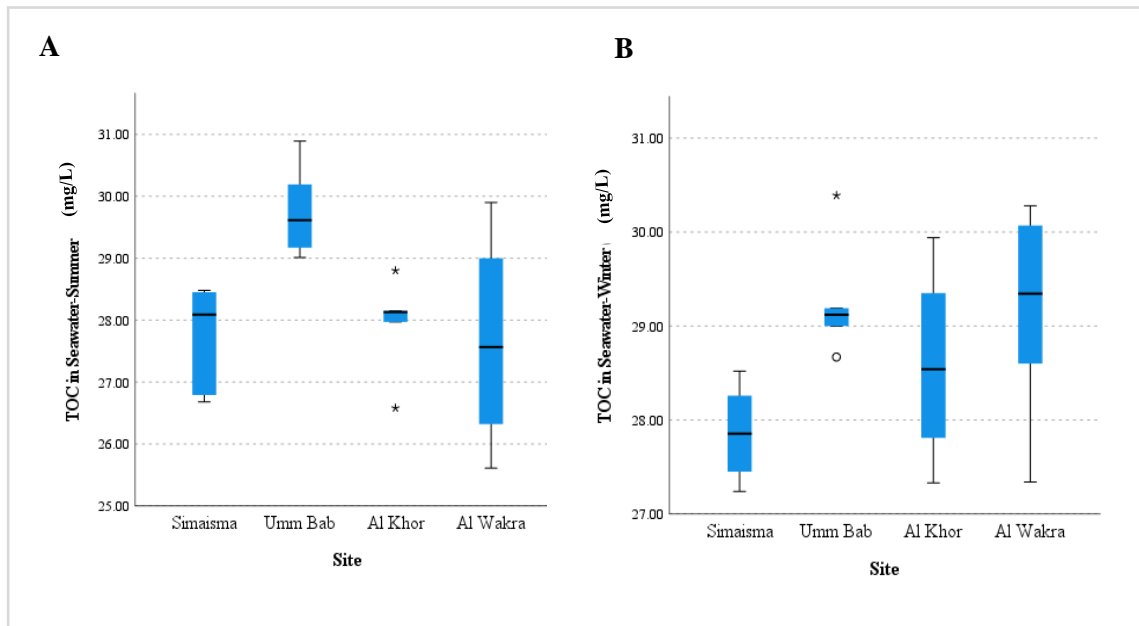


Figure 4. 2: The TOC in seawater samples. (A- In summer seasons. B- In winter seasons).

4.2.1.2 TOC in surface sediment

The TOC content of surface sediment from the four sites was in the range of 0.8 mg/kg to 2.2 mg/kg with an overall seasonally weighted mean of 1.5 mg/kg (Table 4.2). Significantly, higher TOC was observed in Al Khor and Umm Bab in comparison to Simaisma and Al Wakra. The TOC concentration for each site with their replicates is show in Appendix B-1-2.

Table 4. 2: The Mean Concentration of TOC in surface Sediment (mg/kg \pm SD)

	Mar-17	Dec-17	May-18	Nov-18	Weighted mean
Simaisma	1.37 \pm 0.25	1.48 \pm 0.82	1.21 \pm 0.37	1.38 \pm 0.42	1.36
Umm Bab	2.18 \pm 0.22	2.19 \pm 0.19	1.25 \pm 0.15	1.00 \pm 0.38	1.65
Al Khor	1.88 \pm 0.26	2.11 \pm 0.22	2.15 \pm 0.64	1.89 \pm 0.37	2.01
Al Wakra	1.07 \pm 0.06	1.05 \pm 0.06	1.22 \pm 0.61	0.79 \pm 0.06	1.03
Overall mean	1.63	1.71	1.46	1.27	1.51

Al Khor sediment TOC was significantly higher than other sites ($p = 0.031$) in summer (post-hoc Kruskal-Wallis test), while and in winter it was only significantly higher from Al Wakra ($p = 0.013$) (Tukey HSD post-hoc test). Appendix B-2-2 display the statistics used in this section in detail.

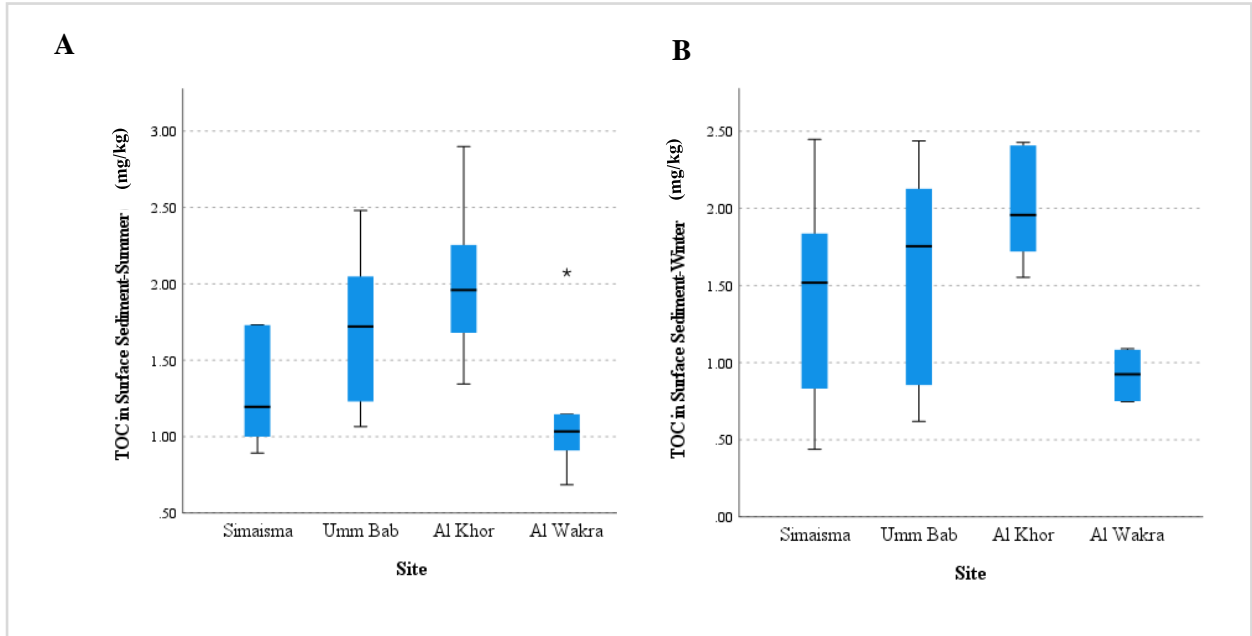


Figure 4. 3: The TOC in surface sediment samples. (A- In summer seasons. B- In winter seasons).

Generally, Al Khor samples had the highest TOC than other sites. Samples collected from the four sites in winter had a wider range than samples collected in summer (Figure 4.3). Comparing levels of TOC in seawater and in sediment shows a non-significant relationship (Figure 4.4).

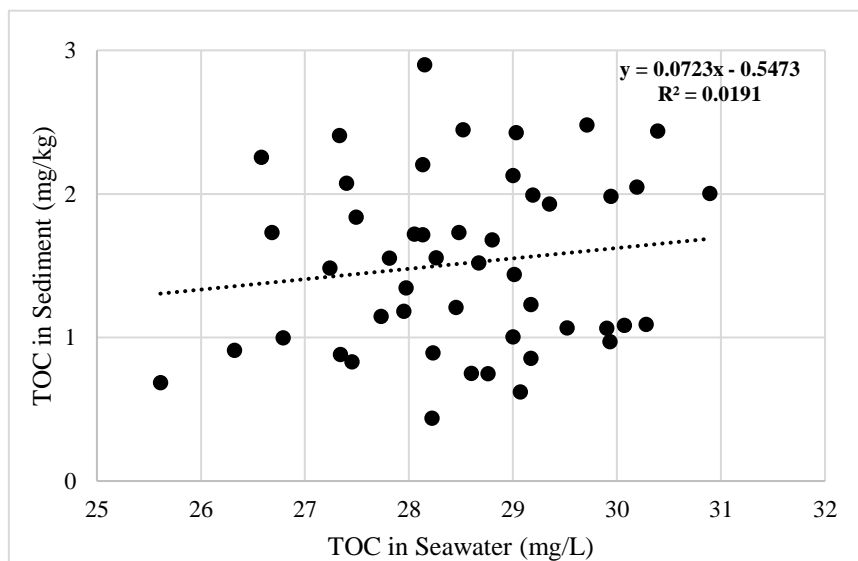


Figure 4. 4: Correlation between TOC in seawater and sediment

4.2.1.3 TOC in Sediment Core

Overall, the TOC level in sediment core samples from all sites ranged from 0.6 mg/kg to 2 mg/kg (Figure 4.5). It can be seen clearly that the TOC level in Al Wakra core samples increased with depth but decreased below 25cm. This is an interesting profile as the surface has the lowest values (0.6 mg/kg) yet deeper (in the past) levels were maximal (2 mg/kg). Likewise, cores from Umm Bab and Al Khor showed decline of TOC level in depth deeper than 20cm. However, cores from Simaisma showed increased of TOC level till 15cm depth, then it decreased in 20cm depth and started to increase again.

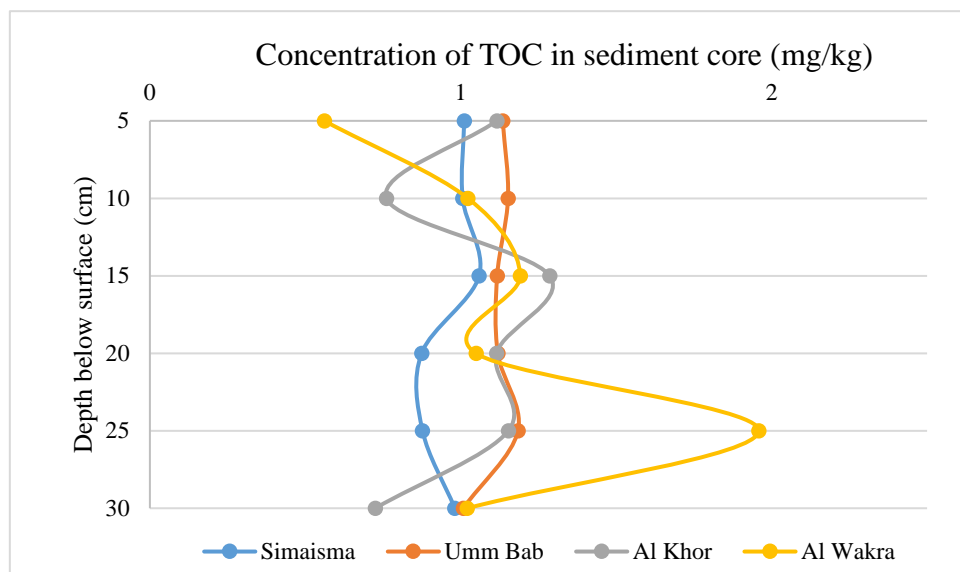


Figure 4. 5: The mean concentration of TOC in sediment core

In general, the TOC concentration in this study in the surface coastal sediments from Qatar's coastline ranged from 0.8 to 2.2 mg/kg. Data regarding the concentration of TOC in the Arabian Gulf are sparse. The earliest data was by [Evans \(1966\)](#) reported levels of TOC in the range of 0.8–1.5 mg/kg. [Hartmann et al. \(1971\)](#) reported that marine sediment in the Arabian Gulf contains a maximum of 2 mg/kg of TOC. Later, in 1992, other researchers reported that the level of TOC within the marine sediments of Kuwait ranged from 0.5–0.8 mg/kg, [Al-Saad et al. \(2017\)](#) reported a TOC range of 0.3–0.9 mg/kg within sediments collected from the Shatt Al-Arab River and North-West Arabian Gulf and more recently [Hassan et al. \(2018\)](#) reported levels between (0.2-0.7 mg/kg) from sediment collected from northern and eastern regions of Qatar coastal zones at water depths varying from 18 to 67 m. TOC concentration reported ranged from 0.2 mg/kg to 2 mg/kg. However, the only available data pertaining to TOC levels in the Qatar coastline itself were published by [de Mora et al. \(2010\)](#), who reported a range of 0.5 mg/kg and 2.3 mg/kg TOC same range compared to our results. It is noted that de Mora et

al.'s data were derived from sediments sampled closer to the coastline of Qatar as our study, where land-based sources of TOC may increase nearshore sediment TOC levels via atmospheric deposition and/or terrestrial runoff. The range of TOC in core samples was (0.6-2 mg/kg). Our TOC results are comparable to data from earlier reports for the Arabian Gulf.

4.2.2 Grain size

4.2.2.1 Surface sediment

The average values for the three categories of sediment particles in the four studied areas are illustrated in Table 4.3. Results confirm that site soil textures were mostly comprised of sand. Overall, sandy particles comprised more than (97.8±1) percentage of the sediment texture collected from Umm Bab and Al Wakra, and more than (58.6±18.3) percentage of the sediment texture collected from Simaisma and Al Khor. Appendix C shows the grain size measurement for all samples with replicates.

Table 4. 3: The mean grain size measurement of surface coastal sediment

Site	Time	% Sand	% Silt	% Clay	Sediment Type
Simaisma	<i>March 2017</i>	69.72± 12.68	27.69±11.11	2.58±1.82	Silty Sand
	<i>December 2017</i>	58.62±18.27	38.74±16.79	2.64±1.47	Silty Sand
	<i>May 2018</i>	81.11±19.53	17.76±17.79	1.13±1.74	Silty Sand
	<i>November 2018</i>	91.28±10.00	8.45±9.61	0.04±0.07	Silty Sand
Umm Bab	<i>March 2017</i>	98.58±1.91	1.42±1.91	0	Sand
	<i>December 2017</i>	99.09±1.12	0.91±1.12	0	Sand
	<i>May 2018</i>	98.89±1.92	1.11±1.92	0	Sand
	<i>November 2018</i>	99.73±0.46	0.27±0.46	0	Sand
Al Khor	<i>March 2017</i>	69.47±6.46	27.94±6.45	2.59±0.11	Silty Sand
	<i>December 2017</i>	72.35±10.76	26.00±10.11	1.65±0.65	Silty Sand
	<i>May 2018</i>	77.03±18.61	20.67±16.46	2.30±2.18	Silty Sand
	<i>November 2018</i>	86.20±1.85	13.18±1.36	0.05±0.02	Silty Sand
Al Wakra	<i>March 2017</i>	97.79±1.04	2.21±1.03	0.01±0.01	Sand
	<i>December 2017</i>	99.91±0.03	0.33±0.41	0	Sand
	<i>May 2018</i>	99.32±1.06	0.68±1.06	0	Sand
	<i>November 2018</i>	99.95±0.09	0.05±0.09	0	Sand

Based on the statistical analysis, the Kruskal-Wallis H test showed that site had a significant effect on the percent sand, silt, and clay ($p < 0.05$). While season showed no significant effect on percent sand, silt and clay. Figure 4.6 shows the overall grain size fraction for each site.

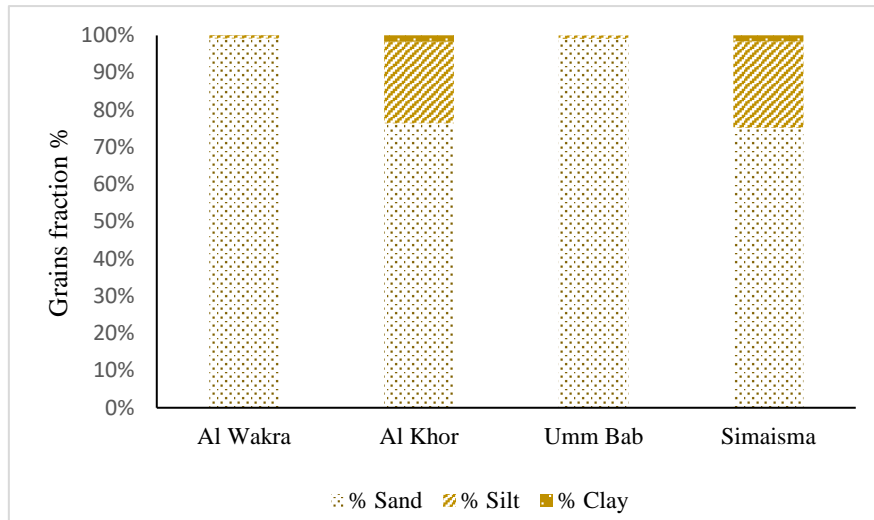


Figure 4. 6: The mean grain size fractions in coastal surface sediment of the four sites in all seasons

4.2.2.2 Sediment Core

Figure 4.7 shows the average values for the sediment particles categories in the four studied areas. It can be seen clearly that no differences were found in core samples sections in all sites. Umm Bab core samples were all sandy from 5cm to 30 cm depth. On the other hand, in the three other sites the sediment core samples were silty sand. Comparing with Al Wakra surface sediment samples which was sandy with more than 97%, core samples which was collected from the foreshore at the same site showed a percentage of silt more than 39.

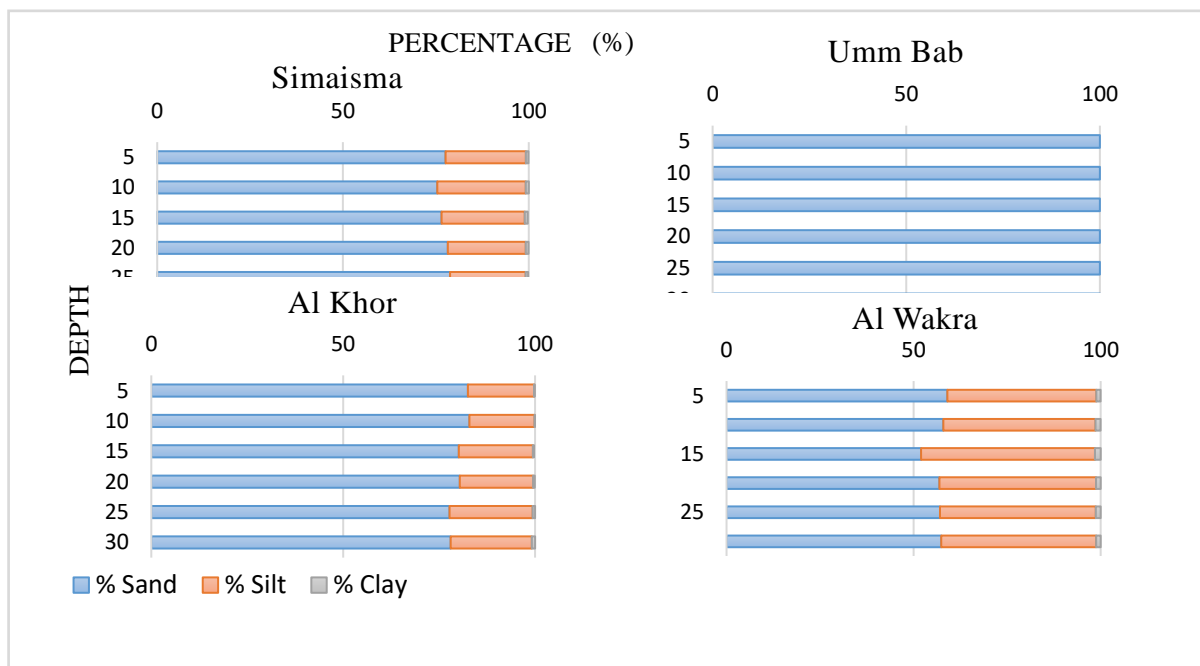


Figure 4. 7: The mean grain size of sediment core samples from the four different locations

4.3 Summary

The overall temperature recorded in the four sites in summer seasons was between (23-29°C), while in winter seasons ranged from 18 to 27°C. In terms of salinity, in summer the levels ranged between 43- 57 psu, whereas in winter they lay between 39- 58 psu) with highest salinity detected in Umm Bab site where there is a desalination plant near the coast. The pH values recorded in summer and winter in the four sites, however, were almost the same ranging from 7.9 to 8.3 and 7.8 to 8.3 respectively.

In general, the grain size fractions of the surface coastal sediments in this study of Qatar's coastline were comparable with local data reported by [Hassan et al., \(2018\)](#) who reported a high sand percentage in the inshore sites with clay fractions reported at offshore sites.

Since small particles (silt and clay) which have a relatively large surface area compared to sand particles, they tend to have a higher concentration of TOC, thus high TOC levels in surface sediment and in surface layer (5cm) of sediment cores were observed in Al Khor site where the sediment showed a higher percentage of silt and clay (21.95% and 1.65%, respectively) than other sites. However, Umm Bab site (which consist of large particles of "sand") showed also high levels of TOC in surface sediment and in surface layer (5cm) of sediment cores, as well as in seawater. These high levels observed in Umm Bab may be related to the site' s geographical position, as Umm Bab is a more enclosed basin which can trap materials and contaminants.

As an overall idea, all the four sites have approximately same range of seawater temperature, pH, TOC in seawater and salinity except Umm Bab site which shows higher salinity levels. The sites could be grouped based on their sediment characteristics, where Umm Bab is consisted of sandy particles and other three sites are silty sand particles, with high TOC level in the Al Khor and Umm Bab sites.

Chapter 5:

**Distribution of organic contaminants (TPHs, PAHs)
in seawater, surface sediment, core sediment, and
oyster tissues around the coastline of Qatar**

5.1 Introduction

Persistent organic chemicals are toxic chemicals that can adversely affect human health and the environment. Because they can be transported by wind and water, persistent organic chemicals generated in one country can affect people and wildlife far from where they are used and released (EPA, 2002). Persistent organic chemicals such as total petroleum hydrocarbons (TPHs) and polyaromatic hydrocarbons (PAHs) are associated with a variety of industrial activities such as refineries, manufacturing of crude oil, spill sites, waste disposal and petrochemical sites (Tolosa et al., 1996; WHO, 2003; Vazquez-Duhalt & Quintero-Ramirez, 2004, p. 447). Once in the environment, these contaminants interact with sediments, the water column and organisms; such interactions are controlled by several physical and chemical processes, and the final result may be chemical release, immobilization, or their transformation into more reactive forms or sub products, which are more effectively available to organisms (National Research Council, 2003).

It is now internationally agreed that the assessment of environmental risks based on ecological quality is best undertaken using an integrated method measuring both chemical and appropriate biological parameters in guardian species (EPA, 2019). As such, bivalve molluscs, including mussels and oysters, have been used extensively in marine coastal monitoring programs. Examples include the U.S. “Mussel Watch” program (NOAA's Mussel Watch Program) in 2015 to 2019 (Johnson et al., 2019) and initiatives in the Arabian Gulf under the guise of ROPME in 2011 (ROPME, 2011). Mussels are ideal sentinel organisms, with significant ecological importance and a wide geographical distribution (Dumbauld et al., 2009). Furthermore, they can bio-accumulate pollutants and exhibit a range of biological responses when stressed or exposed to environmental contaminants. In Qatar, the pearl oyster, *Pinctada radiata* (*P. radiata*) is considered an essential part of the nation's cultural heritage and one of the key economic foundations upon which the country developed. However, the pearl oyster is not immune to environmental stressors and, as Qatar has prospered along with urban and industrial development of coastal areas, *P. radiata* populations have declined significantly (Leitão et al., 2017).

Whereas open water marine environments tend to be relatively free from pollution, the coastal zones, especially in the semi-enclosed water bodies, that are seemingly most affected by the human derived pollutants (Sojinu et al., 2012). The Arabian Gulf, as a branch of the Indian Ocean, is ecologically vulnerable ecosystem and has approximately two-thirds of the

world's proven oil reservoirs (Tolosa et al., 2005). It is an environmentally stressed body of water because over 4.7% of the world's oil related pollution is concentrated on this region (Madany et al., 1998). Various activities have resulted in a significant influx of different types of chemical pollutants to the coastal environment of the Gulf, including those which are known to have a variety of adverse (e.g., reproductive and mutagenic) impacts on marine organisms (Massoud et al., 1996; de Mora et al., 2010; Lyons et al., 2015; Leitão et al., 2017). Chemical contaminants have been found to be present in food products harvested from the sea and certain species of fish and shellfish collected from the Gulf are known to fail international food safety limits (Freije, 2015). In Kuwait, for example, the land-based input of pollutants reaching coastal sediments is mainly from various industrial and municipal discharge points, sewer branches, thermal and chlorinated effluents from power plants, and shipping and dockyard activities (Gevao et al., 2016). The Arabian Gulf region is a semi-enclosed nature and has a peripheral harsh condition, thus problems associated with oil appear to be of greater importance comparing with the other regions. The coastline of Qatar is directly affected by a variety of anthropogenic activities. In recent decades, the industrial and population growth of Qatar has led to a rapid coastal development (Shandas et al., 2017). Thus, Qatar's coastal environment faces many problems because of the environmental impacts of development. Pressures include wastes released in the coastal waters and the resuspension of sediment with construction in coastal areas (Ministry of Development Planning and Statistics, 2017). Primary point sources of pollution include discharge of industrial and sewage effluent within few kilometers of the Qatari shoreline and wastes released from oil and desalination industries (Al-Mamoon & Rahman, 2019, p. 223).

With Qatar relying entirely on seawater for the production of potable water and seafood as the only local source of protein in diet, it is important to determine how these marine and coastal pollutants pose a threat to national water and food security. Moreover, pollution of coastal habitats can lead to a decrease in species diversity (Kurylenko & Izosimova, 2016). As such, protecting Qatar's marine and coastal ecosystems, drinking water and food from chemical contamination is a core component of environmental development within the National Vision 2030, which states that there should be "Management of the environment such that there is harmony between economic growth, social development and environmental protection." (Qatar National Vision 2030, 2008, pg.11).

Environmental research has been performed in some Gulf countries to assess the occurrence of organic contaminants (Total Petroleum Hydrocarbons (TPHs), Polycyclic Aromatic Hydrocarbons (PAHs)) in water, sediment and biota tissues. Five studies have reported the levels of PAHs in Kuwait's marine sediment (Lyons et al., 2015; Beg et al., 2003; Bach et al., 2003 and Saeed et al., 1996). Tolosa et al. (2005) examined the total level of TPHs and PAHs in biota and coastal sediments from Bahrain, UAE, and Oman. Moreover, levels of TPHs in marine sediment from Bahrain and oyster tissues from Oman were reported by de Mora et al. (2010). Two studies have investigated the bioavailability of TPHs in sediments from Saudi Arabia and Kuwait (Fowler et al., 1993; Lyons et al., 2015).

Although the Qatari coastal environment has been impacted by marked industrial expansion and anthropogenic pressure over the last several decades (Advancing Sustainable Development, 2009), few studies have investigated organic contaminants in Qatar's coastal environment such as aliphatic hydrocarbons (TPHs) and aromatic hydrocarbons (PAHs) in sediment and biota. In this context, the 'National Priority Research Program' NPRP 9 project entitled "The Pearl Oyster from national icon to a guardian of Qatar's marine environment" commenced in 2017 and was completed by 2019. Whereas this project deals with a wider range issue, within that framework I focus on analyzing organic contaminants including TPHs and PAHs, using appropriate analytical methods in the seawater, sediment, and pearl oyster tissues. The study aimed to determine the transfer of contaminants from environmental samples to oysters as an early warning tool to assess environmental quality and coastal pollution. Thus, the study aimed to explore the applicability of *P. radiata* as an early warning pollution indicator for organic contaminants.

5.2 Methodology

5.2.1 Sampling and study area

The seawater, coastal sediment, sediment cores, and oyster tissues samples taken from the same sampling sites and strategies followed in Chapter 3. For sample collection locations and techniques, please refer to chapter 2 (section 2.1 and 2.2).

5.2.2 Laboratory techniques protocols

5.2.2.1 Chemicals and reagents

The Organic solvents hexane and methylene chloride (SIGMA-ALDRICH, UK) were used for the dissolution and extraction of samples. Anhydrous sodium sulfate (SIGMA-ALDRICH, United States) and diatomaceous earth were used for the extraction procedure. Dry Glycine, Sodium Carbonate, Calcium Carbonate and Phosphoric Acid were used in TOC analysis. Methanol, Acetonitrile and internal standard mixtures were also used.

5.2.2.2 Glassware and general instruments

For the extraction from the sediment an Accelerated Solvent Extractors (Dionex ASE 350) was used. For the extraction, a mortar and pestle, extraction cells, cellulose filter disks, collection vials (60ml), capes, test tubes, pipettes and spatulas were used. In addition, a solvent evaporator (Dionex SE 500), analytical balance, freezer, gloves, funnels, volumetric flasks, beakers, and GC vials were used. Gas Chromatography/ Flame Ionization Detector (GC/FID) and Gas Chromatography/ Mass Spectrometry (GC/MS) were used for the chromatographic analyses. For TOC analysis, ceramic crucibles and TIC test tubes were used. A 2 mm mesh size sieve was used for grain size analysis.

5.2.2.3 Sample Preparation

For preparation of seawater, surface sediment, sediment cores and pearl oyster tissues samples, please refer to Chapter 3 (section 3.3).

5.2.2.4 Samples Extraction

5.2.2.4.1 Seawater Extraction for GC Analysis

The EPA (3510C) extraction process for organic pollutants from water samples by the liquid-to-liquid extraction was followed ([USEPA, 1996a](#)). Refer to Chapter 3 (section 3.4.1) for full description of the procedure.

5.2.2.4.2 Coastal Sediment and Oyster Tissues Extraction for GC Analysis

To extract the TPHs and PAHs from sediments and biota samples, a Dionex 350 Accelerated Solvent Extractor (ASE) (US-EPA method 8015B) was used (USEPA, 1996b). Chapter 3 (section 3.4.2) presented detailed description of the method.

5.2.2.5 Samples Analysis

5.2.2.5.1 Analysis of TOC and grain Size

The analysis of TOC for seawater and sediment samples, and grain size for sediment samples were described in detail in Chapter 3 (sections 3.4.2 and 3.4.3).

5.2.2.5.2 Analysis of TPHs and PAHs

For the analysis methods and conditions used for analysis of TPHs and PAHs using GC/FID and GC/MS (Accredited by A2LA- ISO 17025), please refer to Chapter 3 (section 3.4.4).

5.2.3 Quality Assurance and Quality Control (QA/QC)

For quality assurance and quality control checks, field blanks and certified reference materials (CRM) were used. For full description of the QA/QC used for organic contaminants, refer to Chapter 3 (Section 3.5.5). The limit of detection (LOD) and CRMs for inorganic contaminants is represented in Chapter 3 (Table 3.8, and Table 3.9 respectively).

5.2.4 Statistical Analysis

For the statistical analyses, Excel and SPSS software were used. Refer to chapter 3 (Section 3.5.6) for full description of statistics used for organic contaminants data.

5.3 Results and Discussion

A total of 216 samples were analysed including 48 samples of surface seawater, 48 samples of surface sediment, 72 sediment core samples and 48 samples of oysters. At the four sites and each sample interval (March 2017, December 2017, May 2018, and November 2018), in-situ parameters (temperature, salinity and pH) of seawater were recorded. In addition, abiotic parameters (TOC and grain size characteristics) were measured in the seawater and sediment samples collected from the four sites two times a year over two years; as well as sediment cores which were collected from the four sites in May 2019 (refer to Chapter 4 for physicochemical parameters data). The levels of organic contaminants (TPHs and PAHs) were quantified in the abiotic matrices (surface seawater, surface sediment, sediment core) and the biotic tissues of Pearl Oyster (*P. radiata*).

5.3.1 TPHs and PAHs in Surface Seawater

The concentrations of TPHs in surface seawater ranged from 1.16 to 271.77 $\mu\text{g/L}$ with an overall seasonally weighted mean of 64.83 $\mu\text{g/L}$. Significantly higher TPHs were observed at all sites in the first sampling (March 2017) compared to other three sample visits with an overall mean of 192.05 $\mu\text{g/L}$. The level of PAHs found in surface seawater from the four sites over the two-year sampling show very low levels and are all less than limit of detection (<LOD).

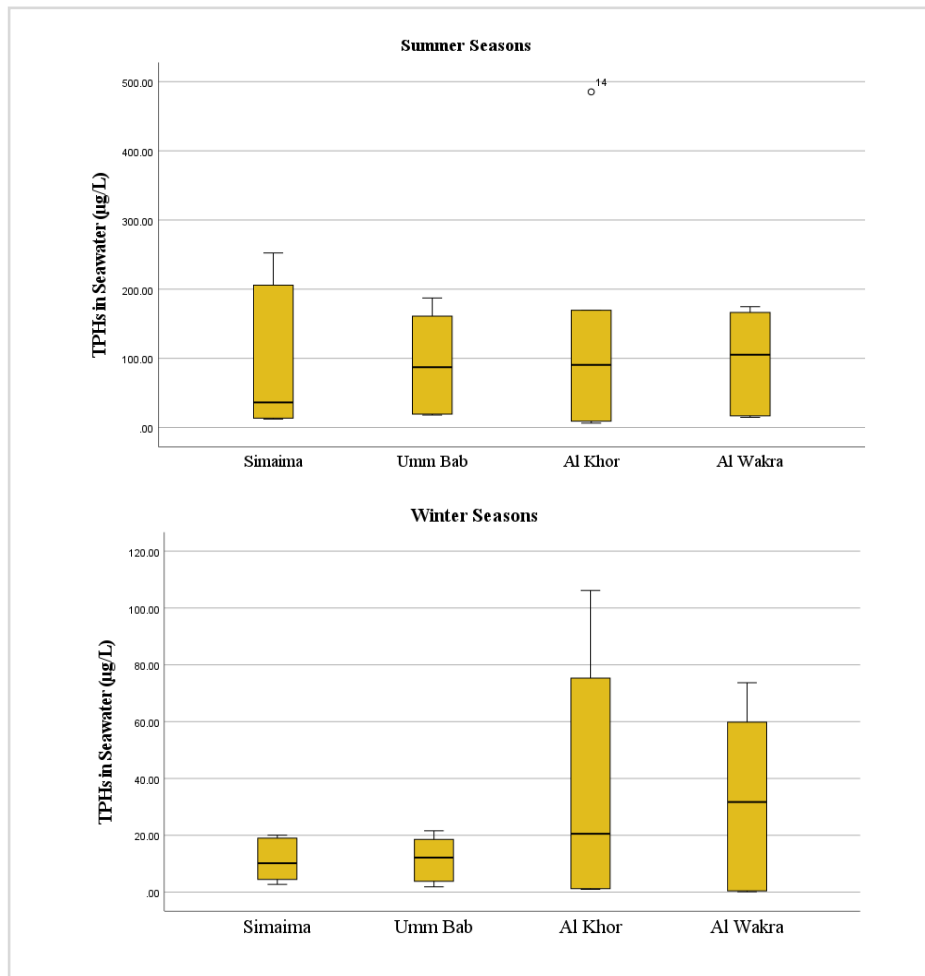


Figure 5. 1: Concentration of TPHs in seawater samples in summer seasons (March 2017 and May 2018) and winter seasons (December 2017 and November 2018).

In general, the concentration of TPHs in surface seawater in the summer season (March 2017 and May 2018) was higher than in the winter season for the same year (December 2017 and November 2018) (Figure 5.1). Although it was found to systematically decrease over time from summer to winter. The TPHs concentration for each site in details presented in Appendix D-1-1. No significant spatial difference of TPHs in summer or winter was observed across the sampling stations.

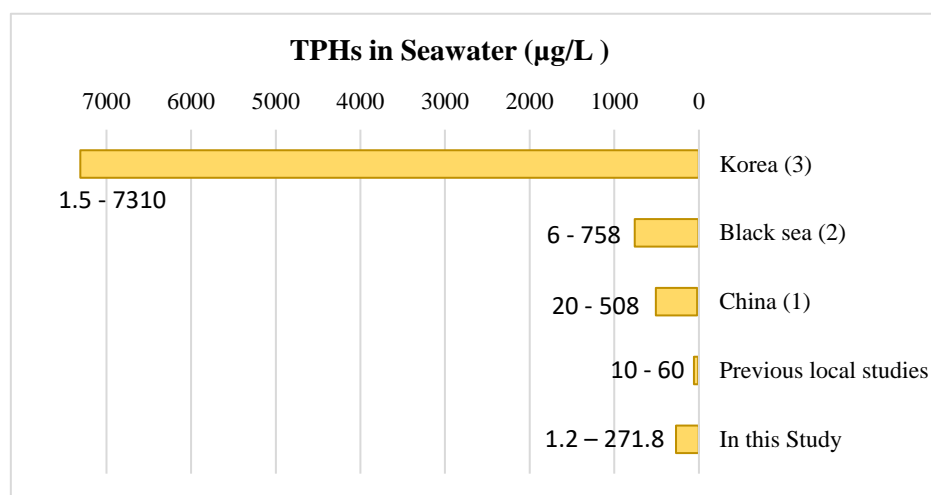


Figure 5. 2: Ranges of TPHs in seawater from different area [(1): [Li et al. \(2010\)](#), (2): [Tığaıuş et al. \(2016\)](#), (3): [Kim et al. \(2013\)](#)]

The Figure 5.2 shows the ranges of TPHs concentration reported from various locations around the world. The concentration of TPHs in seawater from previously reported study from Qatar collected from Al Khor, Al Wakra Harbor, and Doha Harbor in different seasons ranged from 10 to 60 µg/L ([Leitão et al., 2017](#)). Compared to global levels, the TPH levels reported in this study sit within the lower range that has been found worldwide based in selected global studies (1.5 to 758 µg/L) excluding the high level reported in Korea ([Kim et al., 2013](#)). In China, the level was between 20 to 508 µg/L ([Li et al., 2010](#)). [Tığaıuş et al., 2016](#) found a higher level of TPHs in the range of 6- 758µg/L from the Black Sea, while wide range with extremely high value reported from Korea seawater (1.5 to 7310µg/L) by [Kim et al. \(2013\)](#). The highest level detected in Korea was in December 2007 when oil tanker Hebei Spirit released approximately 12,547,000 L of crude oil off the west coast of Korea. Although Qatar sits in Gulf which is close basin and have a lot of economic activity and hydrocarbon exploration, low levels reported in Qatar seawater probably may related to the remobilization of oil by continuing shoreline cleanup activities and subsequent wave/tidal actions.

Even though in this study no PAHs were recorded in seawater samples, [Leitão et al. \(2017\)](#) reported concentration of PAHs in seawater from previously study from Qatar collected from Al Khor, Al Wakra Harbor, and Doha Harbor in different season ranged between 0.06 to 1.37µg/L. In Kuwait, high concentration of PAHs was found (154.89µg/L) ([Saeed et al., 2011](#)). The findings of ([El Nemr and Abd-Allah, 2003](#), [Xiang et al., 2018](#) and [Nizzetto et al., 2008](#)) match the finding of Qatar's seawater profile with a PAHs concentration of (0.047µg/L in Egypt), (0.35µg/L in China) and (0.0007- 0.001µg/L in Atlantic Ocean) respectively. However,

Valavanidis et al. (2008) reported higher level of PAHs from Saronikos Gulf, Greece with average concentration of (113-459 $\mu\text{g/L}$). Low concentration of PAHs observed in seawater samples collected in this study may be due to the relatively high hydrophobicity of PAHs which results in a considerable increase of their ability to accumulate in soil and sediment in comparison to water (Karthikeyan et al., 2001).

5.3.2 TPHs and PAHs in Surface Coastal Sediment

The concentration of TPHs in surface sediment from the four sites ranged between 75.02 and 1751.82 $\mu\text{g/kg}$ with an overall seasonally weighted mean of 440.43 $\mu\text{g/kg}$. High TPHs concentrations were most noticeably in summer in Al Khor site compared to Umm Bab, Simaisma and Al Wakra and less marked in winter. Seasonally, the overall mean concentration of TPHs for all sites in summer 2018 (May 2018) was the highest. Appendix D-1-2 shows the detailed concentration of TPHs in the four sites with their replicates.

The Kruskal-Wallis H test for TPHs in summer seasons across sites showed a significant difference ($p = 0.018$) (Figure 5.3). The post-hoc pairwise comparisons revealed that significant effects have been found between Simaisma and Al Khor ($p = 0.014$). While in winter, no significant differences were observed ($p = 0.237$).

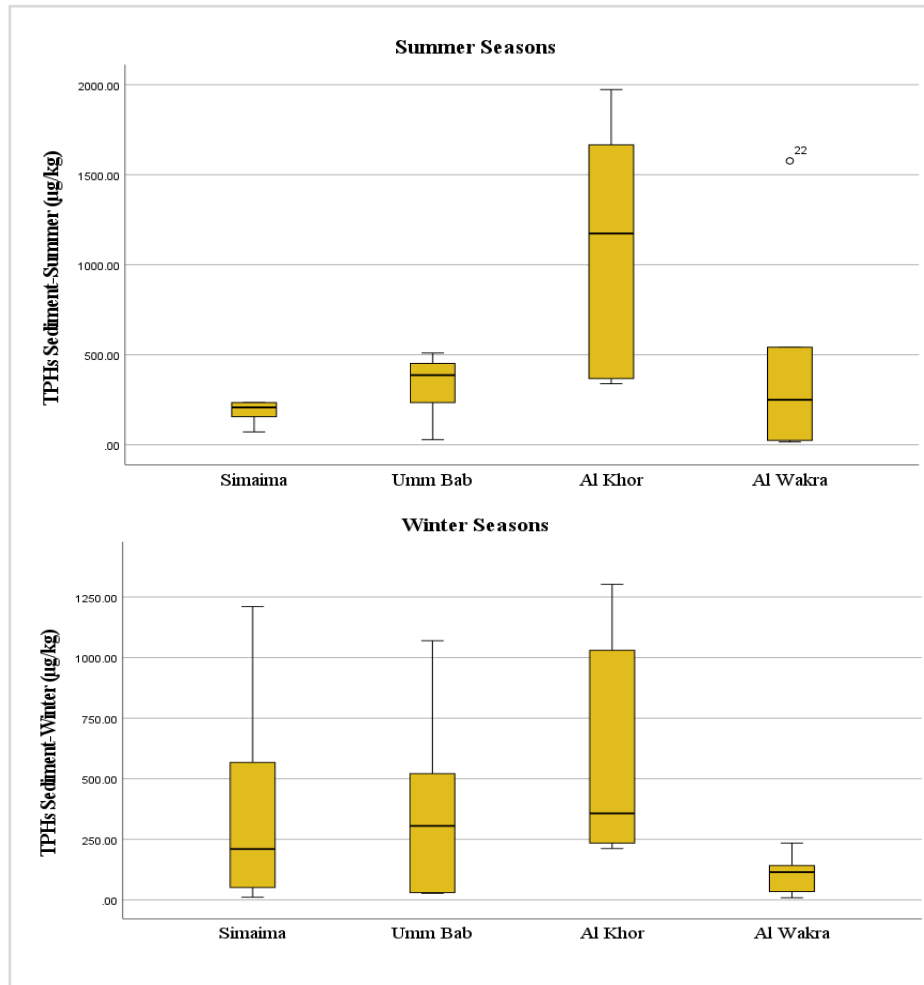


Figure 5. 3: Concentration of TPHs in surface sediment samples in Summer seasons (March 2017 and May 2018) and Winter seasons (December 2017 and November 2018).

The average values of the $\Sigma 16$ PAHs concentrations in surface coastal sediment from the various stations were between 4.25 to 36.73 $\mu\text{g}/\text{kg}$ dry weights with an overall mean of 22 $\mu\text{g}/\text{kg}$. The highest concentration was found in Al Khor, followed by Simaisma then Al Wakra, and the least was in Umm Bab. The PAHs values for the three replicates in each site are illustrated in Appendix E-1-1.

The One-way ANOVA of PAHs in sediment revealed that no significant differences were observed in summer or winter across sites (Figure 5.4). Appendix E-2-1 illustrated the statistics data for TPHs and PAHs in sediment.

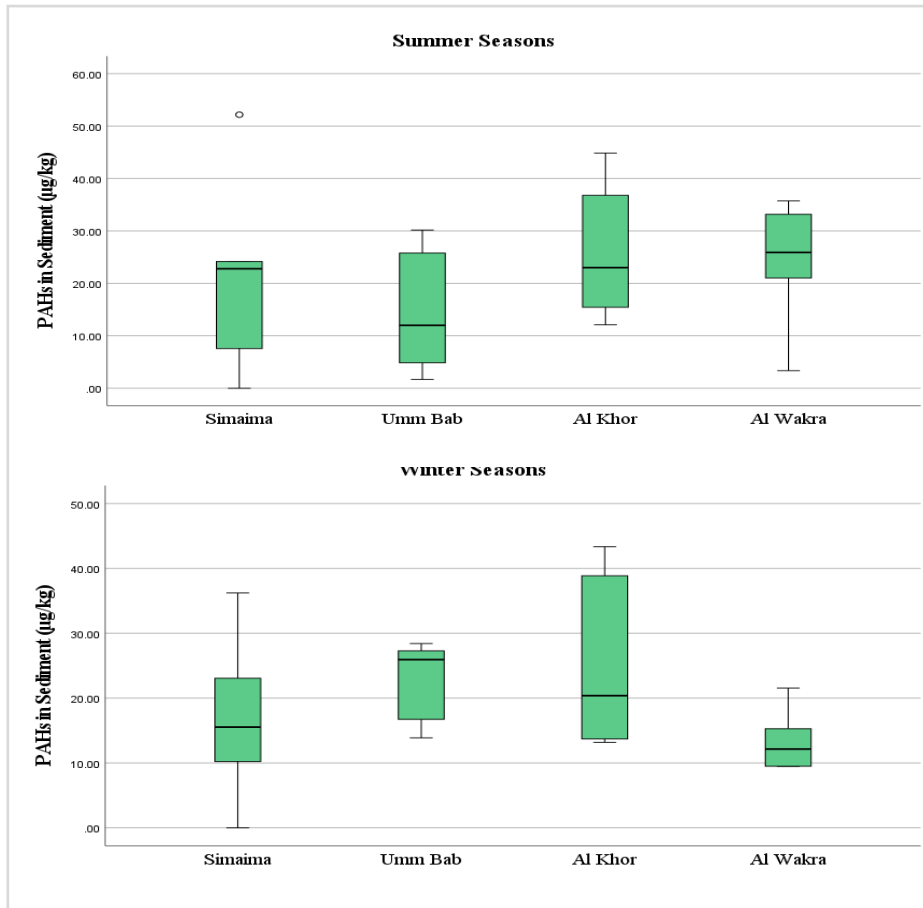


Figure 5. 4: Concentration of PAHs in surface sediment samples in summer seasons (March 2017 and May 2018) and winter seasons (December 2017 and November 2018).

Six PAHs compounds were detected in the sediment in various levels. Pyrene showed high level than other PAHs compounds in all sites and most seasons followed by Anthracene (Figure 5.5). The other four PAHs compounds (Benzo (a) pyrene, Dibenz(a,h) anthracene, Indeno(1,2,3-cd) pyrene and Benzo (ghi) perylene were detected in low level, ranged from (0.02- 5.05 µg/kg).

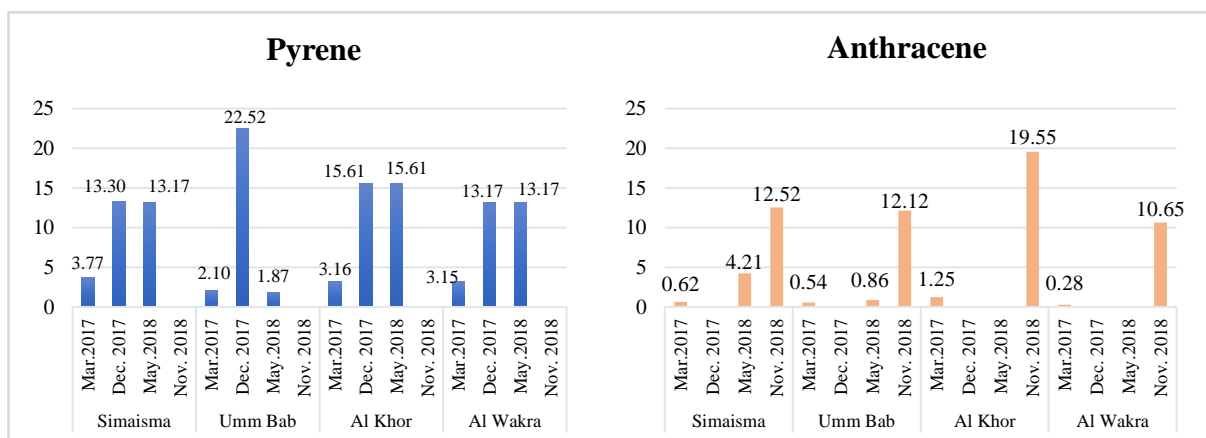


Figure 5. 5: Concentration of most detected PAHs in the surface coastal sediment samples (µg/kg dry weight)

Locally, compared with previous local studies of coastal sediment from Qatar, the TPHs measurement ranged from 75.02 to 1751.82 $\mu\text{g}/\text{kg}$ where in the range of previous local (Table 2.7): 17.3- 79.3 $\mu\text{g}/\text{kg}$ (Rushdi et al., 2017); 160- 1700 $\mu\text{g}/\text{kg}$ (Leitao et al., 2017); and 2200- 84000 $\mu\text{g}/\text{kg}$ (Tolosa et al., 2005). The high levels reported by Tolosa et al. (2005) where from Qatari sites impacted by the oil terminal and refinery plant (Umm Said, Dukhan, Ras Lafan). Moreover, the concentrations of total PAHs (from 4.25 - 36.73 $\mu\text{g}/\text{kg}$) sit within the range of previous local studies (0.29 to 1560 $\mu\text{g}/\text{kg}$). The lowest values were reported by Leitao et al., (2017) and the highest value measured by Soliman et al. (2019).

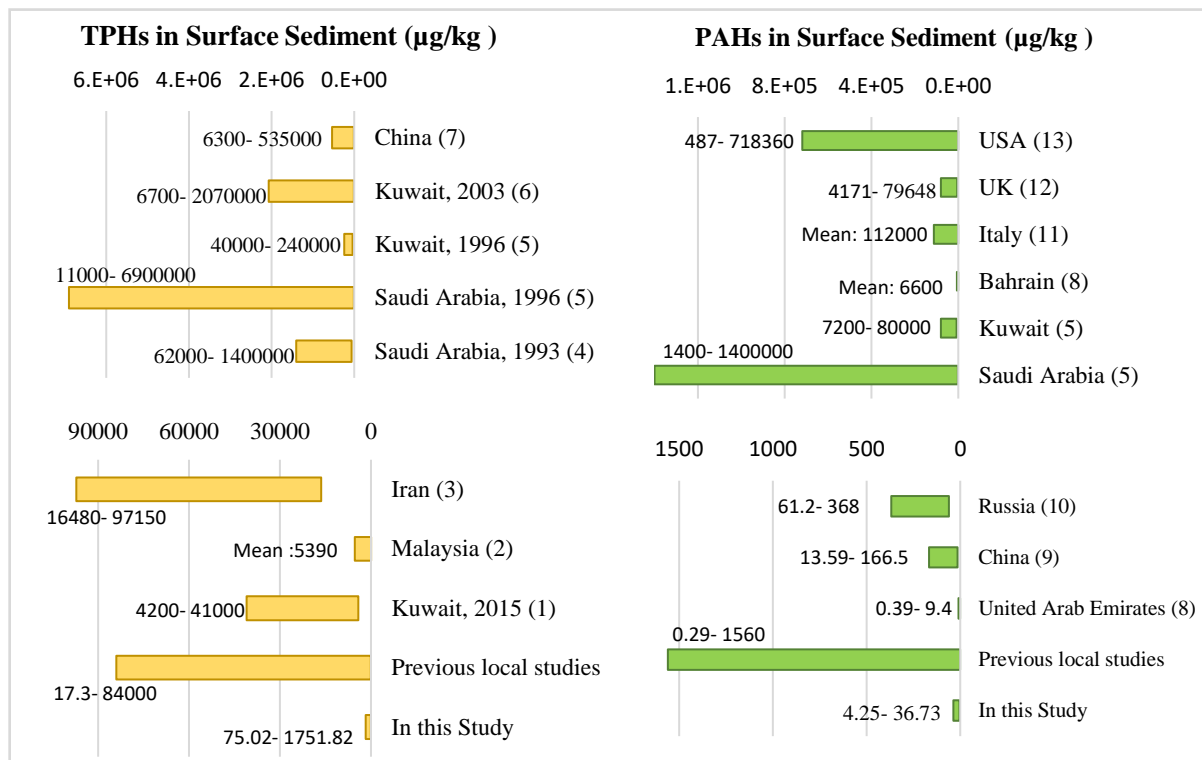


Figure 5. 6: Ranges of TPHs and PAHs in surface sediment from different area [(1): Lyons et al. (2015), (2): Ali et al. (2015), (3): Tehrani et al. (2016), (4): Fowler et al., (1993), (5): Readman et al., (1996), (6): Beg et al. (2003), (7): Zhou et al. (2014), (8): Tolosa et al. (2005), (9): Zhang et al. (2016), (10): Readman et al. (2002), (11): Fabbri (2003), (12): Brettell (2013), (13): Shiaris & Sweet (1986)]

Regionally, compared with previous studies in Arabian Gulf countries, the TPHs levels in sediment reported in this study (75.02 - 1751.82 $\mu\text{g}/\text{kg}$) were lower than other studies (Figure 5.6). The level of TPHs in Saudi Arabia observed by Fowler et al., (1993) and Readman et al., (1996) were 62000–1400000 $\mu\text{g}/\text{kg}$ and 11000- 6900000 $\mu\text{g}/\text{kg}$ respectively. In Kuwait, TPHs levels were between 40,000 to 240000 $\mu\text{g}/\text{kg}$ (Readman et al., 1996), 6700 to 2070000 $\mu\text{g}/\text{kg}$ (Beg et al., 2003), and from 4200–41000 $\mu\text{g}/\text{kg}$ (Lyons et al., 2015). Likewise, Σ PAHs reported in this study compared to other studies from the Arabian Gulf (0.39 – 1400000 $\mu\text{g}/\text{kg}$) were low (Table 2.6). Σ PAHs levels were reported from Saudi Arabia (1400- 1400000 $\mu\text{g}/\text{kg}$,

Readman et al., 1996), Kuwait (7200- 80000 µg/kg, Readman et al., 1996, 1333.6 µg/kg, Beg et al., 2003, and 12.9-190 µg/kg, Lyons et al., 2015), Bahrain (6600 µg/kg, Tolosa et al., 2005), whereas low levels were observed in United Arab Emirates (0.39–9.4 µg/kg, Tolosa et al., 2005).

Globally, concentration of TPHs measured in this study were in low level compared with worldwide region (Figure 30). Ali et al. (2015) reported a 5390 µg/kg of TPHs in surface sediment in Malaysia, where Zhou et al. (2014) examined a range of 6300–535000 µg/kg from surface sediment in China. The coastal sediment from Musa Bay in Iran had a TPHs level between 16480- 97150 µg/kg (Tehrani et al., 2016). Moreover, concentrations of ΣPAHs for Qatar's coastal sediments are low compared to data reported worldwide region (Table 5). Reported ΣPAHs levels include China 13.59-166.5 µg/kg (Zhang et al., 2016), Russia 61.2-368 µg/kg (Readman et al., 2002), Italy 112000 µg/kg (Fabbri, 2003), UK 4171- 79648 µg/kg (Brettell, 2013), 626- 3766µg/kg (Vane et al., 2007), and USA 487-718360 µg/kg (Shiaris & Sweet, 1986). Low levels of TPHs and PAHs reported in this study in coastal surface sediment of Qatar may relate to sediment texture which were mostly comprised of sand (coarse).

The major sources of anthropogenic PAHs are fossil fuel combustion (pyrolytic) and petroleum spillage (petrogenic). PAHs fingerprint ratios, such as phenanthrene to anthracene was applied to evaluate both pyrogenic and petrogenic sources (Chen et al., 2011; Chen et al., 2013). Petrogenic PAHs are often characterized by phenanthrene/anthracene ratio values >10, whereas combustion processes that result in the production of pyrolytic PAHs are specified by low ratios (<10) (Kafilzadeh, 2015). In this study, the values of this ratio for water and sediment samples were lower than 10, indicating that PAHs may be associated to pyrogenic sources (Table 5.1).

Table 5. 1: The range of diagnostic ratios for PAHs sources

Diagnostic ratio	Petrogenic	Pyrolytic	References
phenanthrene/anthracene	>10	<10	(Lang and Cao, 2010) (Kafilzadeh, 2015)
	<15	<10	(Maliszewska-Kordybach et al., 2008)

To sum up, the distribution of petroleum hydrocarbons in surface sediments have an important sign in oil pollution and in understanding temporal variations in the aquatic environments (Al-Saad, 1995). The highest concentration of TPHs in seawater was detected in

Al Khor (271.77 $\mu\text{g/L}$), where [Leitão et al. \(2017\)](#) reported (40 to 50 $\mu\text{g/L}$) from same location. Likewise, the highest TPHs in surface sediment was detected at Al Khor, although the site is relatively free from any industrial or urbanization facility, apart from occasional recreational activity; and the lowest at Al Wakra even though the area is busy with recreational boat traffic and fishing fleet movement. This result may indicate that contamination by diesel oil, which is commonly used in small and private recreational transport, and used by fishing boats, may have taken place in that site in the time of sampling. PAHs are hydrophobic in seawater and predominantly associated with the solid-phase particulate matter which becomes deposited into marine sediments ([Vane et al., 2007](#); [Wang et al., 2011](#); [Zhang et al., 2011](#)). Thus, this may reflect the reason why we found very low concentration of PAHs in seawater samples. Levels of PAHs within sediments are influenced by sediment organic matter content and grain size that affect the sorption of these pollutants onto the solid phase ([Chiou et al., 1998](#); [Wang et al., 2001](#); [Xia and Ball, 1999](#)). The concentration of total organic carbon (TOC) is used as a primary proxy to describe the abundance of organic matter ([Meyers, 2003](#)). The highest concentration of PAHs in surface marine sediment found also in Al Khor site (36.73 $\mu\text{g/kg}$), where the TOC in that sediment was the highest (2.01 mg/kg), and the grain size consist of (1.65 % Clay, 21.95 % Silt). Our finding matches the finding of ([Johnson et al., 2001](#)) and ([Kim et al., 1999](#)), who the first demonstrated that a sediment organic carbon content exceeding 0.1 mg/kg is sufficient to significantly enhance PAHs sorption onto marine sediments, and the later reported that higher levels of PAH are associated with smaller grain size.

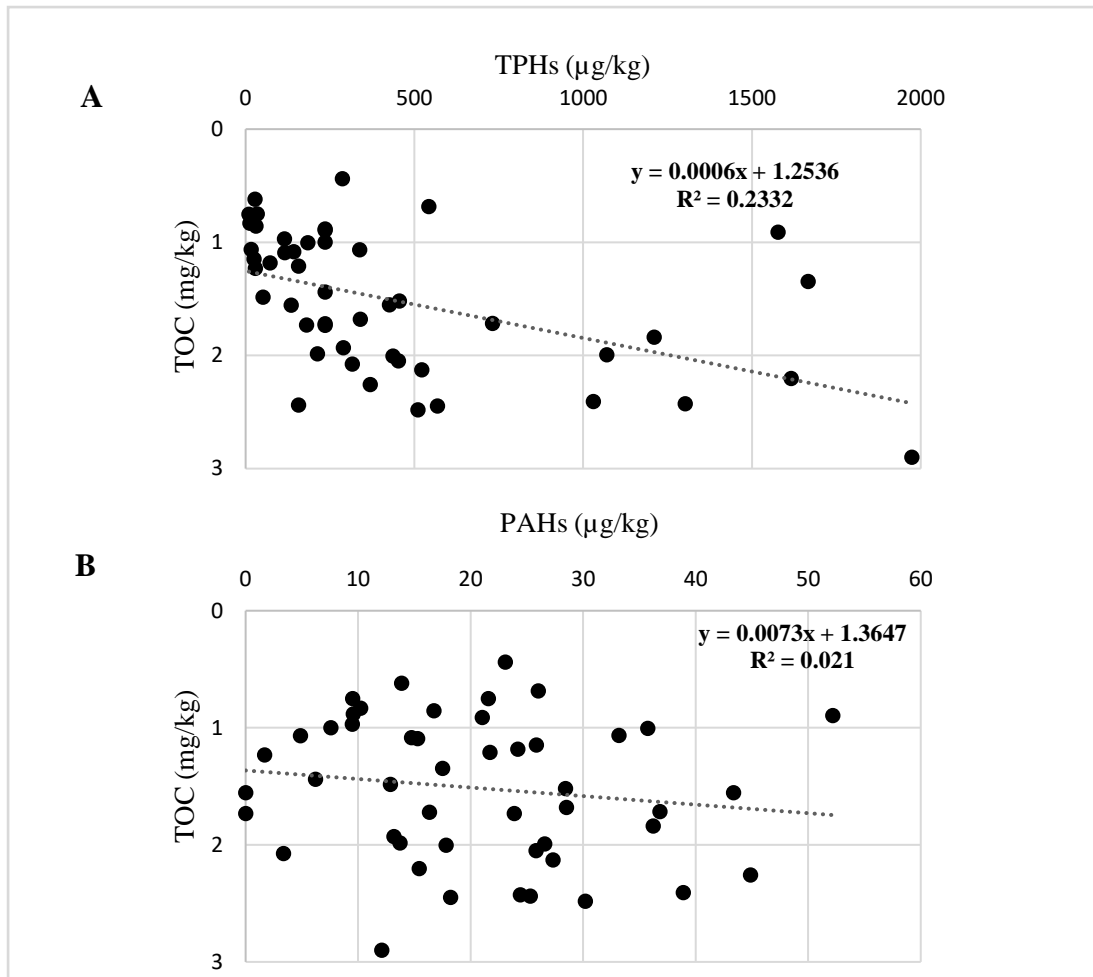


Figure 5. 7: Correlation between TPHs/ PAHs and TOC in surface sediment samples

No correlation between the TPHs or PAHs and TOC in sediments (Figure 5.7 -A and B). This correlation was in agreement with [Al-Khatib \(1998\)](#) who found non-significant correlation between the TPHs in sediments and TOC. This may depend on other factors that have the greatest effects on the TPHs in sediments such as turbid domestic matter that precipitated high levels of TPHs through water column sinking to the sediments or may be due to the benthic algae and aquatic plant closed to sediment that released hydrocarbons to the sediments.

5.3.3 TPHs and PAHs in sediment cores

The levels of TPHs in sediment core samples from the four sites ranged from 7.8 to 768.7 $\mu\text{g}/\text{kg}$ with the highest values measured in all depths at Simaisma (Figure 5.8). In the Simaisma core, the concentrations of TPHs were high at the surface (671.3 $\mu\text{g}/\text{kg}$) then increased to maximum (768.7 $\mu\text{g}/\text{kg}$) in 15cm depth then decreased gradually to minimum (342.3 $\mu\text{g}/\text{kg}$) in 30cm depth. While in Al Wakra core, the levels of TPHs were the highest in surface (439.3 $\mu\text{g}/\text{kg}$) then declined to about half (221 $\mu\text{g}/\text{kg}$) in 10cm, slightly increased in 15cm and then decreased again in 20cm, increased again in 25cm then reduced in 30cm depth to (135.7 $\mu\text{g}/\text{kg}$). Umm Bab core indicated that low levels of TPHs observed in the surface (5cm), while highest level were observed in 10cm (238 $\mu\text{g}/\text{kg}$). Then the levels were gradually declined by depth reaching (18.7 $\mu\text{g}/\text{kg}$) in 30cm depth. On the other hand, Al Khor core shows different trend, high concentrations were detected in bottom depths, 25cm (190 $\mu\text{g}/\text{kg}$) and 30cm (210.5 $\mu\text{g}/\text{kg}$). The TPHs values in the sediment core from each site with their replicates shown in Appendix D-1-3.

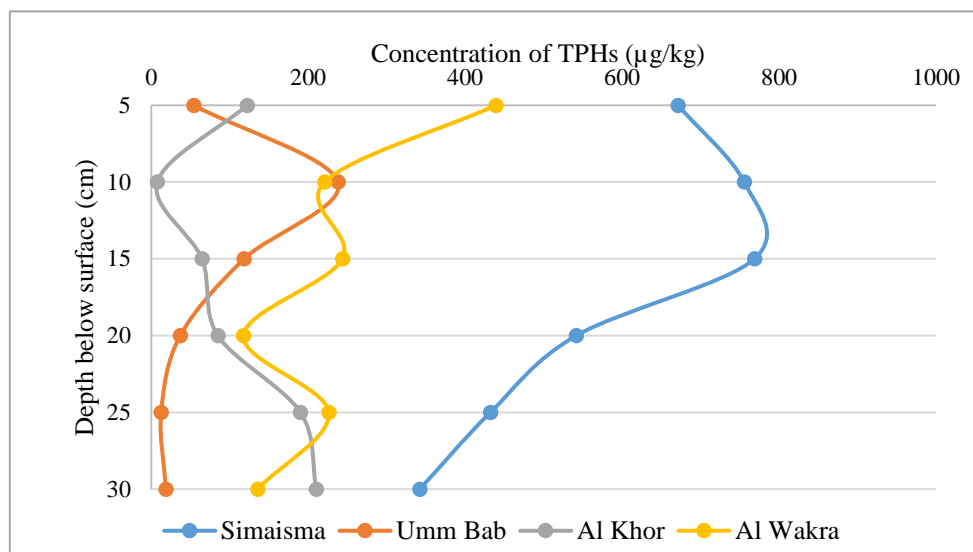


Figure 5. 8: The mean concentration of TPHs in sediment Core ($\mu\text{g}/\text{kg}$)

The Statistical analysis of TPHs results in sediment core samples showed that significant differences was noted among sampling sites (The Kruskal-Wallis H test, $P = < 0.001$) (Figure 5.9.A). The Post-hoc pairwise comparisons revealed that significant effects have been found between Umm Bab and Simaisma ($p = < 0.001$), Al Khor and Simaisma ($p = < 0.001$), and between Al Wakra and Simaisma ($p = 0.021$). Simaisma sediment core samples was significantly higher than the three other sites. No significant differences present between TPHs level and depth (The Kruskal-Wallis H test, $P = 0.877$) (Figure 5.9.B).

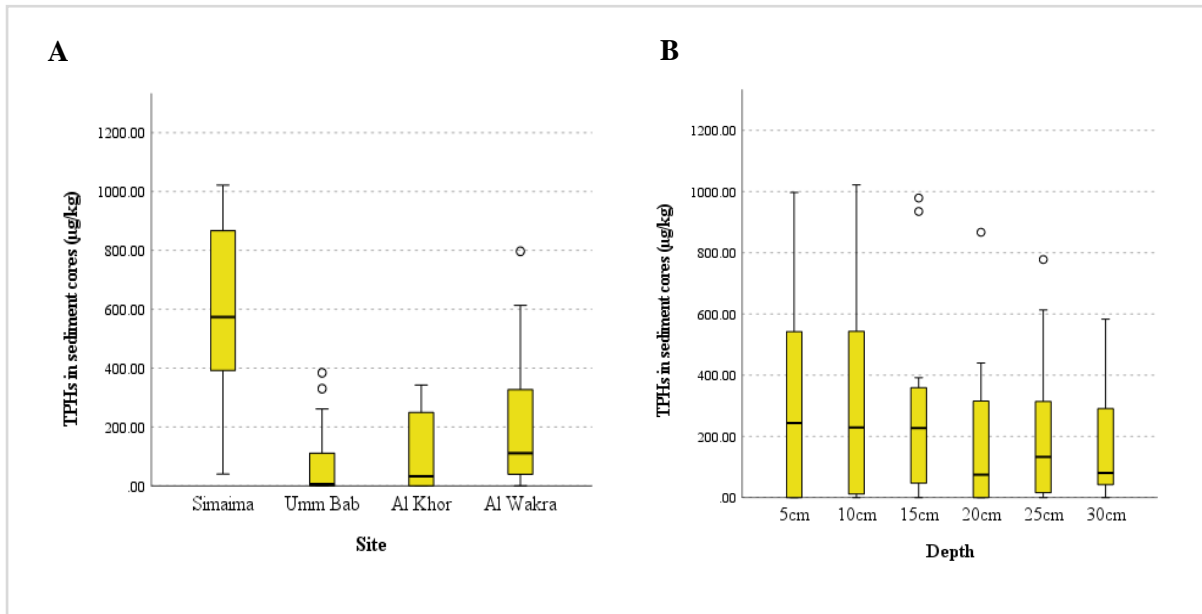


Figure 5. 9: The mean TPHs concentration in sediment cores across sites and depth

The PAHs values of the sediment cores samples are presented in Figure 5.10, which shows different patterns than TPHs. High levels of PAHs were observed in Al Wakra core with a highest concentration detected in 10cm depth (162.3 $\mu\text{g/kg}$). Simaisma, Umm Bab and Al Khor cores shows approximately similar trend. The levels of PAHs were low and showed a slight variation among depth (5 to 30 cm) from 9.9 to 2.6 $\mu\text{g/kg}$, 0.8 to 3.6 $\mu\text{g/kg}$ and from 2.3 to 4.3 $\mu\text{g/kg}$ respectively. The levels of PAHs in individual sites with their replicates are shown in Appendix E-1-2.

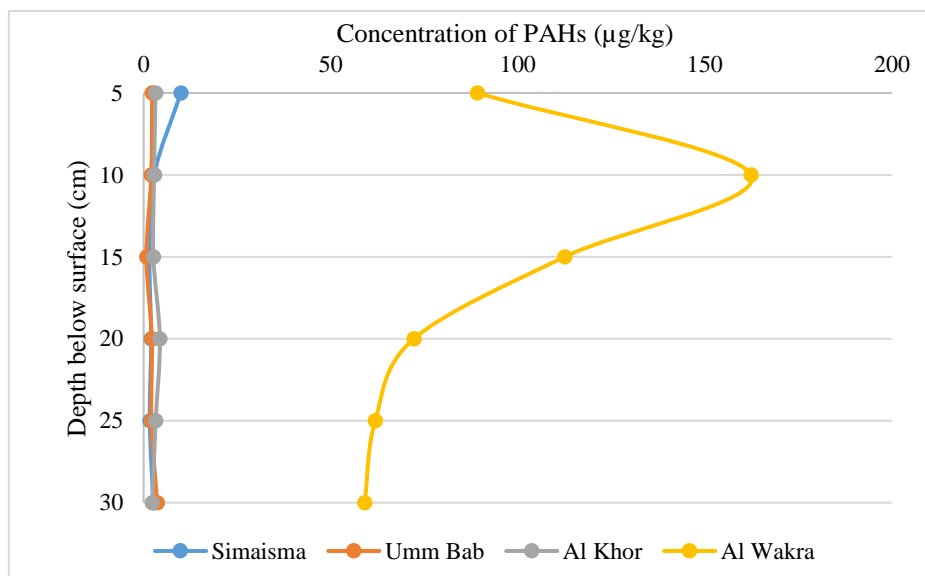


Figure 5. 10: The mean concentration of PAHs in sediment core ($\mu\text{g/kg}$ dry weight)

Significant differences for PAHs results in sediment core samples were observed among sampling sites (Kruskal-Wallis H test, $P = < 0.001$) (Figure 5.11-A). The Post-hoc pairwise comparisons revealed that significant effects have been found between Umm Bab and Al Wakra, Simaisma and Al Wakra, and between Al Khor and Al Wakra with ($p = < 0.001$) for all comparisons. Al Wakra sediment core samples was significantly higher than the three other sites in PAHs concentration. No significant differences present between PAHs level and depth (The Kruskal-Wallis H test, $P = 0.737$) (Figure 5.11-B).

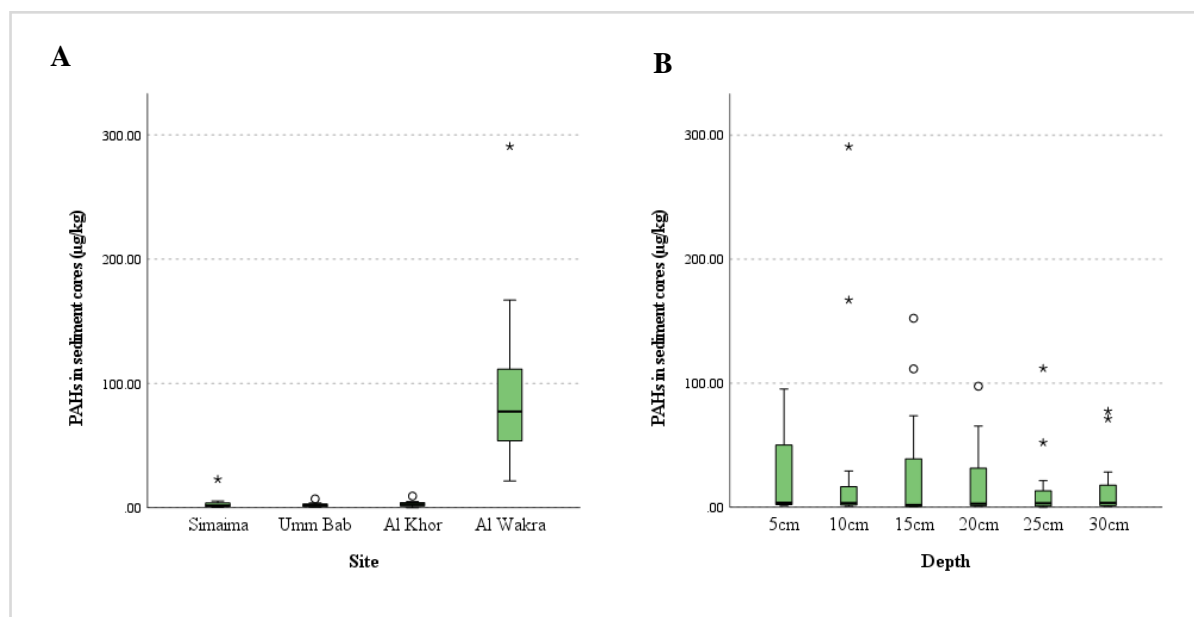


Figure 5. 11: The mean TPHs concentration in sediment cores across sites and depth

Nine PAHs compounds were detected in sediment core samples from Al Wakra area with higher levels compared to other areas (Figure 5.12). Concentration of Phenanthrene, Anthracene, Pyrene, Benzo (a) anthracene, Benzo (k) fluranthene were all higher in Al Wakra in the 10cm depth then dropped gradually by depth. Benzo (a) pyrene showed same pattern, high level was detected in 10cm depth with $10 \mu\text{g}/\text{kg}$ and then declined to $3.7 \mu\text{g}/\text{kg}$ in 30cm depth. Indeno(1,2,3-cd) pyrene was noticed only in 10 and 15 cm depth with 5.5 and $2.6 \mu\text{g}/\text{kg}$ respectively. Moreover, Benzo (ghi) perylene was observed in 5, 10 and 15 cm depth (2 , 3.8 , and $4.4 \mu\text{g}/\text{kg}$ respectively) where it then extremely dropped to less than $0.3 \mu\text{g}/\text{kg}$ in deeper depth. In Simaisma, the core samples showed that the first 5cm had more levels of PAHs compounds than other depth. Benzo (a) pyrene was the highest ($2.9 \mu\text{g}/\text{kg}$) followed by Phenanthrene ($2.7 \mu\text{g}/\text{kg}$) then Dibenz(a,h) anthracene ($1.7 \mu\text{g}/\text{kg}$) and Anthracene ($0.9 \mu\text{g}/\text{kg}$). Al Khor and Umm Bab core samples contained low levels of PAHs compounds (all $< 1 \mu\text{g}/\text{kg}$) in all depth.

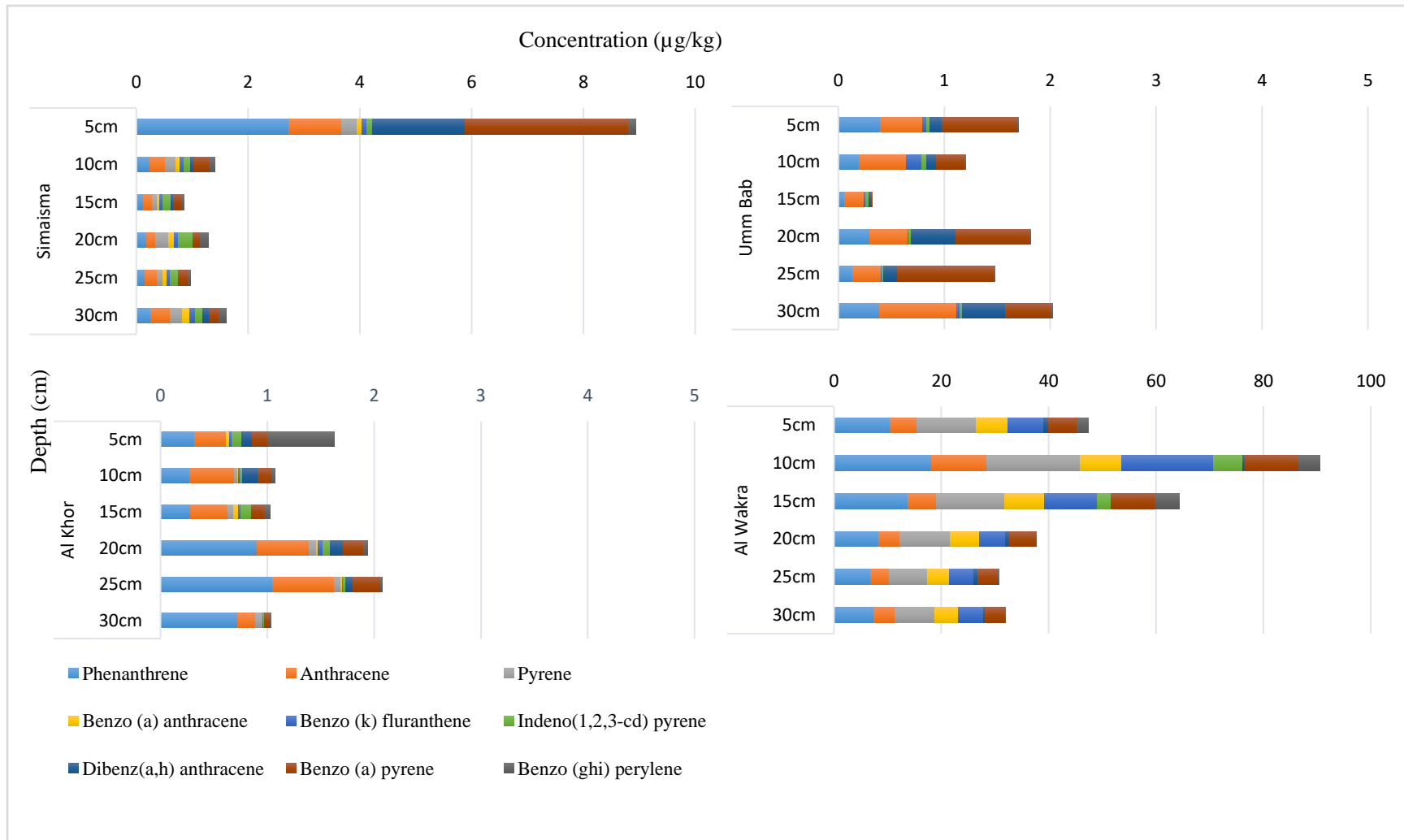


Figure 5. 12: Concentration of detected PAHs in the sediment core samples (µg/kg dry weight)

The concentration profiles of TPHs and PAHs by depth can be seen in Figure 5.13. Overall, although Simaisma was chosen as an offshore pristine location with high bioavailability of bivalves, it shows a high TPHs concentration profile by depth than other sites. The sediment particle size of Simaisma core samples was (75-79% sand, 20-24% silt, 0.6-0.8% clay) and TOC level ranged between 0.9-1 mg/kg. On the other hand, Al Wakra core samples shows a high PAHs levels by depth with TOC content (1-1.2 mg/kg) excluding the 5cm depth and with 52-59% sand, 39-46% silt and 1.1-1.5% clay.

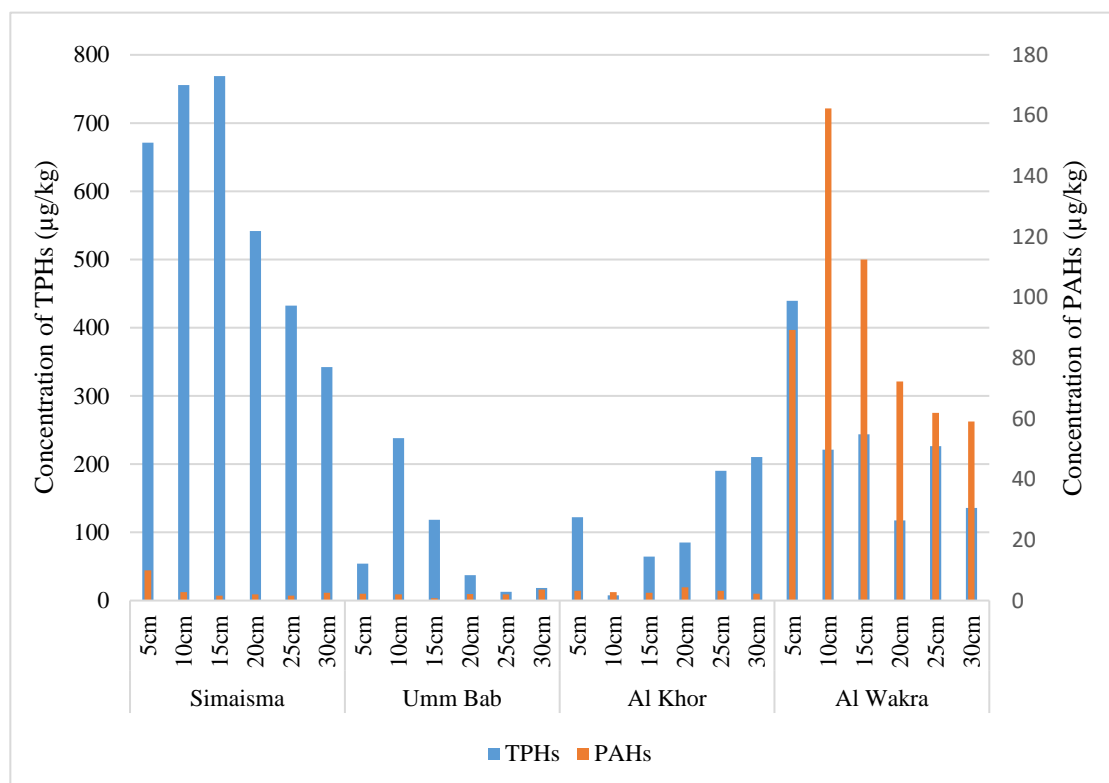


Figure 5. 13: Mean concentration of TPHs and PAHs by depth in sediment core samples

Higher PAHs concentrations found in Al Wakra sediment core compared to other sites may provide insight into factors affecting PAHs concentrations. [Mostafa et al. \(2009\)](#) illustrated that some sediment properties can affect PAHs distribution and concentrations, such as TOC and particle size fractions (sand, silt, clay). Specifically, PAHs concentrations tend to be higher in sediments with higher TOC contents due to the high sorption capacity of organic matter ([Notar et al., 2001](#)). However, a weak correlation was found between TOC and PAH concentrations in this study (Figure 5.14, $R^2 = 0.0178$). Moreover, high level of PAHs in Al Wakra may be due to recreational boat traffic, fishing fleet movement and fueling activities in that area with higher silt % and clay % compared to other sites.

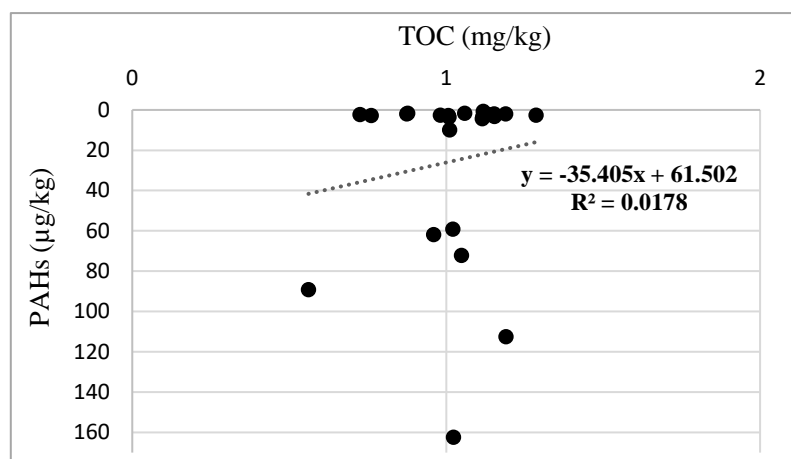


Figure 5. 14: Correlation between TOC content and PAHs level in sediment core samples

In general, the levels of TPHs and PAHs in surface sediment and sediment core samples observed in this study were not compatible. The highest TPHs and PAHs in surface sediment samples were observed in Al Khor site, while in sediment core samples highest TPHs and PAHs in 5 cm depth (surface layer) were observed in Simaisma and Al Wakra respectively. This may be related to the time of sampling, as sediment core samples were collected once in different year than surface sediment (May 2019).

5.3.4 TPHs and PAHs in oyster tissues

The TPH values of oyster tissues samples are presented in Figure 5.15. In general, the TPHs content in pearl oyster tissues collected from the four sites in different seasons ranged from 633.3 to 6666.7 µg/kg dry weight, with the highest concentrations measured at Simaisma. Samples collected from Simaisma showed wide range in both summer (from 1288 to 5316.7 µg/kg) and winter (from 2576.7- 6666.7 µg/kg). While Umm Bab samples showed wider range in summer than winter (from 2603.3 to 4003.3 µg/kg, and from 5726 to 6643.3 µg/kg respectively). In contrast, Al Wakra samples showed the reverse, as the range in winter was wider than summer (1880- 2796.7 µg/kg, and 633.3- 3140 µg/kg respectively). However, samples from Al Khor showed small range in both seasons. Appendix D-1-4 presents the whole TPHs values of oyster tissues in each site with their three replicates.

In summer, no significant differences were observed between sites ($p = 0.621$). Significant difference was observed in winter across sites ($p = 0.040$) (The Kruskal-Wallis H test). The post-hoc pairwise comparisons revealed that significant effects have been found between Al Wakra and Umm Bab ($p = 0.048$).

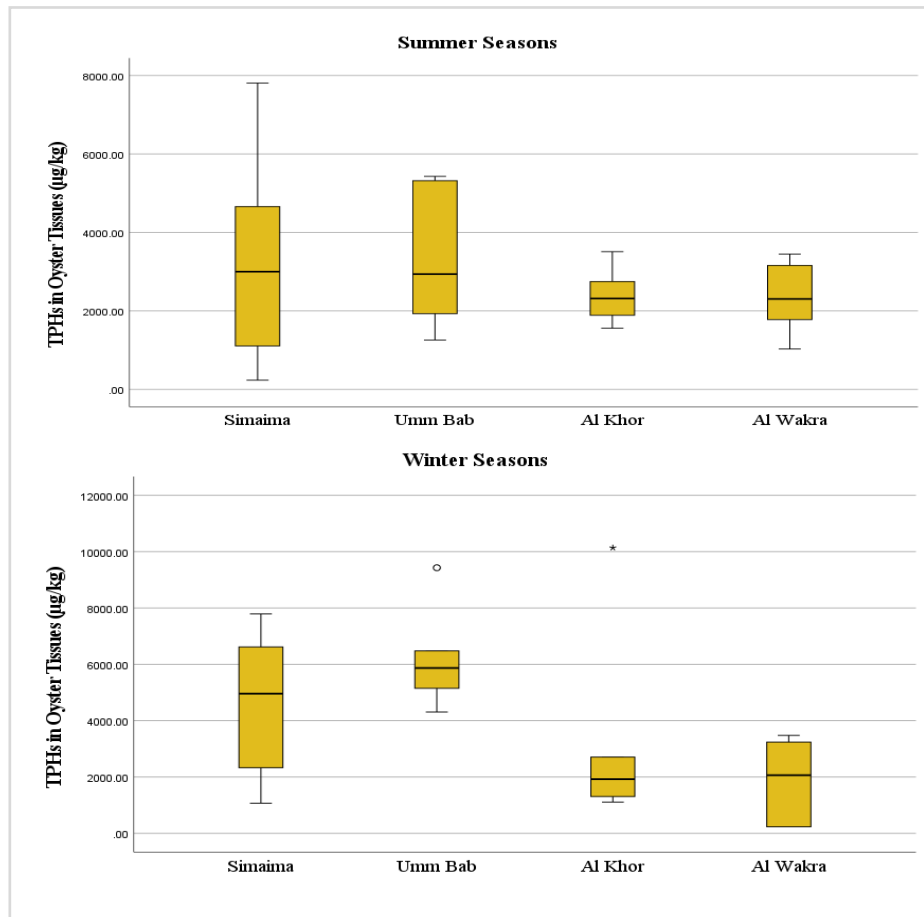


Figure 5. 15: Concentration of TPHs in oyster tissues samples in summer seasons (March 2017 and May 2018) and winter seasons (December 2017 and November 2018).

The concentrations of PAHs in oyster tissues samples showed an extreme variation from 25.9 to 2244 $\mu\text{g}/\text{kg}$ dry weight (Figure 5.16). The highest level of PAHs was measured in Al Wakra. In both seasons, the PAHs level in Al Wakra samples showed a wide range, while Simaisma samples showed small range. Samples collected from Al Khor showed wider range of PAHs in summer than winter. For Umm Bab, the size of PAHs range was approximately same in both seasons. Appendix E-1-3 shows the PAHs values for individual site with their replicates. The statistical analysis showed that no significant differences were observed in summer or winter across sites ($p > 0.05$).

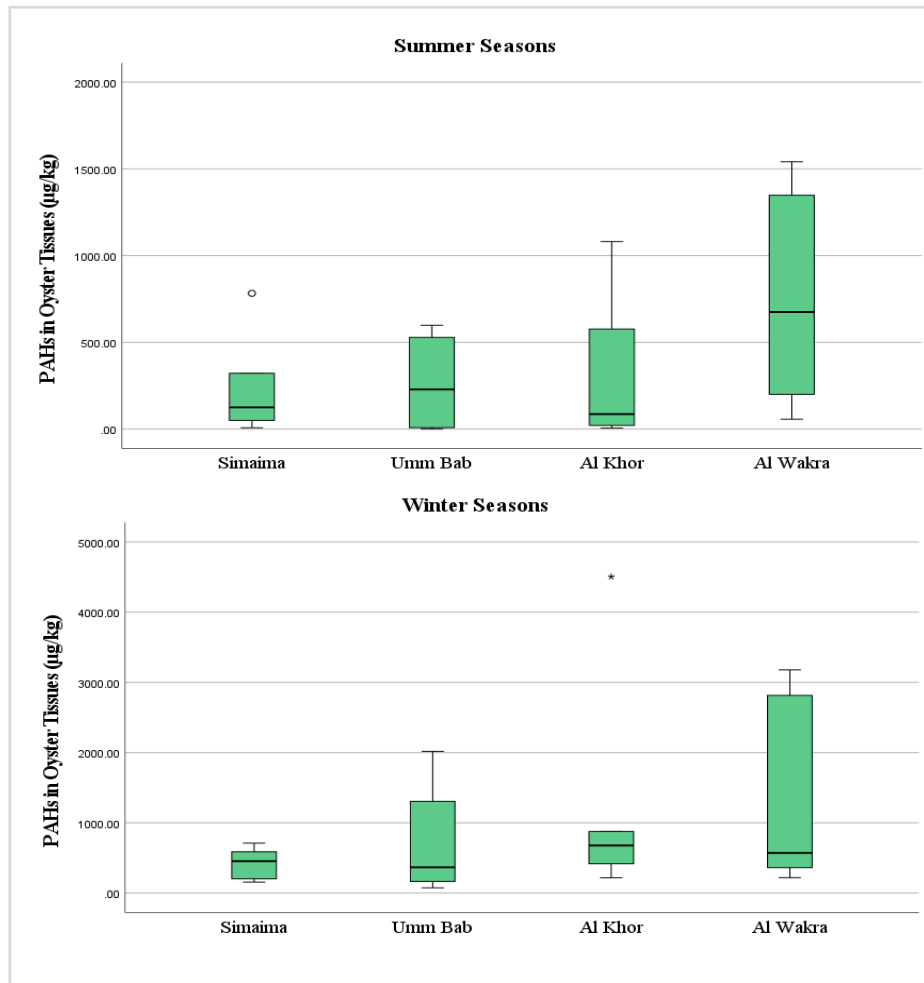


Figure 5. 16: Concentration of PAHs in oyster tissues samples in summer seasons (March 2017 and May 2018) and winter seasons (December 2017 and November 2018).

Eight PAHs compounds were detected in oyster tissues including: Benzo (a) pyrene, Fluorene, Benzo (b) fluranthene, Benzo (k) fluranthene, Indeno(1,2,3-cd), Benzo (ghi) perylene, Dibenz(a,h) anthracene and Chrysene. The highest level of PAHs compounds found in oyster tissues was Benzo (a) pyrene which was detected only in samples collected in winter seasons (winter 2017 and winter 2018) (Figure 5.17). The samples collected in winter 2018 contained higher level of Benzo (a) pyrene than winter 2017. The concentrations found were 1507.2, 1261.9, 374.8, 218.2 $\mu\text{g}/\text{kg}$ dry weight in Al Wakra, Al Khor, Umm Bab and Simaisma tissues samples respectively. Benzo (k) fluranthene showed same pattern as Benzo (a) pyrene, it was detected mostly in winter 2018 with highest concentration found in Umm Bab tissues samples with (436.3 $\mu\text{g}/\text{kg}$ dry weight) and lowest in Simaisma with (213.3 $\mu\text{g}/\text{kg}$ dry weight).

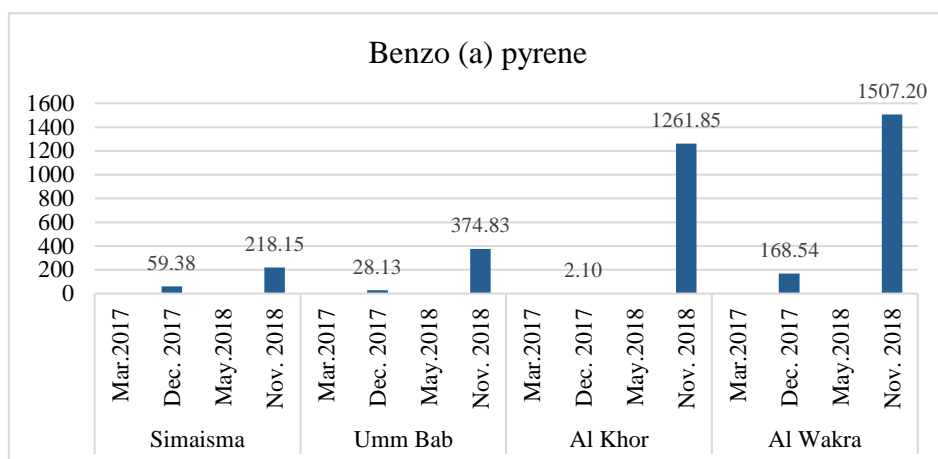


Figure 5. 17: Concentration of highest detected PAHs in the oyster tissues samples ($\mu\text{g}/\text{kg}$ dry weight)

Moreover, Indeno(1,2,3-cd), Benzo (ghi) perylene and Benzo (b) fluranthene detected most in winter seasons. The highest level of Indeno(1,2,3-cd) was found in winter 2017 from Al Khor with ($323.4 \mu\text{g}/\text{kg}$ dry weight) and lowest level found in winter 2018 from Simaisma samples. The Benzo (ghi) perylene highest concentration was found in winter 2017 from Simaisma with $127.5 \mu\text{g}/\text{kg}$ dry weight and lowest found in same site in winter 2018. Low level of Benzo (b) fluranthene found in samples collected in summer 2017 from the four sites, while high level was detected in samples collected in winter 2018 with 315.1, 226.3, 180.2 and 67.4 from Al Wakra, Al Khor, Umm Bab and Simaisma respectively. Chrysene was also noticed in winter seasons samples where it was found in three sites in winter 2017 ($12.3 \mu\text{g}/\text{kg}$ from Umm Bab, $11.4 \mu\text{g}/\text{kg}$ from AlKhor, and 4.4 from Al Wakra). Concentration of Dibenz(a,h) anthracene was fluctuating with high level found in Al Wakra samples in summer 2018 ($49.3 \mu\text{g}/\text{kg}$) and low level noticed in Al Khor in winter 2017 ($0.7 \mu\text{g}/\text{kg}$). Surprisingly, Fluorene was only detected in samples collected from the four sites in summer 2017 with 1323.6, 579.9, 502.2 and $420.6 \mu\text{g}/\text{kg}$ dry weight from Al Wakra, Al Khor, Umm Bab and Simaisma respectively.

Figure 5.18 below shows the levels of TPHs and PAHs reported from different area around the world. The TPHs concentration range reported in *P.radiata* tissues in this study (633.3 - $6666.7 \mu\text{g}/\text{kg}$) was slightly lower than previous study from Qatar (2120 to $7410 \mu\text{g}/\text{kg}$) (Leitão et al., 2017). In contrast, the TPHs concentrations in other Arabian Gulf countries were significantly higher than levels found in this study. These high levels are likely related to the sampling stations and oil contamination from refinery plant. Levels reported were from (22900 to $69700 \mu\text{g}/\text{kg}$) in Bahrain, (20300 to $33900 \mu\text{g}/\text{kg}$) in UAE, and (37600 to 632000) in Oman as described by de Mora et al. (2010). Moreover, Tolosa et al. (2005) reported high levels of

TPHs in oyster tissues in the same Arabian Gulf countries, concentration range were (38500 to 98000 $\mu\text{g}/\text{kg}$, 25600 to 237000 $\mu\text{g}/\text{kg}$, and 23200-130000 $\mu\text{g}/\text{kg}$) in Bahrain, UAE and Oman, respectively. Furthermore, high ranges of TPHs were observed in different areas around the world. [Vaezzadeh et al. \(2017\)](#) studied TPHs in oyster tissues from Malaysia and reported a level from 56661 to 262515 $\mu\text{g}/\text{kg}$, where the oysters collected from site considered to be one of the world's busiest shipping routes where frequent oil spills occur. Research done in Nigeria reported a range of (6370- 8440 $\mu\text{g}/\text{kg}$) in oyster tissues ([Inam et al., 2012](#)).

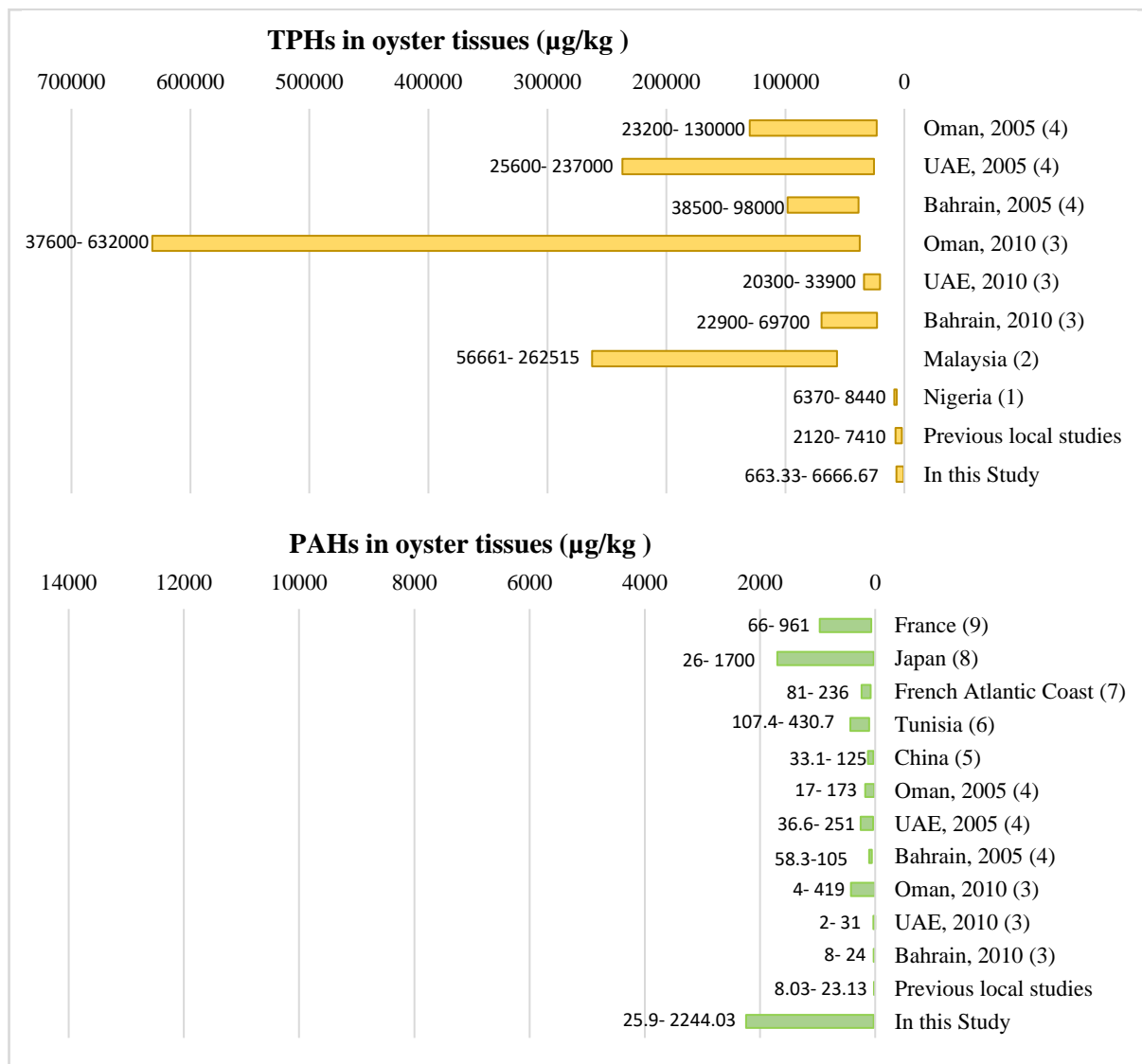


Figure 5. 18: Ranges of TPHs and PAHs in oyster tissues from different area [(1): [Inam et al. \(2012\)](#), (2): [Vaezzadeh et al. \(2017\)](#), (3): [de Mora et al. \(2010\)](#), (4): [Tolosa et al. \(2005\)](#), (5): [Hong et al. \(2016\)](#), (6): [Barhoumi et al. \(2016\)](#), (7): [Acosta et al. \(2015\)](#), (8): [Nakata et al. \(2014\)](#), (9): [Ramdine et al. \(2012\)](#)]

On the other hand, the levels of PAHs observed in this study in *P.radiata* oyster tissues samples (25.9- 2244 µg/kg) were higher than the previous local study observed by [Leitão et al. \(2017\)](#) who reported (8- 23.1 µg/kg) in *P.radiata* tissues from Qatar's coastal environment. Moreover, the levels of PAHs reported from the present study are higher than the range of levels reported in other Arabian Gulf countries (Figure 5.18). [de Mora et al. \(2010\)](#) reported PAHs concentration in oyster tissues between (8- 24 µg/kg) from Bahrain, (2- 31 µg/kg) from UAE, and (4- 419 µg/kg) from Oman. The notable levels of PAHs reported in Oman (419 µg/kg) were in rock oysters from Mina Al Fahal, which have an oil terminal and refinery plant at this site. These levels were lower than a study reported five years earlier in same areas, where the PAHs ranged from (58.3 to 105 and 36.6 to 251) in Bahrain and UAE respectively, while lower level observed in Oman (17 to 173 µg/kg) ([Tolosa et al., 2005](#)). Moreover, similar concentrations were reported in different areas around the world. The range of PAHs measured in oyster tissues were from 33.1 to 125µg/kg in China ([Hong et al., 2016](#)), 107.4- 430.7 µg/kg in Tunisia ([Barhoumi el al., 2016](#)), 81- 236 µg/kg in French Atlantic Coast ([Acosta et al., 2015](#)), 26- 1700 µg/kg in Japan ([Nakata et al., 2014](#)), and 66 to 961 µg/kg in France ([Ramdine et al., 2012](#)).

Overall, the results for pearl oyster tissues showing some indication of oil contamination. High levels of TPHs in pearl oyster tissues were detected in Simaisma, where same trend was observed in sediment cores collected from the same location, while the surface sediment showed low levels. On the other hand, oysters collected from Al Wakra shows high levels of PAHs comparable to sediment cores samples from same site. Thus, this data ensures the fact that oysters are filter feeder and can bio-accumulate contaminants in their tissues ([Funes et al.2006](#)). Which indicate that these sites (Simaisma and Al Wakra) may reflect chronic contamination due to the heavy oil tanker traffic offshore from these locations.

Moreover, Benzo (a) pyrene was the highest PAHs compound detected in pearl oyster tissues (2.1 to 1507.2 µg/kg), exceeding the maximum acceptable levels in bivalve molluscs of 10 µg/kg. According to [Fathallah et al. \(2012\)](#), the EC50 "half maximal effective concentration" for embryos and larvae of bivalve mollusc found to be 0.31 µg/kg. Benzo (a) pyrene can cause potential toxicity to the oysters. [Chen at el., \(2018\)](#) confirmed that this compound induces signal transduction, transcription regulation, cell growth, stress response, and energy metabolism in pearl oyster. Biomagnification studies of benzo(a)pyrene across the food chain system showed higher accumulation of benzo (a) pyrene in mussels ([D'adamo et al., 1997](#)), which may lead to a potential risk to humans through dietary intake. Under EPA's

Guidelines for Carcinogen Risk Assessment (USEPA, 2005), benzo (a) pyrene is “carcinogenic to humans” based on strong and consistent evidence in animals and humans.

The relationship of TPHs between coastal sediment and oyster tissues presented in scatterplot (Figure 5.19). In general, there is a non-significant relationship between the levels of PAHs in coastal sediment and oyster tissues. The four sites show individually a non-significant relationship between levels of PAHs found in the two matrixes.

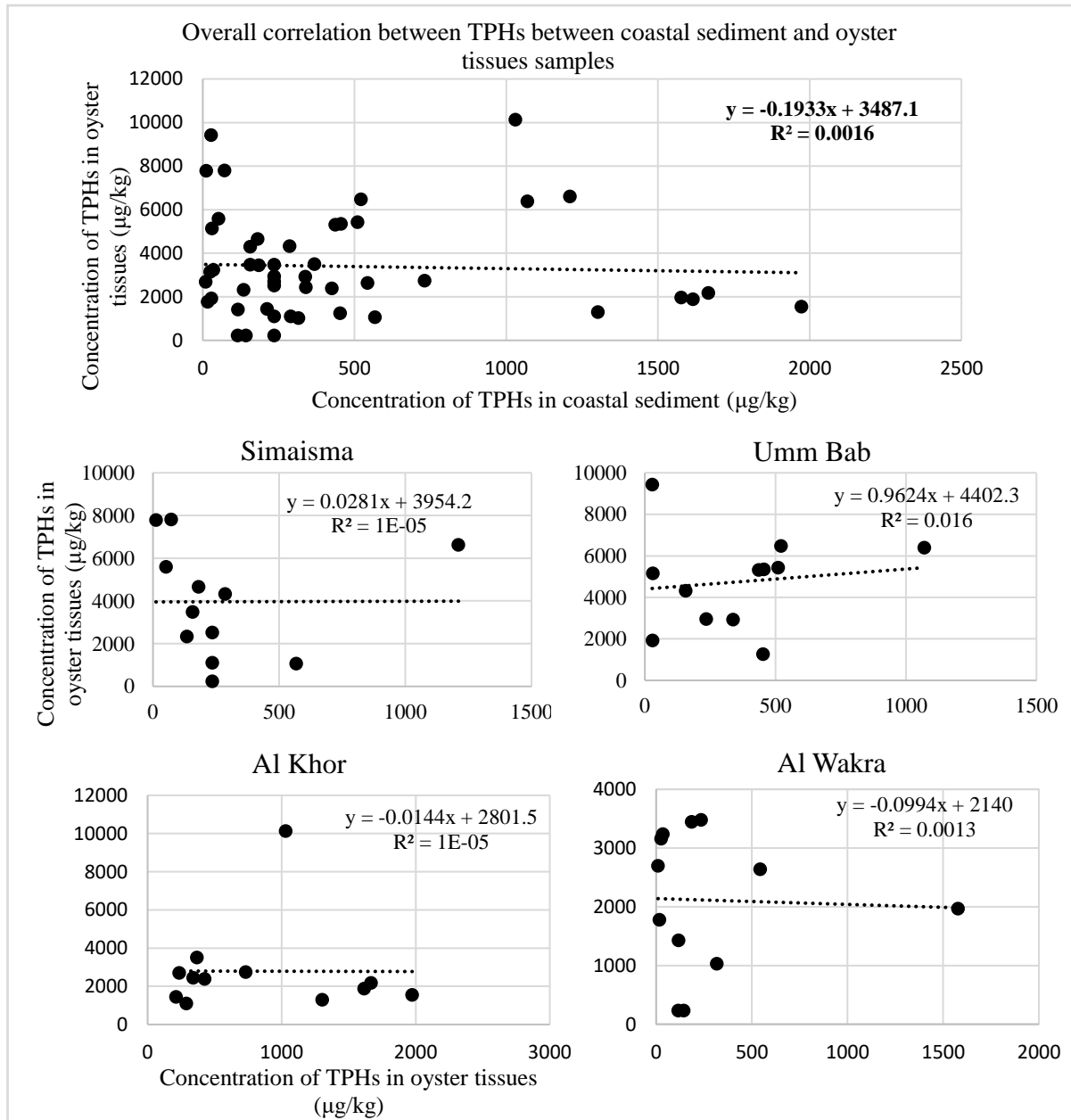


Figure 5. 19: Relationship of TPHs between coastal sediment and oyster tissues

Comparing the levels of PAHs observed in coastal sediment and oyster tissues samples shows non-significant relationship (Figure 5.20). Samples from individual locations show no correlation patterns. In general, none of these relationships statistically significant ($P > 0.05$).

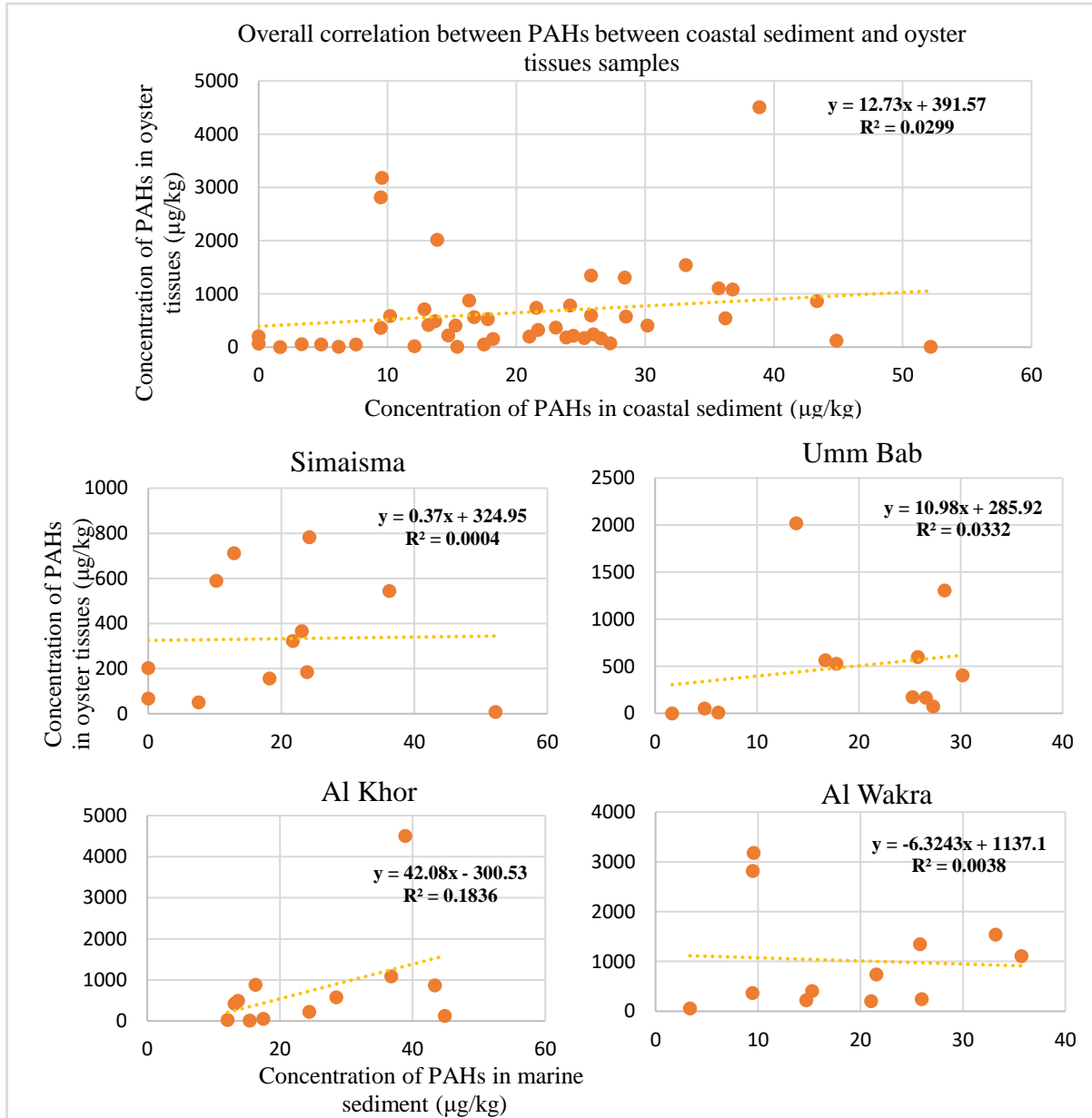


Figure 5. 20: Relationship of PAHs between coastal sediment and oyster tissues

5.3.5 Seasonal Variation of TPHs and PAHs

The overall seasonal variation of TPHs concentration in seawater, coastal sediment and oyster tissues shown in Figure 5.21. The TPHs concentration in seawater samples was higher in summer seasons in both years and in all sites. While the concentration in coastal sediment was higher in winter season samples collected from all sites in 2017, however, high TPHs concentration observed in oyster tissues collected in winter seasons.

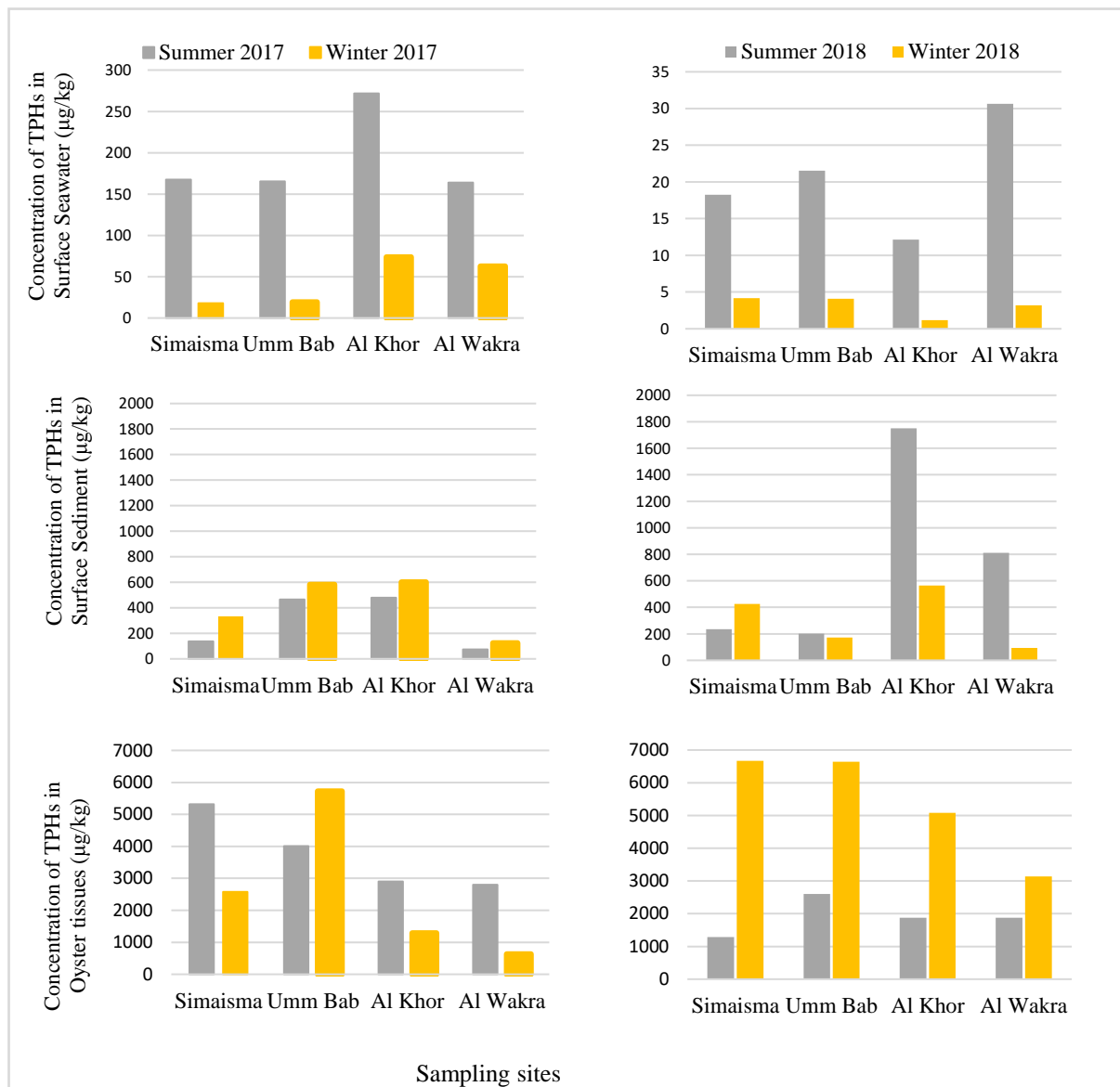


Figure 5. 21: Seasonal variations of TPHs concentration in seawater, surface sediment and oyster tissues

The overall seasonal variation of PAHs concentration in biotic and abiotic matrices illustrated in Figure 5.22. It can be seen clearly that oyster tissues samples in winter seasons accumulated more PAHs in their tissues than in summer season. However, in both seasons from 2017 shows the reverse, more accumulation was happened in summer season. Coastal sediment samples from Umm Bab accumulated more PAHs in winter samples.



Figure 5. 22: Seasonal variations of PAH concentration in the surface coastal sediment and oyster tissues

Generally, the organic contaminants (TPHs and PAHs) were more readily detected in oyster tissues samples than sediment and seawater samples collected from the same locations (Figure 5.23). Comparing the PAHs concentration range in oyster tissues with a worldwide survey ranked as moderate pollution, as the PAHs range recorded in this study in oyster tissues (25.9- 2244µg/kg) were higher than levels reported worldwide based in our selected studies. While comparison of the concentration range found in this study with a worldwide survey of sedimentary PAHs concentrations ranked PAHs contamination in Qatar coastal sediments as

low to moderate pollution. This may be related to the high percentage of sand particles in these sites.

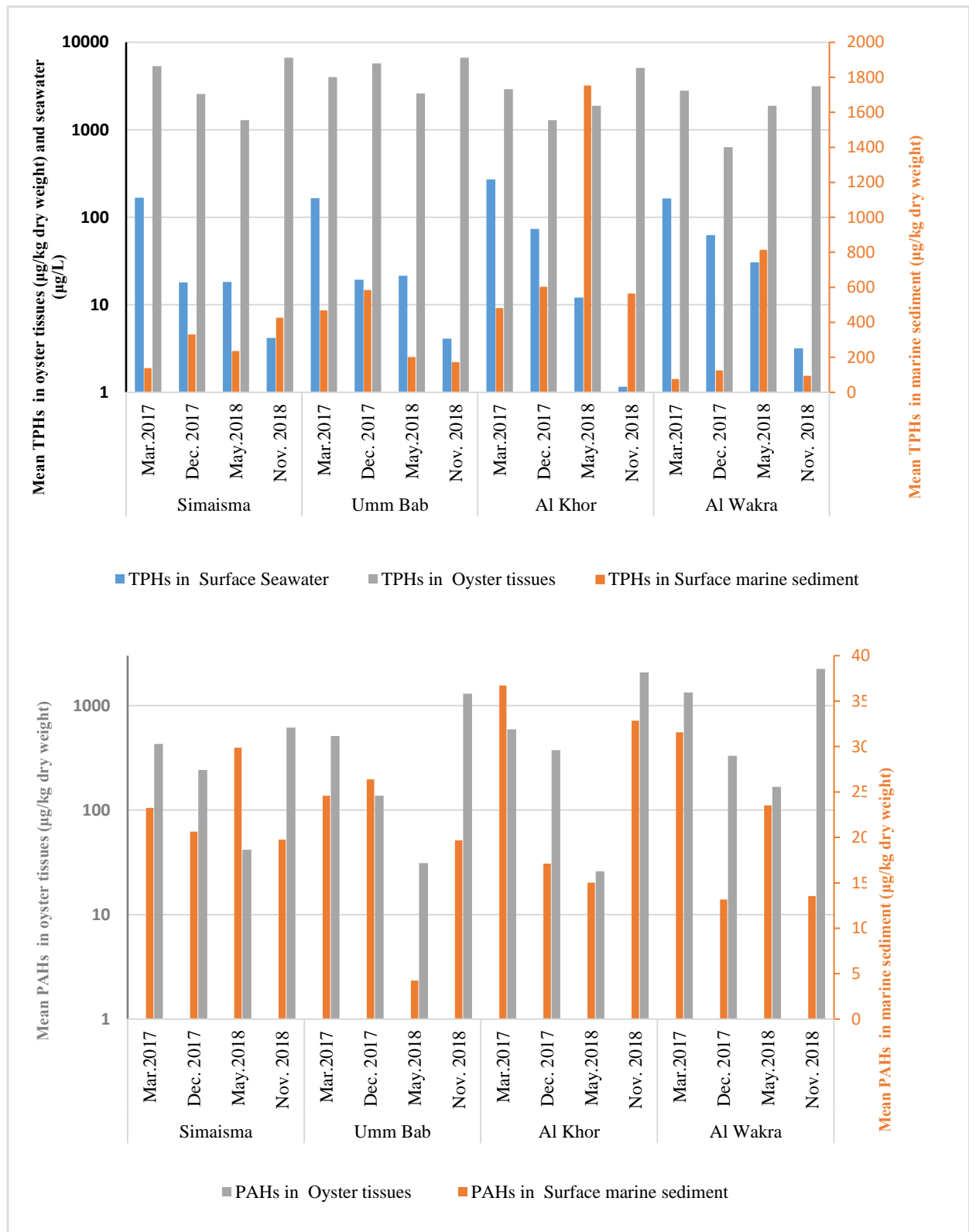


Figure 5. 23: Mean TPHs and PAHs concentration in biotic and abiotic matrixes from Qatar Coastal Environment

To sum up, the surface seawater samples from the four different locations showed negligible levels of PAHs, while TPHs ranged from 1.2 to 271.8 $\mu\text{g/L}$, with highest level recorded in Al Khor. These levels were lower than other studies around the world, but higher than in the previous local studies. The highest TPHs and PAHs levels in surface sediment were also recorded in samples collected from Al Khor where the sediment TOC was found and the sediment texture comprised at greater proportion of finer sediment (e.g., 1.7 % clay, 22% silt). Both the level of TPHs and PAHs in surface sediment were in the low range compared to other studies around the world. The TPHs concentration range reported in *P.radiata* tissues in this study was lower than previous local studies, while PAHs levels were higher than the previous local study and levels reported in other countries. Benzo (a) pyrene, which grouped in the first cluster as the most carcinogenic PAHs compound, was the highest compound detected in oyster tissues. The results show that oyster tissues samples in winter seasons accumulated more PAHs in their tissues than in summer season. Seasonal statistical variation of TPHs in oyster tissues was recorded in Simaisma and Al Wakra sites with highest concentration recorded in Simaisma.

5.4 Conclusion

In this study, an assessment of the organic pollutants (TPHs & PAHs) in seawater, surface coastal sediment, sediment cores and pearl oyster tissues (*Pinctada radiata*), collected from four sites located on the contrasting east and west coasts of the country and in four sampling rounds representing the only two contrasting seasons in Qatar (summer and winter), was made. Pearl oysters were specifically selected for this study as filter feeders due to their tolerance of harsh environmental conditions and availability around Qatar's coastline.

Based on our finding, while levels of TPHs and PAHs in seawater and sediment samples were lower than previous local studies and worldwide studies, the PAHs levels observed in pearl oyster tissues samples (25.9- 2244 $\mu\text{g}/\text{kg}$) were higher than previous studies in Qatar and higher than levels recorded in different areas around the world. Nevertheless, the Al Khor site shows a higher range of TPHs concentration in seawater samples (1.2-271.8 $\mu\text{g}/\text{L}$) than previous local studies (40-50 $\mu\text{g}/\text{L}$), and higher levels of TPHs and PAHs in surface sediment than the other three sites (479.8- 1751.8 $\mu\text{g}/\text{kg}$ and 15- 36.7 $\mu\text{g}/\text{kg}$ respectively). On the other hand, the highest PAHs ranges in oyster samples were observed from Al Wakra and Al Khor (166.7- 2244 $\mu\text{g}/\text{kg}$, and 25.9- 2082.7 $\mu\text{g}/\text{kg}$, respectively) with higher levels reported in winter season than summer. The Al Wakra sediment core reported the highest level of PAHs at all depths compared to the other three sites (89.2- 162.3 $\mu\text{g}/\text{kg}$), while Simaisma core reported the highest TPHs in all depths than other sites (342.3- 768.7 $\mu\text{g}/\text{kg}$).

According to our findings, although the sediments did not seem to have been affected by organic contaminants, high levels of PAHs recorded in oysters collected from Al Wakra and Al Khor, and in seawater collected from Al Khor might represent residual hydrocarbons in these east coast sites of Qatar. Moreover, sediment core sample from Al Wakra reported the highest level of PAHs in all depths than other sites, which might reflect chronic contamination due to the high boat traffic, fishing or fueling activities offshore from this location.

Chapter 6:

**Occurrence of trace metals and total mercury in
seawater, surface sediment, and oyster tissues around
the coastline of Qatar**

6.1 Introduction

Trace metal contamination is a serious and persistent environmental problem due to their toxicity, abundant sources, non-biodegradable and bioaccumulative behavior and they pose potential risk for marine organisms and human health (Gui et al., 2017; Guo et al., 2019; Lu et al., 2019; Wang and Lu, 2018). Trace metals may interfere with the cellular metabolic functions causing harmful side effects (Al Osman et al., 2019). These pollutants may affect marine organisms even at low concentrations: their toxicity arises, not only from their concentration levels, but also from the biochemical role they play in metabolic processes, as well as the extent to which they are absorbed and excreted by marine organisms (Jakimska et al., 2011). Furthermore, their cationic forms are harmful to living organisms as they can readily bind to short carbon chains (Freije, 2015). These forms bioaccumulate in the protein-rich tissues of marine organisms and eventually can affect humans consuming them in their diet. Exposure to certain heavy metals can affect cellular components such as cell membrane, mitochondria, etc. (Wang & Shi, 2001). Mercury is recognized as one of the most hazardous environmental pollutants (WHO, 2017). It is released into the environment by anthropogenic and natural sources such as: volcanoes; industrial runoffs from contaminated soils; as well as gold and ore mining. According to the U.S. Environmental Protection Agency (US EPA), concentrations of total mercury (T-Hg) in biological samples are usually less than 0.1 mg/kg (Risher and Amler, 2005), while levels in sediment vary depending on the level of pollution in the area under study, the proper assessment of which necessitates the analysis of a large number of samples. Moreover, pollution of marine habitats may consequently lead to a decrease in species diversity (Kurylenko & Izosimova, 2016). As such, protecting Qatar's marine ecosystems, drinking water and food from chemical contamination is a core component of the Environmental Development within the National Vision 2030 (MDPS, 2017).

Generally, the degree of chemical contamination in the environment can be indicated by measuring the levels of contaminants accumulated in tissues. Species such as mussels have been reported recently for the monitoring of contaminants of emerging concern (CECs) in Singapore (Bayen et al., 2016) and in Hong Kong (Burket et al., 2018). The pearl oyster (*Pinctada radiata*) is widely distributed throughout the Indo-Pacific and notably in the Arabian Gulf. *P. radiata* live in the benthic zone with relatively long life cycles and good adaptability to a wide range of

environmental changes (Al-Madfa et al., 1998). In Qatar, the pearl oyster is considered being an essential part of the nation's cultural heritage and one of the main economic foundations upon which the nation developed. However, the pearl oyster is not immune to environmental pressures, and as Qatar has prospered and developed coastal urban and industrial areas, oyster beds have been impacted (Smyth et al., 2016).

A wealth of new knowledge exists for heavy metals in seawater, marine sediment, and bivalves in many areas of the world (Yuan et al., 2020; Lu et al., 2019; Lu et al., 2020; Fang and Lien, 2020; Satheeswaran et al., 2019; El-Sorogy and Attiah, 2015; Baltas et al., 2017; and Paul et al., 2021). However, little in recent years is evident for Arabian Gulf countries (Al-Hashimi and Salman, 1985; Fowler et al., 1993; Al-Sayed et al., 1994; de Mora et al., 2004; Juma and Al-Madany, 2008; Naser, 2010, Lyons et al., 2015; and Alharbi and El-Sorogy, 2017). In Qatar, limited studies have examined levels of trace metals in the Qatari coastal environment. Only two published data sets are available for trace metals in Qatari seawater and *P. radiata* tissues (Aboul Dahab and Al-Madfa, 1997 and Leitão et al., 2017) and four studies have reported levels of trace metals in Qatari sediment (Basaham and Al-Lihaibi, 1993; Aboul Dahab and Al-Madfa, 1997; Al-Naimi et al., 2015; Leitão et al., 2017). For total mercury, many studies around the world have reported the levels in seawater and marine sediment. Nevertheless, few studies have measured the total mercury concentration in oyster tissues (Mikac et al., 1985; Eisler, 1987, Fang et al., 2004, Apeti et al., 2012; Ochoa et al., 2013; and Yesudhason et al., 2013). Limited studies are available on the bioavailability of mercury in Qatar's marine environment (Al Madfa et al., 1994; Kreish & Al Madfa, 1999; and Leitão et al., 2017).

In the present study, an attempt has been made to analyze trace metals accumulation that considered to be the most popular toxic metals (including Cd, Cr, Cu, Ni, Pb, Zn and total Hg) in seawater, coastal surface sediment, sediment cores and the abundant bivalve *P. radiata* in order to determine the level and distribution of inorganic contamination in Qatar's coastal environment.

6.2 Methodology

6.2.1 Sampling and Study Area

The seawater, coastal sediment, sediment cores, and oyster tissues samples taken from the same sampling sites and strategies followed in Chapter 3. Sampling collection techniques for the three types of samples are well described in Chapter 3 (Section 3.2).

6.2.2 Laboratory technique protocols

6.2.2.1 Chemicals and Reagents

Nitric acid (HNO₃) (Supra Pure Metal, 65%, Sigma Aldrich), Sulfuric acid (H₂SO₄) (Supra pure, 98%, Merck), Hydrofluoric acid (HF) (reagent grade, 40%, Sigma Aldrich), Tin (II) chloride (reagent grade, 98%, Sigma Aldrich) and Potassium dichromate (EMSURE® ACS) were used. Certified reference material (CRM) NIST-2976 (mussel tissue (trace elements and methylmercury), was sourced from the National Institute of Standards and Technology (Gaithersburg, MD, USA). CRM PACS-3 (Marine Sediment Reference Material for Trace Metals and other Constituents) was purchased from the National Research Council Canada (Ottawa, ON, Canada). Mercuric nitrate standard was used as a stock calibration standard (1001 ± 2 pg/mL, 2%, nitric acid in low TOC water). Argon 99.999% (Buzwair Scientific and Technical Gases, Doha, Qatar) and high-quality type 2 deionised water (~18 MΩ cm) from Thermos Barnstead system (GENPURE UV-TOC Life Technologies Ltd. Paisley, UK) were used.

6.2.2.2 Glassware and General Instruments

Glass jars (500 mL), PP bottles (1 liter), glass amber bottles (1 liter) were used for collection of samples. Teflon tubes, TFM Sample Vessels were used. In addition, hot block, analytical balance, shaker, freezer, gloves, funnels, volumetric flasks and beakers were also used. AdVantage Pro Freeze Dryer, and Planetary Ball Mill, Type PM400 (Retsch, Germany) were used for freeze dry the samples and grind them. Inductively Coupled Plasma-Optical Emission Spectrometry (ICP-OES) (Perkin-Elmer, Optima 7300 DV model) and Mercury Analyzer AULA-254 ASD were used for samples analysis for trace metals and total mercury respectively.

6.2.2.3 Sample Preparation and Analysis

In the field, for all seawater samples, 3mL of nitric acid (1:1) was added for preservation and to maintain a pH < 2. In the laboratory, all sediment and oyster tissues samples were freeze-dried by the AdVantage Pro Freeze Dryer. Then the sediment samples were grinded by Planetary Ball Mill, Type PM400 (Retsch, Germany) to obtain a well-mixed sample. Both the grinded sediment and oyster tissues samples were placed in glass jars prior of extraction.

6.2.2.3.1 Sample Preparation for Trace Metals

6.2.2.3.1.1 Seawater Sample Preparation for Trace Metals

For the trace metals analysis, we followed the Environmental Science Center (ESC) at Qatar University (Accredited by A2LA- ISO 17025) for seawater samples digestion. Refer to Chapter 3 (Section 3.5.1.1) for full description of the method.

6.2.2.3.1.2 Sediment Sample Preparation for Trace Metals

For the coastal sediment and sediment cores samples analyses we followed the procedure used by Environmental Science Center (ESC) at Qatar University for metals analysis in sediment (Accredited by A2LA- ISO 17025). For more detailed in the method, please refer to Chapter 3 (Section 3.5.1.2).

6.2.2.3.1.3 Oyster Tissues Sample Preparation for Trace Metals

The method of Environmental Science Center (ESC) at Qatar University for analysis of metals in biota tissues (Accredited by A2LA- ISO 17025) was used for oyster tissues samples digestion. Detailed description of the digestion method is illustrated in Chapter 3 (Section 3.5.1.3).

6.2.2.3.2 Sample Preparation for Total Mercury

6.2.2.3.2.1 Seawater Sample Preparation for Total Mercury

For total mercury analysis in seawater, we followed the Environmental Science Center (ESC) at Qatar University (Accredited by A2LA- ISO 17025) for seawater samples digestion. Refer to Chapter 3 (Section 3.5.2.1) for full description of the method.

6.2.2.3.2.2 Sediment and Oyster Tissues Samples Preparation for Total Mercury

The sediment and biota samples followed the same procedure for Total Mercury analysis using Method Validation done in Environmental Science Center (ESC) at Qatar University (Abou Elezz et al., 2018) (Accredited by A2LA- ISO 17025). For full detailed of the method, refer to Chapter 3 (Section 3.5.2.2).

6.2.3 Quality Assurance and Quality Control (QA/QC)

For quality assurance and quality control checks, field blanks and certified reference materials (CRM) were used. For full description of the QA/QC used for inorganic contaminants, refer to Chapter 3 (Section 3.5.5). The limit of detection (LOD) and CRMs for inorganic contaminates is represented in Chapter 3 (Table 3.8, and Table 3.10 respectively).

6.2.4 Statistical Analysis

For the statistical analyses, Excel and SPSS software were used. Refer to chapter 3 (Section 3.5.6) for full description of statistics used for inorganic contaminants data.

6.3 Results and Discussion

A total 216 samples were analyzed: 48 samples of seawater; 48 samples of sediment, 72 sediment core samples and 48 samples of oyster tissue. The levels of six trace metals (Cd, Cr, Cu, Ni, Pb, and Zn) and total mercury were quantified in surface seawater, surface coastal sediment, sediment cores and tissues of Pearl Oyster (*P. radiata*). In addition, the TOC and particle sizes were measured in abiotic matrices as well as the temperature, salinity and pH of seawater in the study areas (see Chapter 4).

6.3.1 Trace Metals and Total Mercury in Seawater

The mean concentration range of Cd, Cr, Cu, Ni, Pb, and Zn in seawater were 0 - 1.37, 0 - 3.52, 0 - 3.53, 0.06 - 9.82, 0 - 56.09, and 0.06 - 4.68 µg/L respectively (Table 6.1). The highest trace metal levels detected were Pb > Ni > Zn > Cu > Cr > Cd. In general, most of the trace metals were detected in summer 2017 except zinc, which was at higher levels in winter seasons (Figure 6.1). Appendix F-1-1 showed the trace metals concentration with replicates in detail. Based on statistical analysis, no significant differences were observed in six trace metals between the different sites in summer or winter i.e., the distribution of the six trace metals in summer and winter is the same across the sites.

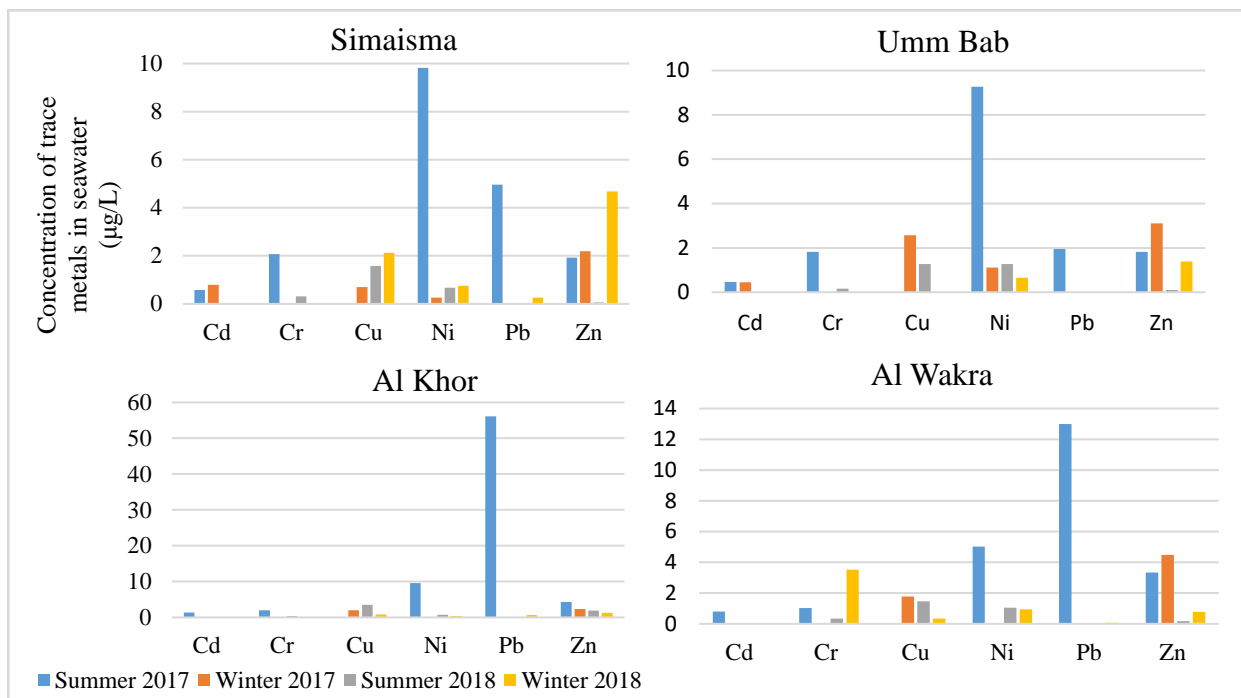


Figure 6. 1: Seasonal variations of trace metals concentration in Seawater samples from the four sites

Table 6. 1: The Mean Concentration of Trace Metals in Surface Seawater ($\mu\text{g/L}$)

Site	Season	Cd		Cr		Cu		Ni		Pb		Zn	
		Mean	STD	Mean	STD	Mean	STD	Mean	STD	Mean	STD	Mean	STD
Simaisma	Mar.17 (Summer)	0.58	0.41	2.07	1.79	0.00	0.00	9.82	8.50	4.96	6.97	1.93	1.71
	Dec.17 (Winter)	0.80	0.14	0.00	0.00	0.70	0.62	0.27	0.23	0.00	0.00	2.20	0.68
	May.18 (Summer)	0.00	0.00	0.32	0.03	1.58	1.21	0.67	0.45	0.00	0.00	0.06	0.07
	Nov.18 (Winter)	0.00	0.00	0.00	0.00	2.13	1.28	0.75	0.56	0.26	0.45	4.68	2.17
Umm Bab	Mar.17 (Summer)	0.46	0.31	1.81	1.57	0.00	0.00	9.27	8.02	1.94	3.37	1.82	2.20
	Dec.17 (Winter)	0.45	0.17	0.00	0.00	2.57	2.46	1.11	1.86	0.00	0.00	3.10	0.69
	May.18 (Summer)	0.00	0.00	0.16	0.10	1.27	1.02	1.28	0.11	0.00	0.00	0.11	0.10
	Nov.18 (Winter)	0.02	0.04	0.00	0.00	0.00	0.00	0.66	0.28	0.00	0.00	1.39	0.80
Al Khor	Mar.17 (Summer)	1.37	2.18	1.98	1.72	0.00	0.00	9.60	8.31	56.09	97.16	4.35	5.40
	Dec.17 (Winter)	0.10	0.11	0.00	0.00	2.02	0.13	0.08	0.13	0.00	0.00	2.37	1.49
	May.18 (Summer)	0.00	0.00	0.42	0.21	3.52	4.83	0.74	0.16	0.00	0.00	1.87	1.66
	Nov.18 (Winter)	0.07	0.08	0.00	0.00	0.84	1.45	0.36	0.54	0.65	1.13	1.29	0.52
Al Wakra	Mar.17 (Summer)	0.80	0.70	1.04	1.80	0.00	0.00	5.02	8.69	12.98	13.18	3.35	2.98
	Dec.17 (Winter)	0.00	0.01	0.00	0.00	1.78	1.33	0.06	0.07	0.00	0.00	4.48	1.77
	May.18 (Summer)	0.00	0.00	0.34	0.07	1.46	0.87	1.05	0.43	0.00	0.00	0.18	0.31
	Nov.18 (Winter)	0.00	0.00	3.52	6.10	0.34	0.35	0.94	0.69	0.06	0.11	0.79	0.80
Water Quality Standards (WQS)*	CMC**	40		1100		4.8		74		210		90	
	CCC***	8.8		50		3.1		8.2		8.1		81	

*WQS, USEPA, National Recommended Water Quality Criteria, 2004.

**CMC: "Criteria Maximum Concentration", is an estimate of the highest concentration of a material in surface water to which an aquatic community can be exposed briefly without resulting in an unacceptable effect.

***CCC: "Criterion Continuous Concentration", is an estimate of the highest concentration of a material in surface water to which an aquatic community can be exposed indefinitely without resulting in an unacceptable effect.

In this study, the concentration of trace metals in the surface seawater samples from the four different locations were in the range of previous local studies. Locally, [Aboul Dahab and Al-Madfa \(1997\)](#) studied Cr distribution in seawater of the eastern side of the Qatari peninsula. Average Cr concentrations in the investigated waters during the period of study were 0.08, 0.66 and 0.54 µg/L respectively for Cr (III), Cr (VI), and particulate phases. In the 10 years following the previous study, only one other has examined the level of trace metals in Qatar's seawater ([Leitão et al., 2017](#)). She showed that most of the heavy metal concentrations in seawater samples collected from Al Khor, Al Wakra Harbor, and Doha Harbor in the range of 0.01 µg/L–4.52 µg/L, with the exception of Zn, which had a range of 13.8µg/L–21.12µg/L during the summer sampling and 27.3 µg/L to 148.57 µg/L during the winter sampling.

Regionally, compared to other studies from Arabian Gulf (Table 2.8), trace metals reported in Qatar's seawater were in the same range except Pb which reported high concentration in Al Khor samples collected in summer 2017. Marine pollution in the territorial water of Bahrain was assessed by analyzing trace metals in seawaters from 23 different sites known as fishing areas in the year 2007, the concentrations of Cd, Cu, Ni, Pb and Zn were in the range of 0.06-5.20, 4.53-119.00, 0.71-20.1, 1.13-2.01 and 4.06-118.0 µg/L, respectively ([Juma and Al-Madany, 2008](#)). The metals (Cd, Cu, Ni, Pb, and Zn) were measured in seawater collected from two stations around Bahrain between March 1991 and March 1992 with mean concentration of 0.13, 0.2, 0.24, 0.14, and 2.99 µg/L ([Al-Sayed et al., 1994](#)).

Globally, a comparison can be made with studies from areas that have similar geographical properties such as Daya Bay (South China Sea) which is a subtropical, semi-enclosed bay that has had as rapid a coastal development as Qatar, the eastern Black Sea region of Turkey where seaport, industrialization, shipyards and various factories lying along the coast as the status of Qatar's coastline, and the Mediterranean Sea coast. [Yuan et al., \(2020\)](#) reported concentrations of five trace metals in seawater from Daya bay (Cd, Cr, Cu, Zn and Pb). The highest trace metal detected in seawater was zinc (mean 12.25 µg/L), followed by copper (mean 1.48 µg/L), lead (mean 0.77 µg/L), chromium (mean 0.72 µg/L), then cadmium (mean 0.08 µg/L). ([Baltas et al., 2017](#)) collected seawater samples from the eastern Black Sea region of Turkey and reported 0.00917 µg/L Cu, 0.00620 µg/L Pb, and 0.00439 µg/L Zn. [El-Sorogy and Attiah \(2015\)](#) reported low levels of trace

metals in seawater of the Mediterranean Sea coast of Egypt, with mean concentration of 1.3×10^{-6} $\mu\text{g/L}$ Zn, 6×10^{-6} $\mu\text{g/L}$ Ni, 6×10^{-6} $\mu\text{g/L}$ Pb, and 4×10^{-6} $\mu\text{g/L}$ Cr.

In comparison to the Water Quality Standards (WQS) from USEPA (Table 6.1), our results may show a potential risk of Pb, Ni and Cu that showed a higher level than the criterion continuous concentration (CCC) set for these metals in seawater. The levels of Pb in Al Khor and Al Wakra seawater samples (56.1 and 13 $\mu\text{g/L}$ respectively) were above the CCC (8.1 $\mu\text{g/L}$). Nickel level in seawater samples collected from Simaisma, Umm Bab and Al Khor (9.8, 9.3 and 9.6 $\mu\text{g/L}$ respectively) were a little higher than the CCC (8.2 $\mu\text{g/L}$). For Cu, slightly higher concentration than CCC (3.1 $\mu\text{g/L}$) was observed in Al Khor seawater (3.5 $\mu\text{g/L}$).

Table 6. 2: The Mean Concentration of Total Mercury in Surface Seawater ($\mu\text{g/L}$)

Season	Site							
	Simaisma		Umm Bab		Al Khor		Al Wakra	
	Mean	STD	Mean	STD	Mean	STD	Mean	STD
Mar.17 (Summer)	0.008	0.008	0.008	0.009	0.005	0.003	0.007	0.006
Dec.17 (Winter)	0.009	0.008	0.024	0.034	0.011	0.011	0.239	0.313
May. 18 (Summer)	0.021	0.024	0.020	0.021	0.112	0.178	0.013	0.016
Nov.18 (Winter)	0.010	0.013	0.043	0.031	0.015	0.013	0.237	0.322

For total mercury, the mean concentration range in seawater samples was 0.005- 0.2 $\mu\text{g/L}$ (Table 6.2). Appendix G-1-1 illustrated the total mercury data. Based on the statistical analysis, no significant differences were observed in summer across sites (Figure 6.2). While in winter, the Kruskal-Wallis H test showed a significant difference. The post-hoc pairwise comparisons revealed that significant effects have been found between Simaisma and Al Wakra ($p = 0.008$). For more detailed in statistical analysis results, refer to Appendix G-2-1.

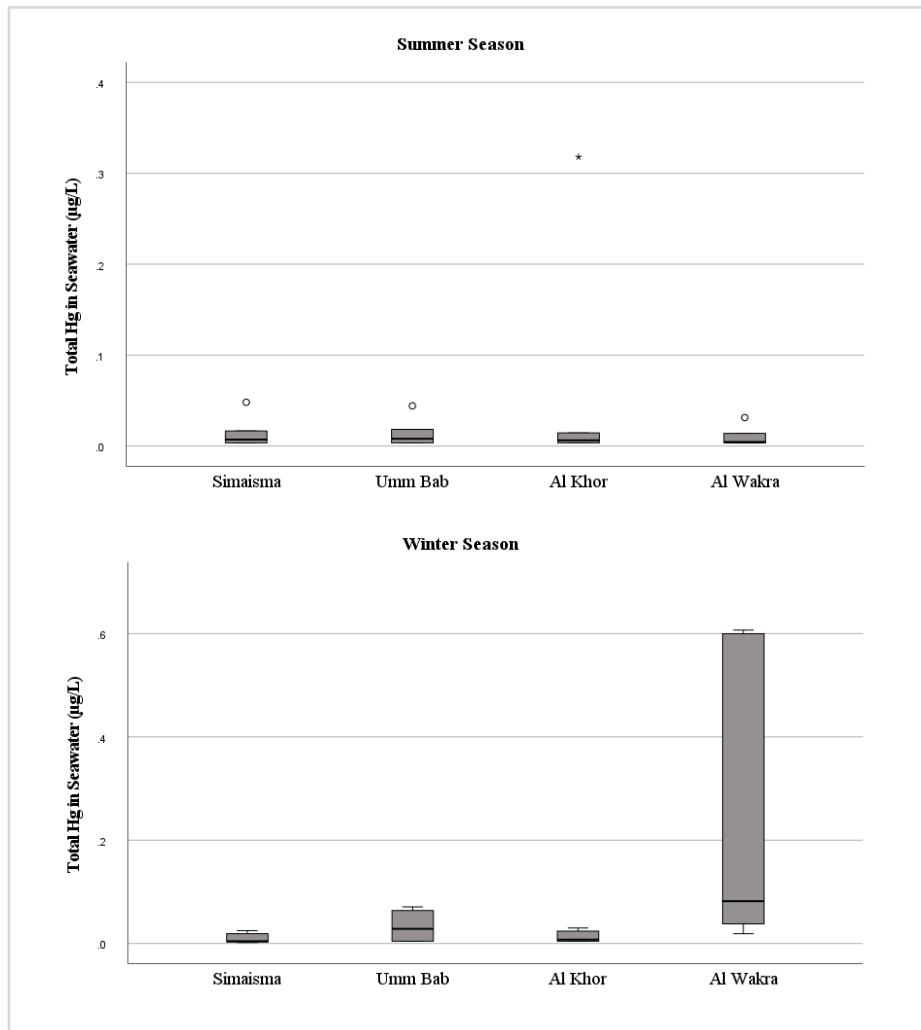


Figure 6. 2: Concentration of Total Mercury in seawater samples in summer and winter seasons

The total mercury concentration observed in this study in the seawater samples were in the range of the previous local studies (0.003- 0.2 µg/L) (Table 2.10). [Al Madfa et al. \(1994\)](#) observed concentration of total mercury in Qatar's seawater ranged between 0.003-0.03 µg/L. After five years, levels slightly became higher with ranged of 0.03 to 0.1 µg/L ([Kreish & Al Madfa, 1999](#)). The latest study done by ([Leitão et al, 2017](#)) reported 0.01- 0.2 µg/L of total mercury in Qatari seawater.

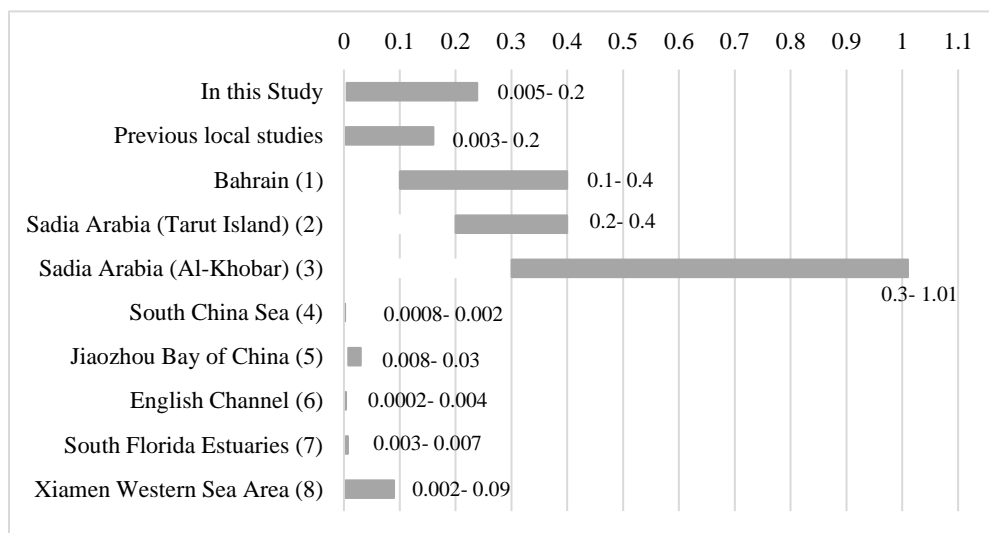


Figure 6. 3: Concentration of total Hg in seawater samples ($\mu\text{g/L}$) [(1): (Juma and Al-Madany, 2008), (2): (Youssef et al., 2016), (3): (Alharbi et al., 2017), (4): (Fu et al., 2010), (5): (Mao et al., 2020), (6): (Cossa and Fileman, 1991), (7): (Kannan et al., 1998), (8): (Liang et al., 2010)]

Regionally, other authors reported higher level of total mercury in seawater from Bahrain (0.1-0.4 $\mu\text{g/L}$, Juma and Al-Madany, 2008), and Sadia Arabia (Tarut Island, 0.2- 0.4 $\mu\text{g/L}$, Youssef et al., 2016 and Al-Khobar, 0.3- 1.01 $\mu\text{g/L}$, Alharbi et al., 2017). Globally, concentration of total mercury measured in this study were little bit high compared with worldwide region (Table 2.9). In South China Sea, the level of total mercury in seawater was ranged between 0.0008 to 0.002 $\mu\text{g/L}$ (Fu et al., 2010). Mao et al., (2020) measured the level of total mercury in surface seawater of the Jiaozhou Bay of China and reported a concentration of (0.008 - 0.03 $\mu\text{g/L}$). Many other studies in seawater reported low levels of total mercury from English Channel, South Florida Estuaries, USA, and Xiamen Western Sea Area with concentration ranged from (0.0002- 0.004 $\mu\text{g/L}$, 0.003- 0.007 $\mu\text{g/L}$, 0.002- 0.09 $\mu\text{g/L}$) respectively (Cossa and Fileman, 1991; Kannan et al., 1998; Liang et al., 2010).

Overall, of the metals detected, most were in the range of 0 to 4.7 $\mu\text{g/L}$, except for Pb and Ni, which had a range of 0.001–56.1 $\mu\text{g/L}$ and 0.06 to 9.8 $\mu\text{g/L}$ respectively. Al Khor seawater samples in summer season showed the highest level of Pb (56.1 $\mu\text{g/L}$), exceeding the WQS (8.1 $\mu\text{g/L}$) and the EC50 (45 $\mu\text{g/L}$) (ILA, 2015). Azlisham et al. (2008) reported that using fishing boats might reflect increased Pb concentrations in the aquatic environments. Thus, high Pb concentration observed in Al Khor might be due to boat transportation traffic in these sites where private boat parks and port located in Al Khor. If Pb moves on the food chain then it can be causing health

impacts. The potential adverse health concerns over the high concentrations of Pb over a short period of time might be anemia, weakness, and kidney and brain damage (NIOSH, 2018). Prolonged exposure to lead may also be at risk for high blood pressure, heart disease, kidney disease, and reduced fertility. The Department of Health and Human Services (DHHS) has determined that lead is probably cancer-causing in humans (US DHHS, 2007). Moreover, Al Khor, Simaisma and Umm Bab samples in summer presented the highest level of Ni with 9.6 µg/L, 9.8 µg/L and 9.3 µg/L respectively. This indicated that there was a source of Ni in these sites that might come from industries effluents in Umm Bab or beach filling in Simaisma or port and mangroves area in Al Khor. Skin contact with nickel-contaminated water may result in nickel exposure that can cause adverse effect to human health including allergic reactions such as skin rashes (Kerr, 2018). For total mercury, the level in Qatari seawater samples is moderately low, in comparison to international standard level in seawater (0.94 µg/L) (USEPA, 2002). In summer, all samples from the four sites showed low range, while in winter samples from Al Wakra showed wide range (0.02 µg/L - 0.6 µg/L) compared to other three sites (Figure 6.2). This observation might be due to recreational beach works in this site or from extensive harbor activities that may leach Hg near the coast.

6.3.2 Trace Metals and Total Mercury in Surface Coastal Sediment

The mean concentration range of Cd, Cr, Cu, Ni, Pb, and Zn in surface coastal sediment from the four sites were in the range of 0- 0.08, 4.10- 14.45, 0.12- 4.19, 3.53- 7.49, 0- 3.35, and 3.10- 14.92 µg/g (Table 6.3). The highest trace metals detected were chromium (4.10- 14.45 µg/g) and zinc (3.10- 14.92 µg/g). Chromium at Al Wakra sediment was significantly higher ($p = 0.028$) from the other three sites in summer while in winter it was only significantly higher from Al Khor ($p = 0.021$) (post-hoc Kruskal-Wallis test).

Figure 6.4 illustrates the seasonal variations pattern of trace metals concentration in coastal sediment samples from four different sites. In general, Cd was observed in very low levels in all sites over different seasons, followed by Pb which had same trend except in winter 2017 where the level was higher than other seasons with highest concentration reported in Al Wakra (3.35 µg/g). In Simaisma, the first year samples results show that Cr, Ni, and Zn had same trend as they detected in high concentration in summer season than winter, while Cu observed in high level in winter. Samples collected in the second year shows that Ni, and Zn were higher in winter, while

Cr and Cu were higher in summer. While in Umm Bab the first year samples results show that Cu, Zn and Pb detected in high concentration in winter, however Cr and Ni were observed in high level in summer. On the other hand, all trace metals in samples collected in the second year were high in winter season. In Al Khor, samples collected in the first year shows that Cu, Pb and Zn had high concentration in winter, while Cr and Ni had high level in summer. However, samples collected in the second year shows that Ni and Zn were higher in winter, while Cr and Cu were higher in summer. For samples collected from Al Wakra in the first year, results show that Cr, Cu, Pb and Zn had high concentration in winter; however, Ni had high level in summer. Samples collected in the second year shows that Ni and Zn were higher in winter; while Cr and Cu had high concentration in summer.

Table 6. 3: The Mean Concentration of Trace Metals in surface coastal sediment ($\mu\text{g/g}$)

Site	Season	Cd		Cr		Cu		Ni		Pb		Zn	
		Mean	STD	Mean	STD	Mean	STD	Mean	STD	Mean	STD	Mean	STD
Simaisma	Mar.17 (Summer)	0.03	0.05	6.98	5.53	1.21	1.98	5.95	3.23	0.20	0.34	8.00	3.36
	Dec.17 (Winter)	0.00	0.00	6.58	4.21	3.20	1.51	4.29	2.84	0.45	0.77	7.82	1.99
	May.18 (Summer)	0.02	0.00	6.02	2.72	1.82	0.76	3.60	1.80	0.00	0.00	4.01	1.41
	Nov.18 (Winter)	0.00	0.00	4.10	2.27	1.51	0.84	4.35	1.93	0.00	0.00	5.82	1.56
Umm Bab	Mar.17 (Summer)	0.00	0.00	6.58	0.87	1.33	1.61	4.66	0.60	0.00	0.00	6.27	1.01
	Dec.17 (Winter)	0.00	0.00	5.26	0.62	3.84	0.80	3.63	0.15	1.81	1.47	8.97	2.44
	May.18 (Summer)	0.03	0.04	12.11	9.85	3.23	1.14	4.10	1.09	0.00	0.00	3.74	1.97
	Nov.18 (Winter)	0.04	0.04	13.38	6.25	4.19	2.29	7.49	1.73	0.54	0.54	7.66	2.20
Al Khor	Mar.17 (Summer)	0.00	0.00	6.94	1.72	0.35	0.32	6.49	1.54	0.00	0.00	9.42	2.46
	Dec.17 (Winter)	0.04	0.03	5.49	1.09	3.52	0.45	5.16	0.76	1.30	1.13	11.02	3.64
	May.18 (Summer)	0.04	0.04	7.27	0.45	3.11	1.25	4.72	1.01	0.00	0.00	6.23	2.53
	Nov.18 (Winter)	0.03	0.03	4.83	0.72	2.47	0.58	5.32	0.72	0.00	0.00	8.18	3.04
Al Wakra	Mar.17 (Summer)	0.00	0.00	12.87	4.74	0.12	0.21	4.34	0.47	0.00	0.00	5.15	0.50
	Dec.17 (Winter)	0.07	0.12	14.45	3.58	3.41	0.88	3.66	0.36	3.35	3.21	14.92	5.95
	May.18 (Summer)	0.08	0.05	13.27	2.43	2.74	0.33	3.53	0.54	0.00	0.00	3.10	0.82
	Nov.18 (Winter)	0.00	0.01	8.46	0.58	1.77	0.34	3.86	0.26	0.00	0.00	7.27	0.83

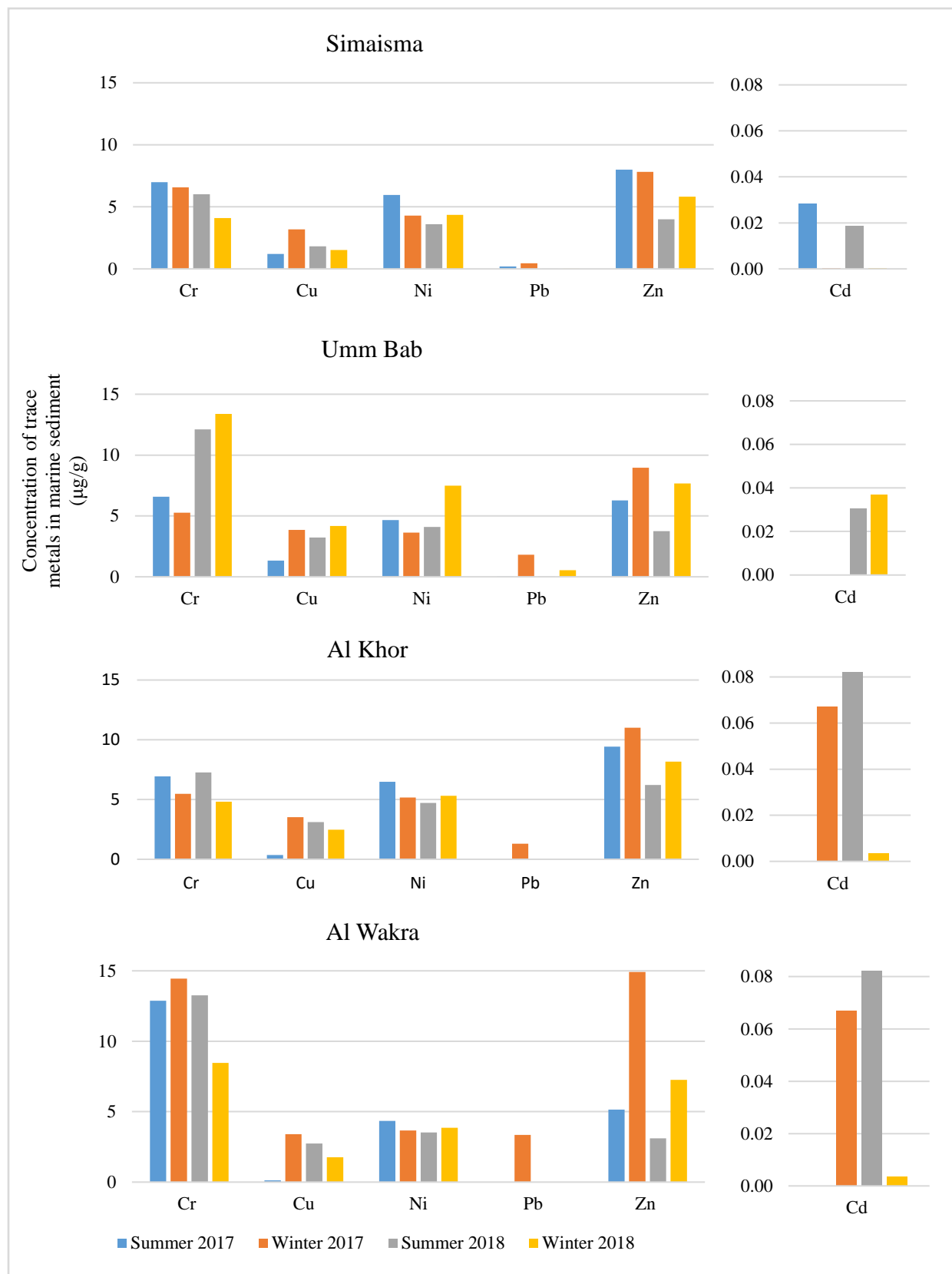


Figure 6. 4: Seasonal variations of trace metals concentration in coastal sediment samples

Compared with previous local studies in coastal sediment from Qatar, the concentrations of trace metals were in the range of previous local studies, ranging from 0.04 to 46.5 $\mu\text{g/g}$, where the lowest values were reported by [Leitao et al., \(2017\)](#) for cadmium and the highest value were measured by [Aboul Dahab and Al-Madfa \(1997\)](#) for chromium. Trace metals (Cr, Co, Cu, Zn, and Ni) concentrations were investigated in coastal sediment from North Western of Qatar with mean concentration of 4, 1, 3, 13, and 6 $\mu\text{g/g}$ respectively ([Basaham and Al-Lihaibi, 1993](#)). [Aboul Dahab and Al-Madfa \(1997\)](#) examined Cr concentration in sediments of the eastern side of the Qatari peninsula with concentration ranged from 11.6 to 46.5 $\mu\text{g/g}$ dry wt. and an average of 25.4 ± 8.7 $\mu\text{g/g}$ dry wt. Concentrations of trace metals in surface sediments along the Qatari Doha Bay from 10 transects each with five stations were studied by ([Al-Naimi et.al., 2015](#)). The overall results of metal analyses were within the international standards criteria, and the results were comparable to the previous studies conducted around Qatar. [Leitão et al. \(2017\)](#) measured levels of trace metals in sediment from three sites around Qatar coastline (AlKhor, Doha Harbor and AlWakra Harbor) during summer and winter seasons. In summer, levels of Cd, Cr, Cu, Ni, and Zn were (0.05, 15.97, 2.92, 1.10 and 4.72 $\mu\text{g/g}$) in AlKhor, and levels of Cd, Cr, Cu, and Zn were (0.06, 1.13, 2.74, and 1.31 $\mu\text{g/g}$) and (0.06, 3.81, 0.74, 0.58, 2.20 $\mu\text{g/g}$) in Doha Harbor and AlWakra Harbor respectively. While in winter, levels of Cd, Cr, Cu, Ni, and Zn were (0.07, 4.90, 2.11, 2.81, and 4.71 $\mu\text{g/g}$) in AlKhor, and levels of Cd, Cr, Cu, and Zn were (0.04, 1.29, 1.08, and 1.37 $\mu\text{g/g}$) and (0.18, 29.80, 9.73, 5.34, and 14.34 $\mu\text{g/g}$) in Doha Harbor and AlWakra Harbor respectively.

Regionally, trace metals reported in Qatar's coastal sediments, compared to other studies from the Arabian Gulf, were low (Table 2.8). An assessment of contamination in coastal sediment due to heavy metals in the Arabian Gulf was conducted during 2000–2001 ([de Mora et al., 2004](#)). This study noted two hotspots in heavy metals in Bahrain and on the east coast of the UAE. Elevated levels of heavy metals Cu, Pb, and Zn with mean concentrations of 48.3, 99.0, and 52.2 $\mu\text{g/g}$ respectively were recorded off the oil refinery in Bahrain. Higher concentrations of heavy metals Cr and Ni were reported at Akkah beach on the east coast of the UAE with maximum concentrations of 303, and 1010 $\mu\text{g/g}$ respectively and attributed to the metal-rich mineralogy of the region. Elevated Cd levels (19.14 $\mu\text{g/g}$) were also reported near a desalination plant off the eastern coastline of Bahrain and attributed to petroleum industries as well as effluents from a variety of factories and industrial facilities ([Naser, 2013](#)). A baseline survey of sediment contamination due to heavy metals was undertaken at twenty-nine locations around Kuwait ([Lyons](#)

et al., 2015). The reported range of trace metals were Cr (108.2–429.0 µg/g), Ni (86.2–169.3 µg/g), Cu (21.7– 53.4 µg/g), Zn (55.3–140.7 µg/g), Cd (<0.178–0.5 µg/g), and Pb (9.7–32.2 µg/g). Previous study in coastal sediment from Kuwait in 1985 reported lower levels of trace metals (Cd, Cu, Ni, Pb and Zn) with mean concentrations of 0.26, 2.59, 10.07, 3.55, and 13.7 µg/g respectively (Al-Hashimi and Salman, 1985). Alharbi and El-Sorogy (2017) measured levels of Cd, Cr, Cu, Ni, Pb and Zn in sediment from Saudi Arabia coastal environment with mean concentration of 0.23, 51.03, 182.97, 75.10, 5.36, and 52.68 µg/g respectively.

Globally, concentration of trace metals measured in this study were in low level compared with selected worldwide region studies (Table 2.7). Fang and Lien (2020) reported levels of trace metals in surface sediment from East China Sea with concentration range of 32.2-142.5 µg/g Cr, 18.2-143.3 µg/g Zn, 13.3-108 µg/g Ni, 6.2-46 µg/g Pb, 1.9-47.1 µg/g Cu, and 0.02-0.36 µg/g Cd. While study conducted in sediments from coastal environment of USA reported lower levels of trace metals with mean concentration of 45.3 µg/g Zn, 32 µg/g Cr, 10.5 µg/g Pb, and 9 µg/g Cu (Paul et al., 2021). Other study investigated the contents of Cu, Zn and Pb in sediment samples collected from Turkey with mean concentration of 576.31 µg/g, 357.02 µg/g, 97.33 µg/g respectively (Baltas et al., 2017). El-Sorogy and Attiah (2015) measured levels Ni, Pb, Zn and Cr in sediment from sea coast of Egypt with mean of 803.2, 405.71, 340.23, and 0.26 µg/g respectively.

For total mercury, the levels in coastal sediment samples collected from the four sites ranged between 0.005 and 0.12 µg/g (Table 6.4). Refer to Appendix G-1-2 for detailed data. Based on the statistical analysis, no significant differences were observed in summer or winter across sites (Figure 6.5). Total mercury was more detected in winter seasons than summer. Refer to Appendix G-2-2 for statistical analysis data.

Table 6. 4: The Mean Concentration of Total Mercury in surface coastal sediment (µg/g)

Season	Site							
	Simaisma		Umm Bab		Al Khor		Al Wakra	
	Mean	STD	Mean	STD	Mean	STD	Mean	STD
Mar.17 (Summer)	0.012	0.008	0.052	0.077	0.100	0.156	0.020	0.010
Dec.17 (Winter)	0.028	0.040	0.019	0.025	0.005	0.000	0.005	0.000
May. 18 (Summer)	0.010	0.008	0.005	0.000	0.029	0.021	0.014	0.008
Nov.18 (Winter)	0.097	0.041	0.053	0.017	0.118	0.043	0.056	0.013

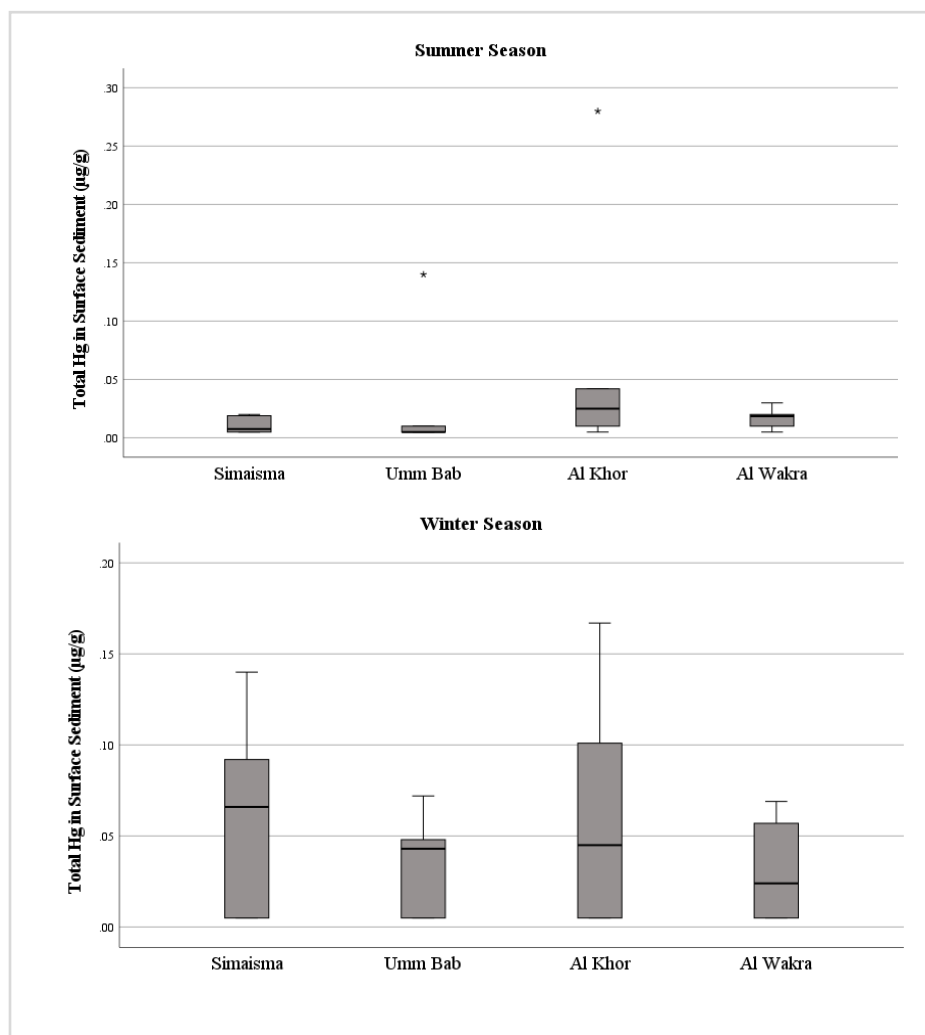


Figure 6. 5: Concentration of Total Mercury in surface sediment samples in summer and winter seasons

The total mercury concentration observed in previous local studies (Figure 6.6) showed that total mercury in coastal sediment of Qatar seems to decline over time. The concentration range were 0.19-1.75 $\mu\text{g/g}$ (Al Madfa et al., 1994), 0.024 - 0.20 $\mu\text{g/g}$ (Kreish & Al Madfa, 1999), 0.01-0.04 $\mu\text{g/g}$ (Leitão et al, 2017), and 0.008-0.03 $\mu\text{g/g}$ (Hassan et al., 2019). However, the concentration of total mercury observed in our study slightly higher compared to levels reported by Leitão et al. (2017) and Hassan et al. (2019), with range of 0.005 to 0.12 $\mu\text{g/g}$.

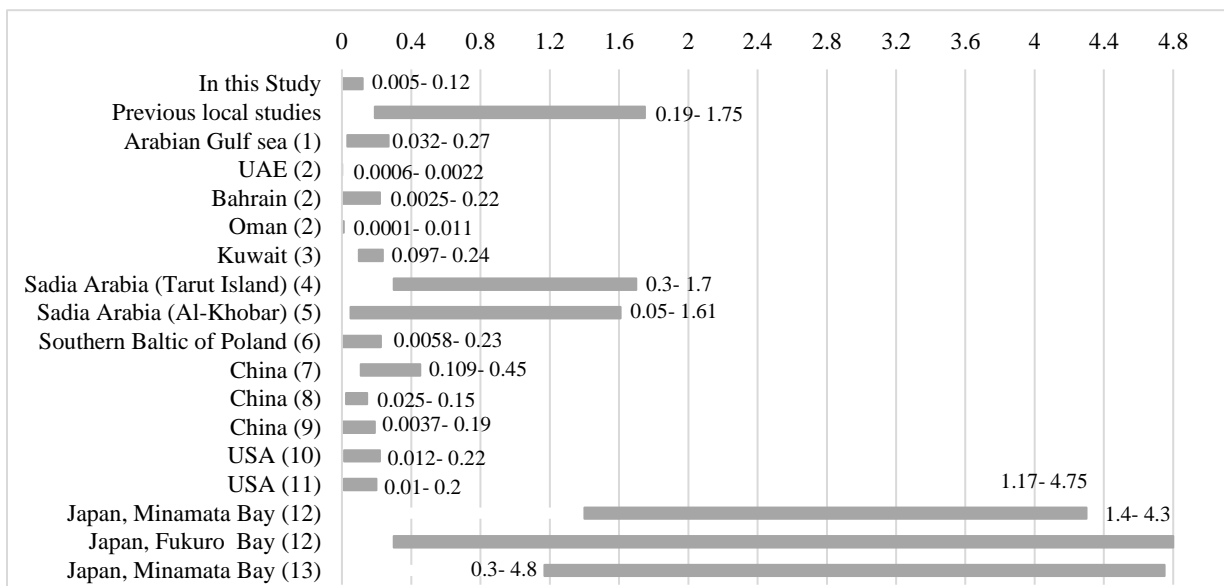


Figure 6. 6: Concentration of total Hg in surface sediment samples ($\mu\text{g/g}$) [(1):(Kureishy and Ahmad, 1994), (2):(de Mora et al., 2004), (3):(Lyons et al., 2015), (4):(Youssef et al., 2016), (5):(Alharbi et al., 2017), (6):(Beldowski et al., 2014), (7):(Yu et al., 2012), (8):(Mao et al., 2020), (9):(Fang and Lien, 2020),(10):(Kannan et al., 1998), (11):(Apeti et al., 2012), (12):(Tomiyasu et al., 2006),(13):(Matsuyama et al., 2011)]

Comparing to other studies in coastal sediment from Arabian Gulf region, the concentration of total mercury detected in this study was in the range found in these countries (0.0001-1.7 $\mu\text{g/g}$). Kureishy and Ahmad (1994) reported (0.032-0.27 $\mu\text{g/g}$) of total mercury from Arabian Gulf sea. de Mora et al. (2004) reported levels of total mercury from UAE, Bahrain and Oman coastal sediment with levels ranged between 0.0006–0.0022 $\mu\text{g/g}$, 0.0025–0.220 $\mu\text{g/g}$, and <0.0001–0.011 $\mu\text{g/g}$ respectively. Concentration of total mercury in Kuwait coastal sediment was ranged from <0.097– <0.236 $\mu\text{g/g}$ (Lyons et al., 2015), while in Saudi Arabia were (0.3- 1.7 $\mu\text{g/g}$, Tarut Island) and (0.05- 1.61 $\mu\text{g/g}$, Al-Khobar) (Youssef et al., 2016; Alharbi et al., 2017).

Likewise, distribution of total mercury in coastal sediment reported in this study was in the range of reported studies from many areas around the world (0.0037- 6.13 $\mu\text{g/g}$) (Table 2.9). The sedimentary mercury in the Southern Baltic of Poland was investigated by Beldowski et al. (2014), who reported concentration of total mercury ranged between 0.0058 to 0.225 $\mu\text{g/g}$. Many authors studied levels of total mercury in coastal sediment of China (Yu et al., 2012; Mao et al., 2020; Fang and Lien, 2020) with concentration ranged between 0.109- 0.453 $\mu\text{g/g}$, 0.0246- 0.14516 $\mu\text{g/g}$, and 0.0037- 0.19 $\mu\text{g/g}$ respectively. Concentration of total mercury in coastal sediment of USA studied in different decade by (Kannan et al., 1998) and (Apeti et al., 2012) who reported same levels with concentration ranged from 0.012- 0.219 and 0.01 - 0.2 $\mu\text{g/g}$ respectively. Tomiyasu et al. (2006) investigated slightly high level of total mercury in surface coastal sediments collected

from Minamata Bay and Fukuro Bay of Japan with concentration ranged from 1.4–4.3 µg/g and 0.3–4.8 µg/g respectively. Moreover, [Matsuyama et al. \(2011\)](#) measured the total mercury in the Minamata Bay and he found (1.17- 4.75 µg/g) approximately same levels reported by the previous author.

To sum up, Al Wakra sediment samples showed the highest levels of Cr and Zn compared with the other three sites (14.45 µg/g and 14.92 µg/g respectively). The anthropogenic sources from harbor activities located along its coast and atmospheric deposition of exhaust particulates from the large volumes of vehicular traffic may explain the elevated levels of Cr in Al Wakra coastal sediment. Moreover, textural characteristics of sediment (% silt and % clay) provided a larger surface area that retained high amounts of trace metals ([Kastratovic et al., 2016](#)). Percent silt and clay were high in Al Wakra sediment cores (42% silt, and 1.3% Clay) in all depth from 5cm to 30cm, although the coastal surface samples were sandy (97% sand). For total mercury, figure 6.5 shows the total concentration in sediment samples in summer and winter. Samples collected in winter from the four sites showed a wider range than samples collected in summer. The highest range was observed in Al Khor samples, where the TOC content in sediment was the highest (2.01 mg/kg) compared to other site and the fine particle size was also high in this site (clay 1.7%, silt 22%). Followed by Simaisma sediment samples that also contain fine particle size (clay 1.6%, silt 23.2%) and TOC content of 1.4 mg/kg less than Al Khor. [Bengtsson and Picado \(2008\)](#) and [Melamed et al. \(1997\)](#) found that TOC content within the sediment enhance the sorption of contaminants such as Hg by providing additional sorption sites by indicating that TOC within coastal sediments possibly plays a vital role in controlling Hg sequestration process. This may indicate that the concentrations of total mercury in sediments of the sampling areas were significantly influenced by TOC contents. Levels of total mercury was compared with the Canadian Sediment Quality Guidelines (SQGs), the threshold effect level (0.170 µg/g) and probable effect level (0.486 µg/g) ([MacDonald et al., 2000](#); [US EPA, 2006](#)) were in the range of unpolluted areas regarding total mercury < 0.13 µg/g, and were nearly four times lower than the threshold effect level.

6.3.3 Trace Metals and Total Mercury in Sediment Cores

The mean concentration range of Cd, Cr, Cu, Ni, Pb, and Zn in sediment cores from the four sites in all depths were in the range of 0.00009- 0.4, 2.9- 32, 0.0001- 9, 0.003- 22.5, 0.0006- 2.7, and 0.0006- 18.6 $\mu\text{g/g}$. The highest trace metals detected in all depths was chromium in Al Wakra site (23.6- 32 $\mu\text{g/g}$) followed by Umm Bab (9.9- 17.6 $\mu\text{g/g}$). Likewise, zinc was more detected in Al Wakra sediment core (8.2- 18.6 $\mu\text{g/g}$) followed by Umm Bab (0.5- 15.3 $\mu\text{g/g}$)

In the Simaisma core, in surface layer (5cm depth) Ni was the highest detected trace metals followed by Cr then Zn (Figure 6. 7). From 10 cm to 30 cm depth, Cr was the highest. While in Umm Bab core, Cr was the highest metal detected in all depths followed by Cu then Zn. In Al Khor core, Cr was the highest metal observed in all depths except in 25cm where Ni showed higher level. Likewise, Al Wakra showed high level of Cr in all depths (23.6 $\mu\text{g/g}$ - 31.96 $\mu\text{g/g}$) followed by Zn (8.2 $\mu\text{g/g}$ - 18.6 $\mu\text{g/g}$) then Cu (6.1 $\mu\text{g/g}$ - 9 $\mu\text{g/g}$).

Statistical analysis of the trace metals (Cd, Cr, Cu, Ni, Pb, and Zn) in the sediment core samples showed that significant differences among sampling sites (The Kruskal-Wallis H test, $P < 0.05$). For Cd, Umm Bab sediment core was significantly higher than the three other sites. For Cr, Cu, Ni, Pb and Zn, the level in Al Wakra sediment core samples was significantly higher than the three other sites.

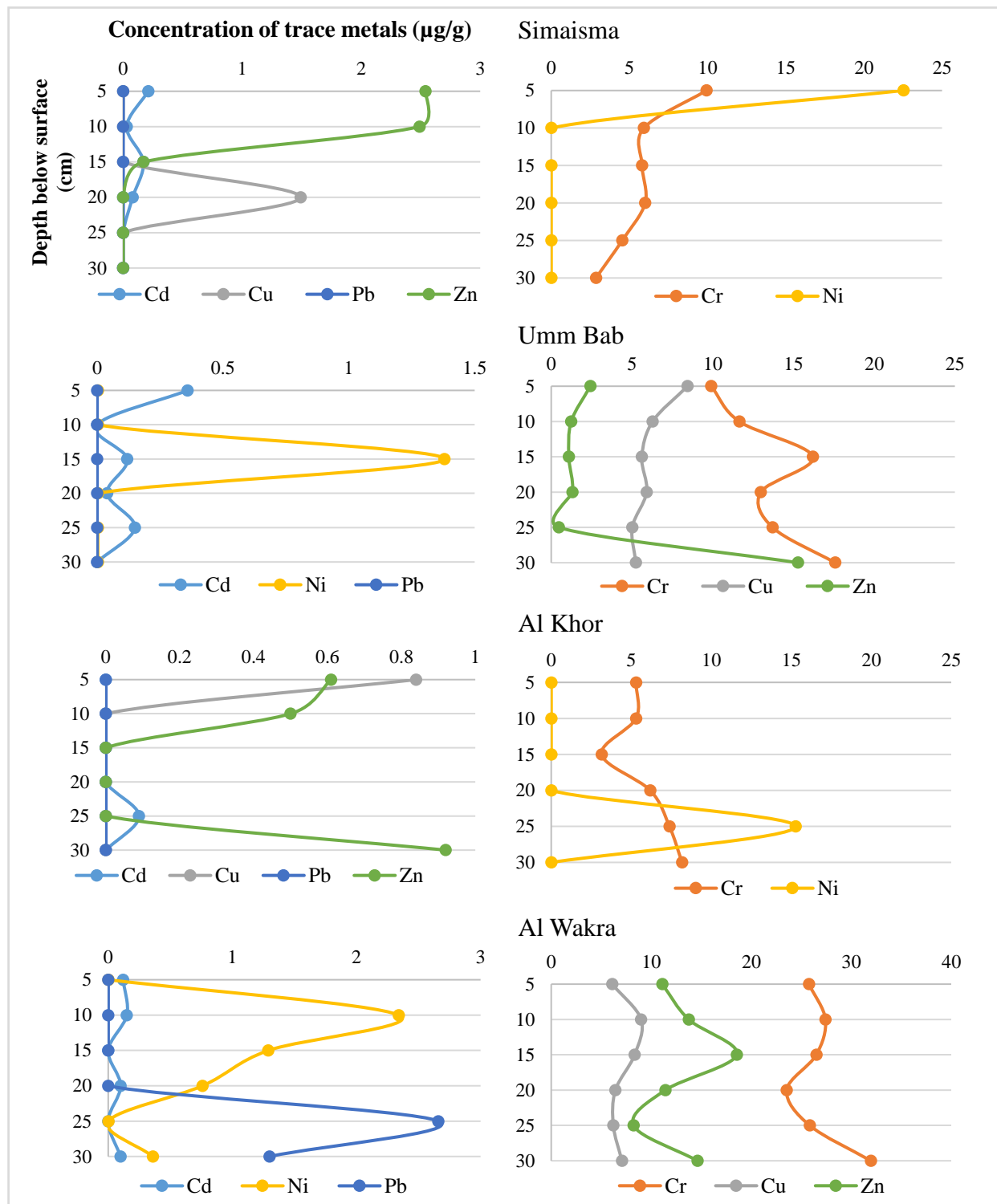


Figure 6. 7: The mean concentration of trace metals in sediment cores from the four sites

For total mercury, the levels in sediment core samples from the four sites ranged from 0.05 to 0.6 $\mu\text{g/g}$ with the highest value measured in all depths at Al Wakra (Figure 6.8). In the Simaisma core, the concentration of total mercury was low at the surface (0.05 $\mu\text{g/g}$) then increased to maximum (0.4 $\mu\text{g/g}$) in 10cm depth then decreased gradually to minimum again (0.05 $\mu\text{g/g}$) in 20cm depth, and then slightly increased to (0.2 $\mu\text{g/g}$) in 25cm depth. While in Umm Bab core, low levels were observed in all depth ranged from (0.1 $\mu\text{g/g}$ - 0.2 $\mu\text{g/g}$). Likewise, Al Khor core showed low levels in all depths ranged between 0.07 $\mu\text{g/g}$ to 0.1 $\mu\text{g/g}$. On the other hand, Al Wakra core shows different trend, slightly higher concentrations were detected in all depths than other cores. At surface (5cm) total mercury was low (0.4 $\mu\text{g/g}$), then slightly increased in 10cm (0.5 $\mu\text{g/g}$) then decreased again in 15cm then increased to maximum in 20cm (0.6 $\mu\text{g/g}$) then decreased till 30 cm to (0.4 $\mu\text{g/g}$).

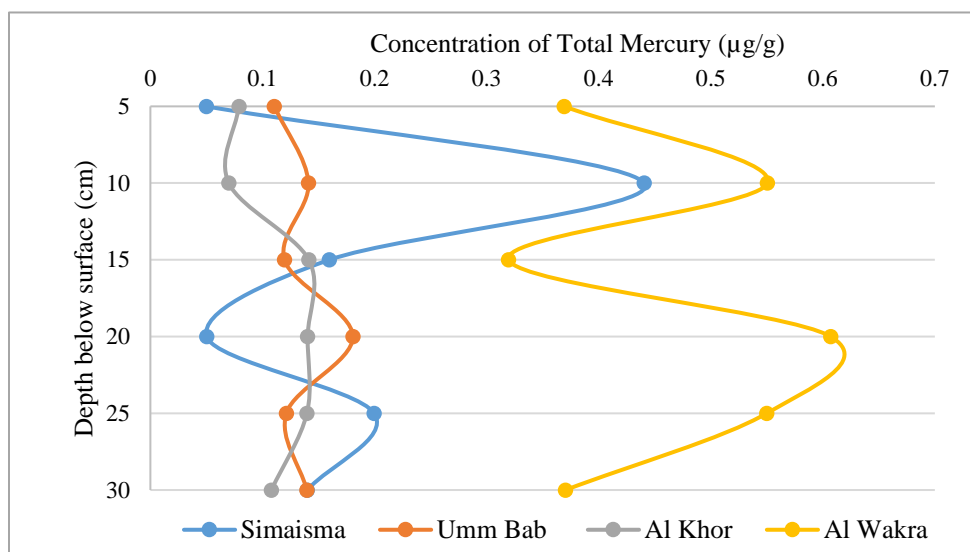


Figure 6. 8: The mean concentration of total mercury in sediment Cores ($\mu\text{g/g}$)

The Statistical analysis showed that significant differences was noted among sampling sites (The Kruskal-Wallis H test, $P= < 0.001$) (Figure 6.9-A). The Post-hoc pairwise comparisons revealed that significant effects have been found between Al Khor and Al Wakra, Umm Bab and Al Wakra, and between Simaisma and Al Wakra. Al Wakra sediment core samples was significantly higher than the three other sites. No significant differences present between Total Mercury level and depth (The Kruskal-Wallis H test, $P= 0.135$) (Figure 6.9-B).

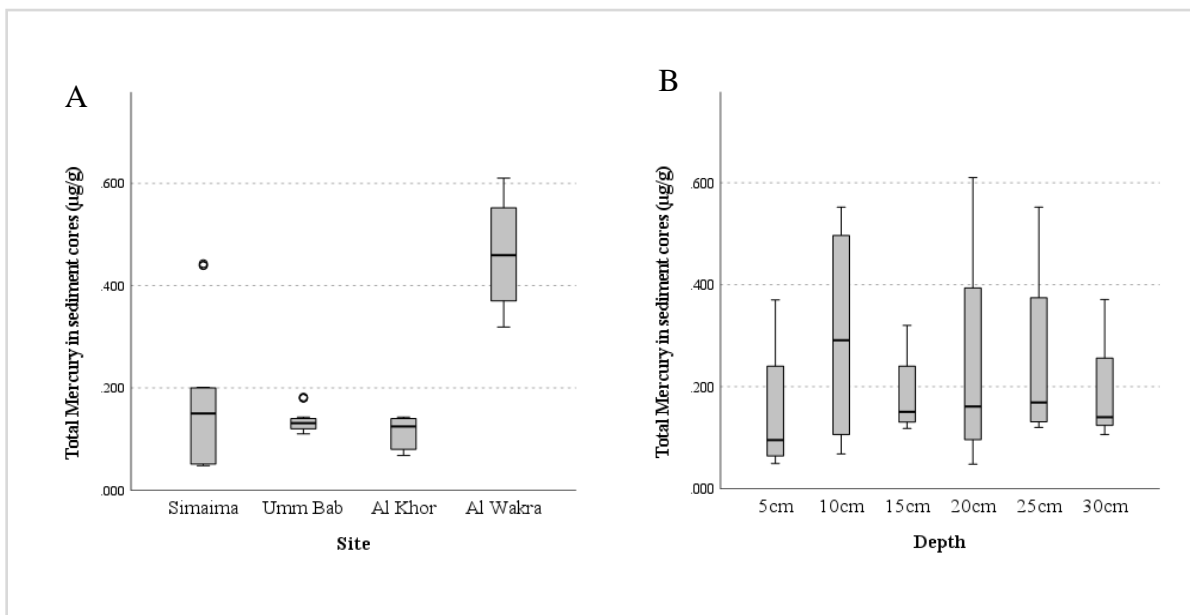


Figure 6. 9: The mean concentration of Total Mercury in sediment cores across sites and depth

Overall, the sediment core samples showed same trend as surface sediment for Al Wakra site, where Cr was the highest trace metal detected in all depths (23.6 µg/g to 32 µg/g) followed by Zn (8.2 µg/g to 18.6 µg/g). Moreover, the highest level of total mercury was reported in Al Wakra sediment core that contained high TOC content as we go deeper and fine grain size fraction with more than 39% of silt in all depth. These results may confirm our thought that grain size of Al Wakra sediment that consist of (42% silt, and 1.3%Clay) may affect the presence of high levels of these trace metals beside with the anthropogenic sources that present in this site including harbor activities, recreational boat traffic and fishing fleet movement.

6.3.4 Trace Metals and Total Mercury in Oyster Tissues

The trace metals concentration in oyster tissues samples are presented in Table 6.5. Zn was the most abundant major trace metals in bivalve tissues (551.8-2807.2µg/g) with highest level detected in oysters collected from Al Wakra, followed by Cd (3.4-10.3 µg/g), Cu (2. 6-10.2 µg/g), Ni (0.8-3.1 µg/g), Cr (0.5-2.6 µg/g), and Pb (0-0.7 µg/g). Appendix F-1-3 shows the trace metals data in detail. The statistical analysis showed that there was a statistically significant for Cr in summer ($p = 0.03$). Al Wakra oyster samples has a significantly higher mean than Umm Bab (Tukey HSD post-hoc test). In winter, significant differences were observed between sites for Cu and Ni with ($p = 0.04$) and ($p = 0.001$) respectively. Significant effects have been found between Al Khor and Al Wakra for Cu, and between Simaisma and Al Wakra for Zn (Tukey HSD post-hoc test).

Table 6. 5: The Mean Concentration of Trace Metals in Tissues of Pearl Oyster (*P. radiata*) ($\mu\text{g/g}$)

Site	Time	Cd		Cr		Cu		Ni		Pb		Zn	
		Mean	STD	Mean	STD	Mean	STD	Mean	STD	Mean	STD	Mean	STD
Simaisma	Mar.17(Summer)	5.99	0.95	0.98	0.77	4.78	3.37	1.59	0.31	0.00	0.00	1768.57	537.21
	Dec.17(Winter)	8.69	2.25	1.06	0.20	4.12	1.11	0.78	0.13	0.67	0.25	1331.12	411.31
	May. 18(Summer)	10.34	3.04	1.30	0.68	7.15	2.15	1.06	0.07	0.00	0.00	1667.42	242.21
	Nov.18(Winter)	6.05	3.34	1.20	0.19	8.73	3.16	1.10	0.28	0.08	0.07	926.22	546.87
Umm Bab	Mar.17(Summer)	6.57	3.01	0.52	0.45	4.58	2.89	1.67	0.70	0.00	0.00	1782.94	640.52
	Dec.17(Winter)	5.88	1.35	1.08	0.35	5.96	1.87	1.58	0.28	0.72	0.15	1072.11	456.94
	May. 18(Summer)	8.32	1.32	0.65	0.73	5.63	1.19	1.22	0.08	0.26	0.45	1718.16	376.44
	Nov.18(Winter)	3.37	0.38	1.20	0.59	5.86	0.72	1.62	0.36	0.15	0.17	551.82	81.32
Al Khor	Mar.17(Summer)	7.80	1.75	0.73	0.49	2.56	0.45	1.34	0.46	0.00	0.00	1522.18	674.02
	Dec.17(Winter)	5.85	1.55	1.99	0.79	4.91	1.20	3.08	3.16	0.62	0.25	1283.48	486.98
	May. 18(Summer)	6.87	2.13	0.73	0.19	6.70	0.52	0.92	0.07	0.40	0.40	1463.04	419.07
	Nov.18(Winter)	3.63	0.38	0.97	0.16	5.26	0.71	2.29	1.97	0.28	0.20	1015.74	306.25
Al Wakra	Mar.17(Summer)	7.31	2.30	2.60	1.67	4.62	2.59	2.02	0.43	0.00	0.00	1769.36	628.89
	Dec.17(Winter)	7.51	1.40	1.65	0.15	7.05	0.46	1.02	0.15	0.25	0.28	2704.88	765.13
	May. 18(Summer)	5.63	0.70	1.40	0.63	7.90	0.60	0.98	0.06	0.00	0.00	2807.18	390.13
	Nov.18(Winter)	5.19	1.31	1.86	0.24	10.19	1.14	2.12	0.46	0.51	0.07	2515.33	650.87

It can be seen clearly that in oyster tissues samples, zinc was detected in high concentration in all sites at all seasons, with higher level detected in summer than winter seasons in Simaisma, Umm Bab and Al Khor except for Al Wakra where higher levels were observed in winter for first year sampling (Figure 6.10). In Simaisma, the samples collected in the first year shows that Cd, Cr, and Pb had same trend as they detected in high concentration in winter season than summer, while Cu and Ni wear observed in high level in summer than winter. Samples collected in the second year shows that Cu, Ni, and Pb were higher in winter than summer, while Cd and Cr were higher in summer than winter. For oyster samples collected from Umm Bab in the first year, results show that Cr, Cu, and Pb detected in high concentration in winter season than summer, however Cu and Ni wear observed in high level in summer than winter. Samples collected in the second year shows that Cr, Cu, and Ni were higher in winter than summer, while Cd and Pb were higher in summer than winter. In Al Khor, the samples collected in the first year shows that Cr, Cu, Ni and Pb were detected in high concentration in winter than summer season, while Cd observed in high level in summer than winter. However, samples collected in the second year shows that Cr and Ni were higher in winter than summer; while Cd, Cu and Pb were higher in summer than winter. For samples collected from Al Wakra in the first year, results show that Cd, Cu, and Pb detected in high concentration in winter season than summer, however Cr and Ni wear observed in high level in summer than winter. Samples collected in the second year shows that Cr, Cu, Ni and Pb were higher in winter than summer; while Cd was higher in summer than winter.

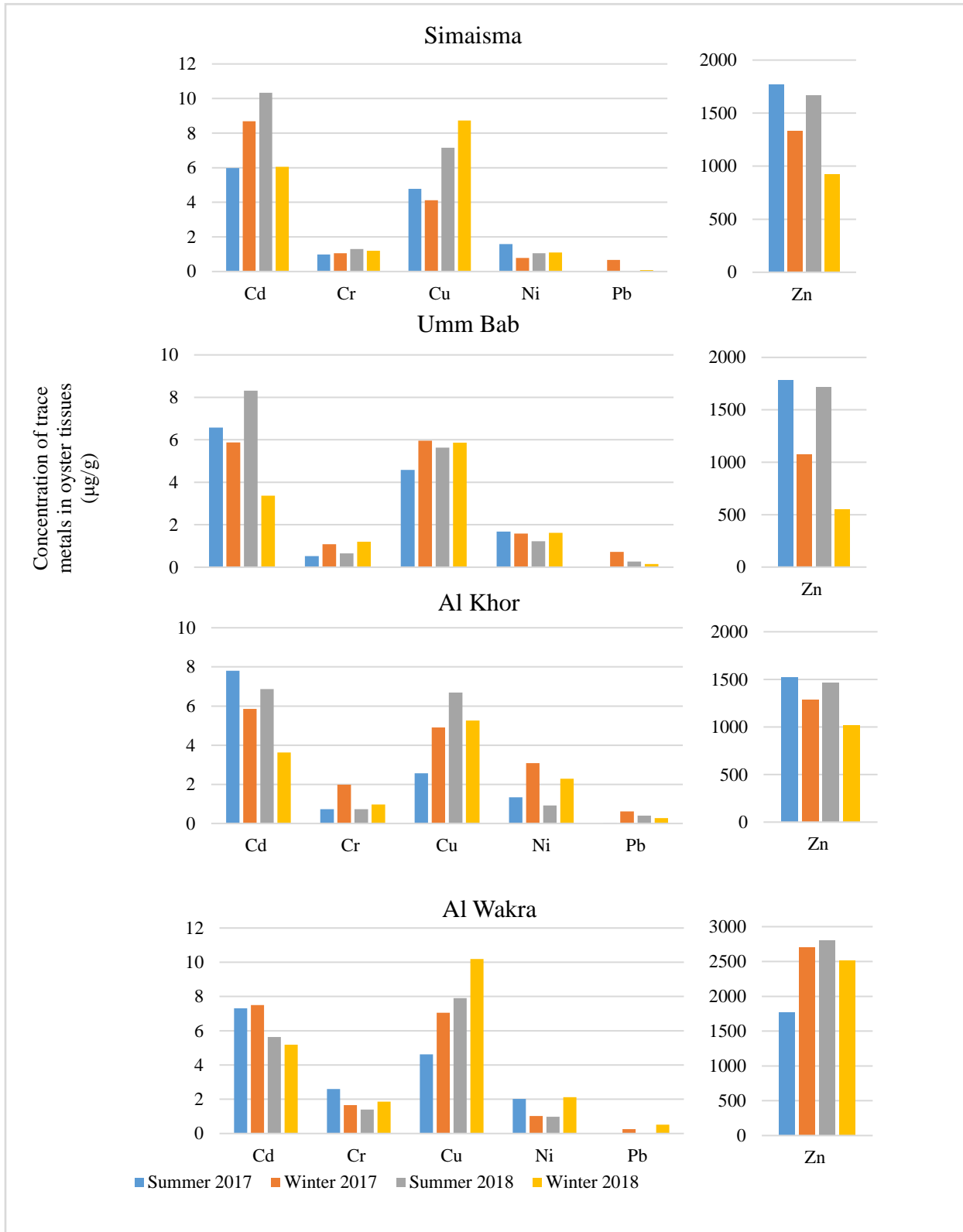


Figure 6. 10: Seasonal variations of trace metals concentration in oyster tissues samples

Levels of trace metals observed in this study in *P. radiata* oyster tissues samples were similar to the findings of the previous local study by [Leitão et al. \(2017\)](#) who reported high levels of Zn. She measured levels of trace metals in *P. radiata* from three sites around Qatar coastline (AlKhor, Doha Harbor and AlWakra Harbor) during summer and winter seasons. In AlKhor and Doha Harbor, the levels for most trace metals were high in winter compared to summer, while in AlWakra the same trend was maintained during the summer and winter. In summer, levels of Cd, Cr, Cu, Ni, Pb and Zn were (9.0, 1.3, 3.8, 0.6, 0.04, and 840.7 µg/g), (0.06, 1.1, 2.7, ND, ND, 1.3 µg/g), and (3.2, 2.6, 12.9, 1.4, 0.3, and 2529.5 µg/g) in AlKhor, Doha Harbor and AlWakra Harbor respectively. While in winter, levels of Cd, Cr, Cu, Ni, Pb and Zn were (7.1, 1.29, 5.75, 0.50, 0.21, and 1792.39 µg/g), (6.35, 1.33, 4.81, ND, 0.10, and 4205.70 µg/g), and (2.45, 2.37, 6.65, 1.28, 0.06, and 2066.83 µg/g) in AlKhor, Doha Harbor and AlWakra Harbor respectively. [Al-Madfa et al. \(1998\)](#) collected pearl oysters *P. radiata* from eight sites around eastern coastline of Qatar to assess trace metals concentrations. The mean concentration of Cd, Cu, Pb, and Ni in *P. radiata* collected from all the sites were 0.49, 2.79, 3.88 and 7.08 µg/g dry weight respectively. This study reported high mean concentrations for Pb and Ni in *P. radiata* collected from areas that were subject to dredging and shipping activities along the Qatari coastline.

Regionally, trace metal concentrations observed in this study in the *P. radiata* samples were in the lower range of the ones observed by [de Mora et al. \(2004\)](#) in pearl oyster specimens from the Arabian Gulf, with the exception of Zn that presented higher values in this study, similar to the levels found in UAE (1261 µg/g), Saudi Arabia (1618 µg/g) and near BAPCO site in Bahrain (4290 µg/g) ([Fowler et al., 1993](#); [de Mora et al. 2004](#)). Moreover, oysters collected from Saudi Arabia showed high level of Ni (260 µg/g), while oysters collected from Oman showed high level of Cu (129.83 µg/g) compared to other countries. During 2000–2001, high concentrations of Pb (3.92 µg/g) were found in pearl oysters near the BAPCO site in Bahrain and relatively high concentrations of Cr (2.36 µg/g), Ni (7.02 µg/g) and Cu (17.3 µg/g) were found in pearl oysters from Abu Dhabi ([de Mora et al., 2004](#)). [Bu-Olayan et al. \(1997\)](#) investigated the contribution of the 1991 oil spill to heavy metal contamination in the pearl oyster, *Pinctada radiata* for their heavy metal contents before and after the spill. Concentrations of copper (Cu), nickel (Ni), lead (Pb) and zinc (Zn) were determined in oyster samples from three coastal stations of Kuwait during 1990 and 1994. In the 1990 samples, the metal mean concentrations in oysters were 0.86 µg/g for Cu, 0.88 µg/g for Ni, 0.56 µg/g for Pb and 0.494 µg/g for Zn, while in the 1994 samples, the metal

mean concentrations for Cu, Ni, Pb and Zn were 55.00, 16.96, 0.57 and 486.61 $\mu\text{g/g}$ respectively. Due to a contribution from the 1991 Gulf War oil spill, the 1994 samples have significantly higher mean concentrations of metals than the 1990 samples. Between March 1991 and March 1992, levels of Cd and Pb were measured in pearl oyster *Pinctada radiata* collected from two stations around Bahrain ranged from (0.25-3.8 $\mu\text{g/g}$) and (1.25-14.0 $\mu\text{g/g}$) respectively (Al-Sayed et al., 1994).

Internationally, the levels of trace metals reported from the present study are in the range of levels reported from different locations worldwide (Table 2.7), and it follows the same trend that Zinc is the most detectable trace metals found in oyster tissues. The most trace metals found in bivalves from South China Sea was zinc (mean 10.78 $\mu\text{g/g}$) but with more high concentration than seawater; other trace metals in bivalves were 3.07 $\mu\text{g/g}$ Cu, 0.9 $\mu\text{g/g}$ Cr, 0.47 $\mu\text{g/g}$ Pb, 0.44 $\mu\text{g/g}$ Cd Yuan et al., (2020). Lu et al. (2020) reported levels of trace metals in oysters from the Pearl River Estuary with high level observed with zinc (mean 4100 $\mu\text{g/g}$), followed by copper (mean 1520 $\mu\text{g/g}$), cadmium (mean 12.4 $\mu\text{g/g}$), nickel (mean 4.17 $\mu\text{g/g}$), chromium (mean 1.66 $\mu\text{g/g}$), then lead (mean 1.46 $\mu\text{g/g}$). Previous study reported that the mean concentrations of Zn, Cu, Cr, Cd, Ni, and Pb in the oyster tissues from the entire Chinese coastal waters were 3346, 1182, 2.57, 8.59, 9.00, and 5.13 $\mu\text{g/g}$, respectively (Lu et al., 2019). Another study in bivalves from southeast coast of India found that Zn and Cu were the highest concentration with 19 and 11.15 $\mu\text{g/g}$, respectively (Satheeswaran et al., 2019). El-Sorogy and Attiah (2015) reported levels of Ni, Zn, Pb, and Cr in bivalves collected from Egypt with mean of 1.92, 1.69, 0.426, and 0.133 $\mu\text{g/g}$, respectively.

The mean concentration of total mercury in oyster tissues samples ranged from 0.007- 1.8 $\mu\text{g/g}$ (Table 6.6). Appendix G-1-3 shows the detailed data. The statistical analysis showed that no significant differences were observed in summer or winter across sites (Figure 6.11).

Table 6. 6: The Mean Concentration of Total Mercury in Tissues of Pearl Oyster (*P. radiata*) ($\mu\text{g/g}$)

Season	Site							
	Simaisma		Umm Bab		Al Khor		Al Wakra	
	Mean	STD	Mean	STD	Mean	STD	Mean	STD
Mar.17 (Summer)	0.540	0.840	1.807	2.662	0.067	0.015	0.133	0.031
Dec.17 (Winter)	0.022	0.007	0.047	0.007	0.032	0.004	0.044	0.023
May. 18 (Summer)	0.062	0.017	0.090	0.047	0.169	0.136	0.056	0.021
Nov.18 (Winter)	0.056	0.027	0.117	0.064	0.035	0.018	0.355	0.369

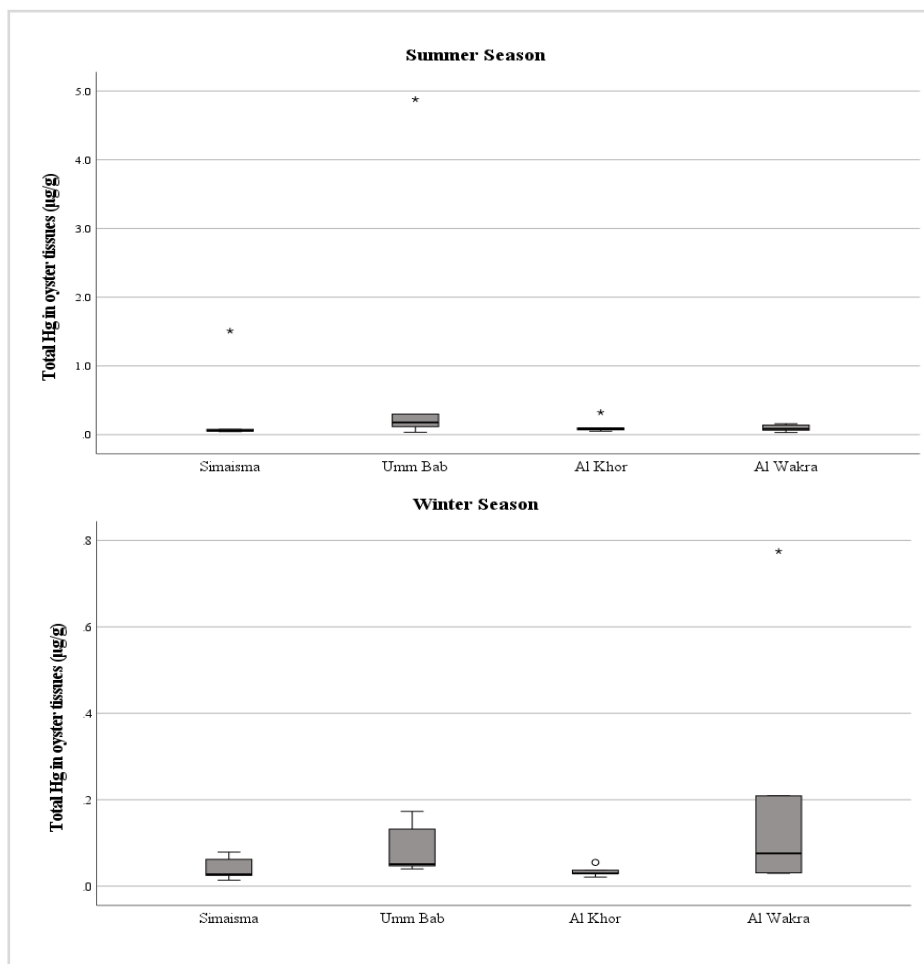


Figure 6. 11: Concentration of Total Mercury in pearl oyster tissues samples in summer and winter seasons

The concentration of total mercury observed in this study in oyster tissues samples was in the range of previous local studies except for samples collected from Umm Bab in summer season who reported higher concentration (1.8 $\mu\text{g/g}$). [Kreish & Al Madfa \(1999\)](#) reported levels of total mercury ranged from 0.038 to 0.065 $\mu\text{g/g}$. The other author reported the maximum total mercury concentration of 0.014 $\mu\text{g/g}$ with an average of 0.008 $\mu\text{g/g}$ ([Al-Maslamani et al., 2015](#)). The latest was ([Leitão et al, 2017](#)) who examined slightly higher concentration of total mercury in oyster tissues ranged between 0.01 to 0.15 $\mu\text{g/g}$.

Few studies around the world reported the total mercury concentration in oysters as shown in (Figure 6.12) with range (0.03- 13.28 $\mu\text{g/g}$). Regionally, [Yesudhason et al. \(2013\)](#) studied the levels of total mercury from Arabian Sea of Oman; he reported a concentration of 0.07 ± 0.03 . Internationally, in the '80^s, high level of total mercury reported in oyster tissues collected from

Minamata Bay of Japan with mean concentration of 10 $\mu\text{g/g}$ (Eisler, 1987). Moreover, Mikac et al. (1985) studied the total mercury level on oysters from Kaštela bay of Yugoslavia and he reported a range of 0.05- 13.28 $\mu\text{g/g}$. In China, especially in Zhejiang, the mean concentration of total mercury in oyster tissues was 0.11 ± 0.04 (Fang et al., 2004). Apeti et al. (2012) investigated the levels of total mercury in oysters from Northern Gulf of Mexico with range of 0.03–0.5. Oysters collected from Ebro Delta of Spain contained total mercury ranged from 0.12–0.27 (Ochoa et al., 2013).

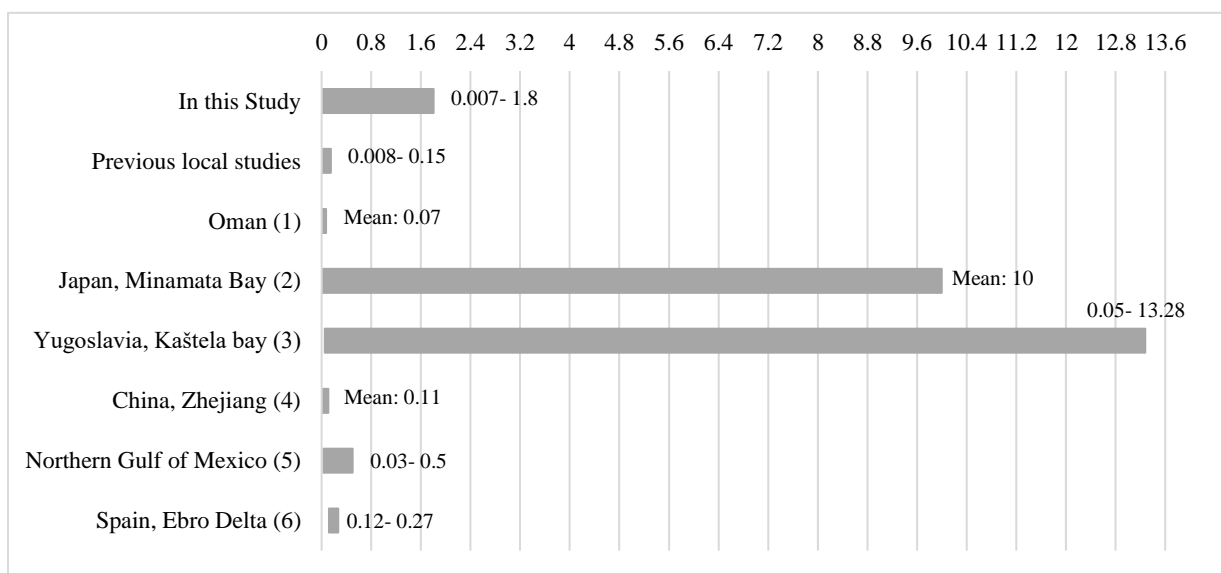


Figure 6. 12: Concentration of total Hg in oyster tissues samples ($\mu\text{g/g}$) from different areas [(1): (Yesudhasan et al., 2013), (2): (Eisler, 1987), (3): (Mikac et al., 1985), (4): (Fang et al., 2004), (5): (Apeti et al., 2012), (6): (Ochoa et al., 2013)]

Figure 6.13 shows the overall total mercury concentration in seawater, surface coastal sediment and pearl oyster tissues samples collected from the four sites in different seasons. The level observed in our study was relatively low in all matrixes. In summer 2017, samples collected from Umm Bab and Simaisma showed the same trend, as the level of total mercury increased as follow (oyster tissues > sediment > seawater). While a different trend was observed in samples collected from Al Wakra in winter 2018 and from Umm Bab in winter 2017 (oyster tissues > seawater > sediment). Sources of Hg might be from the outlet of the cement production plant in Umm Bab (Abdullah, 2020), or from recreational beach works in Al Wakra and Simaisma coast. For seawater samples, it can be seen clearly that in Al Wakra site, high total mercury levels were detected in winter seasons, (winter 2017 and winter 2018) with 0.239 and 0.237 $\mu\text{g/L}$ respectively. While in Al Khor, the highest level was detected in summer 2018 (0.113 $\mu\text{g/L}$). Different trend

noticed in Simaisma and Umm Bab with low levels in all seasons, ranged from (0.008-0.043 µg/L). For coastal surface sediment, the total mercury levels detected in 2018 in all sites were higher in winter than summer season with highest concentration detected in Al Khor. While in 2017, different trend was observed, as the levels of total mercury in summer was higher than winter. For pearl oyster tissues samples, the levels of total mercury in 2017 was higher in summer than winter in all sites, with highest concentration observed in Umm Bab samples (1.81 µg/g) followed by Simaisma (0.54 µg/g). In 2018, same trend was observed in Simaisma and Al Khor, while reverse trend noticed in Umm Bab and Al Wakra with highest concentration detected in oyster tissues collected from Al Wakra in Winter (0.36 µg/g). The highest levels of T-Hg noted in oysters collected from Umm Bab may reflect the presence of the cement production plant in that area. These levels exceeded the permissible limit set for oysters (1 µg/g) (EC, 2001; USEPA, 2002). In vitro results show that mercury may be expected to have an impact on bivalve immune functions in contaminated areas (Gagnaire et al., 2004). Thus, Umm Bab area might cause a risk to oysters and to humans from consumption of seafood with high level of Hg.

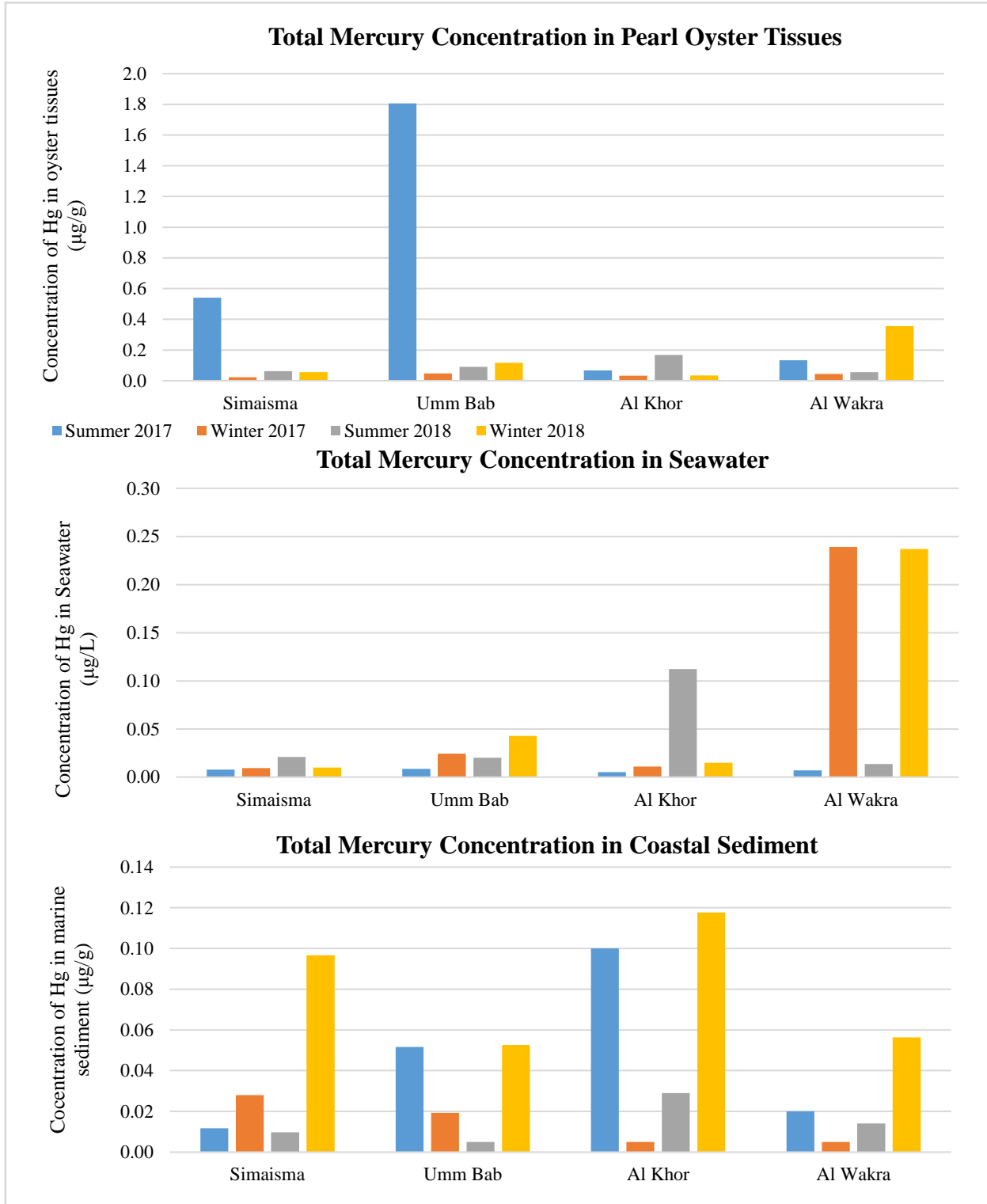


Figure 6. 13: Seasonal variations of total mercury concentration in seawater, coastal sediment, and oyster tissues samples

To sum up, the trace metals in the pearl oyster samples showed the following rank order of accumulation: Zn> Cd>Cu> Ni>Cr>T-Hg>Pb. The level of zinc recorded in pearl oyster tissues in this study was extremely higher than any recorded studies around the world. All the four sites around the coastline of Qatar showed high levels of Zn. The highest concentration noted in oysters collected from Al Wakra with mean concentration of 2288.3 µg/g in summer and 2610.1 µg/g in winter, followed by Umm Bab oysters with 1750.5 µg/g in summer and 812 µg/g in winter. Then Simaisma with mean of 1718 µg/g in summer and 1128.7 in winter and last Al Khor with 1492.6 µg/g and 1149.6 in summer and winter respectively.

Zinc plays an essential role in organisms, where its internal concentration can be regulated to a limited extent depending on the concentrations to which an organism is exposed (WFD-UKTAG, 2010). Zinc acts as natural cofactor in enzyme reactions inside cells and, therefore, oysters ingest high concentrations of this metal in their diets (Silva et al. 2001). The high absorption of Zn by oysters biologically balances with high utilization of this compound in metabolic processes (Suami et al., 2019). Thus, this maybe the reason for its high concentration in soft tissue of *P.radiata* oysters samples. Although Zn concentration in the seawater was below the WQS (81 µg/L) (USEPA, 2004), the level exceeded the maximum limit allowed for oysters (1000 µg/g) according to Australia acceptable limits as recommended by the National Health and Medical Research Council (Hungspreugs and Yaunghthong, 1984). Thus, the Zn levels found in pearl oysters tissues collected from Qatar coastline were significantly elevated in all four sites, which may be indicative of environmental contamination. Leitão et al., (2017) reported same results in oysters collected from Al Wakra Harbor (2529.4 µg/g). Moreover, Al Wakra surface sediment and sediment core also reported the highest level of Zn compering to other three sites with mean concentration range of (3.1 µg/g to 14.9 µg/g) and (8.2 µg/g to 18.6 µg/g) respectively. Thus, this may reflect the potential pollution sources in this site such as harbor activities and fishing boat traffic. Thus, high zinc exposure could cause a risk to oysters and to human from consumption of seafood in that site. Toxicity of Zn evidence to induced copper deficiency with attendant symptoms of anemia and neutropenia (Fosmire, 1990).

6.4 Conclusion

In this study the levels of six trace metals (Cd, Cr, Cu, Ni, Pb and Zn) and total mercury concentration (T-Hg) in seawater, surface coastal sediment, sediment cores and pearl oyster tissues (*P. radiata*) samples collected from four sites around coastline of Qatar have been evaluated. The trace metal concentration trend within seawater follows $Pb > Ni > Zn > Cu > Cr > Cd$. Most were in the range of zero to $4.7 \mu\text{g/L}$, except for Pb and Ni, which had a range of $0.001\text{--}56.1 \mu\text{g/L}$ and 0.06 to $9.8 \mu\text{g/L}$ respectively, where high levels of Pb and Ni observed in summer from (Al Khor and Al Wakra seawater) and (Al Khor, Simaisma and Umm Bab seawater) respectively. Within the surface coastal sediment samples, Al Wakra sediment samples showed the highest levels of Cr and Zn compared to the other three sites, sites where the percent of silt and clay in surface sediments was the highest. Likewise, the Al Wakra sediment core showed the same trend where Cr was the highest trace metal detected in all depths followed by Zn. Data from pearl oyster tissues revealed that Zn was the most abundant major trace metals in bivalve tissues ($551.8\text{--}2807.2 \mu\text{g/g}$), where the recorded range was markedly higher than that recorded in other studies around the world with the highest concentration noted in oysters collected from Al Wakra. For total mercury, levels detected in seawater was moderately low and in the range of the previous local studies. Within the surface sediments, Al Khor samples showed the highest range of total Hg where the TOC content in sediment was the highest compared to the other three sites and the fine grain size was high. However, the Al Wakra sediment core showed the highest level of total Hg where the TOC content was high deeper in the core with a fine grain size fraction more than 39% silt at all depths. Data from oyster tissues showed that levels of total Hg was higher in summer than winter AT all sites, with highest concentration observed in the Umm Bab samples ($1.81 \mu\text{g/g}$).

Chapter 7:

Integration and Discussion

This research project intended to assess environmental contamination around the coastline of Qatar by determining organic and inorganic contaminants using pearl oyster as indicator organism to establish a baseline of contaminants in an aquatic environment. This section will give a brief overview of the findings of the study and an integration of the overall data set. Moreover, some consideration of the temporal and spatial patterns of contaminants will be described, as well as an assessment of the current status of organic and inorganic contaminants in Qatar's coastline in comparison to national and international limits. Finally, recommendations and future research directions and priorities will be highlighted.

7.1 General Finding and Integration

One of the themes that emerged from my analysis of organic (TPHs and PAHs) and inorganic (trace metals and total Hg) contaminants in different matrixes was that most of the contaminants were predominantly detected in pearl oyster tissues (*P. radiata*) rather than other matrixes (Figure 7.1). Thus, oysters play an important role in contaminants' accumulation and cycling due to their high tissue-bioaccumulation and filtering nature. Several previous reports have been described the capacity of oysters to accumulate heavy metals using bioconcentration factor (BCF) (Otchere ,2003 ; Chaharlang et al., 2012; Gawade et al., 2013 ;Birch et al., 2014). Jonathan et al. (2017) demonstrated that Pacific Oysters *Crassostrea gigas* (*C. gigas*) were strong accumulators for Zn, As, Cr and Cu with bioconcentration factor (BCF) values > 1000 which denote significant and slow accumulation of these metals. Oysters are often employed as bio-indicators of organic and inorganic contaminants in the worldwide coastal waters (Phillips and Rainbow, 1994; Rainbow, 1995; Zuykov et al., 2013).

Different patterns of accumulation in oysters, sediment and seawater samples were observed. The trend in the organic and inorganic contaminant mean values found in pearl oyster tissues collected from Simaisma, Umm Bab and Al Khor were in decreasing order of (Zn > Cd > Cu > TPHs > Ni > Cr > PAHs > Pb > T-Hg) except for T-Hg which was higher than Pb only in Umm Bab samples, while oysters from Al Wakra showed different trend (Zn > Cu > Cd > TPHs > Cr > Ni > PAHs > Pb > T-Hg).

For sediment samples collected from Simaisma and Al Khor, the following trend were observed (Zn > Cr > Ni > Cu > TPHs > Pb > T-Hg > PAHs > Cd), while Al Wakra and Umm Bab sediment showed different trend (Cr > Zn > Ni > Cu > Pb > TPHs > Cd > PAHs > T-Hg) where Cr was the most detected trace metal.

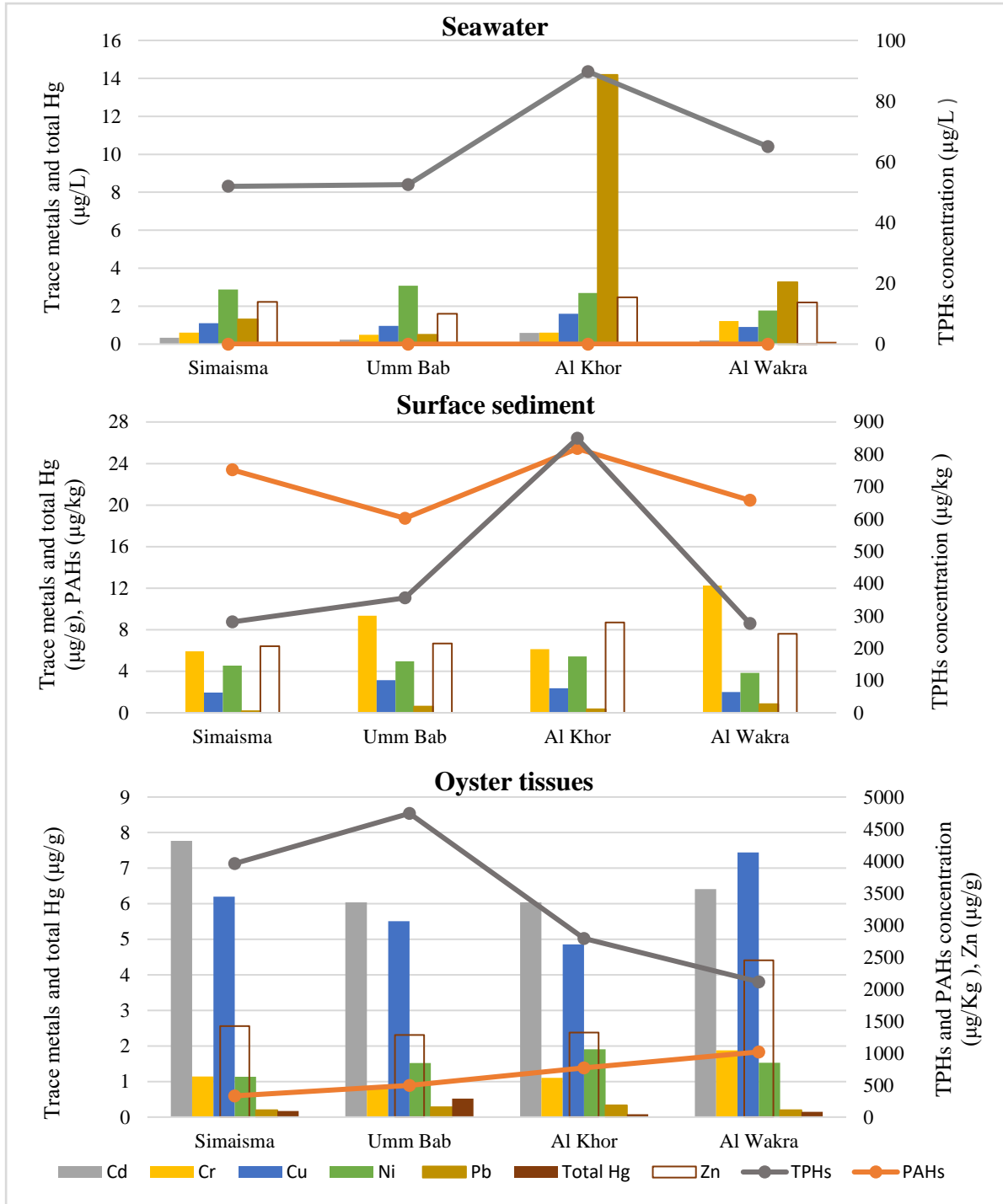


Figure 7. 1: The overall mean concentration of organic and inorganic contaminants from the four sample sites

Seawater samples collected from the four sites showed various trend of accumulation of organic and inorganic contaminants, however, no PAHs compounds were detected in any seawater samples. Simaisma samples followed the trend of (Ni > Zn > Pb > Cu > Cr > Cd > TPHs > T-Hg) while Umm Bab samples followed same trend but by replacement of Pb and Cu position. However, samples from Al Khor showed following trend (Pb > Ni > Zn > Cu > Cr > Cd > TPHs > T-Hg), while for Al Wakra samples (Pb > Zn > Ni > Cr > Cu > Cd > T-Hg > TPHs).

To examine the relationships between all the contaminants, Principal Component Analysis (PCA) and Pearson Correlation were performed using XLSTAT in Excel. Figure 7.2 shows the PCA plot for all the analyzed contaminants (TPHs, PAHs, 6 trace metals and total Hg) as vectors at the four sampling locations (Simaisma, Umm Bab, Al Khor, and Al Wakra) for each matrix as dots. The first plane, corresponding to the projections of all observations on the first (PC1, 63.52%) and second (PC2, 17.06%) principal components, accounted for 80.57% of the total variance. The angles between vectors of different variables show their correlation in this space: small angles represent high positive correlation; right angles represent lack of correlation, opposite angles represent high negative correlation.

The PCA biplot (Figure 7.2) reveals that Al Khor and Al Wakra seawater samples were highly positively correlated with Pb i.e. higher Pb level was observed in seawater samples in these two sites. Ni in sediment samples from the four sites was highly positively correlated with Cr ($P = 0.008$, coefficient $r = 0.5$). Zn in oyster tissues was found to be highly positively correlated with Cu, Cd, and TPHs ($P < 0.0001$, coefficient $r = 0.90$, $P < 0.0001$, coefficient $r = 0.86$, and $P = 0.003$, coefficient $r = 0.60$ respectively). Umm Bab oyster's samples characterized by high value of Total Hg. Total Hg was found to be positively correlated with Cd ($P = 0.03$, coefficient $r = 0.4$) and negatively correlated with Cr and Ni ($P = 0.3$ and 0.08 respectively).

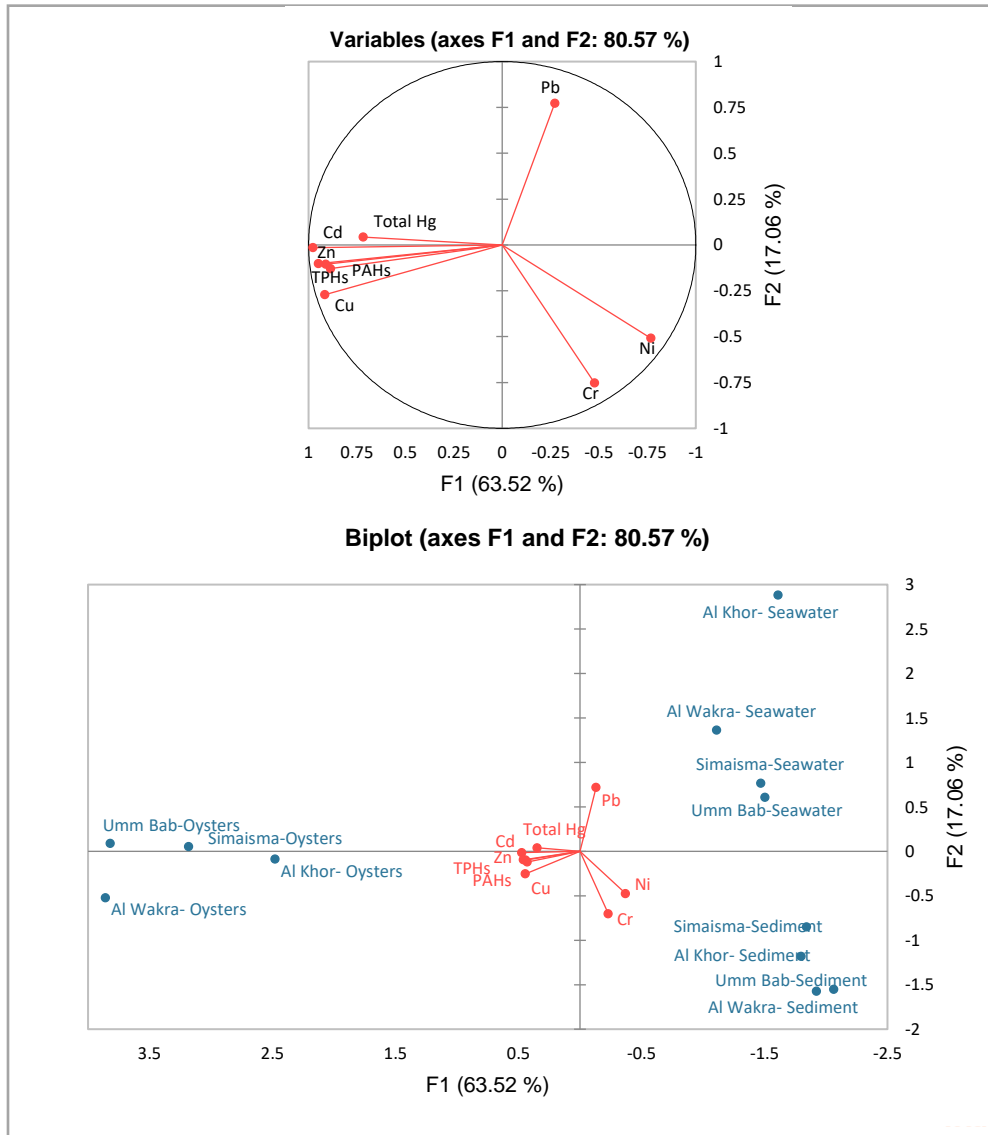


Figure 7. 2: PCA Biplot of organic and inorganic contaminants.

The mean concentration of organic and inorganic contaminants in sediment cores illustrated in Figure 7.3. In sediment core samples, some key feature were observed in some of the analyzed contaminants. The highest TPHs were observed in Simaisma core at all depths, while highest PAHs was detected in Al Wakra core where the optimum level observed in 10cm depth. Cr was observed in all core samples in all depths, with highest level detected in Al Wakra core. Ni was only detected in surface layer (5cm) of Simaisma core; however, the surface sediment samples from all sites reported concentration of Ni (Figure 7.1). This level detected in Simaisma core may indicate a source of Ni pollution in recent time, since no Ni had been observed in other depths. Moreover, trace amount of Ni was detected only in the 10cm depth of Umm Bab core, and

Al Wakra core showed also levels of Ni in 10cm which then decreased as we go deeper. While no Ni detected in Al Khor core. Pb was only detected in Al Wakra core in 25 and 30cm, which may give an indication of Pb pollution in that site in the past. However, the surface sediment samples showed level of Pb that was higher than other sites. Zn and Cu were detected in all depths of Umm Bab and Al Wakra cores.

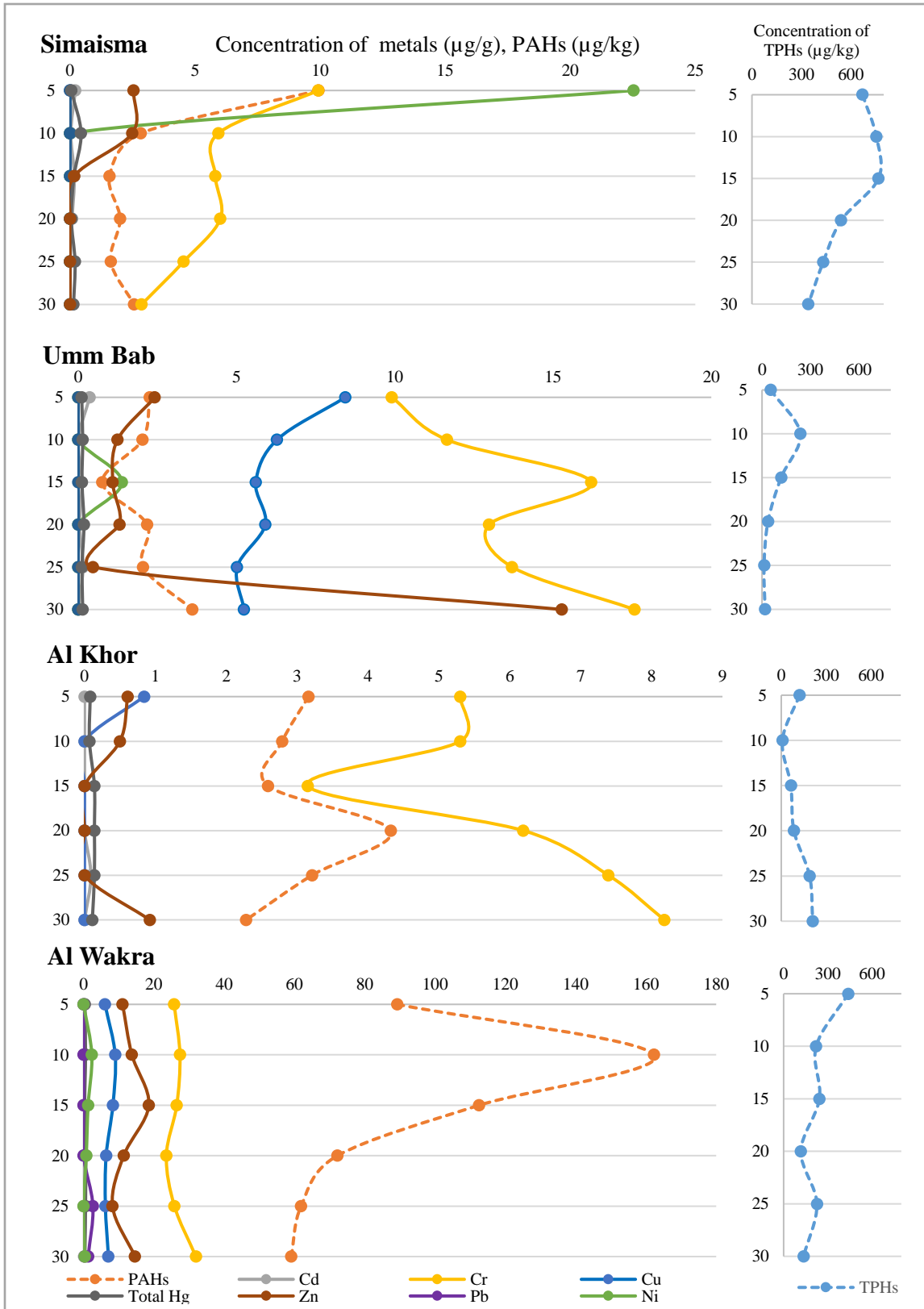


Figure 7. 3: Vertical profiles of mean concentration of organic and inorganic contaminants in sediment cores

7.2 Theoretical Patterns of Organic and Inorganic Contaminants

The potential sources of contaminants at each site are presented in chapter 3 (section 3.1), where the satellite images for each site represent point and nonpoint sources. The organic and inorganic contaminants analyzed in this study were found to have accumulated more in one matrix than others for selected contaminants. In relation to organic compounds (TPHs and PAHs), we noted that levels of TPHs were higher than PAHs in all matrixes from all sites except in the surface sediment samples collected from Simaisma, Umm Bab, and Al Wakra. Levels of TPHs and PAHs followed the following trend of accumulation (oysters > sediment > seawater). Cadmium was highly detected in oyster samples, while very low concentrations were detected in seawater and no levels were detected in surface sediment. Likewise, copper, zinc and T-Hg were also found to have accumulated more in oyster tissues than other matrices. While levels of Cr and Ni were higher in sediment than oyster tissues and seawater samples in all sites. However, Pb showed different pattern of accumulation, where higher level was detected in seawater samples.

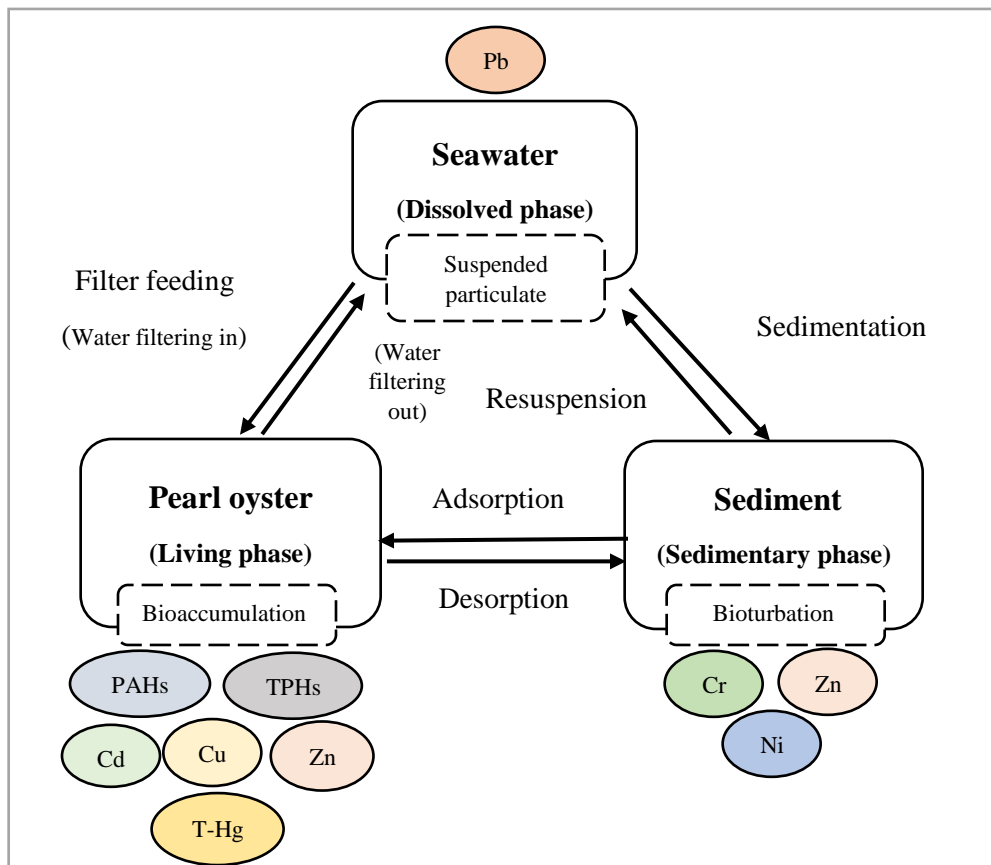


Figure 7. 4: The theoretical accumulation pattern of organic and inorganic contaminants in this study

Figure 7.4 represents an envisaged pattern of accumulation of the studied contaminants, where the highest levels of contaminants detected in each matrix are presented. In coastal environments, contaminants can be partitioned into different phases (dissolved, sedimentary and living phases), and these phases can interact with each other. For example, dissolved metals can be transformed into the sedimentary phase through sedimentation and can be released back into the seawater by resuspension (Yang et al., 2012). Metals in the sedimentary phase can be adsorbed by oysters and released back by desorption. Moreover, bioturbation may impact the release of contaminants by the activities (e.g., feeding and movement) of macrobenthos which live in biogenic structures buried in the sediment and transport contaminants to deeper layers in marine sediments (Black et al., 2008). Filter feeding by oysters can accumulate contaminants by filtration from seawater and releasing back clean water into seawater.

Sediment type has a major effect on transport and accumulation of organics and heavy metals. Thus, the spatial patterns of heavy metals are closely related to sediment types and are often consistent with those of fine-grained sediments (Liang et al., 2019, Wang et al., 2018). This agrees with our finding in this study, where the highest levels of Cr and Zn were detected in Al Wakra, where the sediment comprised more fine particles (42% silt, and 1.3% Clay) than the other sites. It also contained a higher TOC content with deeper. The sources of contaminants in this site include harbor activities, recreational boat traffic and fishing fleet movement. Nickel is a natural element of the earth's crust and it occurs naturally in the environment at low levels in sediment (Kucaj & Abazi, 2015). Thus, this may reflect the slightly higher level of Ni in sediment than other matrices.

Levels of TPHs and PAHs were found to be higher in oyster tissues collected from all sites than sediment and seawater. High hydrophobicity of PAHs may be the reason of low levels in seawater, which make these compounds to accumulate more in sediment rather than seawater (Karthikeyan et al., 2001). Moreover, oysters play a role in filtration of these contaminants (as suspended particulate matter particles) from seawater, as they are a filter feeder. Highest TPHs concentration was detected in Simaisma oysters collected in winter 2018, where same trend was observed in sediment core collected from the same location. However, high PAHs level was observed in Al Wakra oysters where same pattern detected in Al Wakra sediment core in all depths. This indicate the fact that contaminants in sediment can be directly absorbed by oysters and then

accumulated within their bodies. Benzo (a) pyrene was detected only in samples collected in winter seasons, with high level reported in Al Wakra oysters. These data can give an indication of pyrogenic source in Al Wakra and Simaisma sites, which may come from the harbor that have recreational boat traffic and fishing fleet movement in Al Wakra or beach filling and port in Simaisma coast.

Similarly, trace metals including Zn, Cu and Cd, as well as T-Hg found to be more accumulated in oyster tissues. This may estimate the adsorption of this metal from sediment and seawater in these sites, where the point sources of pollution may come from harbor activities and fishing boat traffic in Al Wakra for trace metals, and cement factory in Umm Bab for T-Hg where the cement production industry known to be the major contributors of Hg emissions (Abdullah, 2020).

As illustrated above (Figure 7.4) seawater was slightly more polluted by Pb than sediment and oysters with highest level detected in Al Khor samples. Pb in seawater at Al Khor might be affected by the movement of contaminants by current from the mangrove area and port located in the top of the sampling points. Lead may be partitioning in suspended particles found in surface seawater. In the seawater, heavy metal content is affected by changes in environmental factors such as salinity and pH (Che et al., 2003, Gambrell et al., 1991), but this fact was not confirmed by our finding. Where the levels of most trace metals in seawater were close to each other regardless of salinity and pH levels.

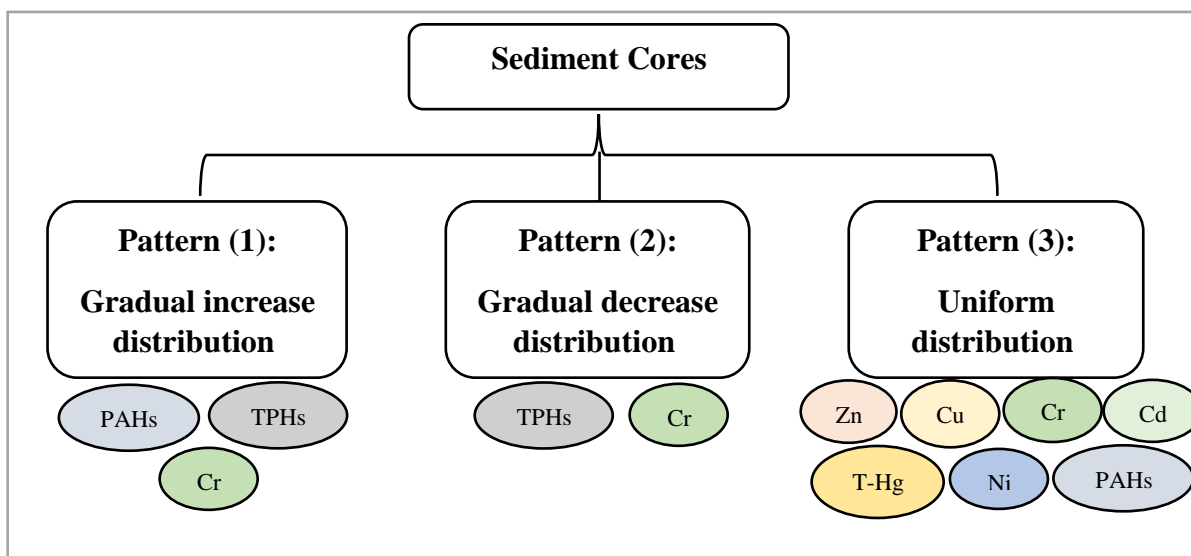


Figure 7. 5: Distribution patterns of organic and inorganic contaminants in the depth profiles of different four cores.

Generally, three distribution patterns of organic and inorganic contaminants occurred in the depth profiles of the four different sites cores (Figure 7.5). Pattern 1 (gradual increase distribution), where gradual increases from the bottom to the top layer. This model was observed for TPHs in Simaisma, Umm Bab and Al Wakra cores, PAHs in Al Wakra core, and Cr in Umm Bab core. Pattern 2 (gradual decrease distribution), where gradual decreases from the bottom to the top layer were observed for Cr in Al Khor cores till 15cm then increase, and in Umm Bab core with just slight increase in 15cm then decreases again; and for TPHs in Al Khor core. Pattern 3 (uniform distribution), where the concentrations varied in a relatively narrow range with increasing depth. This trend was observed for T-Hg in all cores, Zn in Al Wakra core and in Umm Bab core excluding the bottom layer (30cm), Cu and Cd in Umm Bab and Al Wakra cores, Ni in Al Wakra core, and PAHs in Umm Bab, Al Khor and Simaisma cores except the surface layer (5cm) for the latest core.

7.3 Assessment of Current Status of Organic and Inorganic Contaminants in Qatar's Coastal Environment

In this study, as a seawater guideline, Qatar's standard for seawater quality (The Environment Protection Law issued, the Decree No. 30 for the Year 2002) was used. Guidelines for sediment and oysters from other countries were used as no limit is currently set in Qatar for TPHs, PAHs, trace metals and total mercury.

Our results, in general, levels of contaminants seemed low in seawater and sediment, however, in oysters most of the contaminants are higher when compared to international Guideline values given in Table 7.1. Analysis of seawater samples showed that most of the heavy metal concentrations were below the limits set by the Ministry of Environment of Qatar, Environmental Law No. 30/2002. Levels of contaminants in sediment samples were a little higher than water samples, mainly as metals tend to be adsorbed because of their high chemical reactivity. However, all contaminants were below the international permissible limit, and this may reflect the geology of Qatar where the coastal sediment consist of carbonate sediment (Sadooni, 2014), thus natural levels of most metals will be relatively low (Schropp & Windom, 1988). Compared to sediments, oysters showed high levels of contaminants where most of them exceeding the permissible limit. These high levels revealed the fact that these organisms absorb a contaminant into their tissues from the environment that surrounds them. Consequently, a process of bioaccumulation can occur.

Therefore, at some point in time, the contaminant concentration in tissues is greater than that of the surrounding environment.

Table 7. 1: National and international limits for organic and inorganic contaminants

Matrix	Parameter	This study	National permissible limit *	International limit	Reference	Status
Seawater	TPHs	1.2- 271.8 µg/L	5000 µg/L	10000 µg/L	(DPR, 2002)	Below limit
	PAHs	ND	NA	0.20 µg/L	(EU, 2005)	Below limit
	Cd	0 - 1.4 µg/L	700 µg/L	10 µg/L	(WHO, 2003)	Below limit
	Cr	0 - 3.5 µg/L	NA	50 µg/L	(WHO, 2003)	Below limit
	Ni	0.06 - 9.8 µg/L	20000 µg/L	20 µg/L	(BIS, 2009)	Below limit
	Cu	0 - 3.5 µg/L	15000 µg/L	5 µg/L	UK standards**	Below limit
	Zn	0.06 - 4.7 µg/L	----	5000 µg/L	(WHO, 2003)	Below limit
	Pb	0 - 56.1 µg/L	12000 µg/L	50 µg/L	(WHO, 2003)	Above limit
	T-Hg	0.005- 0.2 µg/L	Less than 400 µg/L	0.3 µg/L 0.94 µg/L	UK standards** (USEPA, 2002)	Below limit Below limit
Sediment	TPHs	75-1751.8 µg/kg	NA	30 mg/kg	(FMEnv, 1991)	Below limit
	PAHs	4.3- 36.7 µg/kg	NA	2.5 mg/kg	(USEPA, 2002)	Below limit
	Cd	0- 0.08 µg/g	NA	0.1 µg/g 0.03-0.3 µg/g	(EC, 2005) (UNEP, 1985)	Below limit Below limit
	Cr	4.10- 14.45 µg/g	NA	80 µg/g	(NSPR, 2002)	Below limit
	Ni	3.53- 7.49 µg/g	NA	NA	----	----
	Cu	0.12- 4.19 µg/g	NA	25 µg/g	(USEPA, 1989)	Below limit
	Zn	3.10- 14.92 µg/g	NA	90 µg/g	(USEPA, 1989)	Below limit
	Pb	0- 3.35 µg/g	NA	40 µg/g	(USEPA, 1989)	Below limit
	T-Hg	0.005-0.12 µg/g	NA	0.13 µg/g	(CCME, 2002)	Below limit
Oysters	TPHs	633.3- 6666.7µg/kg	NA	NA	----	----
	PAHs	25.9- 2244µg/kg	NA	0.035 µg/kg	(EU, 2005)	Above limit
	Cd	3.4-10.3 µg/g	NA	1 µg/g, 1.4 µg/g	(EC, 2001), (USEPA, 2002)	Above limit Above limit
	Cr	0.5-2.6 µg/g	NA	12 µg/g	(US FDA, 1993)	Below limit
	Ni	0.8-3.1 µg/g	NA	70 µg/g	(US FDA, 1993)	Below limit
	Cu	2. 6-10.2 µg/g	NA	20 µg/g	(FAO, 1989),	Below limit
	Zn	551.8-2807.2 µg/g	NA	50 µg/g, 200-500 µg/g	(CFIA, 2011), (USEPA, 2002)	Above limit Above limit
	Pb	0.5-2.6 µg/g	NA	0.5 µg/g, 1.7 µg/g	(EU, 2008), (USEPA, 2002)	Above limit Above limit
	T-Hg	0.007- 1.8 µg/g	NA	1 µg/g, 1 µg/g	(EC, 2001), (USEPA, 2002)	Above limit Above limit

NA: Not Available. *Environmental Law No. 30/2002, amended in 2009 by decree Law No. 45. **United Kingdom Quality Standards.

To sum up, even though levels of organic and inorganic contaminants recorded in this study in surface seawater and coastal sediment samples were low and below the international guideline limits, high levels detected in pearl oyster tissues may give an indication of sources of contamination in Qatar coastline. Since coastal sediments are considered to be a useful tool to evaluate contamination, recording of low concentrations indicates non-anthropogenic impact (Memet, 2011). Thus, the estimation that high levels detected in oysters may be due to non-point sources that occur in the four studied sites at specific time or due to regional marine activities surrounding the coastline of Qatar.

7.4 Recommendations and Future Directions

To determine coastal and marine environment quality and measure possible contaminant levels, the integrated wide view provided by bivalves can be crucial (Farrington et al., 2016). In this study, oysters proved to provide a useful perspective indicating bioavailable contaminants.

This study sampled over a two-year period and in different seasons at four sites around the coastline of Qatar; three on the east coast and a fourth on the west coast. It would be worth looking into greater temporal resolution, sampling at a greater frequency during the different seasons (spring, summer, fall, and winter), which may be useful to know the annual pattern of physicochemical parameters in the four different seasons, since this study was limited to summer and winter seasons. Furthermore, increasing span of the sampling by re-sampling where sites have been sampled previously is useful to effectively extend this project since this study limited to the funding period. A further aspect of this would be to look in more detail and date the sediment cores, which could extend the timeline by providing a chronology, and most importantly show pre coastline development (background) conditions.

Moreover, increasing the sampling points to more fully cover the Qatar coastline (west, north, and east) considering the key factors from marine side (such as exposure, regional transport of water and sediment, depth) and land side (such as geology, sediment type on the coast, land use) is recommended. Since this study was limited to a four specific sites as a function of the funding of the project. In addition, looking at mangrove areas to study the distribution and accumulation of contaminants is also suggested, since mangrove vegetation has the characteristic of storing metals, transferring these elements from the sediment and concentrating them in their tissues (MacFarlane et al., 2007). Moreover, mangroves are fine sediment areas and thus potential contaminant stores (compared to the predominantly sandy open coastline site sampled in this study).

In this thesis, I studied both organic (TPHs, PAHs) and inorganic (six trace metals, T-Hg) contaminants, since this study is part of the ‘National Priority Research Program’ NPRP 9 project that aimed to assess the levels of specific organic and inorganic contaminants in Qatar coastal environment. However, other contaminants have been identified in the literature and are considered to also cause serious effects in the coastal environment and ecosystem such as microplastics, antibiotics and organotin (Saha et al., 2021, Zhang et al., 2020, Chung et al., 2020). Little effort to

date has gone into investigating of these contaminants in the Arabian Gulf area and especially in Qatar. Thus, assessing the levels of these other contaminants is suggested.

The selected organic and inorganic contaminants in seawater were below the limits set by the Ministry of Environment of Qatar. However, these contaminants have no national set limits in sediment and oysters. Thus, the Ministry of Environment of Qatar should further consider the setting of standards and guideline for these contaminants in sediment and biota tissues.

Qatar has developed rapidly in the last few decades, but it also pays a lot of attention to its environment, and education and legislation have helped in limiting coastal pollution. However, the country does not sit in isolation; pollutants do not respect international borders, so we need to be aware of pollution level and potential contamination from the wider Gulf. Thus, more regional integrative study overall gulf marine environment should be considered for better understanding of how these marine pollutants move and gets accumulated in different coast. Common monitoring approaches could be a beneficial tool for better assessing contaminants in coastal and marine environment in order to more effectively manage environmental quality across the Arabian Gulf.

References

- Aaseth J, Ajsuvakova O, Skalny A, Skalnaya M, Tinkov A (2018) Chelator combination as therapeutic strategy in mercury and lead poisonings. *Coord Chem Rev* 358:1–12. <https://doi.org/10.1016/j.ccr.2017.12.011>.
- Aboul Dahab O., Al-Madfa H. (1997). Chromium distribution in waters and sediments of the eastern side of The Qatari Peninsula. *Science of The Total Environment*, 196(1):1-11.
- Advancing Sustainable Development. (2009). General Secretariat for Development Planning. Available at: [http://Qatar_Second_National_HDR_Advancing_Sustainable_Development_2009_EN.pdf\(psa.gov.qa\)](http://Qatar_Second_National_HDR_Advancing_Sustainable_Development_2009_EN.pdf(psa.gov.qa))
- Agah H., Elskens M., Fatemi S., Owfi F., Baeyens W., Leermakers M. (2009). Mercury speciation in the Persian Gulf sediments. *Environmental Monitoring and Assessment*, (157), 363–373.
- Agency for Toxic Substances and Disease Registry (ATSDR). *Toxicological Profile for Copper*. Atlanta, GA: Centers for Disease Control; 2002.
- Agency for Toxic Substances and Disease Registry (ATSDR), 2017. ATSDR's substance priority list. Agency for Toxic Substances and Disease Registry <https://www.atsdr.cdc.gov/SPL/>, Accessed date: 25 November 2020.
- Agency for Toxic Substances and Disease Registry (ATSDR), (2014). ToxFAQs™ for Total Petroleum Hydrocarbons (TPH). Retrieved November 30, 2020, from <https://www.cdc.gov/TSP/ToxFAQs/ToxFAQsDetails.aspx?faqid=423&toxid=75#:~:text=Some%20of%20the%20TPH%20compounds,in%20the%20feet%20and%20legs>.
- Akcha, F., Izuel, C., Venier, P., Budzinski, H., Burgeot, T., Narbonne, J.F., 2000. Enzymatic biomarker measurement and study of DNA adduct formation in benzo[a]pyrene-contaminated mussels, *Mytilus galloprovincialis*. *Aquat. Toxicol.* 49, 269–287.
- Al osman M., Yang F., Massey I. (2019). Exposure routes and health effects of heavy metals on children. *Biometals*, 32, 563–573.
- Alharbi T., El-Sorogy A. (2017). Assessment of metal contamination in coastal sediments of Al-Khobar area, Arabian Gulf, Saudi Arabia. *Journal of African Earth Sciences*, 129 (2017) 458-468.
- Alharbi T., Alfaihi H., El-Sorogy A. (2017). Metal pollution in Al-Khobar seawater, Arabian Gulf, Saudi Arabia. *Marine Pollution Bulletin*, (119), 407-415.
- Al-Hashimi A. & Salman H. (1985). Trace metals in the sediments of the northwestern coast of the Arabian Gulf. *Marine Pollution Bulletin*, 16, 118–120.
- Al-Madfa H., Aboul Dahab O., Holail H. (1994). Mercury pollution in doha (Qatar) coastal environment. *Environmental Toxicology and Chemistry*, 13 (5), 725-735.
- Al-Madfa H., Abdel-Moati M., Al-Gimaly F.(1998). *Pinctada radiata* (pearl oyster): a bioindicator for metal pollution monitoring in the Qatari waters (Arabian Gulf). *Bulletin of Environmental Contamination and Toxicology*, 60,245-251.
- Al-Mamoon, A. & Rahman, A. (2019, January). Sea outfall assessment in Qatar: lessons for Bangladesh. Paper presented at the International Conference on Water and Environmental Engineering. Western Sydney University, Dhaka, Bangladesh.
- Al-Maslmani I. , Abdel-Moati M. , Al-Ansari E. , Al-Yafei M. , Soliman Y., Al-Shaikh I. , Rowe G., Wade T., Helmi A., Al-Azhari M., Kuklyte L., Yiğiterhan O.(2015). Bioaccumulation of Mercury in Pearl Oyster (*Pinctada radiata*) from the Coastal Waters of Qatar (Arabian

- Gulf). Paper presented at the Qatar University Life Science Symposium 2015, Qatar, <http://dx.doi.org/10.5339/qproc.2015.qulss2015.16>
- Al-Naimi, H., Al-Ghouti, M., Al-Shaikh, I., Al-Yafe, M., Al-Meer, S., 2015. Metal distribution in marine sediment along the Doha Bay, Qatar. *Environ. Monit. Assess.* 187 (130).
- Al-Saad H.T., Al-Timari A.A.K., Douabul A.A.Z., Hantoush A.A., Nasir A.M, Saleh S.M. (2017). Status of oil pollution in water and sediment from Shatt AlArab Estuary and North-West Arabian Gulf. *Mesopot. J. Mar. Sci.*, 32(1), 9 – 18.
- Al-Sarawi H., Jha A., Al-Sarawi M., Lyons B. (2015). Historic and contemporary contamination in the marine environment of Kuwait: An overview. *Marine Pollution Bulletin*, 100(2).
- Al-Sayed, H.A., Mahasneh, A.M., Al-Saad, J., 1994. Variations of trace metal concentrations in seawater and pearl oyster *Pinctada radiata* from Bahrain (Arabian Gulf). *Mar. Pollut. Bull.* 28, (6), 370–374.
- Al-Taani A., Batayneh A., Nazzal Y., Ghrefat H., Elawadi E., Zaman H. (2014). Status of trace metals in surface seawater of the Gulf of Aqaba, Saudi Arabia. *Mar. Poll. Bull.*, 86, 582-590.
- Alvarenga P., Goncalves A., Fernandes R., Varennes A., Vallini G., Duarte E. (2009). Organic residues as immobilizing agents in aided phytostabilization: (I) effects on soil chemical characteristics, *Chemosphere*, 74, 1292 – 1300.
- Alvarez M., Crespo C., Mattiasson B. (2007). Precipitation of Zn(II), Cu(II) and Pb(II) at bench-scale using biogenic hydrogen sulfide from the utilization of volatile fatty acids. *Chemosphere*, 66, 1677 - 1683.
- Alvarez-Muñoz D., Llorca M., Blasco J., Barcelo D. (2016). Contaminants in the Marine Environment. *Marine Ecotoxicology*, 10.1016/B978-0-12-803371-5.00001-1.
- Apeti DA, Lauenstein GG, Evans DW (2012) Recent status of total mercury and methyl mercury in the coastal waters of the northern Gulf of Mexico using oysters and sediments from NOAA's mussel watch program. *Mar Pollut Bull*, 64, 2399–2408.
- Arcagni, M., Campbell, L., Arribere, M.A., Marvin-DiPasquale, M., Rizzo, A., Ribeiro Guevara, S. (2013). Differential mercury transfer in the aquatic food web of a double basined lake associated with selenium and habitat. *Sci. Total Environ.* 454–455, 170–180.
- Ashour M. M. (1987). Surficial deposits of Qatar Peninsula. Geological Society, London, Special Publications, 35, 361-367, <https://doi.org/10.1144/GSL.SP.1987.035.01.24>.
- Azlisham, M., Vedamanikam, V. J. and Shazilli, N. A. M.(2009). Concentrations of cadmium, manganese, copper, zinc, and lead in the tissues of the oyster (*Crassostrea iredalei*) obtained from Setiu Lagoon, Terengganu, *Malaysia'*, *Toxicological & Environmental Chemistry*, 91:2, 251 — 258.
- Baltasa H., Sirina M., Dalgicb G., Bayraka E., Akdeniz A. (2017). Assessment of metal concentrations (Cu, Zn, and Pb) in seawater, sediment and biota samples in the coastal area of Eastern Black Sea, Turkey. *Marine Pollution Bulletin*, 122, 475–482.
- Barman H., and Bhattacharya K. (2001). Metal contamination of groundwater in a predominantly rural area in Assam, Proceedings of the 10th national symposium on environment, IIT, Mumbai, 161-166.
- Barregard L, Sallsten G, Conradi N. (1999). Tissue levels of mercury determined in a deceased worker after occupational exposure. *Int Arch Occup Environ Health*, 72, 169-73.
- Barregard L, Sallsten G, Schutz A, Attewell R, Skerfving S, Jarvholm B. (1992). Kinetics of mercury in blood and urine after brief occupational exposure. *Arch Environ Health*, 7(3):176-84.

- Basaham A. and Al-Lihaibi S. (1993). Trace Elements in Sediments of the Western Gulf. *Marine Pollution Bulletin*, (27),103-107.
- Basta N., Gradwohl R. (2000). Estimation of Cd, Pb, and Zn bioavailability in smelter contaminated soils by a sequential extraction procedure. *J. Soil Contam.*, 9, 149 – 164.
- Beesley L., Marmiroli M. (2011).The immobilisation and retention of soluble arsenic, cadmium and zinc by biochar. *Environmental Pollution*, 159, 474–480.
- Berlin, M., Zalups, R.K., Fowler, B.A. (2015). Mercury. In: Nordberg, G.F., Fowler, B.A.,Nordberg, M. (Eds.), Handbook on the Toxicology of Metals. Volume II, Specific Metals. Academic Press, London, UK, pp. 1013–1075
- Bełdowski J., Miotk M., Bełdowska M., Pempkowiak J. (2014). Total, methyl and organic mercury in sediments of the Southern Baltic Sea. *Marine Pollution Bulletin*, 87, 388–395.
- Bengtsson, G., Picado, F. (2008). Mercury sorption to sediments: dependence on grain size, dissolved organic carbon, and suspended bacteria. *Chemosphere*, 73, 526–531. <https://doi.org/10.1016/j.chemosphere.2008.06.017>.
- Birch GF, Melwani A, Lee JH, Apostolatos C. (2014). The discrepancy in concentration of metals (Cu, Pb and Zn) in oyster tissue (*Saccostrea glomerata*) and ambient sediment (Sydney estuary, Australia). *Marine Pollution Bulletin*, 36: 236-74.
- BIS. (2009) Drinking water specification, second revision IS 10500. ICS No. 13.060.20. pp. 5–10 Bureau of Indian Standards, New Delhi
- Black F., Gallon C., Flegal A. (2008). Sediment Retention and Release. *Encyclopedia of Ecology*, 3172-3181.
- Boonsaner, M. (2006). Environmental toxicology (4th ed.). Nakhon Prathom: Silpakorn University Press.
- Brettell R. (2013). Source apportionment of polycyclic aromatic hydrocarbons in sediment cores from the humber estuary using molecular distribution, Master thesis, University of East Anglia, Norwich.
- Brook, M.C., Al Shoukri, S., Amer, K.M., Boer, B. and Krupp, F. (2006). Physical and Environmental Setting of the Arabian Peninsula and Surrounding Seas. In Policy Perspectives for Ecosystem and Water Management in the Arabian Peninsula. Eds.
- Burt J. (2014). The environmental costs of coastal urbanization in the Arabian Gulf City Anal. *Urban Trends, Cult. Theory, Policy, Action*, 18,760-770.
- Burt J., Ben-Hamadou R., Abdel-Moati M., Fanning L., Kaitibie S., Al Jamali F., Range P., Saeed S.,Warren C.S. (2017). Improving management of future coastal development in Qatar through ecosystem-based management approaches. *Ocean & Coastal Management*, 148, 171-181.
- Burt J., Ben-Hamadou R., Abdel-Moati M., Warren C. (2017). Improving management of future coastal development in Qatar through ecosystem-based management approaches. *Ocean & Coastal Management*, 148, 171-181.
- Calabrese E, Iavicoli I, Calabrese V, Cory-Slechta D, Giordano J. (2018). Elemental mercury neurotoxicity and clinical recovery of function: a review of findings, and implications for occupational health. *Environ Res* 163:134–148. <https://doi.org/10.1016/j.envres.2018.01.021>
- Canadian Council of Ministers of the Environment (CCME) (2002). Canadian Sediment Quality Guidelines for the Protection of Aquatic Life. Canadian Environmental Quality Guidelines, Canada.

- Carcía A., Montero-Ocampo C. (2010). Improvement of arsenic electro-removal from underground water by lowering the interference of other ions, *Water Air Soil Pollut.*, 205, 237 – 244.
- Carson, P. Hazardous Chemicals Handbook, 2nd ed.; Butterworth Heinemann: Oxford, Woburn, 2002.
- Cavelier, C. (1970). Geologic description of the Qatar Peninsula (Arabian Gulf). Publication of the Government of Qatar, Department of Petroleum Affairs, 39 p.
- CDC "Center for Disease Control and Prevention". (2017). Mercury. Retrieved November 30, 2020, from https://www.cdc.gov/biomonitoring/Mercury_BiomonitoringSummary.html
- Cernichiari E, Brewer R, Myers GJ, Marsh DO, Lapham LW, Cox C, et al. (1995). Monitoring methylmercury during pregnancy: maternal hair predicts fetal brain exposure. *Neurotoxicology*, 16(4), 705-10.
- CFIA, Canadian Food Inspection Agency Fish Products Standards and Methods Manual (2011) Appendix 3: Amend. Number 11 dated 2011, July 20. Canadian guidelines for chemical contaminants and toxins in fish and fish products.
- Chaharlang BH, Bakhtiari AR, Yavari V. (2012). Assessment of cadmium, copper, lead and zinc contamination using oysters (*Saccostrea cucullata*) as biomonitors on the coast of the Persian Gulf, Iran. *Bulletin of Environmental Contamination and Toxicology*, 88(6), 956-61.
- Chang Y., Chang J., Lin T., Hsu Y. (2002). Integrated copper-containing wastewater treatment using xanthate process. *J. Hazard. Mater.*, 94, 89 - 99.
- Chen C. W., Chen C. F. (2011). Distribution, origin, and potential toxicological significance of polycyclic aromatic hydrocarbons (PAHs) in sediments of Kaohsiung Harbor, Taiwan. *Marine Pollution Bulletin*, 63 (5-12), 417-423.
- Chen C., Chen C., Dong C., Kao C. (2013). Assessment of toxicity of polycyclic aromatic hydrocarbons in sediments of Kaohsiung Harbor, Taiwan. *The Science of the Total Environment*, (463), 1174-1181.
- Chen H, Diao X, Wang H, Zhou H. (2018). An integrated metabolomic and proteomic study of toxic effects of Benzo[a]pyrene on gills of the pearl oyster *Pinctada martensii*. *Ecotoxicol Environ Saf*, (156), 330-336.
- Che Y., He Q., and -Q W. (2003). distributions of particulate heavy metals and its indication to the transfer of sediments in the Changjiang Estuary and Hangzhou Bay, China. *Marine Pollution Bulletin*, vol. 46, (1), 123–131.
- Choi KH, Lee HJ, Yang TH, Lee HP, Yum HK, Choi SJ, et al. (1999). A case of pulmonary embolism associated with intravenous mercury injection. *Tuberc Respir Dis.*;46(5):723–728.
- Chung S.W.C, Lau J.S.Y., Lau J. P.K. (2020). Occurrence of organotin compounds in seafood from Hong Kong market. *Marine Pollution Bulletin*, (154), 111116.
- Chung WJ, Kim YS, Lee JD, Kim OH, Kim MH, Bae JH. (1980). A case of mercury poisoning due to herb drug pills. *Korean J Intern Med.*;23(8):719–722.
- Containers, H. (1994). Sediment Sampling (SOP#: 2016). US: EPA
- Cossa D., Fileman C. (1991). Mercury concentrations in surface waters of the English channel: A cooperative study. *Marine Pollution Bulletin*, 22, 4, 197-200.
- Costa C., Teixeira J.P.. (2014). Biomonitoring. In Philip Wexler (Ed.), *Encyclopedia of Toxicology*, (pp. 294–297). Portugal: Portuguese National Institute of Health.
- Covington A. (1997). Modern tanning chemistry. *Chem. Soc. Rev.*, 26, 111 - 126.

- Croxton, A.N., Wikfors, G.H., Schulerbrandt-Gragg, R.D., 2012. Immunomodulation in eastern oysters, *Crassostrea virginica*, exposed to a PAH-contaminated, microphytobenthic diatom. *Aquat. Toxicol.* 118, 27–36.
- Currie LA. (1995). Nomenclature and evaluation of analytical methods, including quantification and detection capabilities. *Pure Appl. Chem.*; 67(10) 1699-1723.
- D'Adamo R., Pelosi S., Trotta P., Sansone G. (1997). Bioaccumulation and biomagnification of polycyclic aromatic hydrocarbons in aquatic organisms, *Marine Chemistry*, 56 (1–2), 45-49.
- Davis, A. (1979). *Pollution Studies with Marine Plankton: Part II. Heavy Metals*, 15, 381–508. [http://doi.org/10.1016/S0065-2881\(08\)60408-3](http://doi.org/10.1016/S0065-2881(08)60408-3)
- de Mora, S., Fowler S., Wyse E., Azemard S. (2004). Distribution of heavy metals in marine bivalves, fish and coastal sediments in the Gulf and Gulf of Oman. *Marine Pollution Bulletin* 49, 410–424.
- de Mora, S., Tolosa, I., Fowler, S.W., Villeneuve, J.-P., Cassi, R., Cattini, C. (2010). Distribution of petroleum hydrocarbons and organochlorinated contaminants in marine biota and coastal sediments from the ROPME Sea Area during 2005. *Mar. Pollut. Bull.* 60 (12), 2323–2349.
- Department of Petroleum Resources (DPR). (2002). EGASPIN soil/sediment target and intervention values for mineral oil (or TPH), environmental guidelines and standards for the petroleum industry in Nigeria. (Revised ed.). The Petroleum Regulatory Agency of Nigeria.
- Do SY, Lee CG, Kim JY, Moon YH, Kim MS, Bae IH, Song HS (2017) Cases of acute mercury poisoning by mercury vapor exposure during the demolition of a fluorescent lamp factory. *Ann Occup Environ Med* 29:19. <https://doi.org/10.1186/s40557-017-0184-x>
- Drexler J., Brattin W. (2007). An in vitro procedure for estimation of lead relative bioavailability: with validation. *Hum. Ecol. Risk Assess.*, 13, 383 – 401.
- Duan J., Lu Q., Chen R., Duan Y., Wang L., Gao L., Pan Y. (2010). Synthesis of a novel flocculant on the basis of crosslinked Konjac glucomannan graft polyacrylamide-co-sodium xanthate and its application in removal of Cu²⁺ ion. *Carbohydr. Polym.*, 80, 436-441.
- Dudzinska M., Clifford D. (1991). Anion exchange studies of lead-EDTA complexes, *React. Polym.*, 16, 71 – 80.
- Eagles-Smith, C.A., Silbergeld, E.K., Basu, N., Bustamante, P., Diaz-Barriga, F., Hopkins, W.A., Kidd, K.A., Nyland, J.F., 2018. Modulators of mercury risk to wildlife and humans in the context of rapid global change. *Ambio*, 47, 170–197.
- EC (2005) Commission regulation (EC) No. 78/2005 amending regulation (EC) No. 466/2001 as regards heavy metals. *Of J Eur Union*, 43–45.
- EC Commission Regulation No. 466/2001 of 8 March 2001, Official Journal of European Communities L77/1 (2001).
- Egorova K.S. and Ananikov V.P. (2017). Toxicity of Metal Compounds: Knowledge and Myths. *Organometallics*, 36, 4071-4090.
- Eisler R. (1987). Mercury hazards to fish, wildlife and invertebrates: a synoptic review. Biological report 85, Contaminant hazard reviews 10, US Fish and Wildlife Service.
- El-Ashtoukhy E., Abdel-Aziz M. (2013). Removal of copper from aqueous solutions by cementation in a bubble column reactor fitted with horizontal screens. *Int. J. Min. Eng.*, 121, 65 – 69.

- El-Katiri, L. and Fattouh, B. (2017). ‘A brief political economy of energy subsidies in the Middle East and North Africa’, *International Development*. URL: <http://journals.openedition.org/poldev/2267>; DOI: <https://doi.org/10.4000/poldev.2267>
- El-Sorogy A., Abdullah Attiah A. (2015). Assessment of metal contamination in coastal sediments, seawaters and bivalves of the Mediterranean Sea coast, Egypt. *Marine Pollution Bulletin*, 101, 867–871.
- Environmental Protection Agency. (2002). Persistent Organic Pollutants: A Global Issue, A Global Response. Retrieved Feb 27, 2021, from [http:// https://www.epa.gov/international-cooperation/persistent-organic-pollutants-global-issue-global-response](http://https://www.epa.gov/international-cooperation/persistent-organic-pollutants-global-issue-global-response)
- Environmental Protection Agency EPA. (2019). Risk Assessment. Retrieved September 14, 2019, from <https://www.epa.gov/risk/about-risk-assessment>
- EU, Commission Regulation (EC), amending Regulation (EC) No 1881/2006 Setting Maximum Levels for Certain Contaminants in Foodstuffs (2008) <http://www.ecolex.org/ecolex/ledge/view/RecordDetails>
- European Union Commission Regulation (EUCR) (2014), European Union Commission Regulation (EU) Amending Regulation (EC) No 1881/2006 as Regards Maximum Levels of Polycyclic Aromatic Hydrocarbons (PAHs) in Traditionally Smoked Meat and Meat Products and Traditionally Smoked Fish and Fishery Products, 2014.
- Eum YO, Kim H, Jung HS, Cheoi KS, Lee MY, Lee WY, et al. (2006). A case of acute renal failure after application of mercury to the skin. *Korean J Nephrol.*;25(6):1019–1023.
- European Union (EU). (2005). Commission Regulation (EC) No 208/2005. *Official Journal of European Union*, L34/3 208/2005.
- Fang J, Wang KX, Tang JL, Wang M, Ren SJ, Wu HY, Wang J (2004) Copper, lead, zinc, cadmium, mercury, and arsenic in marine products of commerce from Zhejiang coastal area, China. *Bull Environ Contam Toxicol*, 73, 583–590.
- Fang T., Lien C. 2020. Mini review of trace metal contamination status in East China Sea sediment. *Marine Pollution Bulletin*, 152, 110874.
- Farrington, J. W., B. W. Tripp, S. Tanabe, A. Subramanian, J. L. Sericano, T. L. Wade, and A. H. Knap. (2016). Edward D. Goldberg’s proposal of “the Mussel Watch”: reflections after 40 years. *Mar. Pollut. Bull.* 110: 501–510.
- Fathallah S., Medhioub M.N., Kraiem M. M. (2012). Photo-induced Toxicity of Four Polycyclic Aromatic Hydrocarbons (PAHs) to Embryos and Larvae of the Carpet Shell Clam *Ruditapes decussatus*. *Bull Environ Contam Toxicol*, (88), 1001–1008.
- Federal ministry of Environment (FMEnv). (1991). Guidelines and standards for environmental pollution control in Nigeria. Nigerian ambient air quality standard.
- Fitzgerald, W.F., Engstrom, D.R., Mason, R.P., Nater, E.A. (1998). The case for atmospheric mercury contamination in remote areas. *Environmental Science & Technology*, 32, 1–7.
- Food and Agriculture Organization of the United Nations (FAO),1989. Report of the Workshop and Study Tour on Mollusk Sanitation and Marketing, Regional Sea Farming Development and Demonstration Project RAS/86/02415–28October. On Line. <http://www.fao.org/docrep/field/003/AB710E24.htm>.
- Fosmire G. J. (1990). Zinc toxicity. Retrieved August 21, 2001, from <https://pubmed.ncbi.nlm.nih.gov/2407097/>
- Fowler F. J., Barry M., Lu-yao G., Roman A, Wasson J., Wennberg J. (1993). Patient-re ported complications and follow-up treatment after radical prostatectomy: The national medicare experience: 1988–1990 (updated June 1993). *Urology*, 42 (6), 622-628

- Fox A., Hughes E., Trocine R., Trefry J., Schonberg S., McTigue N., Lasorsa B., Konar B., Coopere L. (2014). Mercury in the northeastern Chukchi Sea: Distribution patterns in seawater and sediments and biomagnification in the benthic food web. *Deep Sea Research Part II: Topical Studies in Oceanography*, 102, 56-67.
- Fu X., Feng X., Zhang G., Xu W., Li X., Yao H., Liang P., Li J., Sommar J., Yin R., Liu N. (2010). Mercury in the marine boundary layer and seawater of the South China Sea: Concentrations, sea/air flux, and implication for land outflow. *Journal of Geophysical Research: Atmospheres*, (115), D06303.
- Funes, V., Alhama, J., Navas, J. I., López-Barea, J., & Peinado, J. (2006). Ecotoxicological effects of metal pollution in two mollusc species from the Spanish South Atlantic littoral. *Environmental Pollution*, 139(2), 214–223.
- Frenken, K., 2009. Irrigation in the Middle East region in figures AQUASTAT Survey-2008. *Water Rep.* (34)
- Gagnairea B., Thomas-Guyon H., Renault T. (2004). In vitro effects of cadmium and mercury on Pacific oyster, *Crassostrea gigas* (Thunberg), haemocytes. *Fish & Shellfish Immunology*, (16), 501-512.
- Gallego-Lizon T., Pérez de Ortiz E. (2000). Drop sizes in liquid membrane dispersions. *Ind. Eng. Chem. Res.*, 39, 5020 – 5028.
- Gambrell R, Wiesepepe J., Patrick W., and C. Duff M. (1991). effects of pH, redox, and salinity on metal release from a contaminated sediment. *Water, Air, and Soil Pollution*, (57-58), no. 1, pp. 359–367.
- Gawade L, Harikrishna CNV, Sarma VV, Ingole BS. (2013). Variations in heavy metals concentration in the edible oyster *Crassostrea madrasensis*, clam *Polymesoda erosa* and grey mullet *Liza aurata* from coastline of India. *Indian Journal of Science*, 2(4), 59-63.
- Gevao B., Boyle E. A., Carrasco G. G., Ghadban A. N., Zafar J., Bahloul M. (2016). Spatial and temporal distributions of polycyclic aromatic hydrocarbons in the Northern Arabian Gulf sediments. *Marine Pollution Bulletin*, 112, 218–224.
- Goldberg, D. (1995). Emerging problems in the coastal zone for the twenty-first century. *Marine Pollution Bulletin*, 31(4–12), 152–158.
- Goyer R., Golub M., Choudhury H., Hughes M., Kenyon E., Stifelman M. (2004). ISSUE PAPER ON THE HUMAN HEALTH EFFECTS OF METALS. U.S. Environmental Protection Agency, Washington.
- Grandjean P, Budtz-Jorgensen E, White RF, Jorgensen PJ, Weihe P, Debes F, et al. (1999). Methylmercury exposure biomarkers as indicators of neurotoxicity in children aged 7 years. *Am J Epidemiol*;149:301-5.
- Halim C., Amal R., Beydoun D., Scott J., Low G. (2003). Evaluating the applicability of a modified toxicity characteristic leaching procedure (TCLP) for the classification of cementitious wastes containing lead and cadmium. *J. Hazard. Mater.*, 103, 125 – 140.
- Hambidge, M. (2003). Biomarkers of trace mineral intake and status. *The Journal of Nutrition*, 133, 948–955.
- Hamed, M.A. & A.M. Emara. (2006). Marine mollusks as biomonitors for heavy metal levels in the Gulf of Suez, Red Sea. *Journal of Marine Systems*, 60: 220-234.
- Hannam, M.L., Bamber, S.D., Galloway, T.S., Moody, A.J., Jones, M.B., (2010). Effects of the model PAH phenanthrene on immune function and oxidative stress in the haemolymph of the temperate scallop *Pecten maximus*. *Chemosphere*, 78, 779– 784.

- Hassan H., Azenith B. Castillo, Oguz Yigiterhan, Elnaiem Ali Elobaid, Abdulrahman Al-Obaidly, Ebrahim Al-Ansari, Jeffrey Philip Obbard. (2018). Baseline concentrations and distributions of Polycyclic Aromatic Hydrocarbons in surface sediments from the Qatar marine environment. *Marine Pollution Bulletin*, 126, 58-62.
- Hassan H., Ahmed Abou Elezz, Mazen Abuasali, Hamood AlSaadi. (2019). Baseline concentrations of mercury species within sediments from Qatar's coastal marine zone. *Marine Pollution Bulletin*, 142, 595–602.
- Hattula T, Rahola T. (1975). The distribution and biological half-time of ²⁰³Hg in the human body according to a modified whole-body counting technique. *Environ Physiol Biochem*, 5:252-7.
- Hejna, M., Gottardo, D., Baldi, A., Dell’Orto, V., Cheli, F., Zaninelli, M., & Rossi, L. (2018). Review: Nutritional ecology of heavy metals. *Animal*, 12 (10), 2156-2170.
- Hungspreugs M., Yaunghthong C. (1984). The present levels of heavy metals in some mollusks of the upper Gulf of Thailand. *Water, Air and Soil Poll*, (22), 395-402.
- Hursh JB, Greenwood MR, Clarkson TW, Allen J, Demuth S. The effect of ethanol on the fate of mercury vapor inhaled by man. *J Pharmacol Exp Ther* 1980;214(3):520-7.
- Hussain K. et al. (2018) Monitoring and Risk Analysis of PAHs in the Environment. In: Hussain C. (eds) Handbook of Environmental Materials Management. Springer, Cham. https://doi.org/10.1007/978-3-319-58538-3_29-2.
- Hussein H., Lambert L. (2020). A Rentier State under Blockade: Qatar’s Water-Energy-Food Predicament from Energy Abundance and Food Insecurity to a Silent Water Crisis. *Water*, 12, 1051; doi:10.3390/w12041051.
- ILA (International Lead Association). (2015). Lead in Aquatic Environments. London: ILA.
- Inam E., Essien J., Ita B., Etuk H., Kim W. (2012). Petroleum hydrocarbons and trace metal loads in the mangrove oyster (*Crassostrea rhizophorae*) from the Qua Iboe Estuary and adjoining creeks in Nigeria. *Geosystem Engineering*. 15(1).
- International Agency for Research on Cancer (IARC). IARC Monographs on the Evaluation of Carcinogenic Risks to Humans. Volume 58. Beryllium, Cadmium, Mercury, and Exposures in the Glass Manufacturing Industry. 1993. Available at URL: <http://monographs.iarc.fr/ENG/Monographs/vol58/index.phpexternal> icon.
- Islam, M., & Tanaka, M. (2004). Impacts of pollution on coastal and marine ecosystems including coastal and marine fisheries and approach for management: a review and synthesis. *Marine Pollution Bulletin*, 48(7–8), 624–49.
- Islam N., Huq E. , Islam N., Islam A., Ali R., Khatun R., Haque N., Rafiqul Islam, Sultana Nasima Akhter. (2018). Human Health Risk Assessment for Inhabitants of Four Towns of Rajshahi, Bangladesh due to Arsenic, Cadmium and Lead Exposure. *EnvironmentAsia*, 10(2), 168-182.
- Ji HR, Kim TJ, Chyung EJ, Park SY, Yang SK, Kim JT. (1983). A case of acrodynia. *Korean J Dermatol.*, 21(1):125–129.
- Johnson W. E., Kimbrough K. L., and Jacob A. P. (2019). Mussel Watch Program: Great Lakes Monitoring Project Plan under GLRI Action Plan II (20910). Maryland: Silver Spring.
- Jonathan M.P., Muñoz-Sevilla N.P., Góngora-Gómez A.M, Varela R.G.L., Sujitha S.B., Escobedo-Urías D.C, Rodríguez-Espinosa P.F., Villegas L.E.C. (2017). Bioaccumulation of trace metals in farmed pacific oysters *Crassostrea gigas* from SW Gulf of California coast, Mexico. *Chemosphere*, (187), 311-319.

- Jonsson F, Sandborgh-Englund G, Johanson G. (1999). A compartmental model for the kinetics of mercury vapor in humans. *Toxicol Appl Pharmacol*, 155(2):161-8.
- Juang R., Shiau L. (1998). Ion exchange equilibria of metal chelates of ethylenediaminetetraacetic acid (EDTA) with Amberlite IRA-68, *Ind. Eng. Chem. Res.*, 37, 555–560.
- Juma H. and Al-Madany I. (2008). Concentration of heavy metals in the territorial sea water of the Kingdom of Bahrain, Arabian Gulf. *Arab Gulf Journal of Scientific Research*, 26, (1-2), 19-32.
- Juttner K., Galla U. and Schmieder H. (2000). Electrochemical approaches to environmental problems in the process industry, *Electrochim. Acta.*, 45, 2575 – 2594.
- Kannan K., Smith R., Lee R., Windom H., Heitmuller P., Macauley J., Summers J.. (1998). Distribution of Total Mercury and Methyl Mercury in Water, Sediment, and Fish from South Florida Estuaries. *Arch. Environ. Contam. Toxicol.* 34, 109–118.
- Kafilzadeh F. (2015). Distribution and sources of polycyclic aromatic hydrocarbons in water and sediments of the Soltan Abad River, Iran. *The Egyptian Journal of Aquatic Research*, 41, (3), 227-231
- Karavasteva M. (2005). Kinetics and deposit morphology of copper cementation onto zinc, iron and aluminum. *Hydrometallurgy*, 76, 149 – 152.
- Kastratović V., Jaćimović Z., Bigović M., Đurović D., Krivokapić S. (2016). The distribution and accumulation of chromium in the water, sediment and macrophytes of Skadar lake. *Kragujevac J. Sci.* 38, 125-134.
- Karthikeyan, R. and Bhandari, A. (2001). Anaerobic Biotransformation of Aromatic and Polycyclic Aromatic Hydrocarbons in Soil Microcosms: A Review. *Journal of Hazardous Substance Research*, Vol. 3. <https://doi.org/10.4148/1090-7025.1021>
- Kampf, J. and Sadrinasab, M. (2006). The circulation of the Persian Gulf: a numerical study, *Ocean Sci.*, 2, 27–41, <https://doi.org/10.5194/os-2-27-2006>.
- Kaur S, Kaur A, Singh G, Bhatti R (2018) *Mercurius solubilis* attenuates scopolamine-induced memory deficits and enhances the motor coordination in mice. *Int J Neurosci*, 128(3):219–230.
- Kerr M. (2018). Nickel Allergy. Retrieved November 20, 2021 from <http://https://www.healthline.com/health/allergies/nickel>
- Khanmirzaei A., Bazargan K., Moezzi A., Richards B., Shahbazi K. (2013). Single and sequential extraction of cadmium in some highly calcareous soils of Southwestern Iran. *J. Soil Sci. Plant Nutr.*, 13, 153 – 164.
- Kim K., Jahan S., Kabir E., Brown R. (2013). A review of airborne polycyclic aromatic hydrocarbons (PAHs) and their human health effects. *Environmental International*, 60, 71–80.
- Kim M., Hong S., Won J., Yim U., Jung J., Ha S., An J., Joo C., Eunsic Kim E., Han G., Baek S., Choi H., Shim W. (2013). Petroleum hydrocarbon contaminations in the intertidal seawater after the Hebei Spirit oil spill e Effect of tidal cycle on the TPH concentrations and the chromatographic characterization of seawater extracts. *Water Research*, 47(2), 758-768.
- Konyuhov A. I., Maleki B. (2006). The Persian Gulf Basin: Geological History ,Sedimentary Formations, and Petroleum Potential. *Lithology and Mineral Resources*, 41, (4), 344–361.
- Kousi P., Remoudaki E., Hatzikioseyan A., Tsezos M. (2007). A study of the operating parameters of a sulphate-reducing fixed-bed reactor for the treatment of metal-bearing wastewater. In: 17th International Biohydrometallurgy Symposium, Germany, Frankfurt am Main.

- Kreish T. & Al-Muftah A. (1999). Total Mercury Levels In The Coastal Environment Of Qatar (Arabian Gulf). *Qatar University Science Journal*, 274- 284.
- Kroon F., Berry K., Diane L. Brinkman D., Rai Kookana R., Frederic D.L. Leusch F., Steven D. Melvin S., Peta A. Neale P., Andrew P. Negri A., Marji Puotinen M., Jeffrey J. Tsang J., van de Merwe J., Williams M. (2020). Sources, presence and potential effects of contaminants of emerging concern in the marine environments of the Great Barrier Reef and Torres Strait, Australia. *Science of the Total Environment*, 719, 135140.
- Ku Y., Jung L. (2001). Photocatalytic reduction of Cr(VI) in aqueous solutions by UV irradiation with the presence of titanium dioxide. *Water Res.*, 35, 135 -142
- Kucaj E., Abazi U. (2015). Assessment of heavy metals in sediments and phragmites australis in Tirana River, Albania. *European Journal of Physical and Agricultural Sciences*, (3), 2, ISSN 2056-5879.
- Kuppusamy, S., Maddela N. R., Mallavarapu, M. & Kadiyala, V. (2020). Impacts of Total Petroleum Hydrocarbons on human health. *Total Petroleum Hydrocarbons*. Springer, Cham. https://doi.org/10.1007/978-3-030-24035-6_6
- Kureishy .T (1993). Concentration of Heavy Metals in Marine Organisms Around Qatar Before and After the Gulf War Oil Spill. *Marine Pollution Bulletin*, (27), 183-186.
- Kureishy, Tariq W, Ahmed, Mahmoud H. (1994). Total Mercury Distribution In Surface Sediments From The Arabian Gulf. *Qatar Univ. Sci. J.* 14 (2), 390-394.
- Lang Y., Cao Z. (2010). In *Bioinformatics and Biomedical Engineering (iCBBE)*, 2010 4th International Conference on, p. 1.
- Lee HY, Kang GH, Nam KH, Kim MH, Jung BH, Kang HD, et al (2010). Acute mercury vapor inhalation toxicity after burning charms: a case report. *Korean J Crit Care Med.*, 25(3):182–185.
- Lee SH, Kim SH, Kim YK, Woo JY, Han SW, Park IS, et al. Acute respiratory failure and acute renal failure induced by inhalation of mercury vapor. *Korean J Intern Med.* 1991;40(5):712
- Leitão-Ben Hamadou A., Al-Shaikh I., Al-Maslamani I., Al-Ansari E., Hassan H., Ben Hamadou R., Bach S. (2016). First Impact Assessment of Genotoxic Components in the Qatari Marine Environment. *Qatar Foundation Annual Research Conference Proceedings*, Volume 2016 (1), EEPP2749. DOI: <https://doi.org/10.5339/qfarc.2016.EEPP2749>
- Leitão A., Al-Shaikh I., Hassan H., Ben Hamadou R., Bach S. (2017). First genotoxicity assessment of marine environment in Qatar using the local Pearl oyster *Pinctada radiata*. *Regional Studies in Marine Science*, 11, 23–31.
- Leonard E., Pierce L., Gillis P., Wood C., O'Donnell M. (2009). Cadmium trans-port by the gut and Malpighian tubules of *Chironomus riparius*. *Aquat. Toxicol.*, 92, 179 – 186.
- Liang J., Liu J., Xu G., and Chen B. (2019). Distribution and transport of heavy metals in surface sediments of the Zhejiang nearshore area, East China Sea: sedimentary environmental effects. *Marine Pollution Bulletin*, vol. 146, pp. 542–551, 2019.
- Liang Y., Liu X., Yuan D., Gong Z., Zhang Z. (2010). Mercury Species in Seawater and Sediment of Xiamen Western Sea Area Adjacent to a Coal-fired Power Plant. *Water Environment Research*, 82, 4, 335-341.
- Lim HE, Shim JJ, Lee SY, Lee SH, Kang SY, Jo JY, In KH, Kim HG, Yoo SH, Kang KH. (1998). *Korean J Intern Med.* Jul; 13(2):127-30.
- Loganathan P., Hedley M., Grace N. (2008). Pasture soils contaminated with fertilizer derived cadmium and fluoride: livestock effects, *Rev. Environ. Contam. Toxicol.*, 192, 29 – 66.

- Losi M., Amrhein C. and Frankenberger W. (1994). Factors affecting chemical and biological reduction of hexavalent chromium in soil. *Environ. Toxicol. Chem.*, 13, 1727 - 1735.
- Lu G., Pan K., Zhu A., Dong Y., Wang W. (2020). Spatial-temporal variations and trends prediction of trace metals in oysters from the Pearl River Estuary of China during 2011-2018. *Environmental Pollution*, 264, 114812.
- Lu G., Zhu A., Fang H., Dong Y., Wang W. (2019). Establishing baseline trace metals in marine bivalves in China and worldwide: Meta-analysis and modeling approach. *Science of the Total Environment*, 669, 746–753.
- Luna-Acosta, A., H. Budzinski, K. Le Menachb, H. Thomas-Guyon, P. Bustamante. (2011). Persistent organic pollutants in a marine bivalve on the Marennes-Oléron Bay and the Gironde Estuary (French Atlantic Coast)—Part 1: Bioaccumulation. *Science of the Total Environment*, 514, 500-510.
- Lyons B., Barber J., Rumney H., Bolam T., Bersuder P., Law R., Mason C., Smith A., Morris S., Devlin M., Al-Enezi M., Massoud M., Al-Zaidan A., Al-Sarawi H. (2015). Baseline survey of marine sediments collected from the State of Kuwait: PAHs, PCBs, brominated flame retardants and metal contamination. *Marine Pollution Bulletin*, 100, 629–636.
- MacFarlane, G.R.; Koller, C.E.; Blomberg, S.P. (2007). Accumulation and partitioning of heavy metals in mangroves: A synthesis of field-based studies. *Chemosphere*, 69, 1454–1464.
- Maliszewska-Kordybach B.; Smreczak B; Klimkowicz-Pawlas A.; Terelak, H. (2008). Monitoring of the total content of polycyclic aromatic hydrocarbons (PAHs) in arable soils in Poland. *Chemosphere*, 73, 1284–1291.
- MaoL., Liu X., Wang B., Lin C., Xin M., Zhang B-T., Wu T., He M., Ouyang W. (2020). Occurrence and risk assessment of total mercury and methylmercury in surface seawater and sediments from the Jiaozhou Bay, Yellow Sea. *Science of The Total Environment*, 714, 136539.
- Matsuyama A., Eguchi T., Sonoda I., Tada A., Yano S., Tai A. (2011). Mercury speciation in the water of Minamata Bay, Japan. *Water Air Soil Pollut.* 218, 399–412.
- McBride M., Pitiranggon M., Kim B. (2009). A comparison of tests for extractable copper and zinc in metal-spiked and field-contaminated soil, *Soil Sci.*, 174, 439 – 444.
- McDowell MA, Dillon CF, Osterloh J, Bolger PM, Pellizzari E, Fernando R, et al. (2004). Hair mercury levels in U.S. children and women of childbearing age: reference range data from NHANES 1999-2000. *Environ Health Perspect*, 112(11):1165-71.
- Melamed, R., Villas Bôas, R.C., Goncalves, G.O., Paiva, E.C. (1997). Mechanisms of physicochemical interaction of mercury with river sediments from a gold mining region in Brazil: relative mobility of mercury species. *J. Geochem. Explor.* 58, 119–124.
- Memet, V. (2011). Assessment of heavy metal contamination insediments of the Tigris River (Turkey) using pollution indicesand multivariate statistical techniques. *Journal of HazardousMaterials*, 195: 355-364.
- Meyers, P.A. (2003). Applications of organic geochemistry to paleolimnological reconstructions: A summary of examples from the Laurentian Great Lakes. *Org. Geochem.*, 34, 261–289.
- Miettinen JK, Rahola T, Hattula T, Rissanen K, Tillander M. (1971). Elimination of 203Hg-methyl mercury in man. *Ann Clin Res*;3(2):116-122.
- Moorthy B., Gastelum G., Veith A., Wang L., Zhou G., Jiang W. (2019). Mechanistic Role of Cytochrome P450 (CYP) 1 Enzymes in Polycyclic Aromatic Hydrocarbon (PAH)-Mediated Carcinogenesis. *The FASEP Journal*, https://doi.org/10.1096/fasebj.2019.33.1_supplement.509.11Moorthy B., Chu C., Carlin

- D. J. (2015). Polycyclic Aromatic Hydrocarbons: From Metabolism to Lung Cancer. *Toxicological Sciences*, 145(1): 5–15
- Mueller J.G., Cerniglia C.E., Pritchard P.H. (1996). Bioremediation of environments contaminated by polycyclic aromatic hydrocarbons. In: Crawford RL, Crawford DL (eds) *Bioremediation: Principles and Applications*, Cambridge University Press, U.K, 1215-1294.
- Mukhopadhyay M., and Konar S. (1982). Lethal effects of iron on fish and aquatic ecosystem. *Ind. Assoc. Wat. Pollut. Contr. Technol.*, Annual 9, 49 - 162.
- Myers GJ, Thurston SW, Pearson AT, Davidson PW, Cox C, Shamlaye CF, Cernichiari E, Clarkson TW (2009) Postnatal exposure to methyl mercury from fish consumption: a review and new data from the Seychelles Child Development Study. *Neurotoxicology* 30(3):338–349.
- Naser H. (2013). Assessment and management of heavy metal pollution in the marine environment of the Arabian Gulf: A review. *Marine Pollution Bulletin*, 72, 6–13.
- National Ocean Service. (2021). Why is the ocean salty?. Retrieved April 4, 2021, from <https://oceanservice.noaa.gov/facts/whysalty.html#:~:text=The%20average%20salinity%20is%20about,comes%20from%20the%20dissolved%20salts>.
- National Research Council, *Bioavailability of Contaminants in Soils and Sediments: Processes, Tools, and Applications*, National Academies Press, 2003.
- National Standard of PR China (NSPR). (2002) *Marine sediment quality (GB 18668-2002)*. Standards Press of China, Beijing (in Chinese).
- Nemeh A., Van Peteghem A. (1992). Extraction of multicomponent system metals from simulated and industrial effluents by liquid surfactant membranes, *Hydrometallurgy*, 31, 149 – 159.
- Nicklisch, S.C.T., Bonito, L.T., Sandin, S., Hamdoun, A. (2017). Mercury levels of yellowfin tuna (*Thunnus albacares*) are associated with capture location. *Environ. Pollut.* 229, 87–93.
- NIOSH " National Institute for Occupational Safety and Health". (2018). Lead: Health Problems Caused by Lead. Retrieved November 20, 2021, from <http://https://www.cdc.gov/niosh/topics/lead/health.html#:~:text=Exposure%20to%20high%20levels%20of,a%20developing%20baby%27s%20nervous%20system>.
- Nzila A. (2019). Current Status of the Degradation of Aliphatic and Aromatic Petroleum Hydrocarbons by Thermophilic Microbes and Future Perspectives. *Int J Environ Res Public Health*, 15(12): 2782.
- Ochoa V, Barata C, Riva MC (2013). Heavy metal content in oysters (*Crassostrea gigas*) cultured in the Ebro delta in Catalonia, Spain. *Environ Monit Assess*, 185, 6783–6792.
- Ordiano, F.A., Galvan, M.F., Rosiles, M.R. (2011). Bioaccumulation of mercury in muscle tissue of yellowfin tuna, *Thunnus albacares*, of the Eastern Pacific Ocean. *Biol. Trace Elem. Res.* 144, 606–620.
- Otchere FA. (2003). Heavy metals concentrations and burden in the bivalves (*Anadara (Senilia) senilis*, *Crassostrea tulipa* and *Perna perna*) from lagoons in Ghana: Model to describe mechanism of accumulation/excretion. *African Journal of Biotechnology*, 2(9), 280-87.
- Oyo-Ita I. O., Oyo-Ita O. E., Dosunmu M. I., Elarbaoui S. (2016). Distribution and Historical Trends of PAHs Deposition in Recent Sediment Cores of IMO River, S. E. Nigeria. 5th International Conference on Biological, Chemical and Environmental Sciences (BCES-2016) March 24-25, London (UK).
- Pakzadeh B., Batista J. (2011) Chromium removal from ion-exchange waste brines with calcium polysulfide. *Water Res*, 45, 3055 – 3064.

- Paul V., Sankar M., Vattikuti S., Dash P., Arslan Z. 2021. Pollution assessment and land use land cover influence on trace metal distribution in sediments from five aquatic systems in southern USA. *Chemosphere*, 263, 128243.
- Gautam P., Gautam R., Banerjee S., M. C. Chattopadhyaya. (2016). Heavy metals in the environment: Fate, transport, toxicity and remediation technologies. Nava Science Publishers, India.
- Prospero Joseph M., Ginoux P., Torres O., Nicholson S., Gill T. (2002). ENVIRONMENTAL CHARACTERIZATION OF GLOBAL SOURCES OF ATMOSPHERIC SOIL DUST IDENTIFIED WITH THE NIMBUS 7 TOTAL OZONE MAPPING SPECTROMETER (TOMS) ABSORBING AEROSOL PRODUCT. *Reviews of Geophysics* *Reviews of Geophysics*, 1002, doi:10.1029/2000RG000095
- Phillips DJH, Rainbow PS. (1994). Biomonitoring of trace aquatic contaminants. 2nded. London: Chapman and Hall.
- Powers, R.W. (2010). Lexique Stratigraphic International-Saudi Arabia [online] http://paleopolis.rediris.es/LEXICON/KSA/Plate_01.htm (accessed 22 June 2021)
- Qatar National Vision 2030. (2008). General Secretariat For Development Planning. Available at: http://QNV2030_English_v2.pdf (psa.gov.qa)
- Radomyski, A., Lei, K., Giubilato, E., Critto, A., Lin, C., Marcomini, A. (2018). Bioaccumulation of trace metals in aquatic food web. A case study, Liaodong Bay, NE China. *Mar. Pollut. Bull.* 137, 555–565.
- Rahola T, Hattula T, Korolainen A, Miettinen JK. Elimination of free and protein-bound ionic mercury (203Hg²⁺) in man. *Ann Clin Res* 1973;5:214-219.
- Rainbow P.S. (1995). Biomonitoring of heavy metal availability in the marine environment. *Mar. Pollut. Bull.* 31, 183-192.
- Readman J.W., Fillmann G., Tolosa I., Bartocci J., Villeneuve J.-P., Catinni C., Mee L.D. (2002). Petroleum and PAH contamination of the Black Sea. *Marine Pollution Bulletin* 44, 48–62
- Readman J.W., Bartocci J., Tolosa I., Fowler S.W., Oregioni B., Abdulraheem M.Y. (1996). Recovery of the coastal marine environment in the Gulf following the 1991 war-related oil spills. *Marine Pollution Bulletin*, 32 (6), 493-498
- Rice, K.M., Walker Jr., E.M., Wu, M., Gillette, C., Blough, E.R. (2014). Environmental mercury and its toxic effects. *J. Prev. Med. Public Health*, 47, 74–83.
- Richard H. Mckee, M. David Adenuga, Juan-Carlos Carrillo. (2015). Characterization of the toxicological hazards of hydrocarbon solvents, *Critical Reviews in Toxicology*, 45:4, 273-365, DOI: 10.3109/10408444.2015.1016216
- Richer R. (2008). Conservation in Qatar: Impacts of Increasing Industrialization. Qatar: Center for International and Regional Studies.
- Rivers J., Varghese L., Yousif R., Whitaker F., Skeat S., AL-Shaikh I. (2019). The Geochemistry of Qatar Coastal Waters and its Impact on Carbonate Sediment Chemistry and Early Marine Diagenesis. *Journal of Sedimentary Research*, 89, 293–309 .
- Roels HA, Boeckx M, Ceulemans E, Lauwerys RR. (1991). Urinary excretion of mercury after occupational exposure to mercury vapor and influence of the chelating agent meso-2,3-dimercaptosuccinic acid (DMSA). *Br J Ind Med*, 48:247-53.
- ROPME. (2011). ROPME Mussel Watch Programme (RMWP). Retrieved April 24, 2021, from http://www.ropme.org/34_MUSSEL_WATCH_EN.clx

- Rossi, L, Fusi, E, Boglioni, M, Giromini, C, Rebucci, R and Baldi, A. (2014). Effect of Zinc oxide and Zinc chloride on human and swine intestinal epithelial cell lines. *International Journal of Health. Animal Science and Food Safety*, 2, 1–7.
- Ruppert M., Draxler J., Marr R. (1988). Liquid-membrane permeation and its experiences in pilot-plant and industrial scale, *Sep. Sci. Technol.*, 23, 1659 – 1666.
- Rushdi A., Al-Shaikh I., El-Mubarak A., Alnaimi H., Al-Shamary N., Hassan H., Abou Assali M. (2017). Characteristics and sources of anthropogenic and biogenic hydrocarbons in sediments from the coast of Qatar. *Marine Pollution Bulletin*, 124, 56-66.
- Sadooni, F. (2014). Geology of Qatar. Qatar: Environmental Study Center (ESC).
- Saha M., Naik A., Desai A., Nanajkar M., Rathore C., Kumar M., Gupta P. (2021). Microplastics in seafood as an emerging threat to marine environment: A case study in Goa, west coast of India. *Chemosphere*, (270), 129359.
- Sallsten G, Barregard L, Schutz A. (1993). Decrease in mercury concentration in blood after long term exposure: a kinetic study of chloralkali workers. *Br J Ind Med*, 50(9):814-821.
- Sampera E., Rodríguez M., A. De la Rubia M., Prats D. (2009). Removal of metal ions at low concentration by micellar-enhanced ultrafiltration (MEUF) using sodium dodecyl sulfate (SDS) and linear alkylbenzene sulfonate (LAS). *Sep. Purif. Technol.*, 65, 337 - 342.
- Sandborgh-Englund G, Elinder CG, Langworth S, Schutz A, Ekstrand J. (1998). Mercury in biological fluids after amalgam removal. *J Dent Res*;77(4):615-624.
- Satheeswaran T., Yuvaraj P., Damotharan P., Karthikeyan V., Jha D., Dharani G., Balasubramanian T., Kirubakaran R. (2019). Assessment of trace metal contamination in the marine sediment, seawater, and bivalves of Parangipettai, southeast coast of India. *Marine Pollution Bulletin*, 149, 110499.
- Sea Temperature. (2021). Doha. Retrieved April 21, 2021, from <https://seatemperature.net/current/qatar/doha-ad-dawah-qatar-sea-temperature>
- Sheehan, M.C., Burke, T.A., Navas-Acien, A., Breyse, P.N., McGready, J., Fox, M.A. (2014). Global methylmercury exposure from seafood consumption and risk of developmental neurotoxicity: a systematic review. *Bull. World Health Organ.* 92, 254–269.
- Sheppard C., Al-Husiani M, Al-Jamali F., Al-Yamani F., Baldwin R., Bishop J., Benzoni, F., Dutrieux, E., & Dulvy N, Durvasula S., Jones D., Loughland R., Medio D., Manickam, N., Pilling G., Polikarpov I., Price A., Purkis S, Riegl, B., Zainal K. (2010). The Persian/Arabian Gulf: a young sea in decline. *Mar Pollut Bull. Marine Pollution Bulletin*. 60. 13-38. 10.1016/j.marpolbul.2009.10.017.
- Sherlock J, Hislop D, Newton G, Topping G, Whittle K. Elevation of mercury in human blood from controlled ingestion of methyl mercury in fish. *Hum Toxicol* 1984;2:117-131.
- Silva, C. A., Rainbow, P. S., Smith, B. D., and Santos, Z. L. (2001). Biomonitoring of TRACE metal contamination in the Potengi estuary, Natal (Brazil), using the oyster *Crassostrea Rhizophorae*, a local food source. *Water Res.* 35, 4072–4078. doi: 10.1016/S0043-1354(01)00144-0.
- Smith JC, Allen PV, Turner MD, Most B, Fisher HL, Hall LL. (1994). The kinetics of intravenously administered methyl mercury in man. *Toxicol Appl Pharmacol*, 128(2):25125-6.
- Smith JC, Farris FF. (1996). Methyl mercury pharmacokinetics in man: a reevaluation. *Toxicol Appl Pharmacol*;37:245-252.
- Smyth D., Al-Maslamani I., Chatting M., Giraldes B. (2016). Benthic surveys of the historic pearl oyster beds of Qatar reveal a dramatic ecological change. *Marine Pollution Bulletin*, 113(1-2).

- Soliman Y., Al Ansari E., Wade T. (2014). Concentration, composition and sources of PAHs in the coastal sediments of the exclusive economic zone (EEZ) of Qatar, Arabian Gulf. *Marine Pollution Bulletin*, 85, 542–548 .
- Soliman Y., Alansari E., Sericano J., Wade T. (2019). Spatio-temporal distribution and sources identifications of polycyclic aromatic hydrocarbons and their alkyl homolog in surface sediments in the central Arabian Gulf. *Science of the total environment*, 658, 787-797.
- Stentiford G., Massoud M., Al-Mudhhi S., M.A.Al-Sarawi M., M.Al-Enezi, Lyons B. (2014). Histopathological survey of potential biomarkers for the assessment of contaminant related biological effects in species of fish and shellfish collected from Kuwait Bay, Arabian Gulf. *Marine Environmental Research*. (98) 60-67 .
- Schropp S., Windom H. (1988). A GUIDE TO THE INTERPRETATION OF METAL CONCENTRATIONS IN ESTUARINE SEDIMENTS. Tallahassee: Florida Department of Environmental Protection.
- Suami R., Al Salah D., Kabala C., Otamong J. , Mulaji C., Mpiana P., Pote J. (2019). Assessment of metal concentrations in oysters and shrimp from Atlantic Coast of the Democratic Republic of the Congo. *Heliyon*, (5), e03049.
- Suzuki T, Hongo T, Yoshinaga J, Imai H, Nakazawa M, Matsuo N, et al. (1993). The hair-organ relationship in mercury concentration in contemporary Japanese. *Arch Environ Health*, 48(4):221-229.
- Taylan ZS, Ozkoc HB (2007) Bioavailability of aquatic organisms in determination of potential heavy metal pollution. *Journal of BAU FBE*. 9: 17-33.
- Tang Y, Wang X, Jia J (2015) Mercury poisoning presenting as sporadic Creutzfeldt-Jakob disease: a case report. *Ann Intern Med* 162(6):462–463.
- Tchounwou P., Newsome C., Williams J., Glass K. (2008). Copper-induced cytotoxicity and transcriptional activation of stress genes in human liver carcinoma cells. *Metal Ions Biol Med*. 10:285–290
- Tchounwou P., Yedjou C., Patlolla A., and Sutton D. (2014). Heavy Metals Toxicity and the Environment. *National Institution of Health*, 101: 133–164
- Tehrani G., Sany S.B. T., Hashim R., Salleh A. (2016). Predictive environmental impact assessment of total petroleum hydrocarbons in petrochemical wastewater effluent and surface sediment. *Environ Earth Sci*, 75:177
- Thompson L., Darwish W. (2019). Environmental Chemical Contaminants in Food: Review of a Global Problem. *Journal of Toxicology*, vol. 2019, Article ID 2345283, 14 pages.
- Thoppil P., Hogan P. (2010). Persian Gulf response to a wintertime shamal wind event. *Deep Sea Research Part I Oceanographic Research Papers*, 57(8), 946-955.
- Tolosa I., de Mora, S.J., Fowler, S.W., Villeneuve, J.-P., Bartocci, J., Cattini, C. (2005). Aliphatic and aromatic hydrocarbons in marinebiota and coastal sediments from the Gulf and the Gulf of Oman. *Marine Pollution Bulletin*, 50, 1619–1633.
- Tomiyasu T., Matsuyama A., Eguchi T., Fuchigami Y., Oki. K, Horvat M., Rajar R., Akagi H. (2006). Spatial variations of mercury in sediment of Minamata Bay, Japan, *Sci. Total Environ*. 368, 283–290.
- Türe C, Candan M, Böcük H, Yücel H, Ketenoglu O, et al. (2009) Ecology (2ndedn), Anatolian University.
- UNEP. (1985). Reference methods for marine pollution studies, determination of total Hg in marine sediments and suspended solids by cold vapour, *AAS*, 26: 1-28.

- U.S. Department of Health and Human Services. (2007). Toxicological profile for Lead (update) [<http://www.atsdr.cdc.gov/toxprofiles/tp13.pdf> (PDF 4901KB, 582 pages)] Public Health Service Agency for Toxic Substances and Disease Registry.
- USEPA. (United States Environmental Protection Agency). (1982). Office of the Federal Registration (OFR) Appendix A: priority pollutants. Fed Reg., 47:52309.
- USEPA (United States Environmental Protection Agency). (1989). Sediment Classification Methods Compendium. Draft Final Report. United States Environmental Protection Agency, Watershed Protection Division, USA.
- USEPA (United States Environmental Protection Agency). (1996). Method 3510C: Separatory funnel liquid-liquid extraction. CR- ROM, Revision 3, USA.
- USEPA (United States Environmental Protection Agency). (1996). Method 8015B: nonhalogenated organics using GC/FID. CR- ROM, Revision 2, USA.
- USEPA (United States Environmental Protection Agency). (2000). Supplemental Guidance for Conducting for Health Risk Assessment of Chemical Mixtures. EPA/630/R-00/002.
- USEPA (United States Environmental Protection Agency). (2002). Appendix V: median international standards. Environmental Protection Agency. State Water Resources Control Board <http://www.swcb.ca.gov>.
- USEPA. (2004). (United States Environmental Protection Agency). National Recommended Water Quality Criteria. Office of Science and Technology, 4304T.
- USEPA (United States Environmental Protection Agency). (2005). Supplemental guidance for assessing cancer susceptibility from early-life exposure to carcinogens. Risk Assessment Forum, Washington, DC. Available from: <http://www.epa.gov/ncea/raf>.
- USEPA (United States Environmental Protection Agency). (2006). The Great Lakes: Contaminated Sediments. MacDonald, D., Ingersoll, C., Berger, T., 2000. Development and evaluation of consensusbased sediment quality guidelines for freshwater ecosystems. *Arch. Environ. Contam. Toxicol.* 39, 20–31. <https://doi.org/10.1007/sOM440010075>.
- US FDA Food and Drug Administration. Guidance Document for Chromium in Shellfish DHHS/PHS/FDA/CFSAN/Office of Seafood, Washington, DC (1993)
- Vaezzadeh V., Zakaria M., Bong C. (2017). Aliphatic hydrocarbons and triterpane biomarkers in mangrove oyster (*Crassostrea belcheri*) from the west coast of Peninsular Malaysia. *Marine Pollution Bulletin*, 124(1), 33-42.
- Vahter M, Mottet NK, Friberg L, Lind B, Shen DD, Burbacher T. (1994). Speciation of mercury in the primate blood and brain following long-term exposure to methyl mercury. *Toxicol Appl Pharmacol*, 124:221-229.
- Vane C. H., Harrison, I. & Kim, A. W. (2007). Polycyclic aromatic hydrocarbons (PAHs) and polychlorinated biphenyls (PCBs) in sediments from the Mersey Estuary, U.K. *Science of the Total Environment*, 374, 112–126.
- Vaughan, G. O., Al-Mansoori, N., & Burt, J. A. (2019). The Arabian Gulf. In C. Sheppard (Ed.), *World Seas: an Environmental Evaluation (Second Edition) (2 ed., Vol. 2, pp. 1-23)*. Academic Press. <https://doi.org/10.1016/B978-0-08-100853-9.00001-4>
- Waalkes, M. (1995). Metal carcinogenesis. In: Goyer, R.A. and C.D. Klaassen, eds. *Metal toxicology*. New York: Academic Press, 47-67.
- Wang C., Zou X., Feng Z., Hao Z., and Gao J. (2018). Distribution and transport of heavy metals in estuarine-inner shelf regions of the East China Sea. *Science of the Total Environment*, 644, 298–305.

- Wang, S., & Shi, X. (2001). Molecular mechanisms of metal toxicity and carcinogenesis. *Molecular and Cellular Biochemistry*, 222(1–2), 3–9.
- Water Framework Directive - United Kingdom Technical Advisory Group (WFD-UKTAG). (2010). Proposed EQS for Water Framework Directive Annex VIII substances: zinc (For consultation Scotland: WFD-UKTAG).
- WHO. (2003) Malathion in drinking water, background document for preparation of WHO guidelines for drinking water quality. (WHO/ SDE/ WSH/03.04/103)
- WHO. 2017. <https://www.who.int/news-room/fact-sheets/detail/mercury-and-health>, Accessed date: 25 November 2020.
- Wootton, E.C., Dyrinda, E.A., Pipe, R.K., Ratcliffe, N.A. (2003). Comparisons of PAH induced immunomodulation in three bivalve molluscs. *Aquat. Toxicol.* 65, 13–25.
- World Bank Group (2019). Gulf Economic Monitor. Issue 3. Gulf counter:Gulf Cooperation Council Economies.
- Wuana R., Okieimen F., Imborvungu J. (2010). Removal of heavy metals from a contaminated soil using organic chelating acids. *Int. J. Environ. Sci. Technol.*, 7, 485 – 496.
- Yang C P, Lung W S, Kuo J T, Lai J S, Hsu C H. (2012). Using an integrated model to track the fate and transport of suspended solids and heavy metals in the tidal wetlands. *International Journal of Sediment Research*, 27(2): 201–212.
- Yesudhasan P, Al-Busaidi M, Al-Rahabi W, Al-Waili AS, AlNakhaili AK, Al-Mazrooei NA, Al-Habsi SH. (2013). Distribution patterns of toxic metals in the marine oyster *Saccostrea cucullata* from the Arabian Sea in Oman: spatial, temporal, and size variations. *SpringerPlus*, 2, 1–11.
- Yetiv S.A. (1997). *The Persian Gulf Crisis*. Westport: Greenwood Press.
- Yu X., Li H., Pan K., Yan Y., Wang W.X. (2012). Mercury distribution, speciation and bioavailability in sediments from the Pearl River Estuary, Southern China. *Marine Pollution Bulletin*. 64, 1699–1704.
- Yuan Y., Suna T., Wangb H., Liua Y., Ye Pana, Xiea Y., Honghui Huangb H., Fana Z.(2020). Bioaccumulation and health risk assessment of heavy metals to bivalve species in Daya Bay (South China Sea): Consumption advisory. *Marine Pollution Bulletin*, 150, 110717.
- Zhang R., Yu K., Li A., Wang Y., Pan C., Huang X. (2020). Antibiotics in coral reef fishes from the South China Sea: Occurrence, distribution, bioaccumulation, and dietary exposure risk to human. *Science of The Total Environment*, (704),135288.
- Zhang R., Sun Z., Gang Li, Wang H., Cheng J. & Hao M. (2020). Influences of water chemical property on infiltration into mixed soil consisting of feldspathic sandstone and aeolian sandy soil. *Scientific Reports*, 10, 19497. <https://doi.org/10.1038/s41598-020-76548-7>
- Zhou Z, Zhang X, Cui F, Liu R, Dong Z, Wang X, Shengyuan Yu. (2014). Subacute motor neuron hyperexcitability with mercury poisoning: a case series and literature review. *Eur Neurol*, 72(3–4):218–222.
- Zuykov M., Pelletier E., Harper D.A. (2013). Bivalve mollusks in metal pollution studies: from bioaccumulation to biomonitoring. *Chemosphere*, 93, 201-208.

Appendixes

Appendix A: Physical parameters for the four locations from the four sampling rounds in summer and winter.

Appendix A-1: Levels of Physical parameters

Table 1: Physical parameters for the four sites in summer 2017 (March 2017)

Site	Simaisma (27/3/17)			Umm Bab (28/3/17)			Al Khor (29/3/2017)			Al Wakra (16/4/2017)		
	R1	R2	R3	R1	R2	R3	R1	R2	R3	R1	R2	R3
GPS coordinates	N 25°31.969	N 25°32.779	N 25°32.188	N 25°12.193			N 25°40.316	N 25°40.089	N 25°40.051	N 25°09.140	N 25°09.150	N 25°09.136
	E 51°29.537	E 51°30.580	E 51°30.205	E 50°45.881			E 51°32.743	E 51°32.549	E 51°32.568	E 51°37.054	E 51°37.072	E 51°37.073
Temperature (°C)	23.13	23.29	23.65	25.19	25.09	25.19	27.2	29.1	30.4	29.2	28.9	28.8
Conductivity (µS/cm)	61.24	62.5	63.99	80.63	82.01	82.65	69.81	70.63	**	69.25	69.01	68.64
TDS (g/l)	41.27	41.23	42.69	52.2	53.2	53.52	42.52	41.68	**	41.67	41.65	41.47
Salinity (ppt)	42.91	43.7	44.59	56.17*	57.41*	57.81*	44.25	43.19	**	43.22	43.2	42.99
Ph	8.15	8.1	8.24	8.03	8.05	8.08	8.29	8.27	8.29	8.15	8.14	8.13
*near a desalination plant												
** extremely shallow water												

Table 2: Physical parameters for the four sites in winter 2017 (December 2017)

Site	Simaisma (6/12/17)			Umm Bab (7/2/18)			Al Khor (3/12/17)			Al Wakra (3/12/17)		
	R1	R2	R3	R1	R2	R3	R1	R2	R3	R1	R2	R3
GPS coordinates	N 25°31.969	N 25°32.779	N 25°32.188	N 25°12.193			N 25°40.316	N 25°40.089	N 25°40.051	N 25°09.140	N 25°09.150	N 25°09.136
	E 51°29.537	E 51°30.580	E 51°30.205	E 50°45.881			E 51°32.743	E 51°32.549	E 51°32.568	E 51°37.054	E 51°37.072	E 51°37.073
Temperature (°C)	20.46	20.56	20.89	18.95	18.95	18.95	20.04	17.97	18.51	23.90	24.08	23.78
Conductivity (mS/cm)	62.44	62.43	62.58	75.94	75.94	75.94	62.71	63.73	63.67	60.15	61.87	60.53
TDS (g/l)	40.59	40.58	40.68	49.39	49.39	49.39	40.76	41.42	41.38	39.10	40.21	39.35
Salinity (ppt)	42.13	42.13	42.24	52.62*	52.62*	52.62*	42.34	43.1	43.06	40.34	41.65	40.64
Ph	8.16	8.16	8.17	7.81	7.81	7.81	8.11	7.99	8.00	8.15	8.18	8.15
*near a desalination plant												

Table 3: Physical parameters for the four sites in summer 2018 (May 2018)

Site	Simaisma (7/May/18)			Umm Bab (6/May/18)			Al Khor (9/May/18)			Al Wakra (13/May/18)		
	R1	R2	R3	R1	R2	R3	R1	R2	R3	R1	R2	R3
GPS coordinates	N 25°31.969	N 25°32.779	N 25°32.188	N 25°12.193			N 25°40.316	N 25°40.089	N 25°40.051	N 25°09.140	N 25°09.150	N 25°09.136
	E 51°29.537	E 51°30.580	E 51°30.205	E 50°45.881			E 51°32.743	E 51°32.549	E 51°32.568	E 51°37.054	E 51°37.072	E 51°37.073
Temperature (°C)	29.23	28.68	28.89	29.24	28.59	28.48	29.47	29.46	29.29	28.69	27.80	28.31
Conductivity (mS/cm)	63.74	63.56	63.68	80.96	80.91	80.87	64.89	64.62	64.32	62.91	64.34	63.46
TDS (g/l)	41.43	41.31	41.39	52.63	52.59	52.56	42.18	42.00	41.81	40.89	41.82	41.25
Salinity (ppt)	42.94	42.82	42.90	56.55	56.53	56.50	43.81	43.60	43.38	42.32	43.45	42.76
Ph	8.22	8.19	8.22	7.95	7.96	7.96	8.19	8.18	8.14	8.15	8.15	8.15
*near a desalination plant												

Table 4: Physical parameters for the four sites in winter 2018 (November 2018)

Site	Simaisma (19/Nov/18)			Umm Bab (13/Nov/18)			Al Khor (4/Dec/18)			Al Wakra (12/Nov/18)		
	R1	R2	R3	R1	R2	R3	R1	R2	R3	R1	R2	R3
GPS coordinates	N 25°31.969	N 25°32.779	N 25°32.188	N 25°12.193			N 25°40.316	N 25°40.089	N 25°40.051	N 25°09.140	N 25°09.150	N 25°09.136
	E 51°29.537	E 51°30.580	E 51°30.205	E 50°45.881			E 51°32.743	E 51°32.549	E 51°32.568	E 51°37.054	E 51°37.072	E 51°37.073
Temperature (°C)	24.99	24.91	24.97	26.59	26.60	26.60	23.92	23.82	23.92	26.97	26.79	26.97
Conductivity (mS/cm)	63.89	63.89	63.88	82.87	81.92	82.86	63.82	63.88	63.83	59.64	58.03	59.26
TDS (g/l)	41.53	41.53	41.52	53.87	53.87	53.78	41.48	41.52	41.49	38.01	37.72	38.52
Salinity (ppt)	43.18	43.19	43.17	58.2*	58.22*	58.22*	43.15	43.20	43.16	38.49	38.67	39.60
Ph	8.08	8.14	8.15	8.23	8.24	8.23	8.32	8.24	8.33	7.92	7.95	8.07
*near a desalination plant												

Appendix A-2: Parametric and non-parametric tests for physical parameter (Temperature, pH, and salinity)

A-2-1- Temperature

A-2-1-1 Normality and Kruskal-Wallis tests of Temperature in seawater in summer seasons across sites

Tests of Normality

Site	Kolmogorov-Smirnov ^a			Shapiro-Wilk		
	Statistic	df	Sig.	Statistic	df	Sig.
Temperature Summer seasons						
Simaima	.296	6	.108	.751	6	.020
Umm Bab	.313	6	.068	.769	6	.030
Al Khor	.313	6	.066	.847	6	.149
Al Wakra	.229	6	.200 [*]	.946	6	.707

*. This is a lower bound of the true significance.

a. Lilliefors Significance Correction

Hypothesis Test Summary

	Null Hypothesis	Test	Sig. ^{a,b}	Decision
1	The distribution of Temperature Summer seasons is the same across categories of Site.	Independent-Samples Kruskal-Wallis Test	.045	Reject the null hypothesis.

a. The significance level is .050.

b. Asymptotic significance is displayed.

Pairwise Comparisons of Site

Sample 1-Sample 2	Test Statistic	Std. Error	Std. Test Statistic	Sig.	Adj. Sig. ^a
Simaima-Umm Bab	-.667-	4.082	-.163-	.870	1.000
Simaima-Al Wakra	-4.333-	4.082	-1.062-	.288	1.000
Simaima-Al Khor	-10.333-	4.082	-2.532-	.011	.068
Umm Bab-Al Wakra	-3.667-	4.082	-.898-	.369	1.000
Umm Bab-Al Khor	-9.667-	4.082	-2.368-	.018	.107
Al Wakra-Al Khor	6.000	4.082	1.470	.142	.849

Each row tests the null hypothesis that the Sample 1 and Sample 2 distributions are the same.

Asymptotic significances (2-sided tests) are displayed. The significance level is .050.

a. Significance values have been adjusted by the Bonferroni correction for multiple tests.

A-2-1-2 Normality and One-way ANOVA tests of Temperature in seawater in winter seasons across sites

Tests of Normality

Site	Kolmogorov-Smirnov ^a			Shapiro-Wilk		
	Statistic	df	Sig.	Statistic	df	Sig.
Temperature Winter seasons						
Simaima	.314	6	.066	.722	6	.011
Umm Bab	.311	6	.071	.769	6	.030
Al Khor	.306	6	.083	.796	6	.054
Al Wakra	.299	6	.101	.737	6	.015

a. Lilliefors Significance Correction

Hypothesis Test Summary

	Null Hypothesis	Test	Sig. ^{a,b}	Decision
1	The distribution of Temperature Winter seasons is the same across categories of Site.	Independent-Samples Kruskal-Wallis Test	.106	Retain the null hypothesis.

a. The significance level is .050.

b. Asymptotic significance is displayed.

Independent-Samples Kruskal-Wallis Test Summary

Total N	24
Test Statistic	6.113 ^{a,b}
Degree Of Freedom	3
Asymptotic Sig.(2-sided test)	.106

a. The test statistic is adjusted for ties.

b. Multiple comparisons are not performed because the overall test does not show significant differences across samples.

A-2-2- Salinity

A-2-2-1 Normality and Kruskal-Wallis tests of Salinity in seawater in summer seasons across sites

Site	Kolmogorov-Smirnov ^a			Shapiro-Wilk			
	Statistic	df	Sig.	Statistic	df	Sig.	
Salinity Summer seasons	Simaima	.368	6	.011	.747	6	.018
	Umm Bab	.338	6	.030	.854	6	.169
	Al Khor	.191	6	.200 [*]	.970	6	.895
	Al Wakra	.199	6	.200 [*]	.943	6	.684

*. This is a lower bound of the true significance.

a. Lilliefors Significance Correction

Hypothesis Test Summary

	Null Hypothesis	Test	Sig. ^{a,b}	Decision
1	The distribution of Salinity Summer seasons is the same across categories of Site.	Independent-Samples Kruskal-Wallis Test	.001	Reject the null hypothesis.

a. The significance level is .050.

b. Asymptotic significance is displayed.

Independent-Samples Kruskal-Wallis Test Summary

Total N	24
Test Statistic	15.740 ^a
Degree Of Freedom	3
Asymptotic Sig.(2-sided test)	.001

a. The test statistic is adjusted for ties.

Pairwise Comparisons of Site

Sample 1-Sample 2	Test Statistic	Std. Error	Std. Test Statistic	Sig.	Adj. Sig. ^a
Al Wakra-Simaima	1.500	4.082	.367	.713	1.000
Al Wakra-Al Khor	6.500	4.082	1.592	.111	.668
Al Wakra-Umm Bab	14.667	4.082	3.593	<.001	.002
Simaima-Al Khor	-5.000-	4.082	-1.225-	.221	1.000
Simaima-Umm Bab	-13.167-	4.082	-3.225-	.001	.008
Al Khor-Umm Bab	8.167	4.082	2.000	.045	.273

Each row tests the null hypothesis that the Sample 1 and Sample 2 distributions are the same.

Asymptotic significances (2-sided tests) are displayed. The significance level is .050.

a. Significance values have been adjusted by the Bonferroni correction for multiple tests.

A-2-2-2 Normality and Kruskal-Wallis tests of salinity in seawater in winter seasons across sites

Site	Kolmogorov-Smirnov ^a			Shapiro-Wilk			
	Statistic	df	Sig.	Statistic	df	Sig.	
Salinity Winter seasons	Simaima	.314	6	.066	.723	6	.011
	Umm Bab	.312	6	.068	.835	6	.118
	Al Khor	.404	6	.003	.638	6	.001
	Al Wakra	.177	6	.200 [*]	.950	6	.738

*. This is a lower bound of the true significance.

a. Lilliefors Significance Correction

Independent-Samples Kruskal-Wallis Test Summary

Total N	24
Test Statistic	17.716 ^a
Degree Of Freedom	3
Asymptotic Sig.(2-sided test)	<.001

a. The test statistic is adjusted for ties.

Hypothesis Test Summary

	Null Hypothesis	Test	Sig. ^{a,b}	Decision
1	The distribution of Salinity Winter seasons is the same across categories of Site.	Independent-Samples Kruskal-Wallis Test	<.001	Reject the null hypothesis.

a. The significance level is .050.

b. Asymptotic significance is displayed.

Pairwise Comparisons of Site

Sample 1-Sample 2	Test Statistic	Std. Error	Std. Test Statistic	Sig.	Adj. Sig. ^a
Al Wakra-Simaima	9.000	4.076	2.208	.027	.164
Al Wakra-Al Khor	9.917	4.076	2.433	.015	.090
Al Wakra-Umm Bab	17.083	4.076	4.191	<.001	.000
Simaima-Al Khor	-.917-	4.076	-.225-	.822	1.000
Simaima-Umm Bab	-8.083-	4.076	-1.983-	.047	.284
Al Khor-Umm Bab	7.167	4.076	1.758	.079	.472

Each row tests the null hypothesis that the Sample 1 and Sample 2 distributions are the same.

Asymptotic significances (2-sided tests) are displayed. The significance level is .050.

a. Significance values have been adjusted by the Bonferroni correction for multiple tests.

A-2-3- The pH

A-2-3-1 Normality and Kruskal-Wallis tests of pH in seawater in summer seasons across sites

Tests of Normality						
Site	Kolmogorov-Smirnov ^a			Shapiro-Wilk		
	Statistic	df	Sig.	Statistic	df	Sig.
pH Summer seasons						
Simaima	.236	6	.200*	.905	6	.406
Umm Bab	.292	6	.121	.862	6	.196
Al Khor	.248	6	.200*	.863	6	.199
Al Wakra	.392	6	.004	.701	6	.006

*. This is a lower bound of the true significance.

a. Lilliefors Significance Correction

Independent-Samples Kruskal-Wallis Test Summary	
Total N	24
Test Statistic	16.248 ^a
Degree Of Freedom	3
Asymptotic Sig. (2-sided test)	.001

a. The test statistic is adjusted for ties.

Pairwise Comparisons of Site					
Sample 1-Sample 2	Test Statistic	Std. Error	Std. Test Statistic	Sig.	Adj. Sig. ^a
Umm Bab-Al Wakra	-8.083-	4.060	-1.991-	.046	.279
Umm Bab-Simaima	12.750	4.060	3.140	.002	.010
Umm Bab-Al Khor	-15.167-	4.060	-3.735-	<.001	.001
Al Wakra-Simaima	4.667	4.060	1.149	.250	1.000
Al Wakra-Al Khor	7.083	4.060	1.745	.081	.486
Simaima-Al Khor	-2.417-	4.060	-.595-	.552	1.000

Each row tests the null hypothesis that the Sample 1 and Sample 2 distributions are the same.

Asymptotic significances (2-sided tests) are displayed. The significance level is .050.

a. Significance values have been adjusted by the Bonferroni correction for multiple tests.

Hypothesis Test Summary

	Null Hypothesis	Test	Sig. ^{a,b}	Decision
1	The distribution of pH Summer seasons is the same across categories of Site.	Independent-Samples Kruskal-Wallis Test	.001	Reject the null hypothesis.

a. The significance level is .050.

b. Asymptotic significance is displayed.

A-2-3-2 Normality and Kruskal-Wallis tests of pH in seawater in winter seasons across sites

Tests of Normality						
Site	Kolmogorov-Smirnov ^a			Shapiro-Wilk		
	Statistic	df	Sig.	Statistic	df	Sig.
pH Winter seasons						
Simaima	.293	6	.118	.777	6	.036
Umm Bab	.319	6	.056	.692	6	.005
Al Khor	.192	6	.200*	.869	6	.223
Al Wakra	.264	6	.200*	.859	6	.185

*. This is a lower bound of the true significance.

a. Lilliefors Significance Correction

Independent-Samples Kruskal-Wallis Test Summary

Total N	24
Test Statistic	1.931 ^{a,b}
Degree Of Freedom	3
Asymptotic Sig. (2-sided test)	.587

a. The test statistic is adjusted for ties.

b. Multiple comparisons are not performed because the overall test does not show significant differences across samples.

Hypothesis Test Summary

	Null Hypothesis	Test	Sig. ^{a,b}	Decision
1	The distribution of pH Winter seasons is the same across categories of Site.	Independent-Samples Kruskal-Wallis Test	.587	Retain the null hypothesis.

a. The significance level is .050.

b. Asymptotic significance is displayed.

Appendix B: Seasonal concentrations of TOC in seawater, marine sediment, and core sediment from four different sites

Appendix B-1: Concentrations of TOC

B-1-1- TOC in Surface seawater samples

TOC in Surface water (µg/kg)						
		R1	R2	R3	Mean	STD
Simaisma	Round 1	28480.00	28450.00	27950.00	28293.33	297.71
	Round 2	28220.00	28260.00	28520.00	28333.33	162.89
	Round 3	28230.00	26790.00	26680.00	27233.33	864.89
	Round 4	27240.00	27490.00	27450.00	27393.33	134.29
Umm Bab	Round 1	30890.00	29710.00	30190.00	30263.33	593.41
	Round 2	29000.00	30390.00	29190.00	29526.67	753.68
	Round 3	29170.00	29010.00	29520.00	29233.33	260.83
	Round 4	28670.00	29070.00	29170.00	28970.00	264.58
Al Khor	Round 1	28800.00	28130.00	26580.00	27836.67	1138.70
	Round 2	29350.00	29030.00	29940.00	29440.00	461.63
	Round 3	28150.00	28130.00	27970.00	28083.33	98.66
	Round 4	27330.00	27810.00	28050.00	27730.00	366.61
Al Wakra	Round 1	29000.00	29900.00	27730.00	28876.67	1090.24
	Round 2	30070.00	29930.00	30280.00	30093.33	176.16
	Round 3	26320.00	25610.00	27400.00	26443.33	901.35
	Round 4	28760.00	28600.00	27340.00	28233.33	777.77

B-1-2- TOC in Surface marine sediment samples

TOC in Surface Marine Sediment (µg/kg)						
		R1	R2	R3	Mean	STD
Simaisma	Round 1	1730.63	1208.63	1182.40	1373.89	309.23
	Round 2	438.86	1554.82	2447.57	1480.41	1006.42
	Round 3	893.98	997.95	1732.43	1208.12	457.03
	Round 4	1483.71	1837.99	831.10	1384.27	510.76
Umm Bab	Round 1	2003.66	2480.85	2048.00	2177.50	263.64
	Round 2	2127.37	2437.61	1992.47	2185.81	228.25
	Round 3	1230.37	1439.48	1066.14	1245.33	187.12
	Round 4	1518.92	619.75	855.03	997.90	466.30
Al Khor	Round 1	1679.47	1716.29	2255.97	1883.91	322.74
	Round 2	1930.06	2427.87	1984.38	2114.10	273.08
	Round 3	2899.31	2203.34	1345.51	2149.38	778.30
	Round 4	2408.05	1553.00	1720.35	1893.80	453.14
Al Wakra	Round 1	1004.52	1064.07	1146.49	1071.69	71.29
	Round 2	1083.66	970.23	1090.80	1048.23	67.64
	Round 3	910.70	685.04	2074.52	1223.42	745.66
	Round 4	748.96	751.18	880.90	793.68	75.55

Appendix B-2: Parametric and Non-parametric tests for TOC

B-2-1 - TOC in Surface seawater

B-2-1-1- Normality and Kruskal-Wallis tests of TOC in seawater in summer seasons across sites

Tests of Normality							
Site	Kolmogorov-Smirnov ^a			Shapiro-Wilk			Sig.
	Statistic	df	Sig.	Statistic	df	Sig.	
TOC in Seawater-Summer	Simaisma	.257	6	.200 [*]	.809	6	.070
	Umm Bab	.189	6	.200 [*]	.940	6	.659
	Al Khor	.339	6	.030	.808	6	.069
	Al Wakra	.149	6	.200 [*]	.973	6	.909

*. This is a lower bound of the true significance.

a. Lilliefors Significance Correction

Independent-Samples Kruskal-Wallis Test Summary	
Total N	24
Test Statistic	11.178 ^a
Degree Of Freedom	3
Asymptotic Sig.(2-sided test)	.011

a. The test statistic is adjusted for ties.

Pairwise Comparisons of Site					
Sample 1-Sample 2	Test Statistic	Std. Error	Std. Test Statistic	Sig.	Adj. Sig. ^a
Al Wakra-Simaisma	.667	4.082	.163	.870	1.000
Al Wakra-Al Khor	1.000	4.082	.245	.806	1.000
Al Wakra-Umm Bab	11.667	4.082	2.858	.004	.026
Simaisma-Al Khor	-.333-	4.082	-.082-	.935	1.000
Simaisma-Umm Bab	-11.000-	4.082	-2.695-	.007	.042
Al Khor-Umm Bab	10.667	4.082	2.613	.009	.054

Each row tests the null hypothesis that the Sample 1 and Sample 2 distributions are the same.

Asymptotic significances (2-sided tests) are displayed. The significance level is .050.

a. Significance values have been adjusted by the Bonferroni correction for multiple tests.

Hypothesis Test Summary

	Null Hypothesis	Test	Sig. ^{a,b}	Decision
1	The distribution of TOC in Seawater-Summer is the same across categories of Site.	Independent-Samples Kruskal-Wallis Test	.011	Reject the null hypothesis.

a. The significance level is .050.

b. Asymptotic significance is displayed.

B-2-1-1- Normality and Kruskal-Wallis tests of TOC in seawater in winter seasons across sites

Tests of Normality							
Site	Kolmogorov-Smirnov ^a			Shapiro-Wilk			Sig.
	Statistic	df	Sig.	Statistic	df	Sig.	
TOC in Seawater-Winter	Simaisma	.259	6	.200 [*]	.879	6	.263
	Umm Bab	.373	6	.009	.784	6	.042
	Al Khor	.202	6	.200 [*]	.950	6	.739
	Al Wakra	.250	6	.200 [*]	.896	6	.351

*. This is a lower bound of the true significance.

a. Lilliefors Significance Correction

Independent-Samples Kruskal-Wallis Test Summary	
Total N	24
Test Statistic	8.113 ^a
Degree Of Freedom	3
Asymptotic Sig.(2-sided test)	.044

a. The test statistic is adjusted for ties.

Pairwise Comparisons of Site					
Sample 1-Sample 2	Test Statistic	Std. Error	Std. Test Statistic	Sig.	Adj. Sig. ^a
Simaisma-Al Khor	-5.500-	4.082	-1.347-	.178	1.000
Simaisma-Al Wakra	-9.167-	4.082	-2.245-	.025	.148
Simaisma-Umm Bab	-10.667-	4.082	-2.613-	.009	.054
Al Khor-Al Wakra	-3.667-	4.082	-.898-	.369	1.000
Al Khor-Umm Bab	5.167	4.082	1.266	.206	1.000
Al Wakra-Umm Bab	1.500	4.082	.367	.713	1.000

Each row tests the null hypothesis that the Sample 1 and Sample 2 distributions are the same.

Asymptotic significances (2-sided tests) are displayed. The significance level is .050.

a. Significance values have been adjusted by the Bonferroni correction for multiple tests.

Hypothesis Test Summary

	Null Hypothesis	Test	Sig. ^{a,b}	Decision
1	The distribution of TOC in Seawater-Winter is the same across categories of Site.	Independent-Samples Kruskal-Wallis Test	.044	Reject the null hypothesis.

a. The significance level is .050.

b. Asymptotic significance is displayed.

B-2-2- TOC in Surface marine sediment

B-2-2-1- Normality and Kruskal-Wallis tests of TOC in surface marine sediment in summer seasons across sites

Site	Kolmogorov-Smirnov ^a			Shapiro-Wilk		
	Statistic	df	Sig.	Statistic	df	Sig.
TOC in Surface Sediment-Summer						
Simaisma	.257	6	.200 [*]	.858	6	.184
Umm Bab	.202	6	.200 [*]	.935	6	.616
Al Khor	.207	6	.200 [*]	.950	6	.740
Al Wakra	.334	6	.035	.805	6	.065

*. This is a lower bound of the true significance.

a. Lilliefors Significance Correction

Total N	24
Test Statistic	8.860 ^a
Degree Of Freedom	3
Asymptotic Sig. (2-sided test)	.031

a. The test statistic is adjusted for ties.

Sample 1-Sample 2	Test Statistic	Std. Error	Std. Test Statistic	Sig.	Adj. Sig. ^a
Al Wakra-Simaisma	2.500	4.082	.612	.540	1.000
Al Wakra-Umm Bab	8.000	4.082	1.960	.050	.300
Al Wakra-Al Khor	10.833	4.082	2.654	.008	.048
Simaisma-Umm Bab	-5.500-	4.082	-1.347-	.178	1.000
Simaisma-Al Khor	-8.333-	4.082	-2.041-	.041	.247
Umm Bab-Al Khor	-2.833-	4.082	-.694-	.488	1.000

Each row tests the null hypothesis that the Sample 1 and Sample 2 distributions are the same.

Asymptotic significances (2-sided tests) are displayed. The significance level is .050.

a. Significance values have been adjusted by the Bonferroni correction for multiple tests.

Hypothesis Test Summary

	Null Hypothesis	Test	Sig. ^{a,b}	Decision
1	The distribution of TOC in Surface Sediment-Summer is the same across categories of Site.	Independent-Samples Kruskal-Wallis Test	.031	Reject the null hypothesis.

a. The significance level is .050.

b. Asymptotic significance is displayed.

B-2-2-2- Normality and One-way ANOVA for TOC in surface marine sediment in winter seasons across sites

Site	Kolmogorov-Smirnov ^a			Shapiro-Wilk		
	Statistic	df	Sig.	Statistic	df	Sig.
TOC in Surface Sediment-Winter						
Simaisma	.195	6	.200 [*]	.975	6	.925
Umm Bab	.209	6	.200 [*]	.926	6	.546
Al Khor	.205	6	.200 [*]	.914	6	.462
Al Wakra	.199	6	.200 [*]	.875	6	.247

*. This is a lower bound of the true significance.

a. Lilliefors Significance Correction

ANOVA

TOC in Surface Sediment-Winter

	Sum of Squares	df	Mean Square	F	Sig.
Between Groups	3609770.790	3	1203256.930	4.033	.021
Within Groups	5967556.146	20	298377.807		
Total	9577326.936	23			

Multiple Comparisons

Dependent Variable: TOC in Surface Sediment-Winter

Tukey HSD

(I) Site	(J) Site	Mean Difference (I-J)	Std. Error	Sig.	95% Confidence Interval	
					Lower Bound	Upper Bound
Simaisma	Umm Bab	-159.51667-	315.37164	.957	-1042.2218-	723.1884
	Al Khor	-571.61000-	315.37164	.297	-1454.3151-	311.0951
	Al Wakra	511.38667	315.37164	.390	-371.3184-	1394.0918
Umm Bab	Simaisma	159.51667	315.37164	.957	-723.1884-	1042.2218
	Al Khor	-412.09333-	315.37164	.569	-1294.7984-	470.6118
	Al Wakra	670.90333	315.37164	.179	-211.8018-	1553.6084
Al Khor	Simaisma	571.61000	315.37164	.297	-311.0951-	1454.3151
	Umm Bab	412.09333	315.37164	.569	-470.6118-	1294.7984
	Al Wakra	1082.99667[*]	315.37164	.013	200.2916	1965.7018
Al Wakra	Simaisma	-511.38667-	315.37164	.390	-1394.0918-	371.3184
	Umm Bab	-670.90333-	315.37164	.179	-1553.6084-	211.8018
	Al Khor	-1082.99667[*]	315.37164	.013	-1965.7018-	-200.2916-

*. The mean difference is significant at the 0.05 level.

Appendix C: Grain size

C-1-Grain size measurement for Surface marine sediment

Sample Name	Sand	Silt	Clay	Sedimentr type
1703-SIM-SED-1	60.97	34.55	4.48	Silty Sand
1703-SIM-SED-2	84.26	14.88	0.86	Silty Sand
1703-SIM-SED-3	63.94	33.65	2.41	Silty Sand
1703-UmB-SED-1	99.32	0.68	0	sand
1703-UmB-SED-2	96.41	3.59	0	sand
1703-UmB-SED-3	100	0		sand
1703-Alkhore-SED-1	72.5	24.78	2.72	Silty Sand
1703-Alkhore-SED-2	62.05	35.4	2.55	Silty Sand
1703-Alkhore-SED-3	73.86	23.63	2.51	Silty Sand
1703-AIWakra-SED-1	98.88	1.12	0	sand
1703-AIWakra-SED-2	96.81	3.17	0.02	sand
1703-AIWakra-SED-3	97.67	2.33	0	sand
1712-SIM-SED-1	50.36	46.27	3.37	Silty Sand
1712-SIM-SED-2	45.95	50.45	3.6	Sandy Silt
1712-SIM-SED-3	79.56	19.5	0.94	Silty Sand
1712-UmB-SED-1	99.44	0.56	0	Sand
1712-UmB-SED-2	100	0	0	Sand
1712-UmB-SED-3	97.84	2.16	0	Sand
1712-Alkhore-SED-1	81.92	17.03	1.05	Silty Sand
1712-Alkhore-SED-2	60.71	36.95	2.34	Silty Sand
1712-Alkhore-SED-3	74.42	24.03	1.55	Silty Sand
1712-AIWakra-SED-1	99.92	0.8	0	Sand
1712-AIWakra-SED-2	99.94	0.06	0	Sand
1712-AIWakra-SED-3	99.88	0.12	0	Sand

1805-SIM-SED-1	89.28	10.46	0.26	Silty Sand
1805-SIM-SED-2	95.23	4.77	0	Sand
1805-SIM-SED-3	58.82	38.04	3.14	Silty Sand
1805-UmB-SED-1	96.68	3.32	0	Sand
1805-UmB-SED-2	100	0	0	Sand
1805-UmB-SED-3	100	0	0	Sand
1805-Alkhore-SED-1	71.38	26.06	2.56	Silty Sand
1805-Alkhore-SED-2	61.89	33.77	4.34	Silty Sand
1805-Alkhore-SED-3	97.81	2.19	0	Sand
1805-AIWakra-SED-1	100	0	0	Sand
1805-AIWakra-SED-2	99.85	0.15	0	Sand
1805-AIWakra-SED-3	98.1	1.9	0	Sand
1811-SIM-SED-1	79.85	19.43	0.11	Silty Sand
1811-SIM-SED-2	95.59	4.33	0	Sand
1811-SIM-SED-3	98.41	1.59	0	Sand
1811-UmB-SED-1	99.2	0.8	0	Sand
1811-UmB-SED-2	100	0	0	Sand
1811-UmB-SED-3	100	0	0	Sand
1811-Alkhore-SED-1	84.13	14.61	0.06	Silty Sand
1811-Alkhore-SED-2	86.79	13.01	0.06	Silty Sand
1811-Alkhore-SED-3	87.68	11.91	0.03	Silty Sand
1811-AIWakra-SED-1	100	0	0	Sand
1811-AIWakra-SED-2	99.84	0.16	0	Sand
1811-AIWakra-SED-3	100	0	0	Sand

C-2: Statistical analysis for grain size in surface sediment

Tests of Normality

Site	Kolmogorov-Smirnov ^a			Shapiro-Wilk			
	Statistic	df	Sig.	Statistic	df	Sig.	
Sand1	Simaisma	.264	6	.200 [*]	.859	6	.187
	Umm Bab	.300	6	.098	.737	6	.015
	Al Khor	.315	6	.064	.815	6	.080
	Al Wakra	.182	6	.200 [*]	.944	6	.692
Silt1	Simaisma	.277	6	.167	.864	6	.205
	Umm Bab	.300	6	.098	.737	6	.015
	Al Khor	.311	6	.072	.838	6	.125
	Al Wakra	.183	6	.200 [*]	.943	6	.687
Clay1	Simaisma	.213	6	.200 [*]	.925	6	.541
	Umm Bab	.	6	.	.	6	.
	Al Khor	.351	6	.020	.840	6	.130
	Al Wakra	.492	6	<.001	.496	6	<.001

*. This is a lower bound of the true significance.

a. Lilliefors Significance Correction

Hypothesis Test Summary

	Null Hypothesis	Test	Sig. ^{a,b}	Decision
1	The distribution of Sand1 is the same across categories of Site.	Independent-Samples Kruskal-Wallis Test	.001	Reject the null hypothesis.
2	The distribution of Silt1 is the same across categories of Site.	Independent-Samples Kruskal-Wallis Test	.001	Reject the null hypothesis.
3	The distribution of Clay1 is the same across categories of Site.	Independent-Samples Kruskal-Wallis Test	.003	Reject the null hypothesis.

a. The significance level is .050.

b. Asymptotic significance is displayed.

Sites Vs Sand%

Pairwise Comparisons of Site

Sample 1-Sample 2	Test Statistic	Std. Error	Std. Test Statistic	Sig.	Adj. Sig. ^a
Simaisma-Al Khor	-1.000-	4.074	-.245-	.806	1.000
Simaisma-Al Wakra	-11.417-	4.074	-2.803-	.005	.030
Simaisma-Umm Bab	-12.250-	4.074	-3.007-	.003	.016
Al Khor-Al Wakra	-10.417-	4.074	-2.557-	.011	.063
Al Khor-Umm Bab	11.250	4.074	2.762	.006	.035
Al Wakra-Umm Bab	.833	4.074	.205	.838	1.000

Each row tests the null hypothesis that the Sample 1 and Sample 2 distributions are the same.

Asymptotic significances (2-sided tests) are displayed. The significance level is .050.

a. Significance values have been adjusted by the Bonferroni correction for multiple tests.

Sites Vs Clay%

Pairwise Comparisons of Site

Sample 1-Sample 2	Test Statistic	Std. Error	Std. Test Statistic	Sig.	Adj. Sig. ^a
Umm Bab-Al Wakra	-1.167-	3.746	-.311-	.755	1.000
Umm Bab-Simaisma	9.833	3.746	2.625	.009	.052
Umm Bab-Al Khor	-11.000-	3.746	-2.937-	.003	.020
Al Wakra-Simaisma	8.667	3.746	2.314	.021	.124
Al Wakra-Al Khor	9.833	3.746	2.625	.009	.052
Simaisma-Al Khor	-1.167-	3.746	-.311-	.755	1.000

Each row tests the null hypothesis that the Sample 1 and Sample 2 distributions are the same.

Asymptotic significances (2-sided tests) are displayed. The significance level is .050.

a. Significance values have been adjusted by the Bonferroni correction for multiple tests.

Sites Vs Silt%

Pairwise Comparisons of Site

Sample 1-Sample 2	Test Statistic	Std. Error	Std. Test Statistic	Sig.	Adj. Sig. ^a
Umm Bab-Al Wakra	-.833-	4.074	-.205-	.838	1.000
Umm Bab-Al Khor	-11.417-	4.074	-2.803-	.005	.030
Umm Bab-Simaisma	12.083	4.074	2.966	.003	.018
Al Wakra-Al Khor	10.583	4.074	2.598	.009	.056
Al Wakra-Simaisma	11.250	4.074	2.762	.006	.035
Al Khor-Simaisma	.667	4.074	.164	.870	1.000

Each row tests the null hypothesis that the Sample 1 and Sample 2 distributions are the same.

Asymptotic significances (2-sided tests) are displayed. The significance level is .050.

a. Significance values have been adjusted by the Bonferroni correction for multiple tests.

Appendix D: TPHs results for the two-years sampling

Appendix D-1: Concentration of TPHs in seawater, sediment, and pearl oyster tissues

D-1-1- TPHs of surface seawater

TPHs in Surface water (µg/kg)						
		R1	R2	R3	Mean	STD
Simaisma	Round 1	205.783	252.441	43.745	167.323	109.535
	Round 2	20.069	19.000	15.070	18.046	2.633
	Round 3	28.870	12.250	13.622	18.247	9.225
	Round 4	5.326	4.478	2.739	4.181	1.319
Umm Bab	Round 1	161.022	187.260	147.567	165.283	20.187
	Round 2	17.787	18.548	21.607	19.314	2.022
	Round 3	19.371	27.102	18.147	21.540	4.855
	Round 4	1.901	3.835	6.561	4.099	2.341
Al Khor	Round 1	169.538	485.311	160.470	271.773	184.985
	Round 2	106.200	75.327	39.819	73.782	33.217
	Round 3	6.467	9.193	20.793	12.151	7.607
	Round 4	1.230	1.000	1.261	1.164	0.143
Al Wakra	Round 1	150.348	166.429	174.714	163.830	12.389
	Round 2	59.810	73.704	54.536	62.683	9.902
	Round 3	14.730	17.011	60.172	30.638	25.603
	Round 4	0.161	0.449	8.932	3.181	4.983

D-1-2- TPHs of Surface marine sediment

TPHs in Surface Marine Sediment (µg/kg)						
		R1	R2	R3	Mean	STD
Simaisma	Round 1	180.556	156.650	71.845	136.350	57.1278
	Round 2	286.422	134.731	567.729	329.627	219.7088
	Round 3	235.000	235.000	235.000	235.000	0
	Round 4	51.731	1210.432	11.978	424.714	680.7422
Umm Bab	Round 1	436.275	509.804	452.381	466.153	38.65098
	Round 2	521.351	156.219	1069.583	582.384	459.7304
	Round 3	28.741	235.000	337.624	200.455	157.3121
	Round 4	455.446	27.955	30.687	171.363	246.0268
Al Khor	Round 1	339.806	731.068	368.526	479.800	218.0778
	Round 2	289.710	1302.094	212.151	601.318	608.1269
	Round 3	1973.267	1615.842	1666.337	1751.815	193.4379
	Round 4	1030.086	425.765	235.000	563.617	415.0815
Al Wakra	Round 1	184.466	15.842	24.752	75.020	94.88767
	Round 2	142.572	114.770	115.884	124.409	15.73976
	Round 3	1577.228	542.574	315.842	811.881	672.4347
	Round 4	34.623	9.406	235.000	93.010	123.6121

D-1-3- TPHs of core sediment

TPHs in Core Sediment (µg/kg)						
		R1	R2	R3	Mean	STD
Simaisma	5cm	453	997	564	671.33	287.44
	10cm	644	1022	601	755.67	231.65
	15cm	935	979	392	768.67	326.94
	20cm	318	440	867	541.67	288.27
	25cm	778	286	233	432.33	300.53
	30cm	583	39.75	404	342.25	276.84
Umm Bab	5cm	0	162	0	54.00	93.53
	10cm	330	384	0	238.00	207.87
	15cm	94	0	261	118.33	132.19
	20cm	0	0	111	37.00	64.09
	25cm	0	38	0	12.67	21.94
	30cm	0	11	45	18.67	23.46
Al Khor	5cm	325.164	0	41.2594	122.14	177.03
	10cm	0	0	23.364	7.79	13.49
	15cm	0	0	193.742	64.58	111.86
	20cm	0	0	254.857	84.95	147.14
	25cm	0	227.804	342.325	190.04	174.26
	30cm	69.842	249.253	312.348	210.48	125.82
Al Wakra	5cm	0	797	521	439.33	404.73
	10cm	486	128	49	221.00	232.87
	15cm	310	327	94	243.67	129.89
	20cm	0	39	313	117.33	170.57
	25cm	32	34	613	226.33	334.86
	30cm	92	269	46	135.67	117.74

D-1-4-TPHs of pearl oyster tissues

TPHs in oyster tissues (µg/kg)						
		R1	R2	R3	Mean	STD
Simaisma	Round 1	4660.000	3480.000	7810.000	5316.667	2238.444
	Round 2	4330.000	2330.000	1070.000	2576.667	1643.938
	Round 3	235.000	1110.000	2520.000	1288.333	1152.891
	Round 4	5590.000	6620.000	7790.000	6666.667	1100.742
Umm Bab	Round 1	5320.000	5430.000	1260.000	4003.333	2376.433
	Round 2	6480.000	4310.000	6388.000	5726.000	1227.154
	Round 3	1930.000	2950.000	2930.000	2603.333	583.210
	Round 4	5350.000	9430.000	5150.000	6643.333	2415.395
Al Khor	Round 1	2450.000	2750.000	3510.000	2903.333	546.382
	Round 2	1110.000	1310.000	1452.000	1290.667	171.818
	Round 3	1560.000	1890.000	2190.000	1880.000	315.119
	Round 4	10140.000	2400.000	2710.000	5083.333	4381.944
Al Wakra	Round 1	3450.000	1780.000	3160.000	2796.667	892.319
	Round 2	235.000	235.000	1430.000	633.333	689.934
	Round 3	1970.000	2640.000	1030.000	1880.000	808.764
	Round 4	3240.000	2700.000	3480.000	3140.000	399.500

Appendix D-2: Statistical analysis for TPHs

D-2-1 - TPHs in Surface seawater

D-2-1-1- TPHs in Surface seawater in summer

Tests of Normality

Site	Kolmogorov-Smirnov ^a			Shapiro-Wilk		
	Statistic	df	Sig.	Statistic	df	Sig.
TPHs Seawater-Summer						
Simaima	.343	6	.026	.765	6	.028
Umm Bab	.297	6	.106	.795	6	.053
Al Khor	.274	6	.180	.786	6	.044
Al Wakra	.260	6	.200*	.827	6	.101

*. This is a lower bound of the true significance.

a. Lilliefors Significance Correction

Hypothesis Test Summary

	Null Hypothesis	Test	Sig. ^{a,b}	Decision
1	The distribution of TPHs Seawater-Summer is the same across categories of Site.	Independent-Samples Kruskal-Wallis Test	.994	Retain the null hypothesis.

a. The significance level is .050.

b. Asymptotic significance is displayed.

Independent-Samples Kruskal-Wallis Test Summary

Total N	24
Test Statistic	.080 ^{a,b}
Degree Of Freedom	3
Asymptotic Sig.(2-sided test)	.994

a. The test statistic is adjusted for ties.

b. Multiple comparisons are not performed because the overall test does not show significant differences across samples.

D-2-1-2- TPHs in Surface seawater in winter

Tests of Normality

Site	Kolmogorov-Smirnov ^a			Shapiro-Wilk		
	Statistic	df	Sig.	Statistic	df	Sig.
TPHs Seawater-Winter						
Simaima	.270	6	.194	.846	6	.145
Umm Bab	.261	6	.200*	.864	6	.203
Al Khor	.290	6	.126	.834	6	.116
Al Wakra	.264	6	.200*	.832	6	.111

*. This is a lower bound of the true significance.

a. Lilliefors Significance Correction

ANOVA

TPHs Seawater-Winter

	Sum of Squares	df	Mean Square	F	Sig.
Between Groups	3459.324	3	1153.108	1.411	.269
Within Groups	16345.761	20	817.288		
Total	19805.085	23			

D-2-2- TPHs in Surface coastal sediment

D-2-2-1- TPHs in Surface sediment in summer

Tests of Normality

Site	Kolmogorov-Smirnov ^a			Shapiro-Wilk		
	Statistic	df	Sig.	Statistic	df	Sig.
TPHs Sediment-Summer						
Simaima	.276	6	.171	.821	6	.090
Umm Bab	.219	6	.200 [*]	.907	6	.418
Al Khor	.256	6	.200 [*]	.858	6	.182
Al Wakra	.267	6	.200 [*]	.776	6	.035

*. This is a lower bound of the true significance.

a. Lilliefors Significance Correction

Hypothesis Test Summary

	Null Hypothesis	Test	Sig. ^{a,b}	Decision
1	The distribution of TPHs Sediment-Summer is the same across categories of Site.	Independent-Samples Kruskal-Wallis Test	.018	Reject the null hypothesis.

a. The significance level is .050.

b. Asymptotic significance is displayed.

Independent-Samples Kruskal-Wallis Test Summary

Total N	24
Test Statistic	10.086 ^a
Degree Of Freedom	3
Asymptotic Sig.(2-sided test)	.018

a. The test statistic is adjusted for ties.

Pairwise Comparisons of Site

Sample 1-Sample 2	Test Statistic	Std. Error	Std. Test Statistic	Sig.	Adj. Sig. ^a
Simaima-Al Wakra	-3.083-	4.074	-.757-	.449	1.000
Simaima-Umm Bab	-5.500-	4.074	-1.350-	.177	1.000
Simaima-Al Khor	-12.417-	4.074	-3.048-	.002	.014
Al Wakra-Umm Bab	2.417	4.074	.593	.553	1.000
Al Wakra-Al Khor	9.333	4.074	2.291	.022	.132
Umm Bab-Al Khor	-6.917-	4.074	-1.698-	.090	.537

Each row tests the null hypothesis that the Sample 1 and Sample 2 distributions are the same.

Asymptotic significances (2-sided tests) are displayed. The significance level is .050.

a. Significance values have been adjusted by the Bonferroni correction for multiple tests.

D-2-2-2- TPHs in Surface sediment in winter

Tests of Normality

Site	Kolmogorov-Smirnov ^a			Shapiro-Wilk		
	Statistic	df	Sig.	Statistic	df	Sig.
TPHs Sediment-Winter						
Simaima	.246	6	.200 [*]	.832	6	.112
Umm Bab	.210	6	.200 [*]	.872	6	.235
Al Khor	.298	6	.103	.806	6	.067
Al Wakra	.197	6	.200 [*]	.946	6	.709

*. This is a lower bound of the true significance.

a. Lilliefors Significance Correction

ANOVA

TPHs Sediment-Winter

	Sum of Squares	df	Mean Square	F	Sig.
Between Groups	679270.035	3	226423.345	1.534	.237
Within Groups	2952986.738	20	147649.337		
Total	3632256.773	23			

D-2-3- TPHs in sediment Core

D-2-3-1- TPHs vs Sites

Tests of Normality

Site	Kolmogorov-Smirnov ^a			Shapiro-Wilk		
	Statistic	df	Sig.	Statistic	df	Sig.
TPHs in sediment cores						
Simaima	.119	18	.200	.953	18	.468
Umm Bab	.277	18	<.001	.706	18	<.001
Al Khor	.258	18	.003	.771	18	<.001
Al Wakra	.221	18	.020	.855	18	.010

*. This is a lower bound of the true significance.

a. Lilliefors Significance Correction

Hypothesis Test Summary

	Null Hypothesis	Test	Sig. ^{a,b}	Decision
1	The distribution of TPHs in sediment cores is the same across categories of Site.	Independent-Samples Kruskal-Wallis Test	<.001	Reject the null hypothesis.

a. The significance level is .050.

b. Asymptotic significance is displayed.

Pairwise Comparisons of Site

Sample 1-Sample 2	Test Statistic	Std. Error	Std. Test Statistic	Sig.	Adj. Sig. ^a
Umm Bab-Al Khor	-2.917-	6.912	-.422-	.673	1.000
Umm Bab-Al Wakra	-15.167-	6.912	-2.194-	.028	.169
Umm Bab-Simaima	35.361	6.912	5.116	<.001	.000
Al Khor-Al Wakra	-12.250-	6.912	-1.772-	.076	.458
Al Khor-Simaima	32.444	6.912	4.694	<.001	.000
Al Wakra-Simaima	20.194	6.912	2.922	.003	.021

Each row tests the null hypothesis that the Sample 1 and Sample 2 distributions are the same.

Asymptotic significances (2-sided tests) are displayed. The significance level is .050.

a. Significance values have been adjusted by the Bonferroni correction for multiple tests.

D-2-3-1- TPHs vs Depths

Tests of Normality

Depth	Kolmogorov-Smirnov ^a			Shapiro-Wilk		
	Statistic	df	Sig.	Statistic	df	Sig.
TPHs in sediment cores						
5cm	.208	12	.160	.868	12	.062
10cm	.204	12	.181	.868	12	.061
15cm	.224	12	.098	.802	12	.010
20cm	.230	12	.080	.776	12	.005
25cm	.254	12	.031	.818	12	.015
30cm	.259	12	.025	.853	12	.040

a. Lilliefors Significance Correction

Hypothesis Test Summary

	Null Hypothesis	Test	Sig. ^{a,b}	Decision
1	The distribution of TPHs in sediment cores is the same across categories of Depth.	Independent-Samples Kruskal-Wallis Test	.877	Retain the null hypothesis.

a. The significance level is .050.

b. Asymptotic significance is displayed.

D-2-4- TPHs in Oyster tissues

D-2-4-1- TPHs in oyster tissues in summer

Tests of Normality

Site	Kolmogorov-Smirnov ^a			Shapiro-Wilk		
	Statistic	df	Sig.	Statistic	df	Sig.
TPHs Oyster-Summer						
Simaima	.142	6	.200 [*]	.957	6	.795
Umm Bab	.248	6	.200 [*]	.886	6	.296
Al Khor	.135	6	.200 [*]	.974	6	.918
Al Wakra	.157	6	.200 [*]	.964	6	.848

*. This is a lower bound of the true significance.

a. Lilliefors Significance Correction

ANOVA

TPHs Oyster-Summer

	Sum of Squares	df	Mean Square	F	Sig.
Between Groups	5286661.458	3	1762220.486	.603	.621
Within Groups	58463487.50	20	2923174.375		
Total	63750148.96	23			

D-2-4-2- TPHs in oyster tissues in winter

Tests of Normality

Site	Kolmogorov-Smirnov ^a			Shapiro-Wilk		
	Statistic	df	Sig.	Statistic	df	Sig.
TPHs Oyster-Winter						
Simaima	.147	6	.200 [*]	.965	6	.857
Umm Bab	.268	6	.200 [*]	.885	6	.295
Al Khor	.388	6	.005	.657	6	.002
Al Wakra	.211	6	.200 [*]	.865	6	.208

*. This is a lower bound of the true significance.

a. Lilliefors Significance Correction

Hypothesis Test Summary

	Null Hypothesis	Test	Sig. ^{a,b}	Decision
1	The distribution of TPHs Oyster-Winter is the same across categories of Site.	Independent-Samples Kruskal-Wallis Test	.040	Reject the null hypothesis.

a. The significance level is .050.

b. Asymptotic significance is displayed.

Independent-Samples Kruskal-Wallis Test Summary

Total N	24
Test Statistic	8.290 ^a
Degree Of Freedom	3
Asymptotic Sig. (2-sided test)	.040

a. The test statistic is adjusted for ties.

Pairwise Comparisons of Site

Sample 1-Sample 2	Test Statistic	Std. Error	Std. Test Statistic	Sig.	Adj. Sig. ^a
Al Wakra-Al Khor	2.667	4.082	.653	.514	1.000
Al Wakra-Simaima	7.167	4.082	1.756	.079	.475
Al Wakra-Umm Bab	10.833	4.082	2.654	.008	.048
Al Khor-Simaima	4.500	4.082	1.103	.270	1.000
Al Khor-Umm Bab	8.167	4.082	2.001	.045	.272
Simaima-Umm Bab	-3.667-	4.082	-.898-	.369	1.000

Each row tests the null hypothesis that the Sample 1 and Sample 2 distributions are the same.

Asymptotic significances (2-sided tests) are displayed. The significance level is .050.

a. Significance values have been adjusted by the Bonferroni correction for multiple tests.

Appendix E: PAHs results for the two-years sampling

Appendix E-1: Concentration of PAHs in sediment, and pearl oyster tissues samples

E-1-1: PAHs in Surface Marine Sediment

PAHs in Surface Marine Sediment (µg/kg)						
Site		R1	R2	R3	Mean	STD
Simaisma	Round 1	23.88	21.70	24.19	23.26	1.36
Simaisma	Round 2	23.07	0.00	18.204	20.64	3.44
Simaisma	Round 3	52.176	7.574	0	29.88	28.19
Simaisma	Round 4	12.87	36.23	10.21	19.77	14.32
Umm Bab	Round 1	17.80	30.19	25.8	24.60	6.28
Umm Bab	Round 2	27.30	25.29	26.584	26.39	1.02
Umm Bab	Round 3	1.675	6.212	4.862	4.25	2.33
Umm Bab	Round 4	28.42	13.87	16.73	19.67	7.71
Al Khor	Round 1	28.52	36.81	44.86	36.73	8.17
Al Khor	Round 2	13.18	24.42	13.71	17.10	6.34
Al Khor	Round 3	12.094	15.435	17.493	15.01	2.72
Al Khor	Round 4	38.88	43.36	16.34	32.86	14.48
Al Wakra	Round 1	35.73	33.18	25.82	31.58	5.15
Al Wakra	Round 2	14.73	9.48	15.293	13.17	3.21
Al Wakra	Round 3	21.034	25.99	3.354	23.51	3.50
Al Wakra	Round 4	21.56	9.49	9.57	13.54	6.95

E-1-3: PAHs in Oyster tissues

PAHs in oyster tissues (µg/kg)						
Site		R1	R2	R3	Mean	STD
Simaisma	Round 1	184.36	322.33	782.63	429.77	313.27
Simaisma	Round 2	365.83	202.85	156.47	241.72	109.96
Simaisma	Round 3	8.20	50.18	66.72	41.70	30.17
Simaisma	Round 4	711.59	543.91	589.45	614.98	86.71
Umm Bab	Round 1	529.17	404.06	598.57	510.60	98.58
Umm Bab	Round 2	75.10	171.61	165.77	137.49	54.11
Umm Bab	Round 3	1.00	8.83	53.46	31.15	28.30
Umm Bab	Round 4	1307.74	2018.87	564.46	1297.02	727.26
Al Khor	Round 1	576.93	1080.94	122.75	593.54	479.31
Al Khor	Round 2	417.17	217.86	490.97	375.33	141.28
Al Khor	Round 3	21.17	6.28	50.26	25.90	22.37
Al Khor	Round 4	4505.16	865.97	876.97	2082.70	2097.92
Al Wakra	Round 1	1107.74	1541.14	1348.21	1332.36	217.13
Al Wakra	Round 2	220.30	363.01	407.90	330.40	97.96
Al Wakra	Round 3	200.54	242.12	57.31	166.66	96.95
Al Wakra	Round 4	737.32	2815.65	3179.12	2244.03	1317.44

E-1-2: PAHs in Core Sediment

PAHs in Core Sediment (µg/kg)						
Site		R1	R2	R3	Mean	STD
Simaisma	5cm	4.97	2.01	22.8395	9.94	11.269
Simaisma	10cm	3.72	3.99	0.7915	2.83	1.773
Simaisma	15cm	3.81	0.61	0.3275	1.58	1.937
Simaisma	20cm	3.30	1.35	1.3335	2.00	1.133
Simaisma	25cm	2.90	1.26	0.7285	1.63	1.132
Simaisma	30cm	5.39	0.88	1.4075	2.56	2.464
Umm Bab	5cm	1.49	3.00	2.2755	2.26	0.759
Umm Bab	10cm	1.27	1.85	2.9695	2.03	0.865
Umm Bab	15cm	0.69	1.01	0.5635	0.76	0.229
Umm Bab	20cm	1.84	0.96	3.7535	2.18	1.431
Umm Bab	25cm	2.13	0.50	3.5045	2.05	1.502
Umm Bab	30cm	7.09	0.76	2.9895	3.61	3.208
Al Khor	5cm	2.17	3.45	3.8685	3.16	0.883
Al Khor	10cm	1.84	2.56	3.9525	2.79	1.072
Al Khor	15cm	2.17	1.38	4.2045	2.59	1.457
Al Khor	20cm	2.47	9.32	1.1675	4.32	4.383
Al Khor	25cm	0.02	4.88	4.7395	3.21	2.766
Al Khor	30cm	1.37	4.10	1.3795	2.28	1.576
Al Wakra	5cm	95.01	77.42	95.26	89.23	10.230
Al Wakra	10cm	167.07	29.21	290.72	162.33	130.821
Al Wakra	15cm	152.33	111.54	73.75	112.54	39.303
Al Wakra	20cm	65.40	97.54	53.77	72.24	22.672
Al Wakra	25cm	111.98	52.16	21.56	61.90	45.990
Al Wakra	30cm	77.47	71.34	28.42	59.08	26.726

Appendix E-2: Statistical analysis for PAHs

E-2-1: PAHs in Surface Marine Sediment

E-2-1-1: summer

Tests of Normality

Site	Kolmogorov-Smirnov ^a			Shapiro-Wilk		
	Statistic	df	Sig.	Statistic	df	Sig.
PAHs Sediment-Winter						
Simaima	.276	6	.172	.916	6	.477
Umm Bab	.254	6	.200 [*]	.896	6	.350
Al Khor	.239	6	.200 [*]	.918	6	.494
Al Wakra	.226	6	.200 [*]	.885	6	.293

*. This is a lower bound of the true significance.

a. Lilliefors Significance Correction

ANOVA

TPHs Sediment-Winter

	Sum of Squares	df	Mean Square	F	Sig.
Between Groups	679270.035	3	226423.345	1.534	.237
Within Groups	2952986.738	20	147649.337		
Total	3632256.773	23			

E-2-1-2: winter

Tests of Normality

Site	Kolmogorov-Smirnov ^a			Shapiro-Wilk		
	Statistic	df	Sig.	Statistic	df	Sig.
PAHs Sediment-Winter						
Simaima	.138	6	.200 [*]	.986	6	.978
Umm Bab	.310	6	.073	.820	6	.088
Al Khor	.244	6	.200 [*]	.847	6	.149
Al Wakra	.283	6	.145	.828	6	.103

*. This is a lower bound of the true significance.

a. Lilliefors Significance Correction

ANOVA

PAHs Sediment-Winter

	Sum of Squares	df	Mean Square	F	Sig.
Between Groups	458.285	3	152.762	.795	.511
Within Groups	3841.035	20	192.052		
Total	4299.319	23			

E-2-2: PAHs in Core Sediment

E-2-2-1: PAHs vs Sites

Tests of Normality

Site	Kolmogorov-Smirnov ^a			Shapiro-Wilk		
	Statistic	df	Sig.	Statistic	df	Sig.
PAHs in sediment cores						
Simaima	.294	18	<.001	.530	18	<.001
Umm Bab	.154	18	.200 [*]	.840	18	.006
Al Khor	.150	18	.200 [*]	.878	18	.024
Al Wakra	.214	18	.028	.827	18	.004

*. This is a lower bound of the true significance.

a. Lilliefors Significance Correction

Hypothesis Test Summary

	Null Hypothesis	Test	Sig. ^{a,b}	Decision
1	The distribution of PAHs in sediment cores is the same across categories of Site.	Independent-Samples Kruskal-Wallis Test	<.001	Reject the null hypothesis.

a. The significance level is .050.

b. Asymptotic significance is displayed.

Pairwise Comparisons of Site

Sample 1-Sample 2	Test Statistic	Std. Error	Std. Test Statistic	Sig.	Adj. Sig. ^a
Umm Bab-Simaima	3.139	6.976	.450	.653	1.000
Umm Bab-Al Khor	-8.833-	6.976	-1.266-	.205	1.000
Umm Bab-Al Wakra	-39.917-	6.976	-5.722-	<.001	.000
Simaima-Al Khor	-5.694-	6.976	-.816-	.414	1.000
Simaima-Al Wakra	-36.778-	6.976	-5.272-	<.001	.000
Al Khor-Al Wakra	-31.083-	6.976	-4.456-	<.001	.000

Each row tests the null hypothesis that the Sample 1 and Sample 2 distributions are the same.

Asymptotic significances (2-sided tests) are displayed. The significance level is .050.

a. Significance values have been adjusted by the Bonferroni correction for multiple tests.

E-2-2-1: PAHs vs Depth

Tests of Normality

Depth	Kolmogorov-Smirnov ^a			Shapiro-Wilk		
	Statistic	df	Sig.	Statistic	df	Sig.
PAHs in sediment cores						
5cm	.374	12	<.001	.648	12	<.001
10cm	.413	12	<.001	.532	12	<.001
15cm	.433	12	<.001	.620	12	<.001
20cm	.379	12	<.001	.650	12	<.001
25cm	.394	12	<.001	.579	12	<.001
30cm	.387	12	<.001	.622	12	<.001

a. Lilliefors Significance Correction

Hypothesis Test Summary

	Null Hypothesis	Test	Sig. ^{a,b}	Decision
1	The distribution of PAHs in sediment cores is the same across categories of Depth.	Independent-Samples Kruskal-Wallis Test	.737	Retain the null hypothesis.

a. The significance level is .050.

b. Asymptotic significance is displayed.

E-2-3: PAHs in Oyster tissues

E-2-3-1 summer

Tests of Normality

Site	Kolmogorov-Smirnov ^a			Shapiro-Wilk		
	Statistic	df	Sig.	Statistic	df	Sig.
PAHs Oyster-Summer						
Simaima	.237	6	.200*	.806	6	.067
Umm Bab	.279	6	.157	.828	6	.103
Al Khor	.333	6	.036	.772	6	.032
Al Wakra	.280	6	.153	.850	6	.159

*. This is a lower bound of the true significance.

a. Lilliefors Significance Correction

Hypothesis Test Summary

	Null Hypothesis	Test	Sig. ^{a,b}	Decision
1	The distribution of PAHs Oyster-Summer is the same across categories of Site.	Independent-Samples Kruskal-Wallis Test	.261	Retain the null hypothesis.

a. The significance level is .050.

b. Asymptotic significance is displayed.

E-2-3-2 winter

Tests of Normality

Site	Kolmogorov-Smirnov ^a			Shapiro-Wilk		
	Statistic	df	Sig.	Statistic	df	Sig.
PAHs Oyster-Winter						
Simaima	.198	6	.200*	.933	6	.602
Umm Bab	.257	6	.200*	.836	6	.121
Al Khor	.419	6	.001	.645	6	.002
Al Wakra	.326	6	.046	.764	6	.027

*. This is a lower bound of the true significance.

a. Lilliefors Significance Correction

Hypothesis Test Summary

	Null Hypothesis	Test	Sig. ^{a,b}	Decision
1	The distribution of PAHs Oyster-Winter is the same across categories of Site.	Independent-Samples Kruskal-Wallis Test	.483	Retain the null hypothesis.

a. The significance level is .050.

b. Asymptotic significance is displayed.

Appendix F Trace metals results for two years sampling

Appendix F-1: Trace metals concentration in seawater, sediment, and pearl oyster tissues samples

F-1-1: Trace metals concentration in seawater samples

		Metals in Seawater (ug/L)																		
Site	Round	Cd						Cr						Cu						
		R1	R2	R3	Mean	STD	CRMrecovery (%)	R1	R2	R3	Mean	STD	CRMrecovery (%)	R1	R2	R3	Mean	STD	CRMrecovery (%)	
Simaisma	Round 1	0.20000	0.52000	1.02000	0.580	0.413	104.58	3.13	3.07	0.00053	2.067	1.790	95.21	0.000135	0.000135	0.000135	0.000	0.000	109.61	
	Round 2	0.94592	0.75999	0.68218	0.796	0.136	107.83	0.00053	0.00053	0.00053	0.001	0.000	100.02	0.000135	1.1913601	0.8963039	0.696	0.620	86.81	
	Round 3	0.00009	0.00009	0.00009	0.000	0.000	96.6	0.2985415	0.3536287	0.3057338	0.319	0.030	100.4	1.9449507	2.5680158	0.231914	1.582	1.210	94.0	
	Round 4	0.00009	0.00009	0.00009	0.000	0.000	100.1	0.00053	0.00053	0.00053	0.001	0.000	100.3	2.8104563	0.6551818	2.924132	2.130	1.278	98.1	
Umm Bab	Round 1	0.80000	0.19000	0.39000	0.460	0.311	104.58	0.00053	2.72	2.72	1.814	1.570	95.21	0.000135	0.000135	0.000135	0.000	0.000	109.61	
	Round 2	0.48461	0.59730	0.27027	0.451	0.166	107.83	0.00053	0.00053	0.00053	0.001	0.000	100.02	0.000135	4.9053852	2.8118696	2.572	2.461	86.81	
	Round 3	0.00009	0.00009	0.00009	0.000	0.000	96.6	0.1436817	0.0685669	0.2585217	0.157	0.096	100.4	2.2148294	0.195606	1.4090389	1.273	1.016	94.0	
	Round 4	0.00009	0.06874	0.00009	0.023	0.040	100.1	0.00053	0.00053	0.00053	0.001	0.000	100.3	0.000135	0.000135	0.000135	0.000	0.000	98.1	
Al Khor	Round 1	0.23000	0.00009	3.89000	1.373	2.183	104.58	3.16	2.77	0.00053	1.977	1.723	95.21	0.000135	0.000135	0.000135	0.000	0.000	109.61	
	Round 2	0.22641	0.04156	0.03285	0.100	0.109	107.83	0.00053	0.10953	0.00053	0.00053	0.001	0.000	100.02	1.875255	2.1042186	2.0907589	2.023	0.128	86.81
	Round 3	0.00009	0.00009	0.00009	0.000	0.000	96.6	0.2875582	0.6671133	0.3121594	0.422	0.212	100.4	9.0350903	1.5384164	0.000135	3.525	4.834	94.0	
	Round 4	0.00009	0.04438	0.15481	0.066	0.080	100.1	0.00053	0.00053	0.00053	0.001	0.000	100.3	0.000135	0.000135	2.5193828	0.840	1.454	98.1	
Al Wakra	Round 1	1.59000	0.23000	0.59000	0.803	0.705	104.58	0.00053	3.11	0.00053	1.037	1.795	95.21	0.000135	0.000135	0.000135	0.000	0.000	109.61	
	Round 2	0.01015	0.00009	0.00009	0.003	0.006	107.83	0.00053	0.00053	0.00053	0.001	0.000	100.02	3.0200371	1.9450806	0.371186	1.779	1.332	86.81	
	Round 3	0.00009	0.00009	0.00009	0.000	0.000	96.6	0.3882484	0.361755	0.2624443	0.337	0.066	100.4	1.2645821	0.7076522	2.4069829	1.460	0.866	94.0	
	Round 4	0.00009	0.00009	0.00009	0.000	0.000	100.1	10.558732	0.00053	0.00053	3.520	6.096	100.3	0.3394269	0.000135	0.6907423	0.343	0.345	98.1	

Ni						Pb						Zn					
R1	R2	R3	Mean	STD	CRMrecovery (%)	R1	R2	R3	Mean	STD	CRMrecovery (%)	R1	R2	R3	Mean	STD	CRMrecovery (%)
14.88	14.58	0.002985	9.821	8.504	98.58	0.000595	1.94	12.93	4.957	6.973	89.27	2.550	0.001	3.240	1.930	1.706	105.71
0.3852817	0.4086185	0.002985	0.266	0.228	101.03	0.000595	0.000595	0.000595	0.001	0.000	104.09	2.982	1.802	1.804	2.196	0.680	105.68
1.0734809	0.7441683	0.1836062	0.667	0.450	105.8	0.000595	0.000595	0.000595	0.001	0.000	98.5	0.048	0.143	0.001	0.064	0.073	95.6
0.1878935	1.3012377	0.7529456	0.747	0.557	95.9	0.000595	0.000595	0.782325	0.261	0.451	105.8	5.035	2.362	6.654	4.684	2.168	102.8
0.002985	13.97	13.83	9.268	8.024	98.58	5.83	0.000595	0.000595	1.944	3.366	89.27	4.260	1.190	0.001	1.817	2.198	105.71
0.002985	0.0758082	3.2607204	1.113	1.860	101.03	0.000595	0.000595	0.000595	0.001	0.000	104.09	3.133	3.794	2.406	3.111	0.694	105.68
1.2055675	1.407397	1.2216121	1.278	0.112	105.8	0.000595	0.000595	0.000595	0.001	0.000	98.5	0.193	0.128	0.001	0.107	0.098	95.6
0.9784212	0.5047156	0.4838302	0.656	0.280	95.9	0.000595	0.000595	0.000595	0.001	0.000	105.8	2.092	1.573	0.512	1.392	0.805	102.8
14.25	14.55	0.002985	9.601	8.313	98.58	0.000595	0.000595	168.28	56.094	97.156	89.27	0.001	2.650	10.390	4.347	5.399	105.71
0.2279924	0.002985	0.002985	0.078	0.130	101.03	0.000595	0.000595	0.000595	0.001	0.000	104.09	4.068	1.310	1.733	2.370	1.485	105.68
0.7786291	0.8761558	0.5680006	0.741	0.157	105.8	0.000595	0.000595	0.000595	0.001	0.000	98.5	2.414	3.185	0.001	1.867	1.661	95.6
0.002985	0.9837764	0.085493	0.357	0.544	95.9	0.000595	0.000595	1.9615759	0.654	1.132	105.8	0.702	1.461	1.705	1.289	0.523	102.8
0.002985	15.06	0.002985	5.022	8.693	98.58	26.35	0.000595	12.6	12.984	13.179	89.27	4.330	0.001	5.710	3.347	2.979	105.71
0.0303248	0.1389154	0.002985	0.057	0.072	101.03	0.000595	0.000595	0.000595	0.001	0.000	104.09	5.209	5.766	2.461	4.479	1.769	105.68
0.6040563	1.0895258	1.4583939	1.051	0.428	105.8	0.000595	0.000595	0.000595	0.001	0.000	98.5	0.001	0.001	0.542	0.181	0.313	95.6
0.7457656	0.3664487	1.7049035	0.939	0.690	95.9	0.1937261	0.000595	0.000595	0.065	0.112	105.8	0.001	1.608	0.748	0.785	0.805	102.8

F-1-2: Trace metals concentration in surface marine sediment samples

Metals in Marine Sediment (ug/g dry weight)																			
Site	Round	Cd					Cr						Cu						
		R1	R2	R3	Mean	STD	CRMrecovery	R1	R2	R3	Mean	STD	CRMrecovery	R1	R2	R3	Mean	STD	CRMrecovery
Simaisma	Round 1	0.000085	0.000085	0.000085	0.000085	0	101.72	13.30	4.62	3.02	6.981	5.535	101.10	3.48952	0.00014	0.00014	1.163	2.015	94.88
	Round 2	0.000085	0.000085	0.000085	0.000085	0	107.3	2.34	10.76	6.63	6.579	4.208	90.9	1.91767	4.85492	2.81426	3.196	1.505	94.8
	Round 3	0.023257653	0.018348943	0.013975056	0.0185272	0.0046439	113.4	3.03	6.69	8.34	6.022	2.717	100.9	1.61058	1.19230	2.66657	1.823	0.760	92.3
	Round 4	0.000085	0.000085	0.000085	0.000085	0	107.5	6.67	3.25	2.37	4.097	2.272	102.5	2.48000	1.04000	1.02000	1.513	0.837	102.7
Umm Bab	Round 1	0.000085	0.000085	0.000085	0.000085	0	101.72	7.52	5.81	6.42	6.584	0.866	101.10	0.24381	3.18152	0.56725	1.331	1.611	94.88
	Round 2	0.000085	0.000085	0.000085	0.000085	0	107.3	5.51	5.73	4.56	5.264	0.623	90.9	3.04938	4.65334	3.82795	3.844	0.802	94.8
	Round 3	0.014073667	0.077412599	0.000085	0.0305238	0.0412049	113.4	3.68	9.71	22.94	12.111	9.849	100.9	1.98001	4.20700	3.49553	3.228	1.137	92.3
	Round 4	0.03	0.000085	0.08	0.036695	0.040376	107.5	8.19	20.32	11.64	13.383	6.250	102.5	1.62000	6.01000	4.93000	4.187	2.287	102.7
Al Khor	Round 1	0.000085	0.000085	0.000085	0.000085	0	101.72	5.00	7.55	8.28	6.944	1.720	101.10	0.00014	0.44469	0.61367	0.353	0.317	94.88
	Round 2	0.000085	0.056348058	0.064207166	0.0402134	0.0349737	107.3	4.94	6.74	4.77	5.485	1.093	90.9	3.00876	3.83450	3.72426	3.523	0.448	94.8
	Round 3	0.023519132	0.082369493	0.014233652	0.0400408	0.0369506	113.4	7.32	6.79	7.70	7.271	0.455	100.9	4.24777	3.32588	1.77097	3.115	1.252	92.3
	Round 4	0.05	0.05	0.000085	0.0333617	0.0288184	107.5	5.3	4	5.19	4.830	0.721	102.5	3.11000	1.99000	2.30000	2.467	0.578	102.7
Al Wakra	Round 1	0.000085	0.000085	0.000085	0.000085	0	101.72	18.33	10.41	9.87	12.870	4.736	101.10	0.36333	0.00479	0.00014	0.123	0.208	94.88
	Round 2	0.000085	0.000085	0.200858483	0.0670095	0.1159166	107.3	10.62	15.02	17.71	14.449	3.578	90.9	2.44024	4.16843	3.60872	3.406	0.882	94.8
	Round 3	0.048987951	0.135969823	0.061385508	0.0821144	0.0470503	113.4	11.62	16.06	12.12	13.268	2.434	100.9	2.73669	3.06695	2.40541	2.736	0.331	92.3
	Round 4	0.000085	0.000085	0.01	0.00339	0.0057244	107.5	8.13	8.13	9.13	8.463	0.577	102.5	2.07000	1.84000	1.40000	1.770	0.340	102.7

Ni						Pb						Zn					
R1	R2	R3	Mean	STD	CRMrecovery	R1	R2	R3	Mean	STD	CRMrecovery	R1	R2	R3	Mean	STD	CRMrecovery
9.68	3.92	4.26	5.951	3.230	108.44	0.00060	0.00060	0.00060	0.000595	0.000000	107.32	9.95	9.92	4.12	8.001	3.358	108.23
2.28	7.53	3.05	4.286	2.837	104.7	0.00060	1.34	0.00060	0.447624	0.774277	104.6	6.01	7.51	9.95	7.822	1.989	97.8
2.39	2.74	5.66	3.598	1.798	95.2	0.00060	0.00060	0.00060	0.000595	0.000000	102.2	4.20	2.51	5.31	4.005	1.412	96.9
6.28	4.35	2.43	4.353	1.925	102.7	0.00060	0.00060	0.00060	0.000595	0.000000	92.8	7.45	5.68	4.33	5.820	1.565	100
4.84	5.16	3.99	4.664	0.603	108.44	0.00060	0.00060	0.00060	0.000595	0.000000	107.32	6.15	7.34	5.33	6.269	1.011	108.23
3.63	3.79	3.48	3.633	0.152	104.7	0.12	2.63	2.68	1.808989	1.465559	104.6	11.58	8.59	6.74	8.970	2.443	97.8
3.00	5.19	4.11	4.097	1.094	95.2	0.00060	0.00060	0.00060	0.000595	0.000000	102.2	2.87	6.00	2.36	3.744	1.974	96.9
6.36	9.48	6.63	7.490	1.729	102.7	0.00060	1.09	0.52	0.536865	0.544898	92.8	5.71	10.04	7.23	7.660	2.197	100
4.71	7.32	7.43	6.488	1.542	108.44	0.00060	0.00060	0.00060	0.000595	0.000000	107.32	6.58	10.70	10.99	9.422	2.463	108.23
4.33	5.82	5.34	5.162	0.757	104.7	0.00060	1.86	2.05	1.303040	1.132019	104.6	7.12	14.32	11.61	11.016	3.638	97.8
5.74	4.69	3.73	4.721	1.008	95.2	0.00060	0.00060	0.00060	0.000595	0.000000	102.2	7.55	7.83	3.31	6.228	2.534	96.9
5.93	4.53	5.49	5.317	0.716	102.7	0.00060	0.00060	0.00060	0.000595	0.000000	92.8	11.36	7.87	5.31	8.180	3.037	100
4.88	4.10	4.04	4.340	0.469	108.44	0.00060	0.00060	0.00060	0.000595	0.000000	107.32	5.51	5.35	4.58	5.147	0.498	108.23
3.26	3.78	3.95	3.662	0.362	104.7	0.00060	3.66	6.40	3.354307	3.210812	104.6	15.26	8.81	20.70	14.923	5.950	97.8
3.38	4.13	3.09	3.530	0.537	95.2	0.00060	0.00060	0.00060	0.000595	0.000000	102.2	3.72	3.41	2.18	3.102	0.817	96.9
3.61	4.12	3.85	3.860	0.255	102.7	0.00060	0.00060	0.00060	0.000595	0.000000	92.8	6.32	7.64	7.84	7.267	0.826	100

F-1-3: Trace metals concentration in pearl oyster tissues samples

Metals in Oyster tissues (ug/g dry weight)																			
Site	Round	Cd						Cr						Cu					
		R1	R2	R3	Mean	STD	CRMrecovery	R1	R2	R3	Mean	STD	CRMrecovery	R1	R2	R3	Mean	STD	CRMrecovery
Simaisma	Round 1	7.08	5.49	5.39	5.986	0.950	111.81	1.15	1.65	0.13	0.979	0.774	101.10	4.11	8.44	1.80	4.783	3.373	101.02
	Round 2	9.22	6.22	10.62	8.688	2.246	105.4	1.18	0.82	1.16	1.056	0.200	104.0	5.39	3.59	3.38	4.120	1.106	87.9
	Round 3	13.07	7.06	10.88	10.337	3.040	107.1	0.53	1.57	1.81	1.304	0.682	116.5	9.44	5.18	6.84	7.153	2.151	105.6
	Round 4	5.38	9.68	3.1	6.053	3.341	99.3	1.42	1.1	1.09	1.203	0.188	83.97	10.6	10.51	5.09	8.733	3.156	100.29
Umm Bab	Round 1	4.26	9.98	5.48	6.572	3.013	111.81	0.69	0.86	0.01	0.519	0.448	101.10	7.57	4.37	1.81	4.582	2.886	101.02
	Round 2	4.78	7.39	5.46	5.878	1.355	105.4	0.89	0.86	1.48	1.077	0.347	104.0	4.25	5.69	7.95	5.964	1.867	87.9
	Round 3	7.62	9.84	7.50	8.320	1.321	107.1	0.46	1.45	0.03	0.648	0.727	116.5	4.37	5.77	6.75	5.629	1.195	105.6
	Round 4	3.62	2.93	3.57	3.373	0.385	99.3	0.53	1.47	1.61	1.203	0.587	83.97	5.58	6.68	5.33	5.863	0.718	100.29
Al Khor	Round 1	8.56	9.04	5.79	7.797	1.752	111.81	0.21	0.78	1.19	0.727	0.493	101.10	2.91	2.72	2.05	2.559	0.452	101.02
	Round 2	7.61	4.72	5.22	5.851	1.547	105.4	2.68	2.16	1.13	1.989	0.790	104.0	5.98	5.14	3.60	4.909	1.205	87.9
	Round 3	9.02	6.85	4.75	6.873	2.134	107.1	0.58	0.95	0.65	0.727	0.194	116.5	6.50	6.30	7.29	6.696	0.523	105.6
	Round 4	3.21	3.75	3.94	3.633	0.379	99.3	0.85	1.15	0.91	0.970	0.159	83.97	6.07	4.77	4.94	5.260	0.707	100.29
Al Wakra	Round 1	5.36	6.74	9.84	7.313	2.296	111.81	4.07	2.95	0.78	2.600	1.672	101.10	2.99	7.60	3.26	4.618	2.590	101.02
	Round 2	6.99	6.44	9.09	7.505	1.399	105.4	1.50	1.67	1.80	1.652	0.151	104.0	6.55	7.43	7.17	7.048	0.456	87.9
	Round 3	5.17	6.44	5.28	5.628	0.704	107.1	2.02	0.76	1.41	1.399	0.632	116.5	8.28	7.21	8.22	7.905	0.599	105.6
	Round 4	5.19	6.49	3.88	5.187	1.305	99.3	2.14	1.75	1.7	1.863	0.241	83.97	9.14	10.02	11.4	10.187	1.139	100.29

Ni						Pb						Zn					
R1	R2	R3	Mean	STD	CRMrecovery	R1	R2	R3	Mean	STD	CRMrecovery	R1	R2	R3	Mean	STD	CRMrecovery
1.61	1.89	1.27	1.590	0.311	123.51	0.0006	0.0006	0.0006	0.001	0.000	107.32	1803.25	2287.60	1214.86	1768.571	537.209	104.57
0.67	0.75	0.92	0.781	0.126	90.7	0.7084	0.9000	0.3974	0.669	0.254	109.8	1250.95	965.79	1776.61	1331.116	411.308	100.2
1.12	0.99	1.06	1.056	0.067	104.2	0.0006	0.0006	0.0006	0.001	0.000	102.6	1910.29	1425.87	1666.08	1667.417	242.214	112.1
0.99	0.89	1.41	1.097	0.276	95.71	0.1400	0.0006	0.1100	0.084	0.073	105.77	1019.86	1420.22	338.58	926.220	546.866	95.39
1.42	2.46	1.13	1.672	0.699	123.51	0.0006	0.0006	0.0006	0.001	0.000	107.32	1689.96	2464.87	1193.99	1782.942	640.519	104.57
1.39	1.46	1.90	1.581	0.277	90.7	0.8277	0.7888	0.5567	0.724	0.146	109.8	696.21	1580.72	939.40	1072.109	456.944	100.2
1.23	1.30	1.14	1.223	0.079	104.2	0.0006	0.0006	0.7803	0.260	0.450	102.6	1445.28	2147.62	1561.57	1718.155	376.444	112.1
1.3	1.54	2.01	1.617	0.361	95.71	0.0006	0.3400	0.1200	0.154	0.172	105.77	497.21	512.96	645.28	551.817	81.324	95.39
1.13	1.87	1.02	1.341	0.463	123.51	0.0006	0.0006	0.0006	0.001	0.000	107.32	1415.86	2243.04	907.63	1522.177	674.019	104.57
1.38	6.73	1.13	3.078	3.165	90.7	0.8166	0.7127	0.3338	0.621	0.254	109.8	1841.18	942.34	1066.92	1283.481	486.984	100.2
0.91	0.99	0.84	0.916	0.074	104.2	0.4017	0.0006	0.7945	0.399	0.397	102.6	1746.63	1660.81	981.68	1463.039	419.074	112.1
4.56	1.25	1.06	2.290	1.968	95.71	0.4700	0.3000	0.0700	0.280	0.201	105.77	690.9	1299.18	1057.15	1015.743	306.247	95.39
1.52	2.31	2.23	2.020	0.435	123.51	0.0006	0.0006	0.0006	0.001	0.000	107.32	1054.96	2013.70	2239.40	1769.355	628.892	104.57
0.85	1.04	1.16	1.017	0.154	90.7	0.0006	0.5585	0.1969	0.252	0.283	109.8	2114.52	2430.83	3569.30	2704.883	765.129	100.2
0.92	0.96	1.04	0.976	0.061	104.2	0.0006	0.0006	0.0006	0.001	0.000	102.6	2799.51	3201.09	2420.94	2807.178	390.132	112.1
1.93	1.79	2.65	2.123	0.461	95.71	0.4500	0.5000	0.5800	0.510	0.066	105.77	2792.68	2981.58	1771.72	2515.327	650.872	95.39

Appendix F-2: Statistical analysis of trace metals in seawater, sediment, and pearl oyster tissues samples

F-2-1: Trace metals in seawater samples

In summer:

Tests of Normality

Site	Kolmogorov-Smirnov ^a				Shapiro-Wilk		
	Statistic	df	Sig.	Statistic	df	Sig.	
Cd in Seawater-Summer	Simaima	.260	6	.200 [*]	.794	6	.051
	Umm Bab	.264	6	.200 [*]	.803	6	.063
	Al Khor	.448	6	<.001	.533	6	<.001
	Al Wakra	.275	6	.176	.744	6	.018
Cr in Seawater-Summer	Simaima	.381	6	.007	.711	6	.008
	Umm Bab	.372	6	.009	.691	6	.005
	Al Khor	.316	6	.082	.789	6	.047
	Al Wakra	.432	6	<.001	.623	6	<.001
Cu in Seawater-Summer	Simaima	.352	6	.019	.736	6	.015
	Umm Bab	.346	6	.024	.750	6	.020
	Al Khor	.358	6	.016	.596	6	<.001
	Al Wakra	.274	6	.178	.822	6	.092
Ni in Seawater-Summer	Simaima	.381	6	.007	.687	6	.004
	Umm Bab	.385	6	.006	.700	6	.006
	Al Khor	.392	6	.004	.681	6	.004
	Al Wakra	.438	6	<.001	.586	6	<.001
Pb in Seawater-Summer	Simaima	.375	6	.009	.585	6	<.001
	Umm Bab	.492	6	<.001	.496	6	<.001
	Al Khor	.492	6	<.001	.496	6	<.001
	Al Wakra	.390	6	.005	.699	6	.006
Zn in Seawater-Summer	Simaima	.384	6	.006	.712	6	.008
	Umm Bab	.343	6	.026	.674	6	.003
	Al Khor	.325	6	.047	.790	6	.047
	Al Wakra	.350	6	.021	.738	6	.015

*. This is a lower bound of the true significance.

a. Lilliefors Significance Correction

Hypothesis Test Summary

	Null Hypothesis	Test	Sig. ^{a,b}	Decision
1	The distribution of Cd in Seawater-Summer is the same across categories of Site.	Independent-Samples Kruskal-Wallis Test	.959	Retain the null hypothesis.
2	The distribution of Cr in Seawater-Summer is the same across categories of Site.	Independent-Samples Kruskal-Wallis Test	.664	Retain the null hypothesis.
3	The distribution of Cu in Seawater-Summer is the same across categories of Site.	Independent-Samples Kruskal-Wallis Test	.987	Retain the null hypothesis.
4	The distribution of Ni in Seawater-Summer is the same across categories of Site.	Independent-Samples Kruskal-Wallis Test	.912	Retain the null hypothesis.
5	The distribution of Pb in Seawater-Summer is the same across categories of Site.	Independent-Samples Kruskal-Wallis Test	.857	Retain the null hypothesis.
6	The distribution of Zn in Seawater-Summer is the same across categories of Site.	Independent-Samples Kruskal-Wallis Test	.867	Retain the null hypothesis.

a. The significance level is .050.

b. Asymptotic significance is displayed.

In winter:

Tests of Normality

Site	Kolmogorov-Smirnov ^a				Shapiro-Wilk		
	Statistic	df	Sig.	Statistic	df	Sig.	
Cd in Seawater-Winter	Simaima	.315	6	.064	.788	6	.045
	Umm Bab	.243	6	.200 [*]	.869	6	.222
	Al Khor	.339	6	.030	.846	6	.145
	Al Wakra	.492	6	<.001	.496	6	<.001
Cr in Seawater-Winter	Simaima	.	6	.	.	6	.
	Umm Bab	.	6	.	.	6	.
	Al Khor	.	6	.	.	6	.
	Al Wakra	.492	6	<.001	.496	6	<.001
Cu in Seawater-Winter	Simaima	.240	6	.200 [*]	.885	6	.294
	Umm Bab	.397	6	.004	.705	6	.007
	Al Khor	.320	6	.055	.781	6	.039
	Al Wakra	.291	6	.124	.852	6	.163
Ni in Seawater-Winter	Simaima	.250	6	.200 [*]	.925	6	.539
	Umm Bab	.303	6	.091	.747	6	.019
	Al Khor	.323	6	.050	.662	6	.002
	Al Wakra	.247	6	.200 [*]	.813	6	.076
Pb in Seawater-Winter	Simaima	.492	6	<.001	.496	6	<.001
	Umm Bab	.	6	.	.	6	.
	Al Khor	.492	6	<.001	.496	6	<.001
	Al Wakra	.492	6	<.001	.496	6	<.001
Zn in Seawater-Winter	Simaima	.258	6	.200 [*]	.850	6	.156
	Umm Bab	.114	6	.200 [*]	.992	6	.993
	Al Khor	.367	6	.011	.791	6	.049
	Al Wakra	.195	6	.200 [*]	.905	6	.403

*. This is a lower bound of the true significance.

a. Lilliefors Significance Correction

F-2-2: Trace metals in surface sediment samples

In summer:

Tests of Normality

	Site	Kolmogorov-Smirnov ^a			Shapiro-Wilk		
		Statistic	df	Sig.	Statistic	df	Sig.
Cd in Surface Sediment-Summer	Simaima	.310	6	.074	.816	6	.082
	Umm Bab	.355	6	.017	.601	6	<.001
	Al Khor	.290	6	.124	.720	6	.010
	Al Wakra	.277	6	.168	.817	6	.082
Cr in Surface Sediment-Summer	Simaima	.188	6	.200*	.887	6	.303
	Umm Bab	.312	6	.068	.763	6	.027
	Al Khor	.241	6	.200*	.874	6	.241
	Al Wakra	.277	6	.165	.878	6	.260
Cu in Surface Sediment-Summer	Simaima	.189	6	.200*	.924	6	.538
	Umm Bab	.211	6	.200*	.917	6	.486
	Al Khor	.243	6	.200*	.898	6	.360
	Al Wakra	.269	6	.200*	.807	6	.069
Ni in Surface Sediment-Summer	Simaima	.243	6	.200*	.860	6	.188
	Umm Bab	.205	6	.200*	.900	6	.372
	Al Khor	.223	6	.200*	.899	6	.370
	Al Wakra	.232	6	.200*	.938	6	.644
Pb in Surface Sediment-Summer	Simaima	.	6	.	.	6	.
	Umm Bab	.	6	.	.	6	.
	Al Khor	.	6	.	.	6	.
	Al Wakra	.	6	.	.	6	.
Zn in Surface Sediment-Summer	Simaima	.253	6	.200*	.841	6	.132
	Umm Bab	.232	6	.200*	.901	6	.379
	Al Khor	.178	6	.200*	.929	6	.575
	Al Wakra	.166	6	.200*	.943	6	.686

*. This is a lower bound of the true significance.

a. Lilliefors Significance Correction

Hypothesis Test Summary

	Null Hypothesis	Test	Sig. ^{a,b}	Decision
1	The distribution of Cd in Surface Sediment-Summer is the same across categories of Site.	Independent-Samples Kruskal-Wallis Test	.792	Retain the null hypothesis.
2	The distribution of Cr in Surface Sediment-Summer is the same across categories of Site.	Independent-Samples Kruskal-Wallis Test	.028	Reject the null hypothesis.
3	The distribution of Cu in Surface Sediment-Summer is the same across categories of Site.	Independent-Samples Kruskal-Wallis Test	.613	Retain the null hypothesis.
4	The distribution of Ni in Surface Sediment-Summer is the same across categories of Site.	Independent-Samples Kruskal-Wallis Test	.315	Retain the null hypothesis.
5	The distribution of Pb in Surface Sediment-Summer is the same across categories of Site.	Independent-Samples Kruskal-Wallis Test	1.000	Retain the null hypothesis.
6	The distribution of Zn in Surface Sediment-Summer is the same across categories of Site.	Independent-Samples Kruskal-Wallis Test	.124	Retain the null hypothesis.

a. The significance level is .050.

b. Asymptotic significance is displayed.

Pairwise Comparisons of Site

Sample 1-Sample 2	Test Statistic	Std. Error	Std. Test Statistic	Sig.	Adj. Sig. ^a
Simaima-Al Khor	-2.000-	4.082	-.490-	.624	1.000
Simaima-Umm Bab	-2.667-	4.082	-.653-	.514	1.000
Simaima-Al Wakra	-11.333-	4.082	-2.776-	.006	.033
Al Khor-Umm Bab	.667	4.082	.163	.870	1.000
Al Khor-Al Wakra	-9.333-	4.082	-2.286-	.022	.133
Umm Bab-Al Wakra	-8.667-	4.082	-2.123-	.034	.203

Each row tests the null hypothesis that the Sample 1 and Sample 2 distributions are the same.

Asymptotic significances (2-sided tests) are displayed. The significance level is .050.

a. Significance values have been adjusted by the Bonferroni correction for multiple tests.

In winter:

Tests of Normality

	Site	Kolmogorov-Smirnov ^a			Shapiro-Wilk		
		Statistic	df	Sig.	Statistic	df	Sig.
Cd in Surface Sediment-Winter	Simaima	.	6	.	.678	6	.004
	Umm Bab	.380	6	.007	.678	6	.004
	Al Khor	.343	6	.026	.778	6	.037
	Al Wakra	.455	6	<.001	.527	6	<.001
Cr in Surface Sediment-Winter	Simaima	.235	6	.200 [*]	.870	6	.228
	Umm Bab	.242	6	.200 [*]	.820	6	.088
	Al Khor	.270	6	.195	.919	6	.500
	Al Wakra	.249	6	.200 [*]	.845	6	.144
Cu in Surface Sediment-Winter	Simaima	.207	6	.200 [*]	.892	6	.329
	Umm Bab	.160	6	.200 [*]	.983	6	.963
	Al Khor	.174	6	.200 [*]	.927	6	.558
	Al Wakra	.221	6	.200 [*]	.919	6	.500
Ni in Surface Sediment-Winter	Simaima	.221	6	.200 [*]	.889	6	.315
	Umm Bab	.272	6	.189	.857	6	.178
	Al Khor	.226	6	.200 [*]	.889	6	.314
	Al Wakra	.191	6	.200 [*]	.959	6	.814
Pb in Surface Sediment-Winter	Simaima	.492	6	<.001	.496	6	<.001
	Umm Bab	.219	6	.200 [*]	.840	6	.130
	Al Khor	.407	6	.002	.662	6	.002
	Al Wakra	.397	6	.004	.705	6	.007
Zn in Surface Sediment-Winter	Simaima	.195	6	.200 [*]	.961	6	.830
	Umm Bab	.189	6	.200 [*]	.962	6	.835
	Al Khor	.199	6	.200 [*]	.951	6	.751
	Al Wakra	.323	6	.049	.822	6	.091

*. This is a lower bound of the true significance.

a. Lilliefors Significance Correction

Hypothesis Test Summary

	Null Hypothesis	Test	Sig. ^{a,b}	Decision
1	The distribution of Cd in Surface Sediment-Winter is the same across categories of Site.	Independent-Samples Kruskal-Wallis Test	.141	Retain the null hypothesis.
2	The distribution of Cr in Surface Sediment-Winter is the same across categories of Site.	Independent-Samples Kruskal-Wallis Test	.021	Reject the null hypothesis.
3	The distribution of Cu in Surface Sediment-Winter is the same across categories of Site.	Independent-Samples Kruskal-Wallis Test	.178	Retain the null hypothesis.
4	The distribution of Ni in Surface Sediment-Winter is the same across categories of Site.	Independent-Samples Kruskal-Wallis Test	.193	Retain the null hypothesis.
5	The distribution of Pb in Surface Sediment-Winter is the same across categories of Site.	Independent-Samples Kruskal-Wallis Test	.257	Retain the null hypothesis.
6	The distribution of Zn in Surface Sediment-Winter is the same across categories of Site.	Independent-Samples Kruskal-Wallis Test	.237	Retain the null hypothesis.

a. The significance level is .050.

b. Asymptotic significance is displayed.

Pairwise Comparisons of Site

Sample 1-Sample 2	Test Statistic	Std. Error	Std. Test Statistic	Sig.	Adj. Sig. ^a
Al Khor-Simaima	.500	4.082	.123	.903	1.000
Al Khor-Umm Bab	6.667	4.082	1.633	.102	.614
Al Khor-Al Wakra	-10.833-	4.082	-2.654-	.008	.048
Simaima-Umm Bab	-6.167-	4.082	-1.511-	.131	.785
Simaima-Al Wakra	-10.333-	4.082	-2.532-	.011	.068
Umm Bab-Al Wakra	-4.167-	4.082	-1.021-	.307	1.000

Each row tests the null hypothesis that the Sample 1 and Sample 2 distributions are the same.

Asymptotic significances (2-sided tests) are displayed. The significance level is .050.

a. Significance values have been adjusted by the Bonferroni correction for multiple tests.

F-2-3: Trace Metals in pearl oyster tissues samples

In summer:

Site	Tests of Normality						
	Kolmogorov-Smirnov ^a			Shapiro-Wilk			
	Statistic	df	Sig.	Statistic	df	Sig.	
Cd in oyster tissues-Summer	Simaima	.302	6	.092	.855	6	.174
	Umm Bab	.185	6	.200 [*]	.921	6	.512
	Al Khor	.250	6	.200 [*]	.880	6	.268
	Al Wakra	.273	6	.182	.780	6	.039
Cr in oyster tissues-Summer	Simaima	.238	6	.200 [*]	.897	6	.354
	Umm Bab	.178	6	.200 [*]	.934	6	.609
	Al Khor	.164	6	.200 [*]	.989	6	.987
	Al Wakra	.173	6	.200 [*]	.910	6	.436
Cu in oyster tissues-Summer	Simaima	.141	6	.200 [*]	.975	6	.925
	Umm Bab	.193	6	.200 [*]	.955	6	.779
	Al Khor	.272	6	.189	.840	6	.131
	Al Wakra	.317	6	.060	.759	6	.030
Ni in oyster tissues-Summer	Simaima	.226	6	.200 [*]	.887	6	.303
	Umm Bab	.354	6	.018	.685	6	.004
	Al Khor	.330	6	.040	.742	6	.017
	Al Wakra	.263	6	.200 [*]	.823	6	.095
Pb in oyster tissues-Summer	Simaima	.	6	.	.	6	.
	Umm Bab	.492	6	<.001	.496	6	<.001
	Al Khor	.392	6	.004	.702	6	.006
	Al Wakra	.	6	.	.	6	.
Zn in oyster tissues-Summer	Simaima	.138	6	.200 [*]	.989	6	.986
	Umm Bab	.218	6	.200 [*]	.947	6	.720
	Al Khor	.178	6	.200 [*]	.948	6	.722
	Al Wakra	.188	6	.200 [*]	.964	6	.849

*. This is a lower bound of the true significance.
a. Lilliefors Significance Correction

		ANOVA				
		Sum of Squares	df	Mean Square	F	Sig.
Cd in oyster tissues-Summer	Between Groups	8.639	3	2.880	.537	.662
	Within Groups	107.206	20	5.360		
	Total	115.845	23			
Cr in oyster tissues-Summer	Between Groups	7.286	3	2.429	3.766	.027
	Within Groups	12.899	20	.645		
	Total	20.185	23			
Cu in oyster tissues-Summer	Between Groups	10.267	3	3.422	.578	.636
	Within Groups	118.470	20	5.924		
	Total	128.737	23			
Ni in oyster tissues-Summer	Between Groups	.489	3	.163	.699	.564
	Within Groups	4.659	20	.233		
	Total	5.148	23			
Pb in oyster tissues-Summer	Between Groups	.177	3	.059	1.113	.367
	Within Groups	1.060	20	.053		
	Total	1.237	23			
Zn in oyster tissues-Summer	Between Groups	2048726.088	3	682908.696	2.356	.102
	Within Groups	5796266.441	20	289813.322		
	Total	7844992.529	23			

In winter:

Site	Tests of Normality						
	Kolmogorov-Smirnov ^a			Shapiro-Wilk			
	Statistic	df	Sig.	Statistic	df	Sig.	
Cd in oyster tissues-Winter	Simaima	.236	6	.200 [*]	.929	6	.569
	Umm Bab	.231	6	.200 [*]	.917	6	.484
	Al Khor	.214	6	.200 [*]	.882	6	.277
	Al Wakra	.190	6	.200 [*]	.968	6	.878
Cr in oyster tissues-Winter	Simaima	.255	6	.200 [*]	.932	6	.592
	Umm Bab	.274	6	.177	.882	6	.280
	Al Khor	.335	6	.034	.819	6	.087
	Al Wakra	.259	6	.200 [*]	.908	6	.424
Cu in oyster tissues-Winter	Simaima	.290	6	.125	.805	6	.065
	Umm Bab	.237	6	.200 [*]	.957	6	.797
	Al Khor	.198	6	.200 [*]	.923	6	.529
	Al Wakra	.236	6	.200 [*]	.932	6	.598
Ni in oyster tissues-Winter	Simaima	.254	6	.200 [*]	.889	6	.311
	Umm Bab	.249	6	.200 [*]	.886	6	.299
	Al Khor	.374	6	.009	.744	6	.017
	Al Wakra	.227	6	.200 [*]	.926	6	.546
Pb in oyster tissues-Winter	Simaima	.243	6	.200 [*]	.906	6	.409
	Umm Bab	.179	6	.200 [*]	.923	6	.528
	Al Khor	.163	6	.200 [*]	.962	6	.834
	Al Wakra	.284	6	.143	.852	6	.164
Zn in oyster tissues-Winter	Simaima	.202	6	.200 [*]	.973	6	.912
	Umm Bab	.278	6	.162	.805	6	.065
	Al Khor	.250	6	.200 [*]	.918	6	.494
	Al Wakra	.115	6	.200 [*]	.988	6	.985

*. This is a lower bound of the true significance.
a. Lilliefors Significance Correction

		ANOVA				
		Sum of Squares	df	Mean Square	F	Sig.
Cd in oyster tissues-Winter	Between Groups	31.566	3	10.522	2.505	.088
	Within Groups	84.019	20	4.201		
	Total	115.585	23			
Cr in oyster tissues-Winter	Between Groups	1.652	3	.551	2.606	.080
	Within Groups	4.225	20	.211		
	Total	5.877	23			
Cu in oyster tissues-Winter	Between Groups	41.060	3	13.687	3.253	.043
	Within Groups	84.146	20	4.207		
	Total	125.207	23			
Ni in oyster tissues-Winter	Between Groups	9.463	3	3.154	1.986	.148
	Within Groups	31.761	20	1.588		
	Total	41.225	23			
Pb in oyster tissues-Winter	Between Groups	.027	3	.009	.094	.962
	Within Groups	1.897	20	.095		
	Total	1.924	23			
Zn in oyster tissues-Winter	Between Groups	11663633.86	3	3887877.952	15.997	<.001
	Within Groups	4860691.736	20	243034.587		
	Total	16524325.59	23			

F-2-3: Trace Metals in pearl oyster tissues samples

Trace metals Vs. Site:

Tests of Normality							
Site	Kolmogorov-Smirnov ^a			Shapiro-Wilk			
	Statistic	df	Sig.	Statistic	df	Sig.	
Cd	Simaima	.230	18	.013	815	18	.002
	Umm Bab	.216	18	.026	786	18	<.001
	Al Khor	.501	18	<.001	457	18	<.001
	Al Wakra	.309	18	<.001	789	18	.001
Cr	Simaima	.304	18	<.001	836	18	.005
	Umm Bab	.162	18	.200*	909	18	.083
	Al Khor	.189	18	.089	897	18	.050
	Al Wakra	.247	18	.005	822	18	.003
Cu	Simaima	.501	18	<.001	457	18	<.001
	Umm Bab	.266	18	.002	765	18	<.001
	Al Khor	.501	18	<.001	457	18	<.001
	Al Wakra	.251	18	.004	808	18	.002
Ni	Simaima	.501	18	<.001	457	18	<.001
	Umm Bab	.501	18	<.001	457	18	<.001
	Al Khor	.501	18	<.001	457	18	<.001
	Al Wakra	.195	18	.069	825	18	.004
Pb	Simaima	.	18	.	.	18	.
	Umm Bab	.	18	.	.	18	.
	Al Khor	.	18	.	.	18	.
	Al Wakra	.403	18	<.001	652	18	<.001
Zn	Simaima	.386	18	<.001	633	18	<.001
	Umm Bab	.422	18	<.001	550	18	<.001
	Al Khor	.319	18	<.001	779	18	<.001
	Al Wakra	.178	18	.137	907	18	.075

*. This is a lower bound of the true significance.

a. Lilliefors Significance Correction

Hypothesis Test Summary

	Null Hypothesis	Test	Sig. ^{a,b}	Decision
1	The distribution of Cd is the same across categories of Site.	Independent-Samples Kruskal-Wallis Test	.003	Reject the null hypothesis.
2	The distribution of Cr is the same across categories of Site.	Independent-Samples Kruskal-Wallis Test	<.001	Reject the null hypothesis.
3	The distribution of Cu is the same across categories of Site.	Independent-Samples Kruskal-Wallis Test	<.001	Reject the null hypothesis.
4	The distribution of Ni is the same across categories of Site.	Independent-Samples Kruskal-Wallis Test	.016	Reject the null hypothesis.
5	The distribution of Pb is the same across categories of Site.	Independent-Samples Kruskal-Wallis Test	<.001	Reject the null hypothesis.
6	The distribution of Zn is the same across categories of Site.	Independent-Samples Kruskal-Wallis Test	<.001	Reject the null hypothesis.

a. The significance level is .050.

b. Asymptotic significance is displayed.

Appendix G Total mercury results for two years sampling

Appendix G-1: Total mercury concentration in seawater, sediment, and pearl oyster tissues samples

Appendix G-1-1: Total mercury concentration in seawater

Hg in water (ug/L)								
Site		R1	R2	R3	Mean	STD	CRM recovery	Detection limit (LOD)
Simaisma	Round 1	1.67E-02	3.50E-03	3.50E-03	7.90E-03	7.62E-03	101%	7.00E-06
	Round 2	1.90E-02	4.50E-03	4.50E-03	9.33E-03	8.37E-03	100%	9.00E-06
	Round 3	4.82E-02	4.50E-03	9.90E-03	2.09E-02	2.38E-02	96%	9.00E-06
	Round 4	2.50E-02	2.00E-03	3.00E-03	1.00E-02	1.30E-02	0.99	1.00E-06
Umm Bab	Round 1	3.50E-03	3.50E-03	1.84E-02	8.47E-03	8.60E-03	101%	7.00E-06
	Round 2	4.50E-03	4.50E-03	6.40E-02	2.43E-02	3.44E-02	100%	9.00E-06
	Round 3	4.50E-03	4.43E-02	1.17E-02	2.02E-02	2.12E-02	96%	9.00E-06
	Round 4	1.00E-02	7.10E-02	4.70E-02	4.27E-02	3.07E-02	0.99	1.00E-06
Al Khor	Round 1	3.50E-03	3.50E-03	8.20E-03	5.07E-03	2.71E-03	101%	7.00E-06
	Round 2	4.50E-03	4.50E-03	2.40E-02	1.10E-02	1.13E-02	100%	9.00E-06
	Round 3	3.18E-01	4.50E-03	1.45E-02	1.12E-01	1.78E-01	96%	9.00E-06
	Round 4	6.00E-03	3.00E-02	9.00E-03	1.50E-02	1.31E-02	0.99	1.00E-06
Al Wakra	Round 1	3.50E-03	1.40E-02	3.50E-03	7.00E-03	6.06E-03	101%	7.00E-06
	Round 2	7.90E-02	3.80E-02	6.00E-01	2.39E-01	3.13E-01	100%	9.00E-06
	Round 3	4.50E-03	3.14E-02	4.50E-03	1.35E-02	1.55E-02	96%	9.00E-06
	Round 4	1.90E-02	8.50E-02	6.07E-01	2.37E-01	3.22E-01	0.99	1.00E-06

Appendix G-1-2: Total mercury concentration in coastal sediment

Hg in Coastal Sediment (ug/g dry weight)								
Site	Round	R1	R2	R3	Mean	STD	CRM recovery	Detection limit (LOD) (mg/kg)
Simaisma	Round 1	0.005	0.020	0.010	0.012	0.008	94%	0.01
	Round 2	0.005	0.074	0.005	0.028	0.040	100%	0.01
	Round 3	0.005	0.019	0.005	0.010	0.008	95%	0.01
	Round 4	0.140	0.058	0.092	0.097	0.041	96%	0.01
Umm Bab	Round 1	0.140	0.005	0.010	0.052	0.077	94%	0.01
	Round 2	0.048	0.005	0.005	0.019	0.025	100%	0.01
	Round 3	0.005	0.005	0.005	0.005	0.000	95%	0.01
	Round 4	0.045	0.072	0.041	0.053	0.017	96%	0.01
Al Khor	Round 1	0.280	0.010	0.010	0.100	0.156	94%	0.01
	Round 2	0.005	0.005	0.005	0.005	0.000	100%	0.01
	Round 3	0.042	0.040	0.005	0.029	0.021	95%	0.01
	Round 4	0.085	0.101	0.167	0.118	0.043	96%	0.01
Al Wakra	Round 1	0.020	0.010	0.030	0.020	0.010	94%	0.01
	Round 2	0.005	0.005	0.005	0.005	0.000	100%	0.01
	Round 3	0.005	0.018	0.019	0.014	0.008	95%	0.01
	Round 4	0.069	0.057	0.043	0.056	0.013	96%	0.01

Appendix G-1-3: Total mercury concentration in oyster tissues

Hg in Oyster tissues (ug/g dry weight)								
Site	Round	R1	R2	R3	Mean	STD	CRM recovery	Detection limit (LOD) (mg/kg)
Simaisma	Round 1	0.050	1.510	0.060	0.540	0.840	105%	0.01
	Round 2	0.014	0.025	0.028	0.022	0.007	96%	0.01
	Round 3	0.078	0.044	0.063	0.062	0.017	101%	0.01
	Round 4	0.027	0.079	0.062	0.056	0.027	98%	0.01
Umm Bab	Round 1	4.880	0.300	0.240	1.807	2.662	105%	0.01
	Round 2	0.048	0.054	0.040	0.047	0.007	96%	0.01
	Round 3	0.118	0.036	0.117	0.090	0.047	101%	0.01
	Round 4	0.132	0.173	0.047	0.117	0.064	98%	0.01
Al Khor	Round 1	0.080	0.070	0.050	0.067	0.015	105%	0.01
	Round 2	0.030	0.037	0.029	0.032	0.004	96%	0.01
	Round 3	0.081	0.100	0.325	0.169	0.136	101%	0.01
	Round 4	0.021	0.029	0.055	0.035	0.018	98%	0.01
Al Wakra	Round 1	0.160	0.100	0.140	0.133	0.031	105%	0.01
	Round 2	0.030	0.031	0.070	0.044	0.023	96%	0.01
	Round 3	0.072	0.065	0.032	0.056	0.021	101%	0.01
	Round 4	0.209	0.082	0.775	0.355	0.369	98%	0.01

Appendix G-2: Statistical analysis of Total Mercury in seawater, sediment, and pearl oyster tissues samples

Appendix G-2-1: Total Mercury in seawater

In Summer:

Tests of Normality

	Site	Kolmogorov-Smirnov ^a			Shapiro-Wilk		
		Statistic	df	Sig.	Statistic	df	Sig.
Hg in Seawater-Summer	Simaisma	.280	6	.153	.721	6	.010
	Umm Bab	.247	6	.200*	.770	6	.031
	Al Khor	.469	6	<.001	.523	6	<.001
	Al Wakra	.364	6	.013	.705	6	.007

*. This is a lower bound of the true significance.

a. Lilliefors Significance Correction

Hypothesis Test Summary

	Null Hypothesis	Test	Sig. ^{a,b}	Decision
1	The distribution of Hg in Seawater-Summer is the same across categories of Site.	Independent-Samples Kruskal-Wallis Test	.982	Retain the null hypothesis.

a. The significance level is .050.

b. Asymptotic significance is displayed.

In Winter:

Tests of Normality

	Site	Kolmogorov-Smirnov ^a			Shapiro-Wilk		
		Statistic	df	Sig.	Statistic	df	Sig.
Hg in Seawater-Winter	Simaisma	.368	6	.011	.776	6	.036
	Umm Bab	.277	6	.167	.828	6	.103
	Al Khor	.307	6	.080	.791	6	.049
	Al Wakra	.371	6	.010	.712	6	.008

a. Lilliefors Significance Correction

Pairwise Comparisons of Site

Sample 1-Sample 2	Test Statistic	Std. Error	Std. Test Statistic	Sig.	Adj. Sig. ^a
Simaisma-Al Khor	-3.083	4.050	-.761	.447	1.000
Simaisma-Umm Bab	-6.250	4.050	-1.543	.123	.737
Simaisma-Al Wakra	-13.000	4.050	-3.210	.001	.008
Al Khor-Umm Bab	3.167	4.050	.782	.434	1.000
Al Khor-Al Wakra	-9.917	4.050	-2.448	.014	.086
Umm Bab-Al Wakra	-6.750	4.050	-1.666	.096	.574

Each row tests the null hypothesis that the Sample 1 and Sample 2 distributions are the same.

Asymptotic significances (2-sided tests) are displayed. The significance level is .050.

a. Significance values have been adjusted by the Bonferroni correction for multiple tests.

Hypothesis Test Summary

	Null Hypothesis	Test	Sig. ^{a,b}	Decision
1	The distribution of Hg in Seawater-Winter is the same across categories of Site.	Independent-Samples Kruskal-Wallis Test	.010	Reject the null hypothesis.

a. The significance level is .050.

b. Asymptotic significance is displayed.

Appendix G-2-2: Total Mercury in surface sediment

In Summer:

Tests of Normality

	Site	Kolmogorov-Smirnov ^a			Shapiro-Wilk		
		Statistic	df	Sig.	Statistic	df	Sig.
Hg in Seawater-Summer	Simaisma	.287	6	.134	.775	6	.035
	Umm Bab	.464	6	<.001	.519	6	<.001
	Al Khor	.417	6	.002	.623	6	<.001
	Al Wakra	.213	6	.200 [*]	.957	6	.797

*. This is a lower bound of the true significance.

a. Lilliefors Significance Correction

Hypothesis Test Summary

	Null Hypothesis	Test	Sig. ^{a,b}	Decision
1	The distribution of Hg in Seawater-Summer is the same across categories of Site.	Independent-Samples Kruskal-Wallis Test	.251	Retain the null hypothesis.

a. The significance level is .050.

b. Asymptotic significance is displayed.

In Winter:

Tests of Normality

	Site	Kolmogorov-Smirnov ^a			Shapiro-Wilk		
		Statistic	df	Sig.	Statistic	df	Sig.
Hg in Seawater-Winter	Simaisma	.197	6	.200*	.930	6	.580
	Umm Bab	.242	6	.200*	.888	6	.309
	Al Khor	.298	6	.104	.837	6	.122
	Al Wakra	.310	6	.075	.814	6	.078

*. This is a lower bound of the true significance.
a. Lilliefors Significance Correction

ANOVA

Hg in Seawater-Winter

	Sum of Squares	df	Mean Square	F	Sig.
Between Groups	.005	3	.002	.748	.536
Within Groups	.044	20	.002		
Total	.049	23			

Appendix G-2-3: Total mercury in oyster tissues

In Summer:

Tests of Normality

	Site	Kolmogorov-Smirnov ^a			Shapiro-Wilk		
		Statistic	df	Sig.	Statistic	df	Sig.
Hg in oyster tissues-Summer	Simaisma	.480	6	<.001	.515	6	<.001
	Umm Bab	.465	6	<.001	.543	6	<.001
	Al Khor	.402	6	.003	.649	6	.002
	Al Wakra	.182	6	.200*	.959	6	.815

*. This is a lower bound of the true significance.
a. Lilliefors Significance Correction

Hypothesis Test Summary

	Null Hypothesis	Test	Sig. ^{a,b}	Decision
1	The distribution of Hg in oyster tissues-Summer is the same across categories of Site.	Independent-Samples Kruskal-Wallis Test	.314	Retain the null hypothesis.

a. The significance level is .050.
b. Asymptotic significance is displayed.

In Winter:

Tests of Normality

	Site	Kolmogorov-Smirnov ^a			Shapiro-Wilk		
		Statistic	df	Sig.	Statistic	df	Sig.
Hg in oyster tissues-Winter	Simaisma	.337	6	.032	.850	6	.157
	Umm Bab	.360	6	.015	.769	6	.030
	Al Khor	.284	6	.141	.856	6	.177
	Al Wakra	.324	6	.048	.671	6	.003

a. Lilliefors Significance Correction

Hypothesis Test Summary

	Null Hypothesis	Test	Sig. ^{a,b}	Decision
1	The distribution of Hg in oyster tissues-Winter is the same across categories of Site.	Independent-Samples Kruskal-Wallis Test	.035	Reject the null hypothesis.

a. The significance level is .050.
b. Asymptotic significance is displayed.

Pairwise Comparisons of Site

Sample 1-Sample 2	Test Statistic	Std. Error	Std. Test Statistic	Sig.	Adj. Sig. ^a
Simaisma-Al Khor	-.250-	4.081	-.061-	.951	1.000
Simaisma-Umm Bab	-8.000-	4.081	-1.960-	.050	.300
Simaisma-Al Wakra	-9.083-	4.081	-2.226-	.026	.156
Al Khor-Umm Bab	7.750	4.081	1.899	.058	.345
Al Khor-Al Wakra	-8.833-	4.081	-2.165-	.030	.182
Umm Bab-Al Wakra	-1.083-	4.081	-.265-	.791	1.000

Each row tests the null hypothesis that the Sample 1 and Sample 2 distributions are the same.

Asymptotic significances (2-sided tests) are displayed. The significance level is .050.

a. Significance values have been adjusted by the Bonferroni correction for multiple tests.

Appendix G-2-4: Total Mercury in sediment cores

Total Mercury Vs. Sites

Tests of Normality

Hg	Site	Kolmogorov-Smirnov ^a			Shapiro-Wilk		
		Statistic	df	Sig.	Statistic	df	Sig.
	Simaima	.253	18	.004	.784	18	<.001
	Umm Bab	.209	18	.037	.830	18	.004
	Al Khor	.302	18	<.001	.789	18	.001
	Al Wakra	.285	18	<.001	.806	18	.002

a. Lilliefors Significance Correction

Hypothesis Test Summary

	Null Hypothesis	Test	Sig. ^{a,b}	Decision
1	The distribution of Hg is the same across categories of Site.	Independent-Samples Kruskal-Wallis Test	<.001	Reject the null hypothesis.

a. The significance level is .050.

b. Asymptotic significance is displayed.

Pairwise Comparisons of Site

Sample 1-Sample 2	Test Statistic	Std. Error	Std. Test Statistic	Sig.	Adj. Sig. ^a
Al Khor-Umm Bab	6.417	6.968	.921	.357	1.000
Al Khor-Simaima	10.083	6.968	1.447	.148	.887
Al Khor-Al Wakra	-39.500-	6.968	-5.669-	<.001	.000
Umm Bab-Simaima	3.667	6.968	.526	.599	1.000
Umm Bab-Al Wakra	-33.083-	6.968	-4.748-	<.001	.000
Simaima-Al Wakra	-29.417-	6.968	-4.222-	<.001	.000

Each row tests the null hypothesis that the Sample 1 and Sample 2 distributions are the same.

Asymptotic significances (2-sided tests) are displayed. The significance level is .050.

a. Significance values have been adjusted by the Bonferroni correction for multiple tests.

Total Mercury Vs. Depth

Tests of Normality

Hg	Depth	Kolmogorov-Smirnov ^a			Shapiro-Wilk		
		Statistic	df	Sig.	Statistic	df	Sig.
	5cm	.369	12	<.001	.689	12	<.001
	10cm	.274	12	.013	.801	12	.010
	15cm	.365	12	<.001	.701	12	<.001
	20cm	.360	12	<.001	.727	12	.002
	25cm	.362	12	<.001	.676	12	<.001
	30cm	.417	12	<.001	.650	12	<.001

a. Lilliefors Significance Correction

Hypothesis Test Summary

	Null Hypothesis	Test	Sig. ^{a,b}	Decision
1	The distribution of Hg is the same across categories of Depth.	Independent-Samples Kruskal-Wallis Test	.135	Retain the null hypothesis.

a. The significance level is .050.

b. Asymptotic significance is displayed.